Technische Universität München
TUM School of Medicine and Health

The Effect of Coating of Intestinal Anastomoses with Adhesive Biomaterials on Reducing Postoperative Anastomotic Leakage and Its Sequelae

Development of an Innovative *Ex-Vivo* Model for Evaluation of Stability and Pressure Resistance of Gastrointestinal Anastomoses

Kamacay Çıra

Vollständiger Abdruck der von der TUM School of Medicine and Health der Technischen Universität München zur Erlangung einer **Doktorin der Medizin (Dr. med.)** genehmigten Dissertation.

Vorsitz: apl. Prof. Dr. Lutz Renders

Prüfende der Dissertation:

1. Prof. Dr. Helmut Friess
2. apl. Prof. Dr. Rainer Burgkart
3. Prof. Dr. Nicolas Schlegel

Die Dissertation wurde am 18.04.2024 bei der Technischen Universität München eingereicht und durch die TUM School of Medicine and Health am 07.08.2024 angenommen.

Vita brevis, ars longa.

Hippokrates

Abstract

Gastrointestinal surgery is a common medical procedure used to treat various disorders affecting the gastrointestinal tract and associated organs, such as the esophagus, stomach, small intestine, large intestine, rectum, pancreas, liver, and gallbladder. These disorders may include inflammatory, cancerous, non-cancerous, traumatic, or ischemic conditions. When a segment of the gastrointestinal tract is removed due to one of these conditions, it is essential to restore the gastrointestinal continuity by performing an intestinal anastomosis. The choice of anastomotic technique in gastrointestinal surgery often depends on the surgeon's preference, although there are recommended approaches based on specific surgical indications. Anastomotic leakage is the most dreadful complication that may arise following this type of surgery and occurs when the healing of the reconnection site is inadequate, allowing the escape of intestinal contents into the abdominal cavity. This can result in severe infections and potentially life-threatening sepsis.

To address the risk of postoperative anastomotic leakage, various adhesive biomaterials have been investigated for coating intestinal anastomoses. Fibrin adhesives, such as fibrin sealants and collagen-based laminar biomaterials, are particularly promising and have received US Food and Drug Administration approval. Numerous animal studies have generated encouraging results by examining the effects of applying these biomaterials to intestinal anastomoses. These findings have indicated a reduction in postoperative

anastomotic leakage and mortality rates. However, the assessment of these sealants' impact on postoperative anastomotic healing has been confined to a limited number of human studies, both interventional and observational. There has been no comprehensive systematic review and meta-analysis of the outcomes of coating intestinal anastomoses with these biomaterials. Therefore, the overall effect of using fibrin sealants to reduce anastomotic leakage remains uncertain, and no meta-analysis has examined the impact of these biomaterials on postoperative anastomotic leakage rates and associated complications in humans or animals.

Therefore, the primary aim of this thesis was to systematically evaluate the effects of coating all types of intestinal anastomoses with collagen- or fibrin-based adhesive biomaterials, regardless of location and underlying disease, on postoperative anastomotic leakage, its complications, and mortality for human and animal studies. To achieve this, systematic reviews and meta-analyses were conducted, calculating pooled odds ratios with 95 % confidence intervals and performing subgroup analyses for predefined risk factors.

The systematic review and meta-analysis of human studies showed that across 15 studies involving a total of 1,387 patients in the intervention group and 2,243 in the control group, coated intestinal anastomoses were associated with significant benefits. Patients with coated intestinal anastomoses exhibited significantly lower rates of anastomotic leakage, reoperations and major complications according to Clavien–Dindo classification compared to controls. These results remained consistent in sensitivity and subgroup analyses, considering study design, age group, intervention type, anastomotic location, and indication for surgery. Furthermore, length of hospitalization was significantly shorter in the intervention group especially for patients undergoing upper gastrointestinal surgery for a malignant disease.

The systematic review and meta-analysis of animal studies revealed that among the 13 prospective studies (15 data sets) involving 290 animals in the intervention group and 279 animals in the control group, the intervention group exhibited a significantly lower incidence of

anastomotic leakage compared to the control group. Furthermore, within the intervention group, animals with incomplete intestinal anastomoses displayed a significantly reduced susceptibility to anastomotic leakage. Observed results remained stable throughout sensitivity analyses.

Various *ex-vivo* models have been developed to evaluate anastomotic stability and pressure resistance, especially in context of evaluating the biomechanical effect of coating intestinal anastomoses with different adhesive biomaterials. Nevertheless, these models present rudimentary experimental setups and often lack comparability and reproducibility of scientific data. Biomechanical studies are crucial for understanding anastomotic leakage by examining the mechanical behavior and integrity of the anastomotic site. Quantitative measurements, such as bursting pressure, tensile strength, suture holding capacity, and other mechanical parameters, provide valuable insights for identifying potential risk factors and guiding surgical decision-making.

Hence, the secondary aim of this thesis was to develop an innovative *ex-vivo* model for precise and quantitative assessment of gastrointestinal anastomotic quality in terms of stability and pressure resistance, with high comparability, reproducibility, and user-independence. This model aims to enhance the understanding of the biomechanics of intestinal anastomoses and anastomotic leakage without the need for animal testing.

Therefore, an open fluid circulation system was developed, which relies on a modified perfusion bioreactor and incorporates a human machine interface. This system facilitates the controlled intraluminal delivery of a colored phosphate-buffered saline solution into a porcine small intestinal anastomosis, following its passage through a pressure probe. It offers the flexibility to simulate both physiological conditions (low-flow model) and elevated intraabdominal pressure (high-low model). Concurrently, the system enables the monitoring of intraluminal pressure and the temperature of the surrounding phosphate-buffered saline.

Multiple cameras are employed to capture various angles of the anastomosis for comprehensive data recording.

A total of 32 handsewn end-to-end anastomoses were performed, equally distributed between simple interrupted suture and continuous suture techniques, and subjected to two different flow rates, a low-flow model and a high-flow model. This experiment served as a feasibility trial, primarily aimed at assessing the overall functionality of the innovative *ex-vivo* model. Additionally, factors such as adherence to 3R principles, reproducibility, comparability, and user-independence were evaluated to ensure the reliability of the system.

In summary, the comparative analysis revealed several key findings. Firstly, when comparing leakage pressure, the high-flow model exhibited higher leakage pressure for simple interrupted sutured anastomoses, whereas this difference did not apply to continuously sutured anastomoses. Furthermore, the choice of suture technique did not have a significant impact on leakage pressure. Secondly, in terms of bursting pressure, both simple interrupted sutured anastomoses and continuously sutured anastomoses within the high-flow model reached significantly higher bursting pressures compared to the low-flow model. However, no significant differences were observed in bursting pressures between the two suture techniques within the same flow model. Regarding the proportion of bursting pressure at leakage pressure, continuously sutured anastomoses within the high-flow model showed a significantly higher increase in intraluminal pressure until bursting after leakage. These observed phenomena can be ascribed to the viscoelastic properties inherent to biologic tissues, characterized by time-dependent stress-strain responses. Given that the choice of suture technique did not exert a substantial influence on leakage and bursting pressure, it implies that its impact on anastomotic stability and pressure resistance may be limited.

Finally, an investigation system for leakage and bursting location was developed. Images from all four cameras, capturing various angles of the anastomosis, were meticulously

correlated with the corresponding measured pressures in each experimental trial. The anastomosis was systematically divided into eleven equal sections, numbered from -5 to 5, with 0 (or M0) designating the precise location of the mesenteric attachment to the intestine. To streamline data evaluation and presentation, these circular sections were transformed into a linear grid, positioning 0 at the center, -5 to the far left, and 5 to the far right. Subsequently, the grid was further partitioned into two distinct zones: the mesenteric zone (ranging between -1 and +1) and the peripheral zone (encompassing -2 to -5 and +2 to +5), identified as zones M1 and P (P2-P5), respectively.

This analytical approach clearly delineated that the mesenteric zone of the examined anastomoses exhibited significantly higher incidences of both leakage and bursting compared to the peripheral zone. Importantly, this consistent pattern persisted irrespective of the specific experimental series or suture technique employed, strongly indicating a robust association between the occurrence of leakage and the subsequent risk of bursting at the same location within the anastomosis. These findings suggest that the mesenteric insertion site serves as a potential vulnerable point where anastomotic leakage is more likely to occur. Given that surgical procedures frequently involve anastomoses at this location, there is an increased risk of complications related to anastomotic leakage. These results emphasize the importance of careful consideration and appropriate management of the mesenteric insertion site during surgical interventions to minimize the likelihood of anastomotic complications. Moreover, additional research and enhancements in surgical approaches may be necessary to enhance outcomes in this pivotal aspect of anastomotic procedures.

In summary, this thesis leads to the following conclusions:

The application of collagen-based laminar biomaterials or fibrin sealants on intestinal anastomoses can significantly reduce postoperative rates of anastomotic leakage and its sequelae, as evidenced by the performed comprehensive systematic reviews and meta-

analyses covering human and animal studies. Coating intestinal anastomoses may facilitate effective and sustainable leak prevention. However, the validity and robustness of these findings warrant further scrutiny through additional clinical studies. Particular attention should be directed towards investigating the potential risks of anastomotic and adhesive failure resulting from anastomotic infection, with a specific focus on antimicrobial collagen-based sealants. To solidify these conclusions and gain a comprehensive understanding, future research should include more large-scale randomized controlled trials. Additionally, prospective animal studies involving larger mammals, such as pigs, are essential to assess the long-term implications of this intervention and its potential transferability to human patients. Lastly, the development of a highly adhesive collagen-based biomaterial featuring a more user-friendly and efficient application method is imperative for the successful integration of this innovative approach to anastomotic leakage prevention into routine surgical practice.

Finally, the innovative *ex-vivo* model, designed for precise and quantitative assessment of gastrointestinal anastomotic quality in terms of stability and pressure resistance, has demonstrated commendable attributes including comparability, reproducibility, and user-independence. The innovation lies in the comprehensive evaluation of the anastomosis, subjected to controlled conditions. Notably, the significant differences observed between anastomoses in the low-flow model and high-flow model underscore the relevance of the time-dependent response of intestinal tissue to stress, elucidating that the stress-strain response does not manifest instantaneously. The model holds potential for high-throughput experimentation, paving the way for a virtual simulation of anastomotic and intestinal tissue healing without the need for animal experimentation. Collaborative efforts with clinicians and surgeons are essential to refine the *ex-vivo* model, ensuring its alignment with real-world clinical challenges. By integrating their expertise and insights, the *ex-vivo* test setup can become a valuable tool for investigating anastomotic performance and optimizing surgical outcomes.

Furthermore, the *ex-vivo* test setup offers the capability to determine and visualize leakage and bursting pressure, enabling the analysis of weak spots in the anastomosis. This opens avenues for studying the mechanical reinforcement of biologic adhesives used in intestinal anastomoses, potentially leading to innovative approaches for enhancing anastomotic stability and reducing the risk of leakage. Additionally, this platform provides a means to reproducibly compare different suture and anastomotic staple techniques, offering valuable insights into their performance and effectiveness. This information can guide surgeons in selecting the optimal approach for anastomosis. By addressing limitations and harnessing advancements in imaging modalities, artificial intelligence algorithms, tissue engineering, and fostering collaboration with clinicians, the *ex-vivo* test setup holds immense promise in yielding more precise, clinically relevant data. This, in turn, will promote an improved comprehension of anastomotic behavior, translating into enhanced surgical outcomes. One of the central objectives in the future will be the complete digital representation of the anastomotic and intestinal tissue healing processes, thereby eliminating the necessity for animal testing completely.

Zusammenfassung

Die gastrointestinale Chirurgie beinhaltet die Behandlung verschiedener Störungen, die den Gastrointestinaltrakt und zugehörige Organe wie die Speiseröhre, den Magen, den Dünndarm, den Dickdarm, den Mastdarm, die Bauchspeicheldrüse, die Leber und die Gallenblase betreffen. Zu diesen Störungen zählen entzündliche, maligne, benigne, traumatische oder ischämische Erkrankungen. Wenn ein Segment des Gastrointestinaltrakts aufgrund einer dieser Bedingungen entfernt wird, ist es entscheidend, die gastrointestinale Kontinuität durch eine intestinale Anastomose wiederherzustellen. Die Wahl der Anastomosentechnik in der gastrointestinalen Chirurgie hängt in der Regel von der Präferenz des Chirurgen ab, obwohl es empfohlene Ansätze gibt, die auf spezifischen chirurgischen Indikationen basieren. Die Anastomoseninsuffizienz gehört zu den gefährlichsten Komplikationen nach dieser Art von Operation und tritt auf, wenn es zu einer Wundheilungsstörung im Bereich der anastomosierten Darmenden kommt. Dies kann zum Austritt von Darminhalt in die Bauchhöhle führen, was wiederum in einer schweren Infektion und potenziell lebensbedrohlicher Sepsis resultiert.

Um das Risiko postoperativer Anastomoseninsuffizienzen zu minimieren, wurden verschiedene adhäsive Biomaterialien zur Beschichtung der Darmnahtstellen untersucht. Hinsichtlich der Reduktion postoperativer Anastomoseninsuffizienzen stellt die Beschichtung der Darmnahtstellen mit Fibrinklebern und kollagenbasierten laminaren Biomaterialien ein

vielversprechendes Verfahren dar. Zudem besitzen diese Biokleber die Zulassung durch die US-amerikanischen Food and Drug Administration. Zahlreiche Tierversuche haben die Auswirkung dieser Biomaterialien auf Darmnahtstellen untersucht und zeigen ermutigende Ergebnisse hinsichtlich einer Reduktion von postoperativen Anastomoseninsuffizienz- und Sterblichkeitsraten. Die Bewertung des Einflusses dieser adhäsiven Biokleber auf die postoperative Heilung von Anastomosen beschränkt sich jedoch auf eine begrenzte Anzahl von Humanstudien, sowohl interventionelle als auch beobachtende. Der Effekt der Beschichtung von Darmnähten mit adhäsiven Biomaterialen auf die Reduktion von postoperativen Anastomoseninsuffizienzen und den damit assoziierten Komplikationen wurde bisher in keiner systematischen Übersichtsarbeit mit Metaanalyse hinsichtlich zur Schaffung einer wissenschaftlichen Evidenz der vorliegenden Daten untersucht. Daher bleibt der Gesamteffekt der Verwendung adhäsiven Biomaterialen zur Reduktion von Anastomoseninsuffizienzen sowohl bei Human- als auch in Tierstudien unklar.

Daher war das primäre Ziel dieser Dissertation, den Effekt der Beschichtung aller Arten von Darmanastomosen mit kollagen- oder fibrinbasierten adhäsiven Biomaterialien, unabhängig ihrer Lokalisation oder der zugrunde liegenden Erkrankung, systematisch im Hinblick auf die postoperative Anastomoseninsuffizienzrate, den damit assoziierten Komplikationen und der Sterblichkeitsrate sowohl in Human- als auch in Tierstudien zu evaluieren. Um dies zu erreichen, wurden zwei systematische Übersichtsarbeiten und Metaanalysen durchgeführt, bei denen das gepoolte Quotenverhältnis (Odds Ratio) mit einem 95 % -Konfidenzintervallen berechnet und Subgruppenanalysen für vordefinierte Risikofaktoren durchgeführt wurden.

Die systematische Übersichtsarbeit und Metaanalyse von 15 Humanstudien mit insgesamt 1,387 Patienten in der Interventionsgruppe und 2,243 Patienten in der Kontrollgruppe zeigte, dass die Beschichtung von Darmanastomosen mit signifikanten Vorteilen assoziiert war. Patienten in der Interventionsgruppe wiesen signifikant niedrigere

Raten von postoperativen Anastomoseninsuffizienzen, Reoperationen und schwerwiegenden Komplikationen gemäß der Clavien-Dindo-Klassifikation im Vergleich zur Kontrollgruppe auf. Diese Ergebnisse blieben in Sensitivitäts- und Subgruppenanalysen, unter Berücksichtigung von Studiendesign, Altersgruppe, Interventionsart, Lokalisation der Anastomose und Indikation für die Operation, konsistent. Darüber hinaus war die Krankenhausaufenthaltsdauer in der Interventionsgruppe, insbesondere für Patienten, die aufgrund einer malignen Erkrankung des oberen Gastrointestinaltraktes operiert wurden, signifikant kürzer.

Ähnliche Ergebnisse konnten im Rahmen der durchgeführten systematischen Übersichtsarbeit und Metaanalyse von Tierversuchsstudien verzeichnet werden. Unter den 13 prospektiven Studien (15 Datensätze) mit 290 Tieren in der Interventionsgruppe und 279 Tieren in der Kontrollgruppe, zeigte die Interventionsgruppe signifikant niedrigere Inzidenzen von postoperativen Anastomoseninsuffizienzen. Innerhalb der Interventionsgruppe zeigten insbesondere die Tiere, die eine insuffiziente Anastomose in Form von unvollständigen Darmnähten erhalten hatten, eine signifikant reduzierte Anfälligkeit für das Auftreten von postoperativen Anastomoseninsuffizienzen. Die beobachteten Ergebnisse zeigten sich in der Sensitivitätsanalyse stabil.

Im Rahmen der Evaluierung der Effekte von adhäsiven Biomaterialien, wurden diverse *ex-vivo* Modelle entwickelt und zur Evaluation der Stabilität und Druckbeständigkeit von Anastomosen genutzt. Diese Modelle weisen häufig einen Mangel an Vergleichbarkeit und Reproduzierbarkeit wissenschaftlicher Daten auf. Biomechanische Analysen spielen eine entscheidende Rolle bei der Erforschung von Anastomoseninsuffizienzen, indem das mechanische Verhalten und die Integrität der Anastomose untersucht wird. Quantitative Messgrößen wie Berstungsdruck, Zugfestigkeit, Nahtfestigkeit sowie andere mechanische Parameter liefern wertvolle Erkenntnisse zur Identifikation potenzieller Risikofaktoren für Insuffizienzen und unterstützen daher die chirurgische Entscheidungsfindung der Wahl der Anastomosentechnik.

Aus diesem Grund war das sekundäre Ziel dieser Dissertation die Entwicklung eines innovativen *ex-vivo* Modells zur präzisen und quantitativen Bewertung der Qualität von gastrointestinalen Anastomosen in Bezug auf ihre Stabilität und Druckbeständigkeit, mit möglichst hoher Vergleichbarkeit, Reproduzierbarkeit und Nutzerunabhängigkeit. Dieses Modell zielt darauf ab, das Verständnis der Biomechanik von gastrointestinalen Anastomosen und den Anastomoseninsuffizienzen zu verbessern, ohne auf Tierversuche zurückgreifen zu müssen.

Hierfür wurde ein offenes Flüssigkeitszirkulationssystem entwickelt, das auf einem modifizierten Perfusionsbioreaktor basiert und eine Mensch-Maschine-Schnittstelle integriert. Dieses System ermöglicht den kontrollierten intraluminalen Transport einer gefärbten Phosphatpufferlösung vorbei an einer Druckmesssonde, in eine porzine Dünndarmanastomose. Das Modell bietet die Flexibilität, sowohl physiologische (Low-Flow Modell) als auch erhöhte intraabdominale Druckbedingungen (High-Flow Modell) zu simulieren. Gleichzeitig kann das Modell die Überwachung des intraluminalen Drucks und der Temperatur der umgebenden Phosphatpufferlösung gewährleisten. Mehrere Kameras werden eingesetzt, um die Anastomose von verschiedenen Winkeln für umfassende Datenaufzeichnungen zu erfassen.

Insgesamt wurden 32 handgenähte End-zu-End-Dünndarmanastomosen angefertigt, davon 16 mittels Einzelknopfnahttechnik und 16 durch die Anwendung der fortlaufenden Nahttechnik. Diese Anastomosen wurden zwei verschiedenen Durchflussraten ausgesetzt, die dem beschriebenen Low-Flow Modell und dem High-Flow-Modell entsprechen. Das Experiment diente als Machbarkeitsstudie, welche zum Ziel hatte, die Gesamtfunktionalität des innovativen *ex-vivo* Modells zu bewerten. Zusätzlich wurden Faktoren wie die Berücksichtigung der 3R-Prinzipien, Reproduzierbarkeit, Vergleichbarkeit und Benutzerunabhängigkeit bewertet, um die Zuverlässigkeit des Systems sicherzustellen.

Zusammenfassend ergab die vergleichende Analyse mehrere Schlüsselerkenntnisse. Der Insuffizienzdruck war bei den mit Einzelknopfnaht angefertigten Anastomosen im High-Flow-Modell im Vergleich zum Low-Flow-Modell signifikant höher, wohingegen für Anastomosen in fortlaufender Nahttechnik kein derartiger Unterschied festgestellt wurde. Darüber hinaus hatte die Wahl der Nahttechnik keinen signifikanten Einfluss auf den Insuffizienzdruck. Des Weiteren wiesen beide Anastomosentechniken im High-Flow-Modell signifikant höhere Berstungsdrücke im Vergleich zum Low-Flow-Modell auf. Hingegen wurden keine signifikanten Unterschiede im Berstungsdruck zwischen beiden Nahttechniken im gleichen Flussmodell festgestellt.

In Bezug auf den Anteil vom Berstungsdruck bei Erreichen des Insuffizienzdruckes zeigten die in fortlaufender Nahttechnik angefertigten Anastomosen im High-Flow-Modell einen signifikant höheren Anstieg des intraluminalen Drucks bis zum Platzen nach Insuffizienz. Diese beobachteten Phänomene können auf die viskoelastischen Eigenschaften biologischer Gewebe zurückgeführt werden, die durch zeitabhängige Spannungs-Dehnungs-Reaktionen charakterisiert sind. Da die Wahl der Nahttechnik keinen wesentlichen Einfluss auf den Insuffizienz- oder Berstungsdruck hatte, lässt dies darauf schließen, dass ihr Einfluss auf die Stabilität und Druckbeständigkeit von Anastomosen begrenzt sein könnte.

Schließlich wurde anhand der gesammelten Daten ein Untersuchungssystem zur Lokalisation der Insuffizienz- und Berstungsstellen entwickelt. Die Bilder aller vier Kameras, die die Anastomose aus verschiedenen Winkeln aufzeichnen, wurden sorgfältig mit den entsprechenden gemessenen Druckwerten in jedem Experiment in Beziehung gesetzt. Die Anastomose wurde im Rahmen des Querschnittmodels systematisch in elf gleichgroße Abschnitte unterteilt, nummeriert von -5 bis 5, wobei der Referenzpunkt 0 (oder M0) den präzisen Ort der mesenterialen Insertionsstelle am Dünndarm markierte. Um die Auswertung und Präsentation der Daten zu erleichtern, wurden diese kreisförmigen Abschnitte in ein lineares Raster übertragen, wobei 0 in der Mitte, -5 ganz links und 5 ganz rechts platziert

wurden. Das Raster wurde anschließend in zwei verschiedene Zonen unterteilt: die mesenteriale Zone (im Bereich von -1 bis +1) identifiziert als Zone M1 und die periphere Zone (im Bereich von -2 bis -5 und +2 bis +5) identifiziert als P (P2-P5).

Dieser analytische Ansatz verdeutlicht eindeutig, dass Anastomosen im Bereich der mesenterialen Zone im Vergleich zur peripheren Zone signifikant höhere Inzidenzen von Insuffizienzen und Berstungen aufweisen. Diese konsistente Musterung blieb unabhängig von der spezifischen Versuchsreihe oder der angewandten Nahttechnik bestehen und deutet stark auf eine robuste Verbindung zwischen dem Auftreten von Insuffizienzen und dem anschließenden Risiko des Berstens an derselben Stelle innerhalb der Anastomose hin. Diese Ergebnisse legen nahe, dass die mesenteriale Insertionsstelle eine potenzielle Schwachstelle der Anastomose mit erhöhtem Risiko der dortigen Entwicklung der Anastomoseninsuffizienz darstellt. Diese Ergebnisse unterstreichen die Notwendigkeit einer sorgfältigen und präzisen Einbeziehung der mesenterialen Insertionsstelle im Rahmen der Erstellung einer Anastomose, um die Wahrscheinlichkeit von Anastomosenkomplikationen zu minimieren. Des Weiteren könnten weiterführende Optimierungen chirurgischer Anastomosentechniken unter Berücksichtigung der mesenterialen Insertionsstelle als potenzielle Schwachstelle notwendig sein, um die postoperativen Ergebnisse zu verbessern.

Zusammenfassend führen die in dieser Dissertation gewonnenen Erkenntnisse zu folgenden Schlussfolgerungen:

Die Beschichtung von Darmanastomosen mit Fibrinklebern oder kollagenbasierten laminaren Biomaterialien kann das Auftreten von postoperativen Anastomoseninsuffizienzen und den damit assoziierten Komplikationen reduzieren. Daher könnte dieses Verfahren zur effektiven und nachhaltigen Prävention von Anastomoseninsuffizienzen beitragen. Die Validität und Robustheit dieser Erkenntnisse bedürfen weiterer genauer Prüfung durch zusätzliche klinische Studien. Es ist wichtig, spezielles Augenmerk darauf zu legen, die

potenziellen Risiken von Anastomoseninsuffizienzen und dem Haftungsversagen von Bioklebern aufgrund von Anastomoseninfektionen zu untersuchen. Dabei sollte der Fokus auf antimikrobiell beschichteten, kollagenbasierten Bioklebern liegen. Hierfür sollten zukünftig größer angelegte randomisierte kontrollierte Studien durchgeführt werden. Zusätzlich sind prospektive Tierversuchsstudien mit größeren Säugetieren, wie beispielsweise Schweinen, notwendig, um die langfristigen Auswirkungen dieser Intervention zu evaluieren und die potenzielle Übertragbarkeit auf Patienten zu überprüfen. Schließlich ist die Entwicklung eines hochadhäsiven kollagenbasierten Bioklebers mit einer benutzerfreundlicheren und effizienteren Anwendungsmethode für die erfolgreiche Integration dieses innovativen Ansatzes zur Prävention einer Anastomoseninsuffizienz in die routinemäßige chirurgische Praxis unerlässlich.

In Bezug auf das innovative *ex-vivo* Modell kann festgehalten werden, dass ein vergleichbares, reproduzierbares und benutzerunabhängiges Verfahren zur präzisen und quantitativen Bewertung der gastrointestinalen Anastomosenqualität in Bezug auf Stabilität und Druckbeständigkeit entwickelt wurde. Die Innovation liegt in der umfassenden biomechanischen Bewertung der Anastomose unter kontrollierten Bedingungen. Insbesondere unterstreichen die signifikanten Unterschiede zwischen den Anastomosen im Low-Flow- und High-Flow-Modell die Bedeutung der zeitabhängigen Reaktion des Darmgewebes auf mechanischen Stress, was darauf hinweist, dass die Spannungs-Dehnungs-Reaktion nicht sofort auftritt. Zudem bietet das Modell Potenzial für die Durchführung von Hochdurchsatzexperimenten, die wiederum genug Daten bieten, um eine virtuelle Simulation der Wundheilung von Anastomosen und Darmgewebe zu entwickeln, ohne auf Tierversuche angewiesen zu sein. Die enge Zusammenarbeit mit Klinikern und Chirurgen ist essenziell für die Weiterentwicklung des *ex-vivo* Modells, um letztlich den Anforderungen und Herausforderungen der klinischen Praxis gerecht zu werden. Durch die Integration ihrer Expertise und Erkenntnisse kann das Modell als wertvolles Instrument zur Bewertung

technischer Schwachstellen bei der Anastomosenanfertigung genutzt werden und so dazu beitragen, chirurgische Ergebnisse zu optimieren.

Zusätzlich ermöglicht das *ex-vivo* Modell die Bestimmung und Visualisierung von Insuffizienz- und Berstungsdrücken, wodurch die Analyse von Schwachstellen der Darmanastomose ermöglicht wird. Aufgrund dessen könnte das Modell eine nützliche Anwendung zur Bewertung der Auswirkungen der mechanischen Nahtverstärkung von Anastomosen mittels adhäsiver Biomaterialien darstellen. In dieser Anwendung könnte das Modell dazu beitragen, innovative Ansätze zur mechanischen Nahtverstärkung zu entwickeln, um die Stabilität von Anastomosen zu verbessern und somit das Risiko von Insuffizienzen zu reduzieren. Des Weiteren könnten mit dem Modell unterschiedliche Naht-, Stapler- und Anastomosentechniken reproduzierbar verglichen werden und somit Einblicke in deren Leistungsstärke und Effektivität bieten. Die hierbei gewonnen Erkenntnisse können Chirurgen dabei unterstützen, die optimale Technik zur Anlage einer Darmanastomose auszuwählen.

Durch die Nutzung von fortgeschrittenen Bildgebungstechnologien, künstlicher Intelligenz, Tissue-Engineering und der Zusammenarbeit mit klinischen Experten birgt das innovative *ex-vivo* Modell ein großes Potenzial, präzise und klinisch relevante Daten zu generieren. Dies wird wiederum zu einem verbesserten Verständnis des Verhaltens von Anastomosen führen und letztendlich zu verbesserten chirurgischen Ergebnissen beitragen. Ein zentrales Ziel in der Zukunft wird die vollständige digitale Darstellung der Heilungsprozesse von Anastomosen und Darmgewebe sein, um den Einsatz von Tierversuchen gänzlich zu vermeiden.

Contents

Contents

Contents

I Abbreviations

1. List of abbreviations for the main text

°	Degree
$°C$	Degrees Celsius
Chi^2 or χ^2	Chi-squared test (heterogeneity)
CO_2	Carbon Dioxide
$>$	Greater than
$<$	Less than
$\pm$	Plus-minus
%	Percentage or frequency
3D	Three-dimensional
3R	3R principles (reduction, refinement, replacement)
A_C	Number of events in the control group
ACS	American Chemical Society
A_E	Number of events in the experimental group
AL	Anastomotic leakage
ARRIVE	Animal in Research: Reporting In Vivo Experiments guidelines for reporting animal research
B_C	Number of non-events in the control group
B_E	Number of non-events in the experimental group
BMI	Body Mass Index
BP	Bursting pressure
C-BLB	Collagen-based laminar biomaterial
C-DMC	Clavien-Dindo major complications
CI	Confidence interval
cm	Centimeter
cP	Centipoise
CPR	Center of Preclinical Research
CS	Continuous suture technique
CS-CON-HF	Handsewn sufficient small intestinal end-to-end anastomoses using simple continuous suture technique, tested in the high-flow model
CS-CON-LF	Handsewn sufficient small intestinal end-to-end anastomoses using simple continuous suture technique, tested in the low-flow model
CSV	Comma-separated values file
df	Degree of freedom
dyn/cm	Dyne per centimeter
e.g.	Exempli gratia
EEA	End-to-end anastomosis
Etc.	Et cetera
FDA	United States Food and Drug Administration
FE	Fixed-effect model meta-analysis
F. S.	Felix Stocker (surgical resident)
FS	Fibrin Sealant
Full HD	Full High Definition (a video resolution standard with a resolution of 1920 x 1080 pixels)
g	Gram
HF	High-flow model
HMI	Human-machine interface

I Abbreviations

I^2	I-squared (measure of heterogeneity)
ID	Identification
IND	Inner diameter
JASP	JASP Team (*2021; JASP (Version 0.16) [Computer software]*)
jpg or JPEG	Joint Photographic Experts Group
K. C.	Kamacay Cira (surgical resident)
K2RANICH	Kollagener Biokleber und Vlies zur Reduktion der Anastomosen-Insuffizienz in der Chirurgie
kg/m^2	Kilogram per square meter
kg/m^3	Kilogram per cubic meter
LabVIEW	Laboratory Virtual Instrumentation Engineering Workbench (*LabVIEW 2021 SP1 f2; National Instruments, USA*)
LED	Light-emitting diode
LF	Low-flow model
log	Logarithm
LP	Leakage pressure
Mbyte	Megabyte
MD	Mean difference
min	Minute
ml	Milliliter
mm	Millimeter
$mmHg$	Millimeters of mercury
mRNA	Messenger ribonucleic acid
$msec$	Millisecond
NI-myRIO	NI-myRIO Controller
NOS	Newcastle-Ottawa Scale for cohort studies
NRS	Non-randomized interventional study
OR	Odds ratio
p	Probability value
P-A. N.	Philipp-Alexander Neumann (surgical specialist)
PBS	Phosphate-buffered saline solution
PCS	Prospective cohort study
PDS	Polydioxanone
POD	Postoperative day
PROSPERO	International Prospective Register of Systematic Reviews of the National Institute for Health Research
px	Pixel
Q	Difference of the chi-squared statistic
RCS	Retrospective cohort study
RCT	Randomized controlled study
RE	Random-effect model meta-analysis
RevMan	Review Manager software version 5.3. (*Nordic Cochrane Centre, Copenhagen, Denmark*)
RoB 2	Revised Cochrane Risk of Bias 2 tool for randomized controlled trials
ROBINS-I	Risk of Bias in Non-Randomized Studies - of Interventions tool for non-randomized controlled studies
SBS	Simple interrupted suture technique
SBS-CON-HF	Handsewn sufficient small intestinal end-to-end anastomoses using interrupted suture technique, tested in the high-flow model
SBS-CON-LF	Handsewn sufficient small intestinal end-to-end anastomoses using interrupted suture technique, tested in the low-flow model
SC	Sample chamber

I Abbreviations

SD	Standard deviation
SE	Standard error
SEM	Standard error of the mean
S. N. J.	Saskia Nicole Janett (doctoral candidate and medical student)
SND	Standard normal deviate
S. R.	Stefan Reischl (radiology resident)
SYRCLE	Systematic Review Centre for Laboratory Animal Experimentation Tool for Animal Studies
TSD	Test for subgroup difference
USB-C	Universal Serial Bus Type-C
z-value	z-statistics (measure of the asymmetry in the funnel plot)

2. List of abbreviations for the figures

"o"	Bursting points
"x"	Leakage points
°	Degree
$°C$	Degrees Celsius
Chi^2 or χ^2	Chi-squared test (heterogeneity)
CO_2	Carbon dioxide
©	Copyright
$>$	Greater than
$<$	Less than
$=$	Equals
↑	Significantly higher
↓	Significantly lower
*	$p < 0.05$
**	$p < 0.01$
***	$p < 0.001$
%	Percentage or frequency
AL	Anastomotic leakage
AF	Anatomical forceps
BC-PBS	Blue-colored phosphate-buffered saline solution
BP	Bursting pressure
C	Camera
CF	Custom-made aluminum square-shaped frame
CI	Confidence interval
CM	Custom-made 3D-printed stabilization brackets
cm	Centimeter
CS	Simple continuous suture technique
CS-CON-HF	Handsewn sufficient small intestinal end-to-end anastomoses using simple continuous suture technique, tested in the high-flow model
CS-CON-LF	Handsewn sufficient small intestinal end-to-end anastomoses using simple continuous suture technique, tested in the low-flow model
CW	Custom-made plastic walls with cutouts
df	Degree of freedom
EEA	End-to-end anastomosis
FFS	Fluid-filled syringe
FI	Fluid influx
I^2	I-squared (measure of heterogeneity)
IA	Intestinal anastomosis
IIP	Increase of intraluminal pressure
IS	Iris scissors
IV	Inverse variance
LED	Light-emitting diode
LLP	Laboratory lifting platform
LP	Leakage pressure
MD	Measuring device
M-H	Mantel-Haenszel method
mm	Millimeter
$mmHg$	Millimeters of mercury
$msec$	Milliseconds

I Abbreviations

n	Number
N/A	Not available
NH	Needle holder
NI-myRIO	NI-myRIO controller
ns	Non-significant
P	Pressure
p	Probability value
PBS	Phosphate-buffered saline solution
PDS	Polydioxanone
PMP	Pressure measurement probe
R	Ruler
SBS	Simple interrupted suture technique
SBS-CON-HF	Handsewn sufficient small intestinal end-to-end anastomoses using interrupted suture technique, tested in the high-flow model
SBS-CON-LF	Handsewn sufficient small intestinal end-to-end anastomoses using interrupted suture technique, tested in the low-flow model
SC	Sample chamber
SD	Standard deviation
SW	Stainless steel screw
t	Time
t_1	Start to LP Time
t_2	LP to BP Time
$t_{(1+2)}$	Start to BP Time
T	Tube
Tau^2	Tau-squared (heterogeneity)
TV	Three-way valve
Z	Z-statistics (statistical significance of the overall effect)
Zone M1 or Zone M (M0+M1)	Mesenteric zone
Zone P(P2 – P5)	Peripheral zone
ZT	Zip ties

3. List of abbreviations for the tables

$\pm$	Plus-minus
↔	No difference
↑	Significantly higher
↓	Significantly lower
%	Percentage or frequency
✓	yes
-	no
5-FU	5-Fluorouracil
α-SMA	Histologic staining scores for fibroblastic activity
BP	Bursting pressure
C	Control group
C-BLB	Collagen-based laminar biomaterial
CI	Confidence interval
cm	Centimeter
col-1	Collagen type 1
col-3	Collagen type 3
CS	Simple continuous suture technique
CS-CON-HF	Handsewn sufficient small intestinal end-to-end anastomoses using simple continuous suture technique, tested in the high-flow model
CS-CON-LF	Handsewn sufficient small intestinal end-to-end anastomoses using simple continuous suture technique, tested in the low-flow model
DC	Distal colon
E	Esophagus
E-G	Esophagogastric junction
EEA	End-to-end anastomosis
ES	End-to-side
F	Female
FE	Fix-effects model meta-analysis
FS	Fibrin sealant
GIT	Gastrointestinal tract
I	Intervention group
I^2	I-squared (measure of heterogeneity)
IS	Interrupted suture
LP	Leakage pressure
M	Male
min	Minute
ml	Milliliter
mm	Millimeter
$mmHg$	Millimeters of mercury
MMP	Matrix metalloproteinase
mRNA	Messenger ribonucleic acid
$msec$	Milliseconds
n	Number
N/A	Not available
NR	Non-resorbable suture material
NRS	Non-randomized study
NS	No suture
OS	Observational study
OR	Odds ratio
p	Probability value

I Abbreviations

PC	Proximal colon
PCS	Prospective cohort study
PI	Proximal intestine
POD	Postoperative day
R	Resorbable suture material
RCS	Retrospective cohort study
RCT	Randomized controlled trial
RE	Random-effects model meta-analysis
RT-R	Rubber-tube removal
SBS	Simple interrupted suture technique
SBS-CON-HF	Handsewn sufficient small intestinal end-to-end anastomoses using interrupted suture technique, tested in the high-flow model
SBS-CON-LF	Handsewn sufficient small intestinal end-to-end anastomoses using interrupted suture technique, tested in the low-flow model
SD	Standard deviation
SE	Side-to-end
SEM	Standard error of the mean
SI	Small intestine
U	Unknown
VEGF	Vascular endothelial growth factor
WMD	Weighted mean difference

4. List of abbreviations for the supplementary tables

3D	Three-dimensional
AC	Allocation concealment
ACS	American Chemical Society
ARRIVE	Animal in Research: Reporting In Vivo Experiments guidelines for reporting animal research
B	Blinding
BC	Baseline characteristics
C. I.	Color index
cm	Centimeter
g	Gram
ID	Inner diameter
IOD	Incomplete outcome data
H	High risk of bias
L	Low risk of bias
LED	Light-emitting diode
M	Moderate risk
M5	Metric thread size designation (5 mm diameter)
MF	Manufacturer number
ml	Milliliter
mm	Millimeter
N	No
n	Number
NI-myRIO	NI-myRIO controller
NOS	Newcastle-Ottawa Scale for cohort studies
NRS	Non-randomized controlled study
OBS	Other sources of bias
PC	Polycarbonate
PDS	Polydioxanone
PE	Polyethylene
PN	Product number
PTFE	Polytetrafluoroethylene
PVC	Polyvinyl chloride
RH	Random housing
ROA	Random outcome assessment
RoB 2	Revised Cochrane Risk of Bias 2 tool for randomized controlled trials
ROBINS-I	Risk of Bias in Non-Randomized Studies - of Interventions tool for non-randomized controlled studies
RCT	Randomized controlled trial
SC	Some concerns
SG	Sequence generation
SOR	Selective outcome reporting
U	Unclear risk of bias
USB-C	Universal Serial Bus Type – C
USP	United States Pharmacopeia
UV	Ultraviolet
WD	Wall thickness
wt	Weight
Y	Yes

II Introduction

The content presented in **Chapter II** has been adapted and modified from the publication authored by Cira et al., 2022 [1], and Cira et al., 2024 [2].

1. Brief introduction and aim of the study

Gastrointestinal surgery is commonly performed in general surgery and is a treatment for diseases affecting the gastrointestinal tract and associated organs, which include the esophagus, stomach, small intestine, large intestine, rectum, pancreas, liver and gallbladder. Gastrointestinal disorders, including inflammatory, cancerous, non-cancerous, traumatic or ischemic disease, may present an indication for gastrointestinal surgery. When a segment of the gastrointestinal tract is resected due to one of the mentioned pathologic conditions, the gastrointestinal continuity needs to be restored. Therefore, the two formerly distant portions of the intestine can be reconnected to each other by performing an intestinal anastomosis. [3]

Intestinal anastomoses belong to one of the most frequently performed surgical procedures. In 1826, Antoine Lembert (1802-1851) introduced his development of an improved intestinal suture technique underlining the importance of serosal apposition using inverted sutures. Several years later, Nicholas Senn (1844-1908, Chicago) reviewed approximately 60 different intestinal suture techniques which’s history he classified from an anatomico-practical standpoint into three epochs, namely ancient, modern and recent. Senn considered the recent epoch to have commenced with the introduction of aseptic suturing by Lord Joseph Lister (1827-1912) in 1867. [4-7] This concept transformed intestinal anastomosis from a potentially life-threatening procedure into a safe and routine surgical practice. [5]

Alongside various described suture techniques, the Murphy button (New York Medical Record, December 10, 1982) revolutionized the field of intestinal anastomosis as the first popular sutureless technique, acting as a stapling prototype. [8] Despite limited clinical success

due to anastomotic necrosis and a narrow intestinal lumen, the Murphy button served as a precursor for the subsequent development of modern stapling devices. [9-14]

Currently, the choice of intestinal anastomotic technique primarily relies on the surgeon's preference, although there are recommended approaches based on specific surgical indications.

However, anastomotic leakage (AL) poses a significant postoperative complication when wound healing is inadequate. This complication can lead to the escape of contaminated intestinal contents into the abdominal cavity, resulting in severe infection and life-threatening sepsis. [15, 16] AL remains a substantial challenge in visceral surgery [17-29], with varying rates depending on the location of the intestinal anastomosis. Upper gastrointestinal anastomoses, such as those involving the esophagus or esophagogastric junction, exhibit AL rates of up to 19.5 % [22, 28], while lower gastrointestinal anastomoses, particularly colorectal procedures, present AL rates of up to 25.6 % [19, 21, 23].

Notably, despite continuous improvements in surgical techniques and perioperative treatment regimens, AL is associated with considerable mortality rates ranging from 4.3 % to 43.8 %. [22, 30-32] Moreover, it can contribute to both local [33] and distant tumor recurrences [34] in patients with malignant diseases. In this context it is not surprising that AL is associated both with great personal suffering for affected patients, as well as with considerable socio-economic burdens for the healthcare systems. For patients undergoing intestinal surgery for colorectal cancer, AL increases the total clinical and economic burden by 0.6–1.9 times. [35] Therefore, preventing AL is a challenging task in the field of surgery, particularly given its multifactorial etiology and the complex pathophysiological processes involved, which are subject to ongoing research. [36, 37]

To mitigate the risk of postoperative AL, various adhesive biomaterials have been experimentally investigated for coating intestinal anastomoses over the course of several decades. [38, 39] Surgical glues, including cyanoacrylate preparations initially employed in

military settings for skin wounds, have been subsequently applied to enhance the mechanical strength of intestinal anastomoses. After application, the surgical glue rapidly forms a stable but flexible connection with the intestinal tissue, which was considered advantageous. [40, 41]. Additionally, synthetic and genuine adhesive biomaterials, such as sterile polyethylene plastic sheets [42], fibrin adhesives [38, 39], and collagen fleeces [38], have been explored to provide supplementary support to anastomoses. While fibrin adhesives have primarily been employed for hemostatic purposes in gastrointestinal surgery and minimally-invasive procedures, their use has also been studied in anastomotic healing. [43] Fibrin sealants (FS) and collagen-based laminar biomaterials (C-BLB) are one of the most promising adhesives, as they have been acknowledged across various surgical specialties and were approved in their liquid form by the United States Food and Drug Administration (FDA) in 1998. [44]

A significant body of research, involving numerous animal models, has produced promising findings regarding the positive effects of coating intestinal anastomoses with biomaterials. These interventions have shown to reduce postoperative AL and mortality rates. [45-57] However, the assessment of the impact of these sealants on postoperative anastomotic healing remains limited, with only a few interventional [58-65] and observational [66-71] studies in humans.

Despite the extensive investigation of adhesive biomaterials in animal models, a comprehensive systematic review and meta-analysis of the outcomes have not yet been conducted. Consequently, the overall effect of coating intestinal anastomoses with C-BLBs on reducing AL remains uncertain. Furthermore, no meta-analysis has examined the impact of coating intestinal anastomoses with C-BLBs or FSs on postoperative AL rates and associated sequelae in humans.

The primary objective of this thesis was to systematically assess the effects of coating various types of intestinal anastomoses with collagen- or fibrin-based adhesive biomaterials, irrespective of location and underlying disease, on postoperative AL, its accompanying

complications, and mortality for human and animal studies. Therefore, systematic reviews and meta-analyses were conducted, calculating pooled odds ratio (OR) with 95 % confidence intervals (CI) and performing subgroup analyses for prespecified risk factors were performed.

To evaluate the effect of coating intestinal anastomoses with adhesive biomaterials and, consequently, anastomotic stability and pressure resistance, various *ex-vivo* models have been developed. [45, 46, 48-50, 52, 53, 56] However, these models often reveal a lack of comparability and reproducibility of scientific data. Biomechanical studies play a crucial role in comprehending AL by unravelling the mechanical behavior and integrity of the anastomotic site. Quantitative measurements, including bursting pressure (BP), tensile strength, suture holding capacity, and other mechanical parameters of anastomotic tissues, offer valuable insights for identifying potential risk factors, developing preventive strategies, and guide surgical decision-making. [72-75] These measurements help in determining the optimal suture technique, suture material, or reinforcement methods to enhance the strength and integrity of the anastomosis. [76-79]

Therefore, the secondary objective of this thesis was to develop an innovative *ex-vivo* model for quantitative and precise determination of gastrointestinal-anastomotic quality in terms of stability and pressure resistance with high comparability, reproducibility, and user-independence. The *ex-vivo* test-setup aimed to increase the understanding of the biomechanics of intestinal anastomoses and therefore AL, without the need for animal testing.

2. Background and current state of research

2.1 Intestinal anastomotic techniques and wound healing

It has been stated that the key to a successful anastomosis is the accurate union of two viable bowel ends with complete avoidance of tension. Furthermore, an adequate blood supply plays a critical role in the creation of a bowel anastomosis. [3] The principles of wound healing have often been investigated using cutaneous models due to their ease of generation and real time visualization. [80] Based on these principles, healing of intestinal anastomoses has been studied in different experimental models, drawing a conclusive overview of healing physiology which can be divided into three phases: the inflammatory phase, the proliferative phase and the remodeling phase.

The inflammatory phase represents the initial stage of intestinal wound healing, typically occurring within the first four days following intestinal anastomosis. During this phase, processes such as hemostasis, provisional wound closure, and wound debridement take place. [80, 81] The balanced and controlled secretion of pro- and anti-inflammatory factors plays a key role during inflammation. An imbalance of these factors might disturb adequate wound healing, predisposing to impaired wound healing. [80-82]

After the inflammatory phase, the intestinal wound healing progresses into the proliferative phase, characterized by processes such as angiogenesis, re-epithelization, collagen synthesis and production of extracellular matrix. The primary goal of this phase is to cover and protect the intestinal wound while restoring the different layers of the intestine. [81, 82]

The stability and resistance of the intestinal anastomosis depend mainly on the collagen formation induced by myofibroblasts migrating and proliferating into the healing tissue. In subsequent stages of anastomotic healing, the stable layer of collagen undergoes turnover and remodeling of the collagen types and fibers to restore the full mechanical stability, by forming a stable, functional scar. [80-82]

The remodeling phase represents the last and the longest stage of wound healing, extending over several weeks after the proliferative phase. The objective of this phase is the maturation of the wound and the remodeling of collagen and vasculature, aiming to increase strength and restore the intestinal integrity of the newly formed tissue. [80-83] Collagen rearrangement primarily occurs through the breakdown of type 3 collagen and its replacement with type 1 collagen, mediated by matrix metalloproteases. [82, 84] Therefore, balanced regulation of these enzymes plays a key role in collagen remodeling, as increased activity can impair wound healing by accelerating collagen breakdown. In addition to collagen remodeling, the initially disorganized vasculature network undergoes remodeling to form an organized network. [80-83]

Despite the intrinsic healing mechanisms, several risk factors can compromise intestinal anastomotic healing. Factors such as infection, certain microbial influences, malnutrition, advanced age, and certain comorbidities (exempli gratia (e.g.), diabetes, smoking) have been identified as risk factors for impaired healing. These factors can disrupt the delicate balance of the healing process, leading to complications such as AL, fistula formation, and delayed wound healing. [85-87]

Intestinal anastomotic healing is influenced not only by patient-related factors but also by various surgical factors, including blood supply, tension at the suture site and anastomotic technique applied. [85, 86] Surgeons play a crucial role in ensuring the successful healing of intestinal anastomoses by considering and implementing appropriate surgical techniques and practices.

Several technical aspects have been identified that affect anastomotic healing, either positively or negatively. In general, intestinal anastomotic techniques can be classified based on their configuration to [88]:

a. end-to-end anastomosis (EEA) (**Figure 1**)
b. side-to-side anastomosis (**Figure 2**)

   a. isoperistaltic side-to-side anastomosis (**Figure 2**)
   b. anisoperistaltic side-to-side anastomosis (**Figure 2**)

c. side-to-end anastomosis

d. end-to-side anastomosis

e. special forms (e.g., Kono-S-Anastomosis [89])

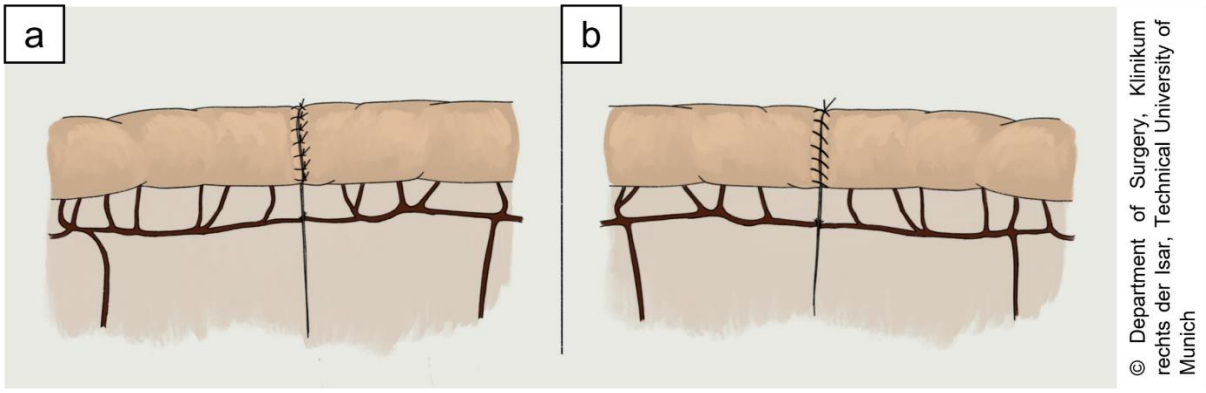

Figure 1. Handsewn end-to-end anastomosis. (a) Simple interrupted suture technique (SBS). (b) Simple continuous suture technique (CS). © Department of Surgery, Klinikum rechts der Isar, Technical University of Munich. *(Cira et al., Gastro-News 2023)* [88]

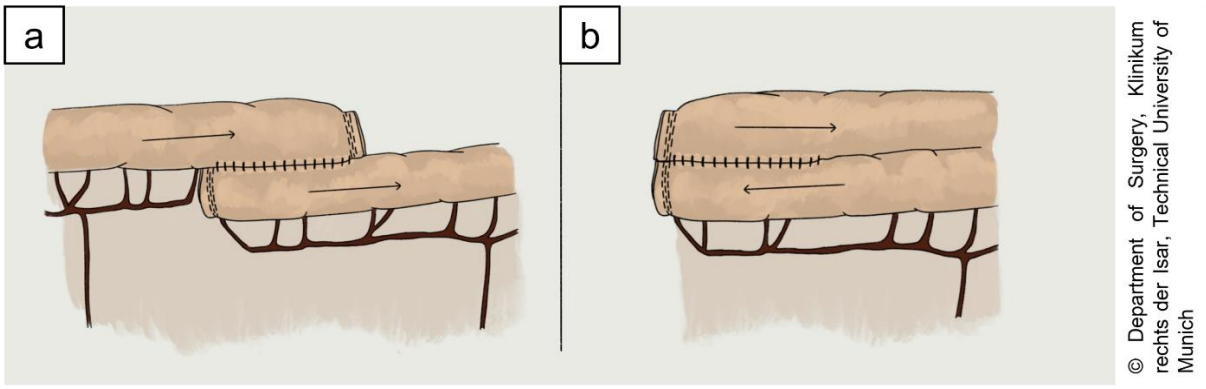

Figure 2. Stapled side-to-side anastomosis. (a) Isoperistaltic configuration. (b) anisoperistaltic configuration. © Department of Surgery, Klinikum rechts der Isar, Technical University of Munich. *(Cira et al., Gastro-News 2023)* [88]

The most frequently performed intestinal anastomoses are the EEA (**Figure 1**) and the side-to-side anastomosis (**Figure 2**), which can be further subclassified into an iso- (**Figure 2. a**) and anisoperistaltic (**Figure 2. b**) anastomosis. The classical intestinal anastomosis is performed via a handsewn technique and can be differentiated mainly based on applied suture

techniques. Commonly employed suture techniques include the continuous (**Figure 1. b**) and interrupted (**Figure 1. a**) suture techniques (CS and SBS).

2.2 Biomechanics

The behavior of a solid body subjected to various types of loading can be studied in the subject of material science, specifically mechanics of a material. The motion of matter and the forces that cause such motion are studied in mechanics and can be applied to the analysis of any existing dynamical system. A classical subject of physics and engineering is the analysis of stress, deformation, and stability of thin-walled tubes. [75]

2.2.1 Gastrointestinal biomechanics

Biomechanical studies are of paramount importance in the understanding of AL as they elucidate the mechanical behavior and integrity of the anastomotic site. Determining the stresses and strains in biological structures when forces are acting on them represent the principle objective of biomechanics. The biomechanical behavior of biological structures, including gastrointestinal tissue and thereby gastrointestinal anastomoses, can be obtained by determining the quantities from close to the unloaded state up to loads causing failure. [72-75]

Gastrointestinal tissue exhibits viscoelastic characteristics, enabling it to store and release energy when subjected to stress and strain. [72-75] Therefore, the deformation of gastrointestinal tissue is finite, and due to its heterogeneous laminated structure, the viscoelastic component and anisotropy prevail. Furthermore, the stress-strain relationship of this tissue is non-linear and time-dependent, meaning that the stress-strain response does not occur instantly. [73-75, 90]

According to studies of Dobrin et al. [72] and Roach et al. [91], the non-linear elastic behavior observed in arterial tissues can be attributed to the unique properties of collagen. Collagen exhibits the ability to withstand circumferential wall forces at higher stress levels, providing protection against overdistention and damage at elevated intraluminal pressure. This

property ensures that the tissue can easily distend within the physiological range and facilitates fluid flow. It is worth noting that excessive distention can lead to plastic deformation, where the biological tissue is unable to return to its original unstressed state. [72-75, 90, 91] These findings from Dobrin et al.'s [72] and Roach et al.'s [91] studies can be extrapolated to gastrointestinal tissue, given its collagen-rich nature, making collagen a key determinant of the non-linear stress-strain relationship and shaping the characteristic curves. [75, 90]

Other important forces to consider while studying the biomechanics of gastrointestinal tissue are the external forces from the environment the gastrointestinal tract is part of and the forces the gastrointestinal tract generates by itself. External forces can be applied from the out- or the inside of the gastrointestinal lumen, causing deformation and influencing the forces. Therefore, distensibility and stiffness are commonly used to describe deformation and resistance to it. [75]

2.2.2 Tensile tests and bursting pressure measurement

Tensile tests and BP measurements are two widely used methods for evaluating the mechanical properties of biological tissues, including intestinal tissue. These methods offer several advantages for assessing the stability and pressure resistance of intestinal anastomoses and are commonly employed in research investigating AL [45, 46, 48-50, 52, 53, 56]. Both tensile tests and BP measurements provide advantages over other methods commonly used to evaluate the mechanical properties of biological tissues. They are quantitative and allow for direct measurement of tissue strength and pressure resistance. Additionally, they are relatively easy to perform and offer high reproducibility and accuracy. [72-75] The concept of evaluating bursting strength in experimental anastomoses was initially described by Chlumsky et al. in 1899 [92], and since then, it has undergone modifications in numerous experimental studies.

The bursting strength of a material, such as biological tissue, can be quantified by two parameters: BP, representing the maximum intraluminal pressure, and bursting wall tension, corresponding to the maximal wall tension observed at the point of disruption. These parameters are determined in accordance with Laplace's law. [72-75] BP measurements involve placing a tissue sample within a pressure chamber and gradually increasing the pressure until the tissue ruptures. This method provides information on the maximum pressure that the tissue can withstand before failure, a critical parameter in evaluating the pressure resistance of intestinal anastomoses. BP measurements are particularly useful in evaluating the integrity of anastomoses and can help identify potential sites of leakage. [45, 46, 48-50, 52, 53, 56]

In-vitro, the tensile test is commonly used to measure the uniaxial force required to break a wound. [93] However, the bursting strength method, recognized for its enhanced capacity to accurately reflect physiological strain, involves a multiaxial assessment that identifies the weakest site of the anastomosis, where leakage is more prone to occur. [94, 95] A study conducted by Christensen et al. [96] integrated the detection of intracolonic physiological pressure with radiologic measurements, demonstrating the synchrony between maximum pressure and anastomotic disruption.

Several studies in the literature have explored the use of adhesive biomaterials for anastomotic coverage. However, the majority of these studies have employed non-standardized testing setups, making it challenging to draw meaningful conclusions or make effective comparisons. For instance, studies that utilized ad hoc setups or non-uniform pressure application methods have reported varying results, making it challenging to assess the true effectiveness of bioadhesives in promoting anastomotic stability. [45, 46, 48-50, 52, 53, 56]

An *ex-vivo* model, similar to the one depicted in **Figure 3**, has been commonly employed in various studies [45, 47-50, 52-54, 56, 57] for measuring BP of anastomosed intestinal

segments. In this model, the anastomosed intestinal segment is connected to a fluid-filled syringe, with a pressure measurement probe attached at the other end. The syringe and the sensor are tightly secured to the intestinal segment to prevent fluid leakage from the anastomosis. The measurement process entails manually injecting fluid into the anastomotic lumen while the pressure measurement probe records the intraluminal pressure, displayed as a curve on a monitoring device. Visual inspection, aided by a camera positioned above the setup, allows for detection of any leakage or bursting of the anastomosis, resulting in fluid escaping with a simultaneously occurring drop in pressure observed on the device graph.

Despite its widespread usage, the *ex-vivo* BP measurement setup has encountered significant challenges related to user-dependence and irreproducibility. Inconsistencies arise from variations in the injection speed of the fluid during experiments, external disturbances impacting the pressure sensor, and inadequate visualization of the entire anastomosis due to the setup's limitations. Additionally, the positioning of the anastomosis may impede the detection of initial leaks, potentially compressing them under the weight of the anastomosis.

The absence of a physiologically simulated environment and the potential temperature discrepancies of the injected fluid further limit the applicability of this model. Moreover, the orientation of the anastomosis in a lying position introduces pressure disparities, with higher pressure observed at the inferior part compared to the superior part of the anastomosis. These factors collectively contribute to the limitations of the *ex-vivo* model for measuring BP in anastomotic evaluations.

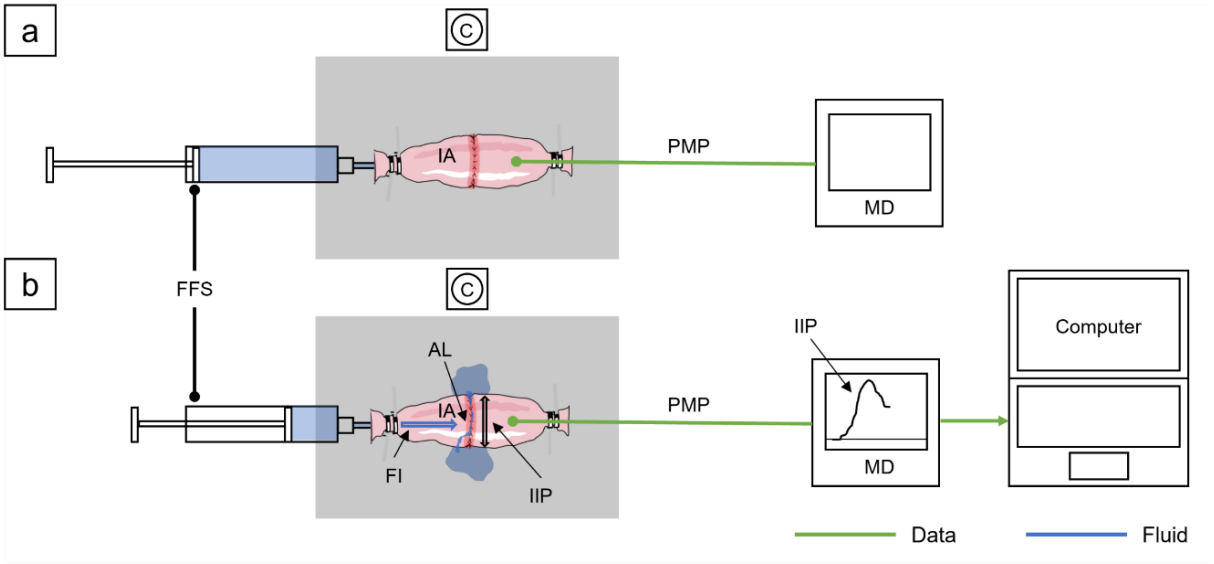

Figure 3. Commonly utilized *ex-vivo* model for bursting pressure measurement in gastrointestinal anastomoses. (a) The anastomosed intestinal segment is connected to a fluid-filled syringe (FFS), with a pressure measurement probe (PMP) attached at the other end, and both the syringe and the sensor are firmly secured to prevent fluid leakage from the anastomosis (IA). The PMP is connected to a measuring device (MD). (b) During the measurement process, fluid is manually injected into the anastomotic lumen while the PMP records the intraluminal pressure, displayed as a curve on a MD. Visual inspection facilitated by a camera (C) positioned above the setup enables the detection of leakage or bursting of the anastomosis. Such events are characterized by fluid escaping and a concurrent drop in pressure observed on the device graph. *AL = Anastomotic leakage; FI = Fluid influx; IA = Intestinal anastomosis; IIP = Increase of intraluminal pressure.*

2.2.3 Examination of bursting pressure

Depending on the surrounding atmospheric pressure and temperature [97]:

a. water has a density of 992 – 1000 kg/m^3, and air has a density of 0.120 – 12 kg/m^3

b. water has a viscosity of 0.656 – 1.792 cP (centipoise), and air has a viscosity of 0.0158 – 0.198 cP

c. water has a surface tension with air of 69.6 – 75.6 dyn/cm (dyne per centimetre) [97]

In summary, water has a higher density, viscosity and surface tension than air, influencing its behavior in leakage. The greater viscosity and surface tension of water prevents its leakage through, for example, a small hole in the intestinal anastomosis, while these forces do not prevent air from leaking through the same hole in the anastomosis. These physical properties are important to consider when evaluating for anastomotic BP since air tends to leak earlier

than fluid. Thus, a test setup should be capable of performing a hydrostatic fluid leak test and a pneumatic air leak test to evaluate the resistance of the suture line against increasing intraluminal pressures.

2.2.3.1 Perfusion Bioreactor

The perfusion bioreactor (**Figure 4**), originally developed by Micheler et al. [98-100], is an integrated system comprising two technologies: information technology and fluid power technology. The system consists of several key components, including a controller, a human-machine interface (HMI), sensors, actuators, a fluid system, and a sample chamber (SC). Notably, the controller operates autonomously without the need for an external computer, functioning as a WLAN-enabled embedded system. The prototype of the perfusion bioreactor was further optimized by Berndt et al. [101] and Hangleiter et al. [102].

The information technology system encompasses components such as the HMI, the NI-myRIO controller (*National Instruments, USA*), and the carbon dioxide (CO_2) controller. Within this system, the user's instructions, including test parameters, are received by the NI-myRIO controller through the HMI. Micheler et al. [98-100] utilized a touch display (*ITEAD Studio, China; Type: NX8048K070-011C*) to input information and display results. The controller is capable of measuring and calculating various test parameters, as well as generating signals that are subsequently displayed on the touch display. Both the controller and the display are synchronized to ensure coordinated functioning. Moreover, the controller regulates the perfusion of the bioreactor by receiving continuous feedback signals from the pressure sensor.

To maintain a consistent CO_2 value in Micheler's experiments [98-100], a CO_2 controller was incorporated to ensure constant maintenance of the desired CO_2 level. [98-102] (**Figure 4**)

The fluid power technology consists of several components, including a pressure sensor, a temperature sensor, a peristaltic pump, a SC, and a medium reservoir. Micheler et al. [98-

100] developed a closed fluid circulation system for conducting experiments. The peristaltic pump is utilized to transport the medium from the reservoir to the SC and back. To measure the hydrostatic pressure generated by the peristaltic pump, a pressure sensor (*AMSYS, Germany; Type: AMS 5812-0150-D*) with a built-in sensor chamber and adapter (*Arthrex, USA*) is installed downstream of the pump. Additionally, a separate temperature sensor is installed to monitor the temperature of the medium, SC, and fluid within the peristaltic pump. [98-102] (**Figure 4**)

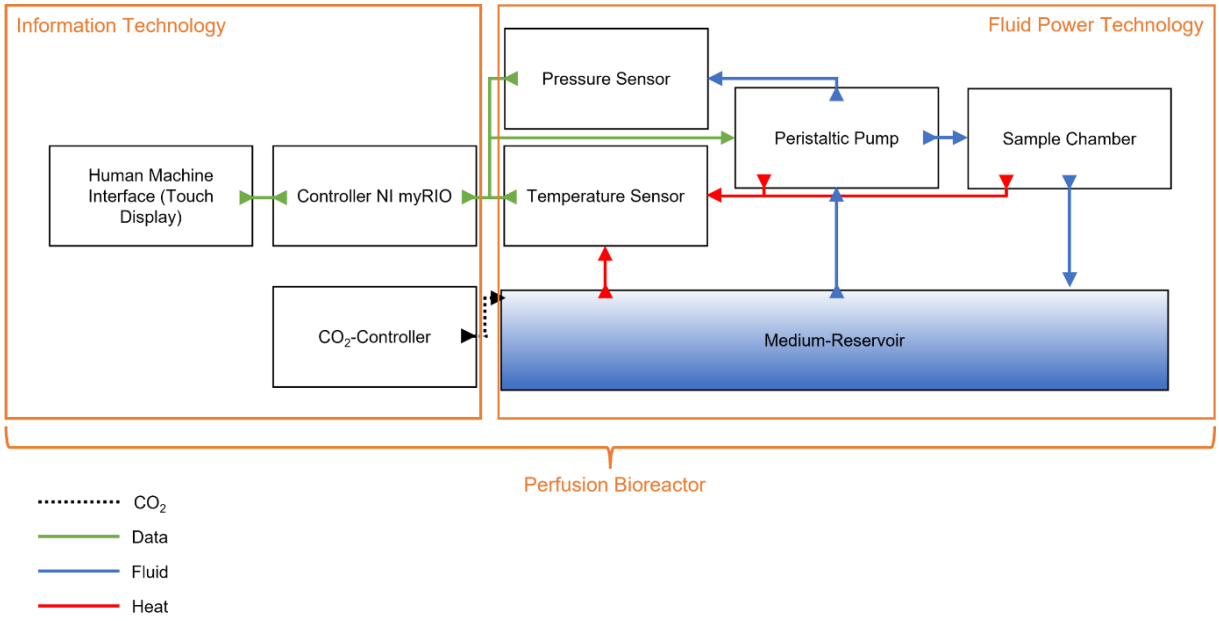

Figure 4. Perfusion bioreactor. Process description of the perfusion bioreactor, encompassing both information technology and fluid power technology. *(Modified from Micheler 2018a and Micheler et al., Curr. Dir. Biomed. Eng 2021*) [98-100]

For the programming of the bioreactor's measurement and control technology, the Laboratory Virtual Instrumentation Engineering Workbench (LabVIEW) software (*LabVIEW 2021 SP1 f2; National Instruments, USA*) [103] was utilized. LabVIEW serves as a development environment, system-design platform, and graphical coding language. User interfaces are seamlessly integrated into the development cycle using LabVIEW, allowing the software to be structured on different levels based on a program flowchart.

Virtual instruments (VIs) are functional blocks that encompass and execute calculations. Each VI can function as a SubVI (subroutine) within another VI or independently as a

standalone VI. A VI consists of a block diagram, a front panel (user interface), and a connector pane. The connector pane facilitates the connection of VIs, enabling the definition of data flow as each VI can have inputs and outputs. Controls serve as user inputs to supply information to the VI, while indicators display results based on the inputs received by the VI. Together, controls and indicators are used to construct the front panel of the user interface. [103]

Field-Programmable Gate Arrays are programmable silicon chips that can be configured using pre-built logic blocks, forming the foundation of VIs. The pre-built logic blocks are programmed using a configuration file. Unlike software, the performance of Field-Programmable Gate Arrays remains unaffected by the number of central processing unit cores, as they operate independently. [103] In Micheler et al.'s study [98-100], the software for the touch display and the controller was programmed on a computer, and the final file was transferred to a terminal device (e.g., a computer), effectively decoupling the software from the computer. [98-100] Users can control the previously developed software through the touch display using graphical input. Event-based data packets are exchanged between the touch display and the controller using a serial interface known as "universal asynchronous receiver-transmitter". [98-102]

Micheler et al. [99] utilized the Nextion Software (*Nextion Editor*) to insert pre-built elements into the development environment through a "drag-and-drop" mechanism, enabling individual adjustments. The user interface can be subdivided into different areas, such as navigation, current status, or processes. This interface allows users to initiate test sequences, perform operations such as aborting tests, and input specific test parameters or comments. [98-102]

III Materials and methods

The content presented in **Chapter III.1** has been adapted and modified from the publication authored by Cira et al., 2022 [1]. The content presented in **Chapter III.3** has been adapted and modified from the publication authored by Cira et al., 2024. [2]

1. Systematic review and meta-analysis of human studies

1.1 Literature search

1.1.1 Inclusion criteria

For this systematic review and meta-analysis studies evaluating the effect of coating intestinal anastomoses with adhesive biomaterials were included based on the following criteria:

1. human trials
2. study designs:
    a. randomized controlled trials (RCTs)
    b. non-randomized controlled studies (NRSs)
    c. observational studies (prospective or retrospective):
        i. comparative cohort studies
        ii. comparative case-control studies
        iii. nested case-control studies
        iv. cross-sectional studies
3. publication status and publication language:
    a. abstracts or full-text articles published in the electronic medical databases from January 1, 1964, to January 17, 2022
    b. articles, published in the following languages: English, German or Spanish
4. baseline characteristic of examined patients:

a. any age group (pediatric; young adults, middle-aged adults; elderly adults)
b. any sex or gender
c. any underlying condition

5. surgical characteristics of examined patients: any abdominal surgical procedure with the formation of an intestinal anastomosis
    a. any surgical approach (conventional (open) approach; laparoscopic approach; hand-assisted or laparoscopic assisted approaches)
    b. any timing of surgery (elective surgery, urgent, or emergent surgery)
    c. intestinal anastomoses of the upper and lower gastrointestinal tract (esophagus; stomach; small intestine; large intestine; rectum)
    d. any type and technique of intestinal anastomosis
        i. handsewn or stapled anastomoses
        ii. any type of suture material and suture technique
            - CS; SBS
            - single-layer anastomoses; double-layer anastomoses; inverting or everting anastomoses
            - any technique (EEAs; end-to-side anastomoses; side-to-side anastomoses)
6. characteristics of the intervention group:
    a. criteria mentioned in 1. – 5. and intestinal anastomoses coated or reinforced with a commercially available adhesive biomaterial (C-BLB; FS)
    b. C-BLB or FS
        i. animal derived or synthetic
        ii. regardless of manufacturer
        iii. with or without additional substances embedded
7. characteristics of the control group:

   a. criteria mentioned in 1. – 5. and intestinal anastomoses not coated or reinforced with any products
8. postoperative outcomes reported:
   a. any postoperative clinical outcome (without restrictions)

1.1.2 Exclusion criteria

Studies were excluded based on the following criteria:

1. any studies other than human trials (e.g., animal studies; *in-vivo* or *ex-vivo* studies*; in-vitro* studies)
2. study design:
   a. reviews and/ or meta-analyses
   b. case-reports or case-series
   c. studies without a control group
3. publication status and publication language:
   a. unpublished articles
   b. languages other than English, German or Spanish
4. surgical characteristics of examined patients:
   a. any abdominal surgical procedure without the formation of an intestinal anastomosis
   b. any anastomoses other than intestinal anastomoses (e.g., hepatobiliary anastomoses; biliodigestive anastomoses; pancreaticointestinal anastomoses)
   c. any procedure other than intestinal anastomoses (e.g., surgical closure of intestinal defects both transmural and non-transmural; creation of intestinal stumps or pouches)
   d. coating or reinforcing intestinal anastomoses with a commercially available adhesive biomaterial in the setting of an operative revision (e.g., secondary to postoperative complication such as AL or fistula formation)

e. intestinal anastomoses coated or reinforced with an adhesive biomaterial not commercially available or not based on collagen and/ or fibrin

1.2 Search strategy

Using predefined search items, a comprehensive systematic literature search was conducted to identify studies published in the electronic medical databases PubMed (MEDLINE), Web of Science, Scopus, and Cochrane Library. The exact search strategy is depicted in **Supplementary Table 1.** To ensure the identification of all potentially relevant studies, reference lists of reviews and included studies were manually examined, and additional web searches were conducted. In the event of inadequate or insufficient data presentation, corresponding authors of the studies were contacted to provide the required information. The final search was conducted on January 17, 2022.

1.3 Study selection and documentation

In terms of quality assurance, all studies were assessed manually and independently by two investigators (surgical residents: Kamacay Cira (K. C.) and Felix Stocker (F. S.)). Studies identified during the search process were exported to the reference management tool EndNote X9 (*EndNote X9; The EndNote Team, Clarivate 2013; Philadelphia, PA*). Before screening of identified studies, duplicate records were removed by computer-based tools (EndNote X9), followed by a secondary manual exclusion.

In accordance with the predefined eligibility criteria, titles and abstracts of identified studies were manually assessed and studies not coinciding with these criteria were excluded. The remaining abstracts and full-text articles were retrieved and more precisely assessed for eligibility.

Any discrepancies and disagreements concerning eligibility were discussed and resolved in consensus with a third investigator (surgical specialist: Philipp-Alexander Neumann (P-A.

N.)). The accuracy of the search results and selection process was assessed independently by the third investigator (P-A. N.).

1.4 Data collection and extraction

The data of the included studies were extracted, collected, and analyzed manually and independently by two investigators (K. C.; F. S.) onto a Microsoft Excel spreadsheet (*Home and Student 2019 edition; Microsoft, Redmond, WA*). If the included studies reported outcomes for two or more discrete data sets, they were included separately in the analyses. The accuracy of the extracted data was independently assessed by a third investigator (radiology resident: Stefan Reischl (S. R.)). Arising discrepancies or disagreements during this process were discussed and resolved in consensus with a fourth investigator (P-A. N.).

If available, the following data were collected for each study:

1. general information and study design:
    a. author and year of publication; country of publication
    b. study design and inclusion period
    c. study and ethical approval; funding
    d. blinding of study participants; matching of examined patient groups
    e. studies' individual inclusion and exclusion criteria
2. baseline characteristics:
    a. number of patients in the intervention and control group
    b. mean (standard deviation (SD)) or median (range) age of patients in the intervention and control group
    c. sex of patients in the intervention and control group
    d. Body Mass Index (BMI) (kg/m^2) of patients in the intervention and control group
    e. underlying disease of patients in the intervention and control group
3. surgical characteristics:
    a. indication for surgery for patients in the intervention and control group
    b. surgical intervention performed for patients in the intervention and control group

   c. procedure technique applied in general and for patients in the intervention and control group
   d. type, number and location of intestinal anastomoses
   e. number of surgeons
   f. any type of additional intervention for patients in the intervention and control group
   g. type of adhesive biomaterial used to coat or reinforce intestinal anastomoses of patients in the intervention group
4. any postoperative outcomes for patients in the intervention and control group

1.5 Risk of bias assessment

The risk of bias of included studies were systematically assessed by two investigators independently (K. C.; F. S.) and in accordance with the Cochrane Handbook for Reviews of Interventions. [104-106] Any emerging disagreements or discrepancies in the assessment of risk of bias were discussed and resolved with a third investigator (S. R.). The following tools were used:

1. Revised Cochrane Risk of Bias 2 (RoB 2) tool for RCTs[107]
2. Risk Of Bias In NRS - of Interventions (ROBINS-I) tool [108] for NRSs
3. Newcastle-Ottawa Scale (NOS) for cohort studies [109]

The revised RoB 2 tool [107] consists of five domains evaluating the risks of bias:

1. prior the intervention, bias due to randomization process
2. after the intervention, bias due to:
   a. deviation from intended interventions
   b. missing outcome data
   c. measurement of outcomes
   d. selection of reported results

Within each domain, RCTs can be divided into different risk of bias grades based on a set pattern of predefined questions: low risk of bias, some concerns or high risk of bias. The overall risk of bias judgement is based on the results of the individually queried domains and can be categorized likewise into low risk of bias, some concerns and high risk of bias. [107]

For NRSs, the ROBINS-I tool [108] can be applied to assess the studies risk of bias. This tool consists of seven domains with a set pattern of predefined questions:

1. two domains prior the intervention, bias due to:
    a. confounding
    b. selection of participants into the study
2. one domain at the intervention, bias due to classification of interventions
3. four domains after the intervention, bias due to:
    a. deviations form intended interventions
    b. missing data
    c. measurement of outcomes
    d. selection of reported results

Within each domain, NRSs can be divided into five categories: low risk of bias, moderate risk of bias, serious risk of bias, critical risk of bias, or no information. [108]

As described in the revised RoB 2 tool [107], the overall risk of bias judgement is based on the results of the seven different domains and can be categorized likewise into low risk of bias, moderate risk of bias, serious risk of bias, or critical risk of bias. [108]

The NOS score [109] is an established and commonly used tool to assess the quality of observational studies. The tool uses a "star system" by which the quality of a cohort study is judged on three different categories:

1. selection of the study groups (maximum four stars):
    a. representativeness of the exposed cohort

   b. selection of the non-exposed cohort
   c. ascertainment of exposure
   d. demonstration that outcome of interest was not present at the start of the study
2. comparability of the study groups (maximum two stars):
   a. comparability of cohorts based on the design and analysis – controlled for critical factor(s)
   b. comparability of cohorts based on the design and analysis – controlled for additional factor(s)
3. outcome of interest of the study groups (maximum 3 stars):
   a. assessment of outcome
   b. follow-up period long enough for outcomes to occur
   c. adequacy of follow-up of cohorts

The risk of bias for a cohort study increases as the number of stars decreases. For this study, a NOS score of greater than (>) 7 was defined as high quality cohort study, a score of 5-7 as moderate quality cohort study, and a score of less than (<) 5 as low quality cohort study. [109]

2. Systematic review and meta-analysis of animal studies

2.1 Literature search

2.1.1 Inclusion criteria

For this systematic review and meta-analysis studies evaluating the effect of coating intestinal anastomoses with C-BLBs were included based on the following criteria:

1. animal studies
2. study designs: prospectively conducted *in-vivo* animal studies
3. publication status and publication language:
    a. full-text articles published in the electronic medical databases from January 1, 1962, to October 6, 2021
    b. articles, published in all languages in Latin script
4. baseline characteristic of examined animals:
    a. any animal species
    b. any age group
    c. any sex
    d. any underlying condition
5. surgical characteristics of examined animals: any abdominal surgical procedure with the formation of an intestinal anastomosis
    a. any surgical approach (conventional (open) approach; laparoscopic approach; hand-assisted or laparoscopic assisted approaches)
    b. any timing of surgery (elective surgery, urgent or emergent surgery)
    c. intestinal anastomoses of the upper and lower gastrointestinal tract (esophagus; stomach; small intestine; large intestine; rectum)
    d. any type and technique of intestinal anastomoses
        i. handsewn or stapled anastomoses

ii. any type of suture material and suture technique any technique (EEAs; end-to-side anastomoses; side-to-side anastomoses)
    - CS; SBS
    - single-layer anastomoses; double-layer anastomoses; inverting or everting anastomoses

6. characteristics of the intervention group:
    a. criteria mentioned in 1. – 5. and intestinal anastomoses coated or reinforced with a commercially available C-BLB (animal derived or synthetic; regardless of manufacturer; with or without additional substances embedded)
7. characteristics of the control group:
    a. criteria mentioned in 1. – 5. and intestinal anastomoses not coated or reinforced with any products
8. any experimental or clinical outcome depicting anastomotic healing:
    a. any postoperative outcome (without restrictions)

2.1.2 Exclusion criteria

Studies were excluded based on the following criteria:

1. any studies other than animal studies (e.g., human trials; *in-vivo* or *ex-vivo* studies; *in-vitro* studies)
2. study design:
    a. abstracts or conference proceedings
    b. reviews and/ or meta-analyses
    c. case-reports or case-series
    d. studies without a control group
3. publication status and publication language:
    a. unpublished articles
    b. languages using non-Latin script

4. surgical characteristics of examined animals:
    a. any abdominal surgical procedure without the formation of an intestinal anastomosis
    b. any anastomoses other than intestinal anastomoses (e.g., hepatobiliary anastomoses; biliodigestive anastomoses; pancreaticointestinal anastomoses)
    c. any procedure other than intestinal anastomoses (e.g., surgical closure of intestinal defects both transmural and non-transmural; creation of intestinal stumps or pouches)
    d. coating or reinforcing intestinal anastomoses with a commercially available C-BLB in the setting of an operative revision (e.g., secondary to postoperative complication such as AL or fistula formation)
    e. intestinal anastomoses coated or reinforced with a C-BLB not commercially available or not based on collagen (e.g., FS)

2.2 Search strategy

A comprehensive systematic literature search was conducted using predefined search items to identify studies published in the electronic medical databases PubMed (MEDLINE), Cochrane Library, Scopus, and Web of Science. The exact search strategy is depicted in **Supplementary Table 2**. To ensure the identification of all potentially relevant studies, reference lists of reviews and included studies were manual examined, and additional web searches were conducted. In case of inadequate or insufficient data presentation, corresponding authors of the studies were contacted to provide the required information. The final search was conducted on October 6, 2021.

2.3 Study selection and documentation

In terms of quality assurance, all studies were assessed manually and independently by three investigators (K. C.; F. S.; S. R.). Studies identified during the search process were exported

to the reference management tool *EndNote X9*. Before screening of identified studies, duplicate records were removed by computer-based tools (*EndNote X9*), followed by a secondary manual exclusion.

In accordance with the predefined eligibility criteria, titles and abstracts of identified studies were manually assessed, and studies not coinciding with these criteria were excluded. The remaining full-text articles were retrieved and more precisely assessed for eligibility.

Any discrepancies and disagreements concerning eligibility were discussed and resolved in consensus with a fourth investigator (P-A. N.). The accuracy of the search results and selection process was assessed independently by the fourth investigator (P-A. N.).

2.4 Data collection and extraction

The data from the included studies were manually extracted, collected, and analyzed by two investigators (K. C.; F. S.) using a Microsoft Excel spreadsheet. If the included studies provided outcomes for multiple distinct datasets, each dataset was included separately in the analyses. A third investigator (S. R.) independently assessed the accuracy of the extracted data. Any discrepancies or disagreements that arose during this process were discussed and resolved by consensus with a fourth investigator (P-A. N.).

If available, the following data were collected for each study:

1. general information and study design:
    a. author and year of publication; country of publication
    b. study design
    c. study and ethical approval; funding
    d. studies individual inclusion and exclusion criteria
2. baseline characteristics:
    a. animal genus and species
    b. number of animals in the intervention and control group

   c. sex of animals in the intervention and control group
3. surgical characteristics:
   a. surgical intervention performed for animals in the intervention and control group
   b. procedure technique applied in general and for animals in the intervention and control group
   c. type, number and location of intestinal anastomoses
   d. type of suture material utilized to create intestinal anastomoses
   e. type, brand and manufacturer of C-BLB used to coat or reinforce intestinal anastomoses of animals in the intervention group
   f. any type of additional intervention for patients in the intervention and control group
4. any experimental or clinical outcome depicting anastomotic healing (any postoperative outcome (without restrictions)) for animals in the intervention and control group

2.5 Risk of bias assessment

The risk of bias and the quality of reporting of included studies were systematically assessed independently by two investigators (K. C.; F. S.). Any emerging disagreements or discrepancies in the assessment of risk of bias were discussed and resolved with a third investigator (S. R.) and a fourth investigator (P-A. N.). The following tools were used:

1. Systematic Review Centre for Laboratory Animal Experimentation (SYRCLE) tool for animal studies [110]
2. Animal in Research: Reporting *In Vivo* Experiments (ARRIVE) guidelines for reporting animal research [111]

The SYRCLE [110] tool was developed based on the RoB 2 [107] tool. Overall, five items of the RoB 2 [107] were adopted in the SYRCLE [110] tool while the remaining five were adapted for animal studies. The SYRCLE [110] tool consists of 10 entities:

1. selection bias due to:
    a. sequence generation (allocation sequence)
    b. baseline characteristics
    c. allocation concealment
2. performance bias due to:
    a. random housing
    b. blinding
3. detection bias due to:
    a. random outcome assessment
    b. blinding
4. attrition bias due to:
    a. incomplete outcome data
5. reporting bias due to:
    a. selective outcome reporting
6. other
    a. other sources of bias

Each item consist of questions which can be answered with "yes", "no", or "unclear". The judgment, whether the item is judged as either low, high, or unclear risk of bias depends on the given answer, whereby "yes" indicated a low risk of bias, "no" indicates a high risk of bias, and "unclear" indicates that not sufficient data is present for conclusive judgement.

The quality of reporting was evaluated according to the ARRIVE guidelines for reporting animal research [111], consisting of a checklist of 20 items. These items included in the checklist represent the minimum of information that should be reported by all scientific publications of animal research to be of good quality. [111] The 20 items examine:

1. title (accurate and concise description)
2. abstract (includes background, objectives, methods, key findings and conclusions)

3. introduction
    a. background
    b. objective
4. methods
    a. ethical statement
    b. study design (randomization, blinding)
    c. experimental procedures (description of the procedure and explanation why this procedure was chosen)
    d. experimental animals (characteristics such as species, sex or weight)
    e. housing and husbandry
    f. sample size
    g. allocating animals to experimental groups
    h. experimental outcomes
    i. statistical methods
5. results
    a. baseline data
    b. numbers analyzed (number of animals analyzed)
    c. outcomes and estimation
    d. adverse events
6. discussion
    a. interpretation/ scientific implications
    b. generalizability/ translation
    c. funding

2.6. Registration in the international prospective register of systematic reviews of the national institute for health research

The study was registered in the International Prospective Register of Systematic Reviews of the National Institute for Health Research (PROSPERO: Identification (ID) 183085).

3. Development of an innovative *ex-vivo* model for evaluation of stability and pressure resistance of gastrointestinal anastomoses

3.1 Chemicals and consumable materials

A list of all utilized chemicals, reagents, parent solutions, surgical and consumable materials, laboratory equipment, hardware, and software is depicted in **Supplementary Table 3**Error! Reference source not found.**.**

3.2 Biological material – Porcine small intestine

The porcine small intestine bears a striking resemblance to the human small intestine in terms of microscopic and macroscopic characteristics, as demonstrated by previous studies [112, 113]. Therefore, an *ex-vivo* model utilizing porcine small intestinal tissue was selected as the preferred approach for conducting all experiments. The selection of the tissue source for the experiments was guided by ethical considerations, specifically adhering to the principles of the 3 R's—reduction, replacement, and refinement of animal experiments. [114] In line with these principles, the porcine small intestine used in the study was sourced from the Center of Preclinical Research (CPR) affiliated with the Klinikum rechts der Isar of the Technical University of Munich. Consequently, all animal products utilized in this research were obtained as byproducts from animals already sacrificed for unrelated experimental purposes. This approach eliminated the necessity to sacrifice additional animals specifically for the purposes of this study.

The porcine small intestine was obtained promptly after the sacrifice of the animals and underwent a thorough cleaning process using water before being utilized. To mitigate the potential impact of tissue degeneration on experimental outcomes, the harvested tissue was stored in a refrigerator, maintained at a temperature of four degrees Celsius ($°C$), and kept moisturized for a maximum of twelve hours. Any unused intestinal tissue during this time period was placed in a 3.7 % Formalin solution, prepared by combining 100 ml of American Chemical

society (ACS) reagent with a 37 weight % concentration in water and 10-15 % methanol as a stabilizer, with an additional 900 ml of water (*Sigma-Aldrich Chemie GmbH*). This preserved tissue was intended for future use in feasibility experiments.

3.3 Innovative *ex-vivo* model for evaluation of stability and pressure resistance of gastrointestinal anastomoses

During the course of this thesis, an innovative *ex-vivo* test setup was developed with the objective of creating a model for the precise and quantitative assessment of gastrointestinal anastomotic quality in terms of stability and pressure resistance. (**Figure 5 and Figure 6**) The model aimed to achieve high comparability, reproducibility, and independence from user variations. Based on predefined requirements, the model was engineered and constructed in collaboration with the team from the "*Kollagener Biokleber und Vlies zur Reduktion der Anastomosen-Insuffizienz in der Chirurgie (K2RANICH)*" project in the Laboratory of Biomechanics and Tissue Engineering at the Department of Orthopaedics and Sports Orthopaedics at Klinikum rechts der Isar in Munich, Germany. The project members involved in the collaboration were P-A. N, Prof. Dr. Rainer Burgkart, Dr. Andreas Obermeier, Carina Micheler, and Saskia Nicole Janett (S. N. J).

The designed model consists of five main components: the anastomotic unit, the test unit, the sensor unit, the mechanical drive unit, and the control unit. (**Figure 5. c**) Drawing upon the perfusion bioreactor developed by Micheler et al. [98-100], the integrated system can be further categorized into two technologies: information technology and fluid power technology. (**Figure 5. b and Figure 5. d**) The key components of the integrated system in this model include a HMI, a controller, actuators, sensors, a fluid system, and a SC. (**Figure 5. a and Figure 5. d**)

3.3.1 Information technology

The information technology system, as previously described by Micheler et al. [98-100], involves the use of a HMI to receive user instructions, including test parameters, which are

then transmitted to the NI-myRIO controller. (**Figure 4**) In the newly developed model, a laptop was utilized for data entry and result display. The controller receives feedback signals from the pressure sensor and is capable of recording them at a rate of one measurement every 100 milliseconds ($msec$). To maintain a physiological body temperature within the SC, a temperature sensor was connected to the controller, enabling continuous monitoring and regulation of the temperature upon activation. (**Figure 5 and Figure 6**)

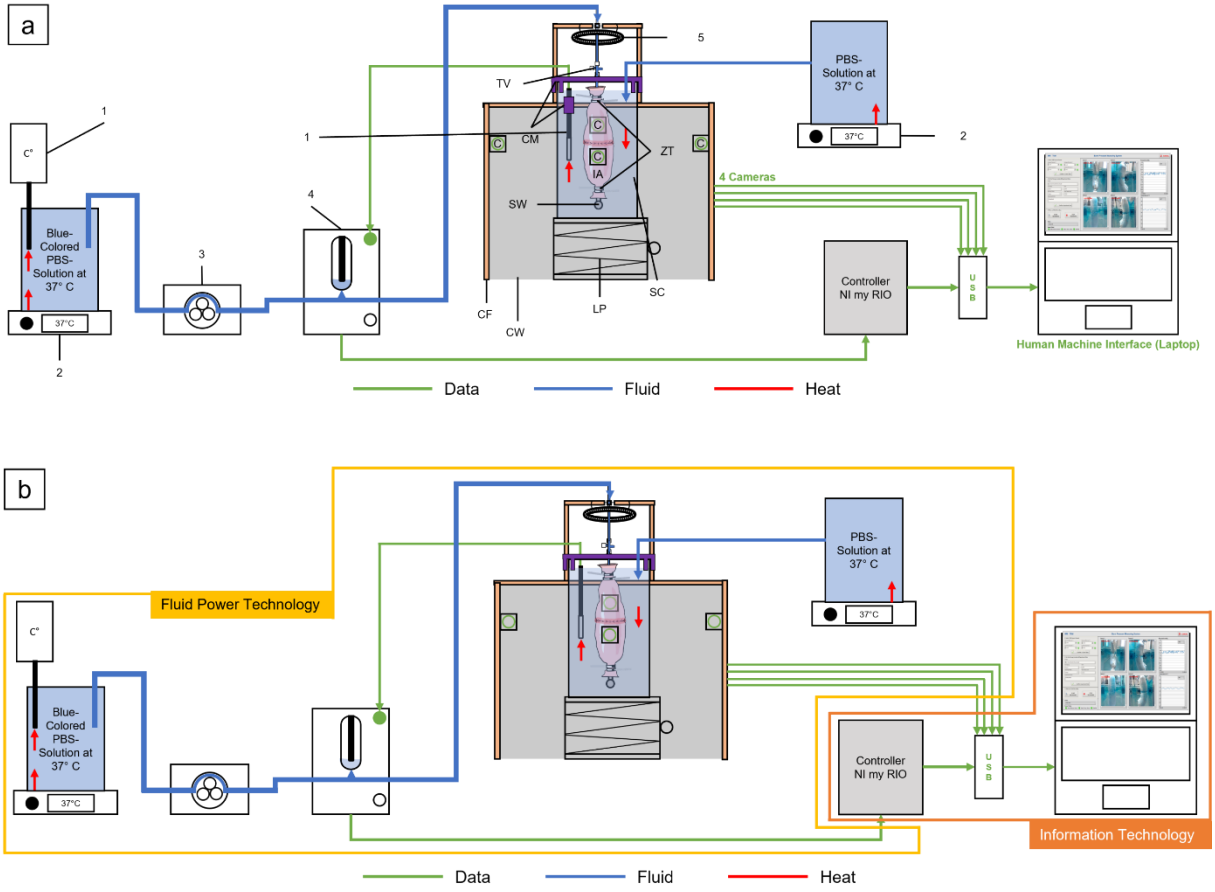

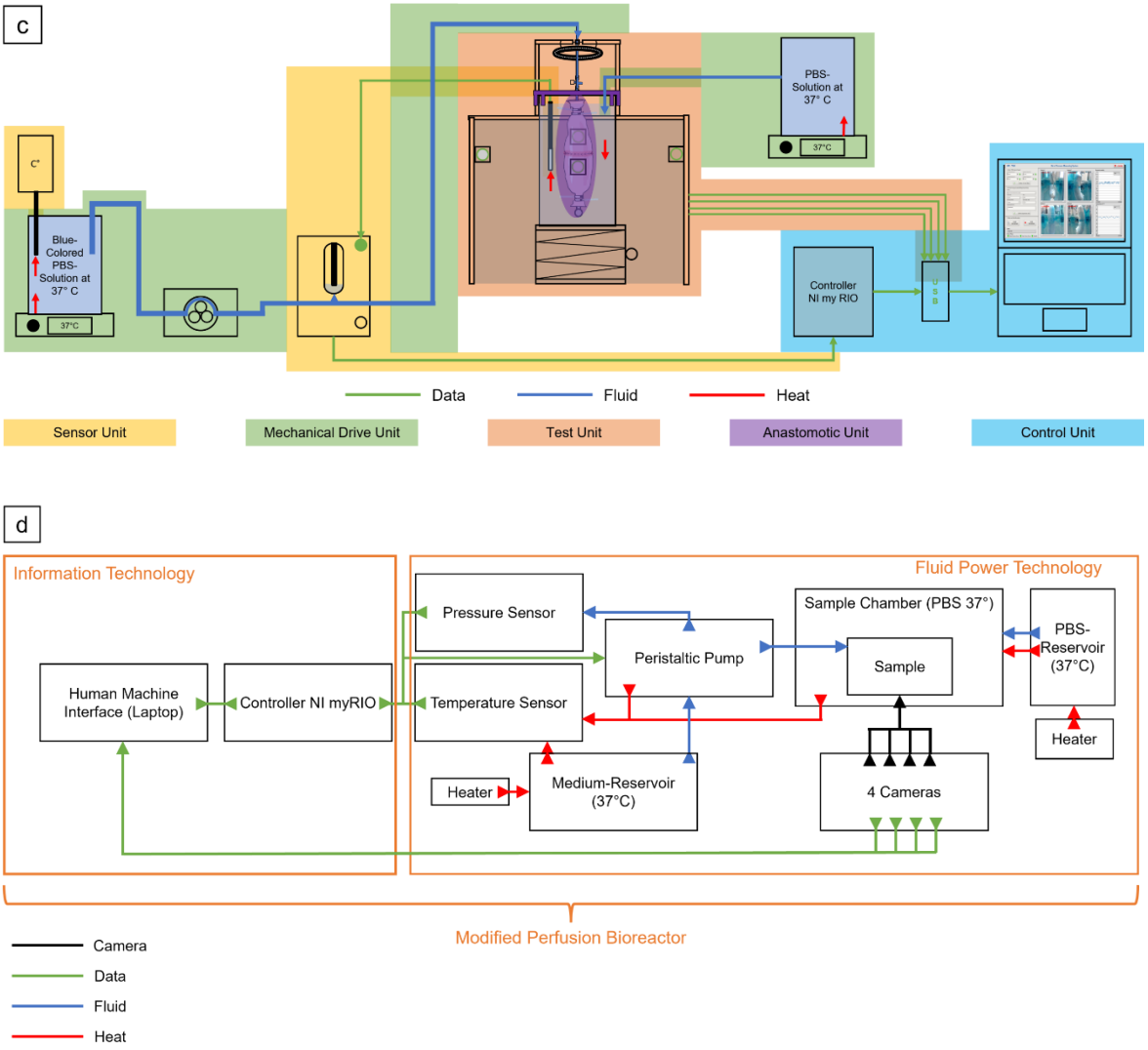

Figure 5. Schematic representation of the innovative *ex-vivo* model for evaluation of stability and pressure resistance of gastrointestinal anastomoses. (a) Key components in the test configuration. (b) Two technologies: information technology and fluid power technology. (c) Main units of the experimental setup: sensor unit; mechanical drive unit; test unit; anastomotic unit; control unit. (d) Modified perfusion bioreactor. Process description of the modified perfusion bioreactor, encompassing both information technology and fluid power technology. *C = Camera; CF = Custom-made aluminum square-shaped frame; CM = Custom-made 3D-printed stabilization brackets; CW = Custom-made plastic walls with cutouts; IA = Intestinal anastomosis; LLP = Laboratory lifting platform; SC = Sample chamber; SW = Stainless steel screw; TV = Three-way valve; ZT = Zip ties; 1 = Temperature sensor; 2 = Heater; 3 = Peristaltic pump; 4 = Pressure sensor; 5 = LED Ring light. (Adapted from Cira et al., Langenbecks Arch Surg 2024* [2]*; Modified from Micheler 2018a and Micheler, Geck, Charitou et al., Curr. Dir. Biomed. Eng 2021* [98-100]*)*

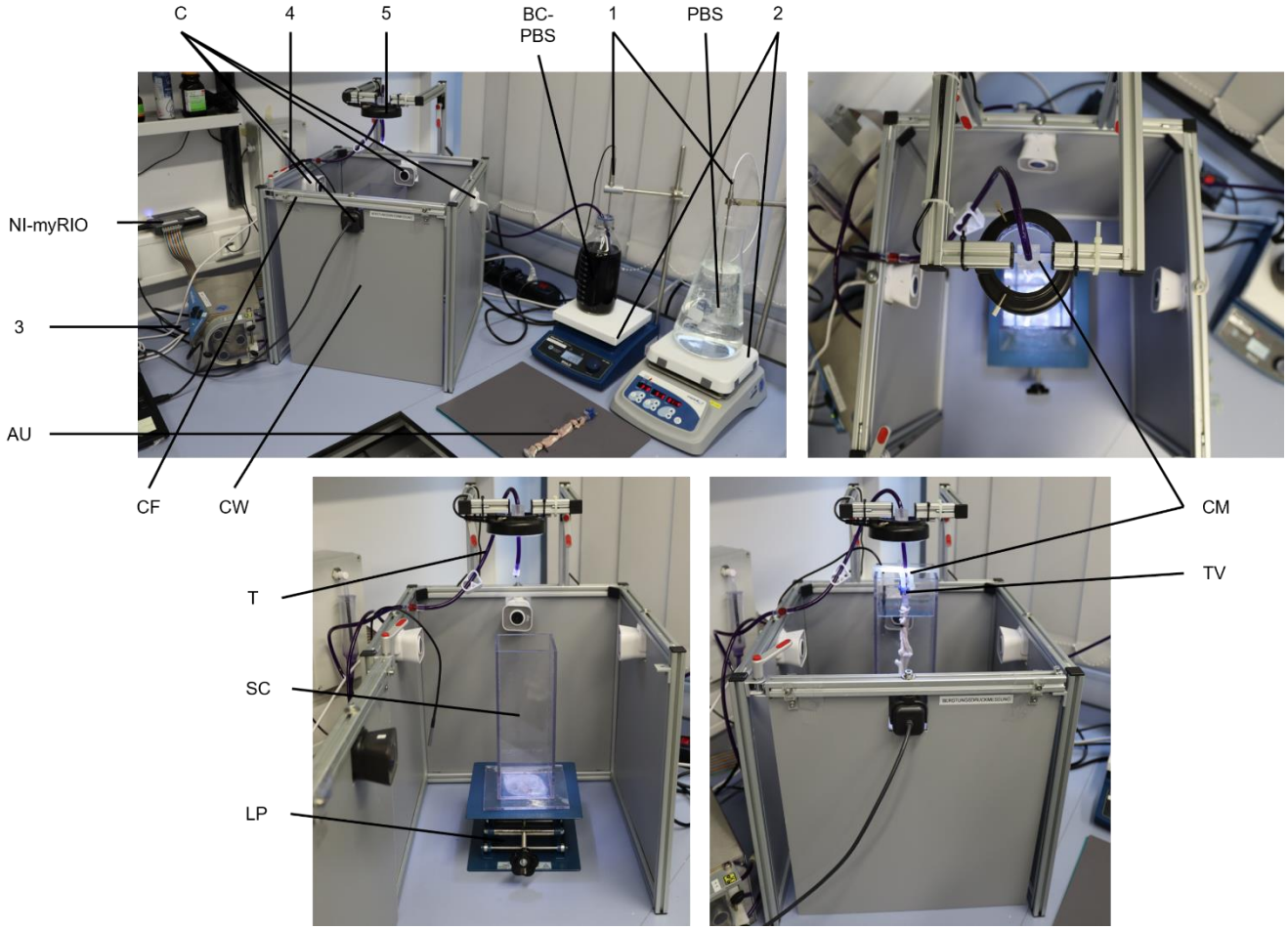

Figure 6. Innovative *ex-vivo* model for evaluation of stability and pressure resistance of gastrointestinal anastomoses. *BC-PBS = Blue-colored PBS-solution at 37 °C; C = Camera; CF = Custom-made aluminum square-shaped frame; CM = Custom made 3D-printed stabilization brackets; CW = Custom-made plastic walls with cutouts; LLP = Laboratory lifting platform; NI-myRIO = NI-myRIO controller; PBS = PBS-solution at 37 °C; SC = Sample*

chamber; TV = Three-way valve; T = Tube; ZT = Zip ties; 1 = Temperature sensor; 2 = Heater; 3 = Peristaltic pump; 4 = Pressure sensor; 5 = LED Ring light. (Adapted from Cira et al., Langenbecks Arch Surg 2024) [2]

3.3.2 Fluid power technology

The fluid power technology system of the *ex-vivo* test setup operates as an open fluid circulation system. It employs a peristaltic pump to transport a specific medium, in this case, a methyl green solution. This solution is prepared by dissolving one gram (g) of methyl green solution (*Carl Roth GmbH & Co. KG*) and one phosphate-buffered solution (PBS) tablet (*EMD Millipore Corporation; Sigma-Aldrich Chemie GmbH*) in one liter of distilled water (*SAV Liquid Production GmbH*).

The pump transports the solution from a reservoir into the anastomosis, passing through the mechanical drive unit, sensor unit, test unit, and anastomotic unit. After the peristaltic pump, a pressure sensor with an integrated sensor chamber or adapter was installed to measure the hydrostatic pressure generated. Additionally, a separate temperature sensor (*Conrad Electronic, Deutschland*) was integrated to monitor the temperature of the medium and the SC.

Similar to Micheler's prototype [98-100], the LabVIEW software was utilized to program the measurement and control technology of the bioreactor, and the resulting program was subsequently transmitted to the controller. (**Figure 5 and Figure 6**)

3.3.3 Main components of the model

3.3.3.1 Anastomotic unit

The anastomotic unit is constructed by inserting a 16.8 g stainless-steel screw into the distal end of the anastomosis, leaving only the screw end exposed outside the anastomosis. Two zip ties are tightly fastened around the distal end of the anastomosis, securing the previously inserted screw with a minimum distance of 0.5 – 1 centimeter (cm). This meticulous sealing technique ensures prevention of leakage during testing and provides slight weighting to maintain a predominantly vertical position within the SC. The proximal end of the anastomosis accommodates the insertion of the connection unit. (**Figure 5 and Figure 7**)

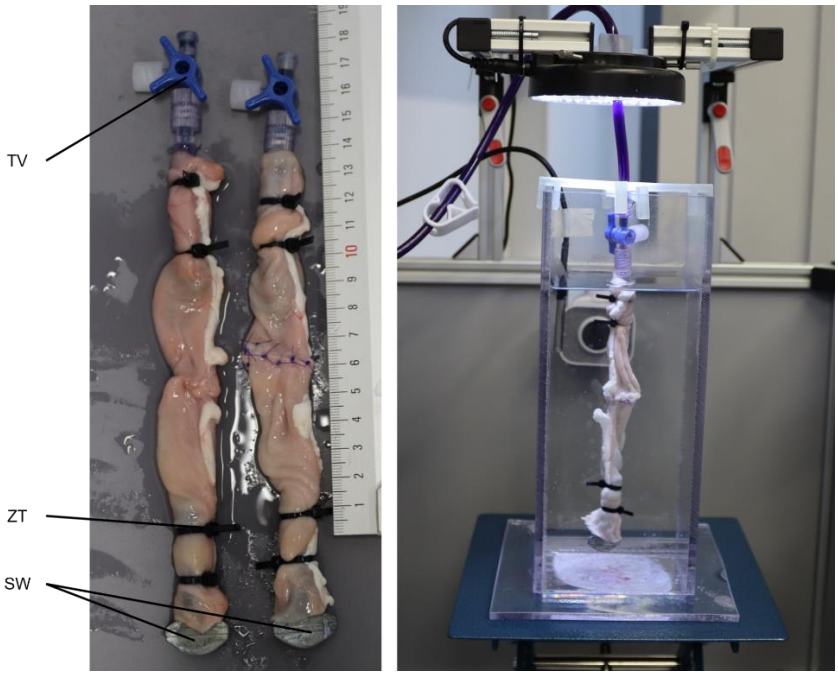

Figure 7. Anastomotic unit. *SW = Stainless steel screw; TV = Three-way valve; ZT = Zip ties. (Adapted from Cira et al., Langenbecks Arch Surg 2024)* [2]

A female Luer-Lock adapter (*RCT Reichelt Chemietechnik GmbH + Co*.) connects both ends of a custom-cut tube (*Arthrex GmbH*). At one end of the tube, the female Luer-Lock adapter is affixed to a three-way valve (*B. Braun SE; Germany*). To ensure precise testing conditions, the tube and three-way valve undergo a comprehensive flushing process with methyl green-colored PBS solution, effectively eliminating any trapped air. This meticulous procedure prevents the ingress of air into the closed anastomotic lumen, mechanical drive, and sensor unit, thereby safeguarding the integrity of pressure measurements. Subsequently, the anastomosis is positioned in the SC filled with PBS maintained at 35 – 39 °C. The three-way valve is connected to the tube from the mechanical drive unit. (**Figure 8**)

3.3.3.2 Test unit

The test unit functions as the central component of the *ex-vivo* model, consisting of a custom-made transparent plastic square-shaped container with a single opening at the top serving as the SC. To replicate the intraabdominal physiological environment at body temperature, the

SC is filled with a PBS solution maintained at 35 – 39 °C. For precise positioning during testing, a laboratory lifting platform (*JUCHHEIM Laborgeräte GmbH*) is utilized. The SC is encased by a custom-made aluminum square-shaped frame (*Item Industrietechnik GmbH*) with custom-made plastic walls (*Item Industrietechnik GmbH*), featuring cutouts for four cameras (*Logitech Europe S.A.*) strategically placed on each side to capture the experiment.

The front of the frame is equipped with a manually operated lifting gate mechanism, facilitating easy opening and closing. Additionally, a second elevated frame (*Item Industrietechnik GmbH*) is centrally positioned above the SC, securing a Light-emitting diode (LED) ring light (*Omegon.de*) with commercially available zip ties (*TRU COMPONENTS; Conrad Electronic SE*) directly over the SC. To avoid potential contact with liquid materials, electric wires are securely fastened along the frame using zip ties.

The fluid-transporting tube is fed through the middle of the LED ring light via a three-dimensional (3D)-printed feed connection and connected to the anastomotic unit. A supplementary 3D-printed stabilization bracket complements the chamber setup. For comprehensive documentation of the experiment, four Logitech cameras are positioned on each side of the frame's wall, capturing the experiment and ensuring a thorough record of the entire circumference of the anastomosis. Logitech webcams with a full high definition (Full HD) resolution of 1920 x 1080 pixels (px) are employed, resulting in an original size of 4 x 6 Megabytes (Mbyte) (Red, Green, Blue).

The Universal Serial Bus Type-C (USB-C) transmission rate stands at 4 x 1 Mbyte (Joint Photographic Experts Group (jpg)), while the frame rate remains at a minimum of 25 frames per second with at least two frames per measurement. (**Figure 5, Figure 6, Figure 7, and Figure 8**)

3.3.3.3 Sensor unit

The sensor unit is equipped with a pressure (*Amsys GmbH & Co. KG*) and temperature sensor, both housed within a watertight box featuring an opening for pressure equalization. This sensor unit, initially designed by Micheler et al. [98-100] for a perfusion bioreactor (**Figure 4**), has been implemented according to the model's requirements. A temperature probe within the SC ensures continuous temperature recording. The pressure sensor is directly linked to the tube through which the fluid flows in the open circulatory system, providing accurate measurements of the intraluminal pressure. (**Figure 5 and Figure 6**)

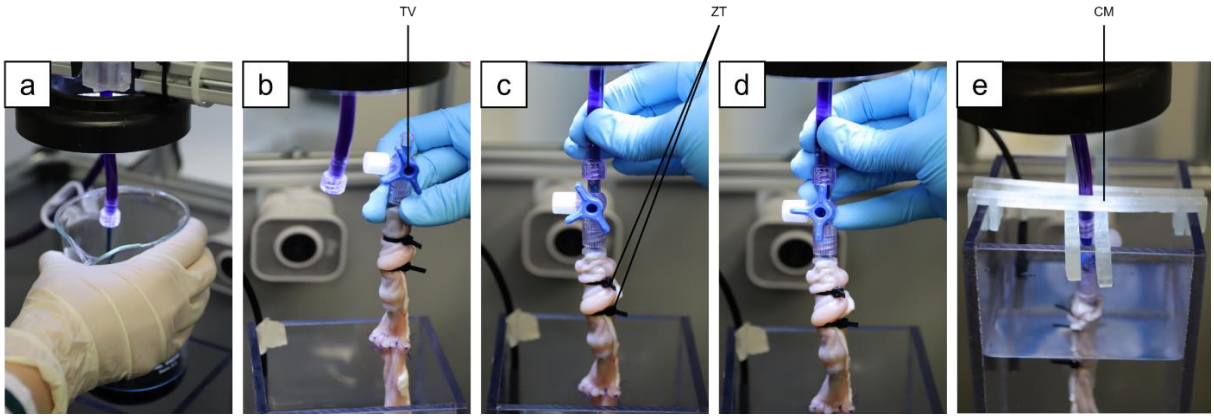

Figure 8. Connection of the intestinal anastomosis to the mechanical drive unit. The figure illustrates the steps involved in connecting the intestinal anastomosis to the mechanical drive unit for experimental testing: (a) The flushing process with methyl green-colored PBS solution effectively eliminates any trapped air. (b) The flushed and closed three-way valve is securely connected to the intestinal anastomoses using zip ties, ensuring a tight seal. (c) The flushed and closed three-way valve is then connected to the flushed and airless tube from the mechanical drive unit. (d) The flushed three-way valve is subsequently opened, allowing controlled fluid flow during the experiment. (e) Finally, the intestinal anastomosis is carefully positioned in the SC, filled with a PBS solution maintained at a temperature range of 35 – 39 °C, establishing a physiological environment for testing. *CM = Custom made 3D-printes stabilization brackets; TV = Three-way-valve; ZT = Zip ties. (Adapted from Cira et al., Langenbecks Arch Surg 2024)* [2]

3.3.3.4 Mechanical drive unit

The mechanical drive unit facilitates fluid flow to the anastomosis through the tube using an externally provided peristaltic pump (*Ismatec; VWR International GmbH*). For optimal performance, it is recommended to replace the fluid system's tubing after approximately 100 tests or upon initial use to prevent potential tearing. The actual flow rate of the peristaltic pump at various device-speed levels was manually tested, as it may slightly deviate from the flow

rates outlined in the device manual. The tube connects to the peristaltic pump, efficiently transporting methyl green-colored PBS solution at a temperature of 35 – 39 °C, simulating the body's internal physiological environment. This fluid is sourced from a commercially available glass bottle made from borosilicate glass (*DURAN Schott; Avantor, Inc; VWR International GmbH*), commonly used in the laboratory sector. The fluid is directed into the anastomotic lumen, passing through the pressure sensor and connection unit, thereby forming an open circulatory system. The temperature maintenance is ensured by a heater (*witeg Labortechnik GmbH*). (**Figure 5, Figure 6, and Figure 7**)

3.3.3.5 Control unit

The control unit of this model represents a modified version of a bioreactor originally designed by Micheler et al. [98-100]. The bioreactor underwent customization, transforming it into an automated, software-controlled system with an HMI. This advanced setup enables simultaneous recordings of the intraluminal pressure within the tube and the anastomosis, as well as the surrounding temperature of the anastomosis within the SC, while simultaneously capturing camera footage. The real-time capable controller, NI myRIO (*National Instruments, USA*), is programmed using the LabVIEW development environment, effectively overseeing and regulating the operations of the adapted bioreactor. (**Figure 5 and Figure 6**)

Figure 9. Human machine interface during an experiment. The figure displays the HMI on a laptop used during the experiment. 1 = Camera activation: allows the user to activate the cameras for recording; 2 = Enter experimental data: enables inputting relevant experimental data; 3 = Start recording

of the experiment: initiates the recording of the experiment; 4 = Stop recording of the experiment: halts the recording process; 5 = Video and sensor status: provides information on the status of videos and sensors; 6 = Four cameras capturing the anastomosis: shows the real-time footage from the four cameras capturing the anastomosis during the experiment; 7= Pressure measurement: displays the intraluminal pressure measurement in $mmHg$ during the experiment; 8 = Temperature measurement during the experiment: shows the temperature measurement in $°C$ recorded during the experiment. *(Adapted from Cira et al., Langenbecks Arch Surg 2024)* [2]

3.3.4 Feasibility study and functional validation of the innovative *ex-vivo* model

A feasibility study and functional validation of the innovative *ex-vivo* model was conducted with the primary objective of evaluating the overall functionality of the new test setup, while also assessing the reproducibility, comparability, and user-independence. The secondary aim was to investigate the differences in anastomotic stability and pressure resistance when employing two distinct anastomotic techniques under two different flow rate conditions.

3.3.4.1 Flow rate models

Under normal physiological conditions, the fluid flow rate in the proximal small intestine exhibits variations depending on whether it is measured during fasting or after meals. In fasting subjects, a fluid flow rate of approximately 2.5 ml/minute (ml/min) [115, 116] can be observed, while after meals, the fluid flow rate can increase to around 20 ml/min [117-121].

To simulate a physiological increase in intraluminal intestinal pressure under normal conditions, a fluid flow rate of about 20 ml/min was selected and defined as the low-flow model (LF). This flow rate reflects a moderate increase in fluid influx, akin to the rise in intraabdominal pressure observed during regular activities.

For simulating a sudden increase in intraluminal pressure, such as during Valsalva maneuvers, coughing, or jumping, the intraluminal intestinal flow rate was increased tenfold to 200 ml/min, defined as the high-flow model (HF). This higher flow rate represents a substantial surge in fluid influx, simulating the abrupt elevation in intraabdominal pressure associated with forceful expiration or physical activities.

It is important to note that resting intraabdominal pressure typically ranges from 2 – 4 $mmHg$, but it can increase during various activities. For instance, jumping can elevate intraabdominal pressure to 170 $mmHg$, coughing to 100 $mmHg$, the Valsalva maneuver to 40 $mmHg$, and simply standing to 20 $mmHg$. [122, 123] The resting intraluminal pressure in the small intestine varies among the literature, estimated to be 6 – 13 $mmHg$ [123-125], and can reach 20 – 30 $mmHg$ during various peristaltic activities [126].

Given these variations, a fluid flow rate of 200 ml/min was chosen as the HF rate to emulate the sudden increase in intraluminal intestinal fluid influx associated with activities like Valsalva maneuvers or coughing. By selecting these flow rates, the experimental models aimed to replicate the changes in intraabdominal pressure observed during different physiological states, providing a basis for studying the effects of pressure on anastomotic stability and pressure resistance. It is important to note that the goal is not to precisely replicate *in-vivo* intestinal stress but rather to induce stress on the tissue wall in a manner reflective of observed human stress situations. This approach allows analysis of biomechanical behavior, specifically stretching and stiffness.

3.3.4.2 Sample preparation and anastomotic technique

Figure 10 illustrates the instruments and materials required to create the anastomotic unit.

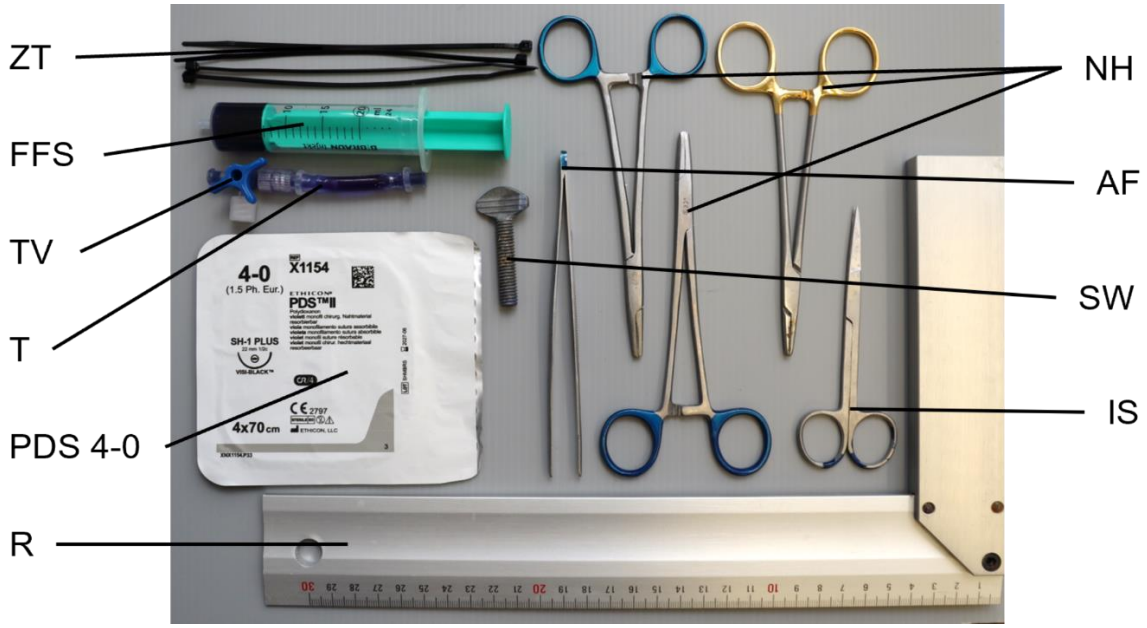

Figure 10. Instruments and materials for creating the anastomotic unit. *AF = Anatomical forceps; FFS = Fluid-filled syringe; IS = Iris scissors; NH = Needle holder; PDS = Polydioxanone; R = Ruler; SW = Stainless steel screw; T = Tube; TV = Three-way valve; ZT = Zip ties. (Adapted from Cira et al., Langenbecks Arch Surg 2024)* [2]

The porcine small intestines were carefully dissected into 20 cm long segments before their utilization in the experiment. (**Figure 11**) Prior to performing the intestinal anastomosis, the tissues underwent a rehydration process and were heated to 37 °C, following the method described by Daristotle et al. [127]. This rehydration process involved submerging the segments in PBS solution preheated to 37 °C for two minutes, followed by exposure to 37 °C ambient air for four minutes, with this two-step process repeated twice. (**Figure 11**)

Preliminary testing revealed that the porcine small intestinal surface dehydrated rapidly when exposed to 37 °C ambient air for two minutes. To ensure the biomechanical stability of the tissue, the 20 cm long porcine small intestines used in the experiments were pre-rehydrated for at least five minutes in 37 °C PBS solution both before and after performing the intestinal anastomosis. (**Figure 11**)

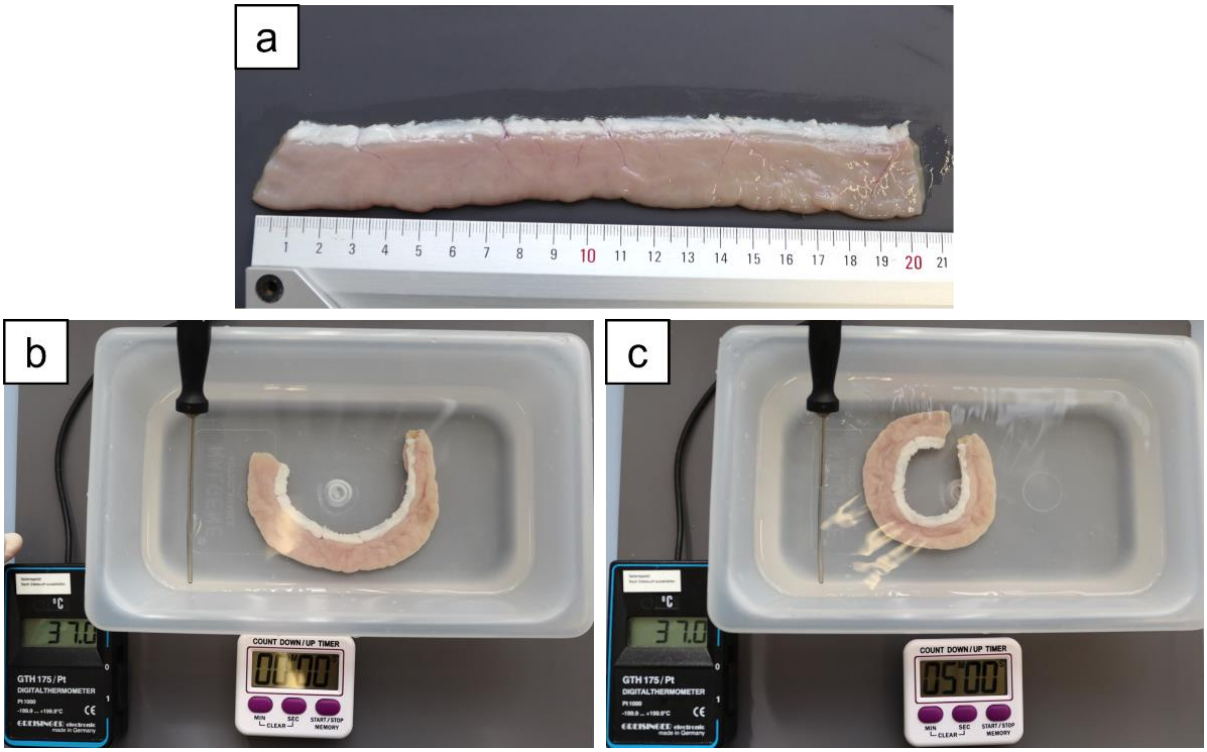

Figure 11. Preparation and rehydration of porcine small intestine. (a) The porcine small intestines were meticulously dissected into 20 cm long segments before their utilization in the experiment. (b) Prior to performing the intestinal anastomosis, the tissues underwent a rehydration process and were heated to 37 $°C$. (c) The porcine small intestines used in the experiments were pre-rehydrated for at least five minutes in 37 $°C$ PBS solution both before and after performing the intestinal anastomosis. *(Adapted from Cira et al., Langenbecks Arch Surg 2024)* [2]

To perform an EEA intestinal anastomosis, the intestinal segment was incised at the middle (10 cm) using a disposable scalpel (*FEATHER; SOCOREX ISBA SA*) (**Figure 12. a**) and dissected vertically into two parts with dissecting iris scissors (*Entrhal Medical GmbH*) (**Figure 12. b**). The mesenterial border of the segment's midline incision was freed from adipose tissue and vessels, ensuring at least 1 cm clearance on each side (**Figure 12. c**). Depending on the experimental series, the following anastomotic techniques were employed: handsewn sufficient small intestinal EEA using the SBS technique (**Figure 13**) or handsewn sufficient small intestinal EEA using the CS technique (**Figure 14**).

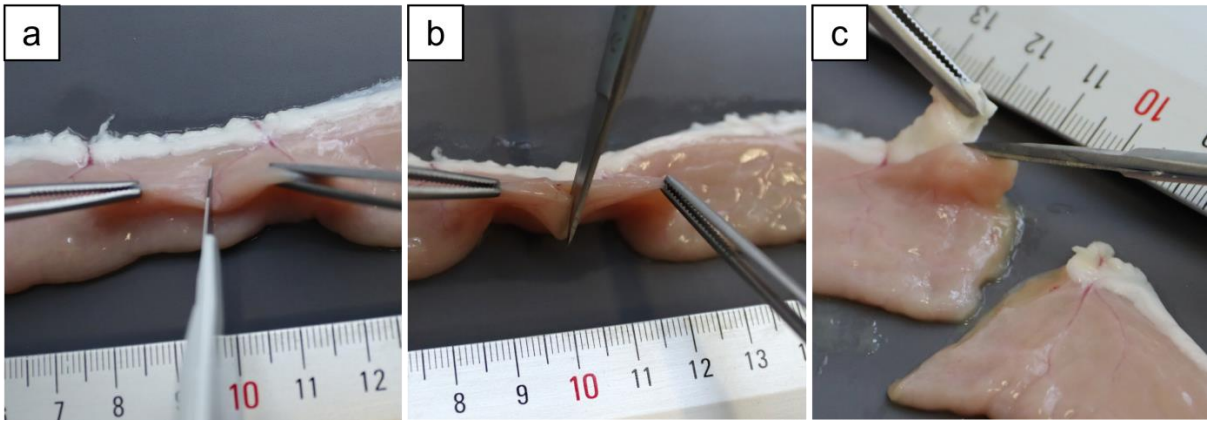

Figure 12. Sample preparation. (a) The intestinal segment was incised at its middle (10 cm) using a disposable scalpel. (b) Vertical dissection in two parts was performed using dissecting iris scissors. (c) The mesenterial border of the incision was cleared of adipose tissue and vessels, leaving a 1 cm clearance on each side.

In total, 32 handsewn sufficient small intestinal EEAs were performed on formalin-fixed porcine small intestinal tissue obtained from the CPR. Prior to testing, the tissue was prepared as described in section **Chapter III.3.2**. The tissue was prepared by one investigator (K. C.) who prepared 16 anastomoses using the SBS technique and 16 anastomoses using the CS technique, in a random order. Subsequently, another investigator (doctoral candidate and medical student: S. N. J.) randomly divided the anastomoses further into the following four groups for the study:

1. Experimental series 1: eight handsewn sufficient small intestinal EEA using the SBS technique were created. (**Figure 13**) These anastomoses were subsequently tested in the LF model (SBS-CON-LF).
2. Experimental series 2: eight handsewn sufficient small intestinal EEA were created using the SBS technique. (**Figure 13**) These anastomoses were subsequently tested in the HF model (SBS-CON-HF).
3. Experimental series 3: eight handsewn sufficient small intestinal EEA using the CS technique were created. (**Figure 14**) These anastomoses were subsequently tested in the LF model (CS-CON-LF).

4. Experimental series 4: eight handsewn sufficient small intestinal EEA using the CS technique were created. (**Figure 14**) These anastomoses were subsequently tested in the HF model (CS-CON-HF).

In experimental series 1 and 2, the handsewn sufficient small intestinal EEA using the SBS technique was performed using 4-0 Polydioxanone (PDS) (*Ethicon Deutschland Johnson & Johnson Medical GmbH*) suture material. A seromuscular stay suture was placed five millimeters (mm) from the incision site at the proximal and distal ends of the intestinal segments. Interrupted sutures were placed between the two stay sutures, with a 5 mm distance to the intestinal margin and a stitch distance of 5 mm. After the anterior site of the intestinal segments was securely closed, the intestinal segment was rotated by 180 degrees (°) to visualize the unsutured posterior intestinal segment, and the anastomosis was closed from the antimesenteric border to the mesenteric border. This was done by passing the stay suture at the antimesenteric border 180° posteroinferior and the stay suture at the mesenteric border 180° anterosuperior. The intestinal segment was rotated back to its initial position, passing the stay sutures 180° back. Finally, both stay sutures were tied. Each suture was knotted six times. (**Figure 13**)

In experimental series 3 and 4, the handsewn sufficient small intestinal EEA using the CS technique was performed using 4-0 PDS suture material. (**Figure 14**)

The first seromuscular stitch was placed 5 mm apart from the incision site at the mesenterial border, adapting both segment endings. The suture was knotted twice above the midline. Then, a stay suture was placed at the antimesenteric border, again 5 mm apart from the incision line. This suture was loosely knotted once. The intestinal segments were sutured with a continuous seromuscular technique from the mesenteric border to the antimesenteric border. The first seromuscular stitch was passed through one intestinal segment, and the thread was pulled through and tightened by the assistant (S. N. J). Then, the second seromuscular stitch was made obliquely to the mesentery, ensuring a clean adaptation

between the two intestinal segments. This technique ensures a clean adaption between the two intestinal segments. [128] (**Figure 14**)

After closing the anterior site, the intestinal segment was turned by 180° to visualize the unsutured posterior intestinal segment. The stay suture of the antimesenteric end was passed anteroinferiorly, and the fixed thread of the initial suture, located at the mesenteric border, was passed posterosuperiorly. The assistant (S. N. J) tightened the thread of the initial suture, and the stay suture was removed. The anastomosis was closed from the antimesenteric to the mesenteric border. After completing the anastomosis, both suture ends were securely tied together with six knots. (**Figure 14**)

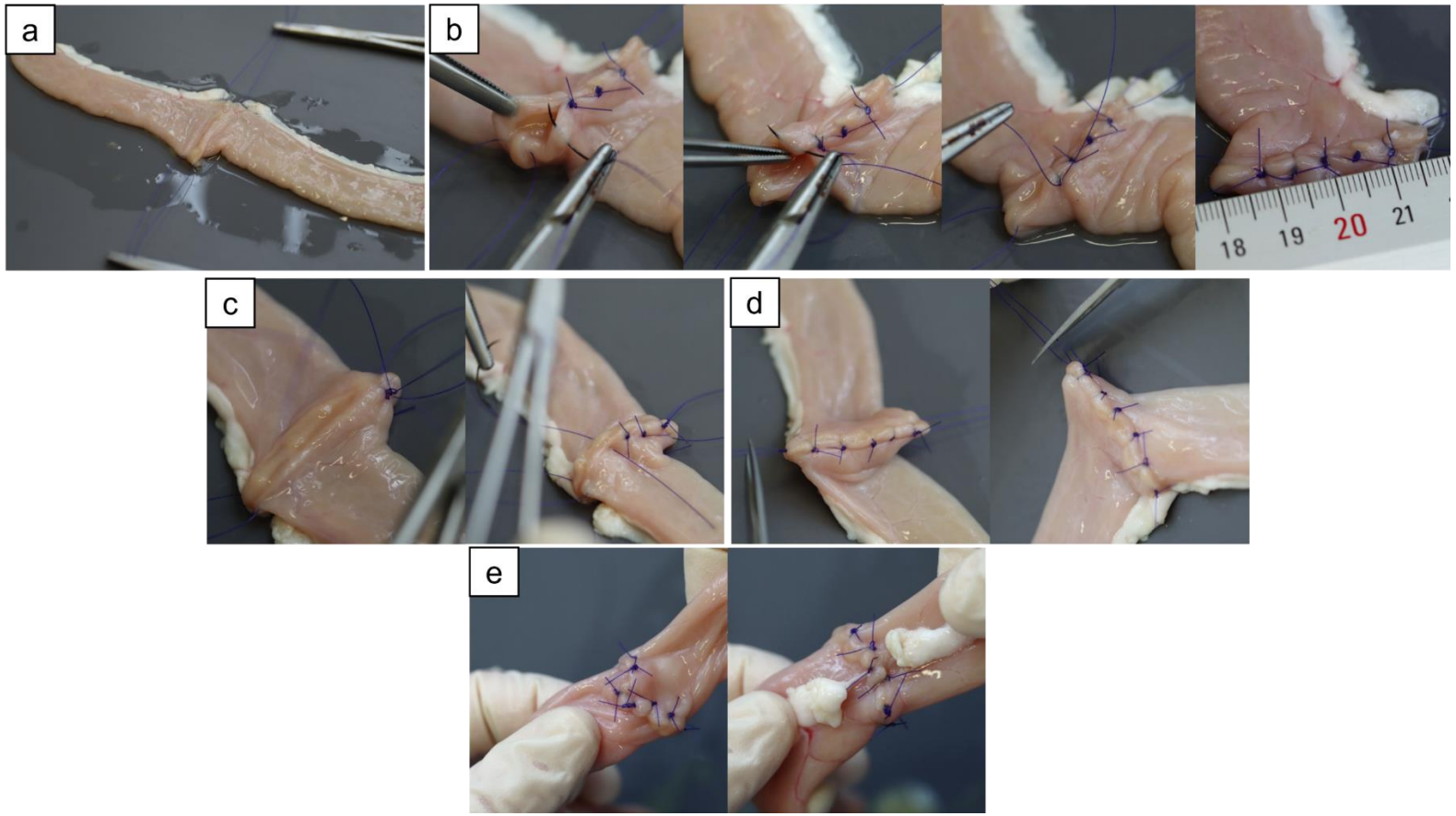

Figure 13. Handsewn sufficient small intestinal end-to-end anastomosis using the simple interrupted suture technique. (a) A seromuscular stay suture was placed 5 mm away from the incision site at the proximal and distal ends of the intestinal segments. (b) Interrupted sutures were placed between the two stay sutures, maintaining a 5 mm distance to the intestinal margin, with a stitch distance of 5 mm. (c) After securely closing the anterior site of the intestinal segments, the intestinal segment was rotated by 180° to visualize the unsutured posterior segment, and the anastomosis was closed from the

antimesenteric border to the mesenteric border. (d) Finally, both stay sutures were tied. (e) Completed handsewn sufficient small intestinal EEA using interrupted suture technique, anterior and posterior views. *(Adapted from Cira et al., Langenbecks Arch Surg 2024)* [2]

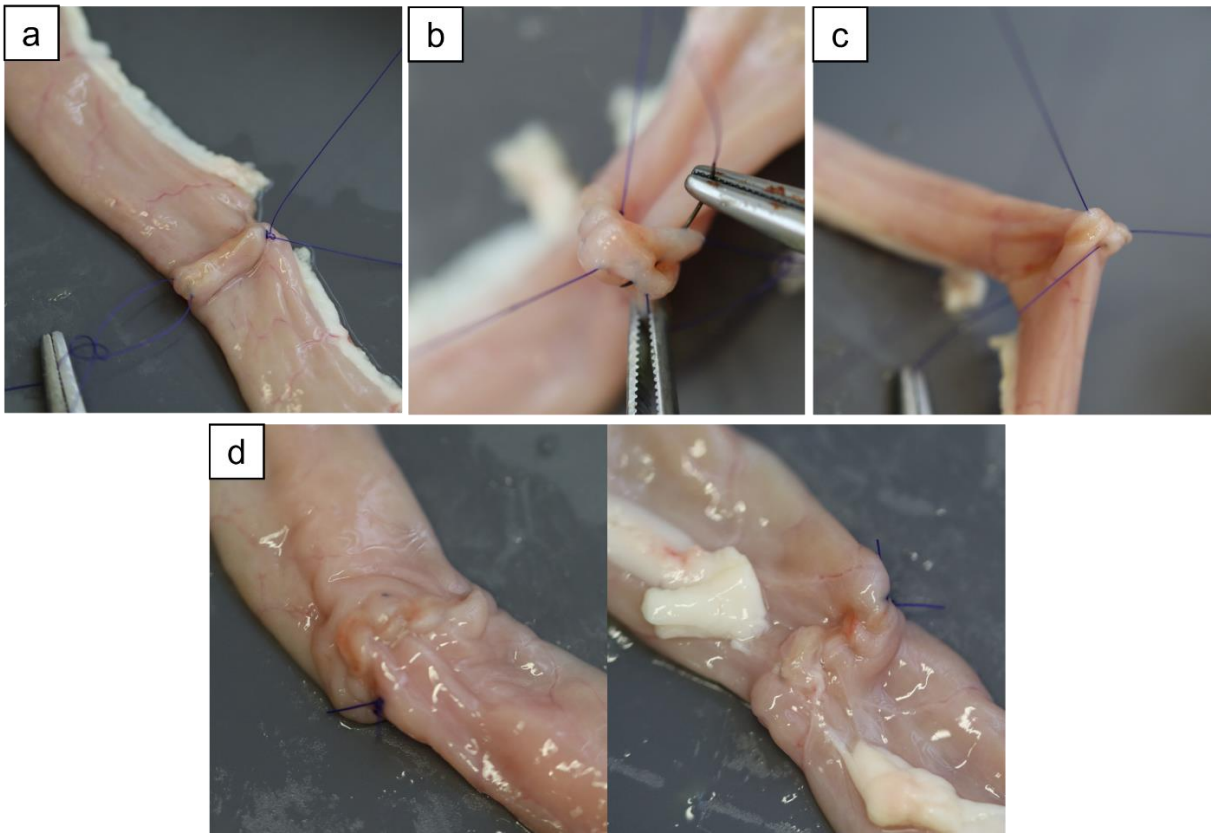

Figure 14. Handsewn sufficient small intestinal end-to-end anastomosis using the simple continuous suture technique. (a) The first seromuscular stitch was placed 5 mm from the incision site at the mesenteric border, ensuring proper adaptation of both segment endings. A stay suture was positioned at the antimesenteric border, also 5 mm from the incision line. (b) Using the continuous seromuscular technique, the intestinal segments were sutured from the mesenteric border to the antimesenteric border. (c) After closing the anterior site, the intestinal segment was rotated by 180° to visualize the unsutured posterior intestinal segment, and the anastomosis was closed from the antimesenteric to the mesenteric border. (d) Finally, both suture ends were securely tied together with six knots. *(Adapted from Cira et al., Langenbecks Arch Surg 2024)* [2]

3.3.5 Data analysis

All experimental data, including images and text files, were meticulously organized and stored in a predefined folder on the Microsoft computer system. The text file, which can be accessed through Microsoft Excel (*Version 2307; Microsoft, Redmond, WA*), contains essential general information such as the name of the test system, test name, user, start date, start time, bursting mode, flow rate level, flow rate (3.2 inner diameter (IND)), pump speed

(revolutions per min), start pressure (runtime experiment in), and manually included experiment information.

Each specific test measurement point's data comprises the date, time stamp, runtime of the experiment ($msec$), temperature ($°C$), pressure (mm of mercury ($mmHg$)), pressure difference ($mmHg$), mean pressure ($mmHg$), and pressure temperature ($°C$). Image files were automatically saved and categorized according to their recording order, with automatic time stamp-based file naming. Additionally, the images were sorted into folders corresponding to the respective cameras that captured them (e.g., cam01-Images; cam02-Images et cetera (etc.)), facilitating efficient retrieval and analysis of specific images.

Upon exporting the data to Microsoft Excel, the runtime was standardized to zero. Subsequently, the first pressure difference value closest to the acquired time stamp was identified, adhering to specific criteria, which required the value to be either greater than or equal to zero and not followed by negative values. In certain cases where leakage occurred at the onset of the test, negative pressure difference values were accepted. This exception was based on the assumption that, at that particular time, the outflow from the anastomotic lumen might outweigh the influx, leading to a temporary occurrence of negative intraluminal anastomotic pressure.

Following this data preprocessing, comprehensive analyses were conducted, such as quantitative analyses of anastomotic performance and time intervals (**Chapter III.3.3.5.1.1** – **3.3.5.1.4**), including interrelated analyses derived from experimental outcomes (**Chapter III.3.3.5.2**), and leakage and bursting location analyses (**Chapter III.3.3.5.3**).

The pressure difference data was plotted using GraphPad Prism (*Version 8.0.2. San Diego, CA: GraphPad Software, 2020*), with the y -axis representing pressure difference and the x-axis representing runtime zeroed ($msec$). To visualize the images in a video format, we utilized a specialized video converter programmed in LabVIEW by Carina Micheler. This allowed for the efficient transformation and review of all images.

3.3.5.1 Quantitative analysis of anastomotic performance and time intervals

The data generated with the innovative *ex-vivo* model enables accurate measurements of various parameters related to anastomotic stability and pressure resistance. The primary focus of this analysis was to evaluate the performance of the porcine small intestinal EEAs under controlled fluid flow conditions. The assessment of anastomotic stability and pressure resistance is of paramount importance in surgical practice, as it directly influences patient outcomes and the success of gastrointestinal surgical procedures. [72-75] Hence, the investigation aimed to thoroughly understand the biomechanical characteristics of anastomotic sites under both physiological and stress-induced conditions.

To achieve this objective, the study meticulously examined and analyzed key parameters, such as start pressure, leakage pressure (LP), BP, and various time intervals between critical events during the experimental process. (**Figure 15**) These measurements provide valuable insights into the integrity and endurance of anastomotic sites under different intraluminal pressures, simulating diverse physiological and forceful expiratory activities. Through a comprehensive data analysis, factors influencing anastomotic stability were investigated, with a specific focus on the time of leakage occurrence relative to bursting and the assessment of pressure and time differences between leakage and bursting events. This analysis enabled a comparison of the occurrence of leakage and bursting in different proportions, facilitating the evaluation of potential variations based on suture methods or flow rate models.

All the following parameters were compared between the experimental groups to determine if there were differences between the groups based on flow model or anastomotic technique.

3.3.5.1.1 Start pressure

The start pressure was defined as the pressure difference measured at the initiation of each experiment. The acquired images and data were meticulously examined to identify the precise

time stamp corresponding to the beginning of the experiment. Subsequently, the data sheet was scrutinized to identify the first pressure difference value closest to the acquired time stamp, meeting the criteria of being either greater than or equal to zero and not followed by negative values. An exception was made in cases where leakage occurred at the very start of the test, accepting negative pressure difference values. This exception was made based on the assumption that at that particular time, the outflow from the anastomotic lumen might outweigh the influx, leading to a temporary occurrence of negative intraluminal anastomotic pressure. (**Figure 15**)

3.3.5.1.2 Leakage pressure analysis

LP was defined as the pressure difference measured at the moment of the first visible AL. The identification of the initial leakage involved a manual screening of all acquired images (two frames per measured value) from all four cameras. Upon detecting the first leak in one image from one camera view, the corresponding pressure difference was extracted from the data sheet by locating the corresponding time stamp. For the images from the other camera views, the images with time stamps closest to the previously mentioned one were selected for analysis. (**Figure 15**)

3.3.5.1.3 Bursting pressure analysis

BP was defined as the peak pressure recorded during each experimental trial. This parameter was determined by identifying the highest value from the dataset of pressure differences obtained in each experiment, utilizing the "MAX" function in Microsoft Excel. To ensure the accuracy and validity of the acquired BP, a meticulous process of manual data and image verification was undertaken to ensure alignment with the actual bursting event. The time stamp associated with the measurement of BP was used to identify the corresponding image captured from one camera view. Similarly, for images from other camera views, those with time stamps

closest to the previously mentioned value were selected for further analysis and validation. (**Figure 15**)

3.3.5.1.4 Time interval analysis

The analysis of time intervals entailed investigating and comparing different durations during the experimental process. The primary focus of this analysis was on the absolute numerical values of time measured in $msec$. This approach enables a direct comparison of time intervals between various experimental groups, providing valuable insights into the duration required for the pressure to increase from the start of the experiment to the point of leakage or bursting, as well as the time required for the pressure to increase from leakage to bursting. By assessing these time intervals in a standardized manner, it allows for a comprehensive understanding of the temporal dynamics associated with the occurrence of leakage and bursting in the experimental setting. (**Figure 15**)

Three key time intervals were examined:

1. Start to LP Time: This represents the time interval (measured in $msec$) between the initiation of the experiment and the moment when the anastomotic site begins to leak, marked by the attainment of LP.
2. Start to BP Time: This represents the time interval (measured in $msec$) between the initiation of the experiment and the occurrence of bursting at the anastomotic site.
3. LP to BP Time: This represents the time interval (measured in $msec$) between the occurrence of leakage and the subsequent bursting event, represented by the time difference between LP and BP.

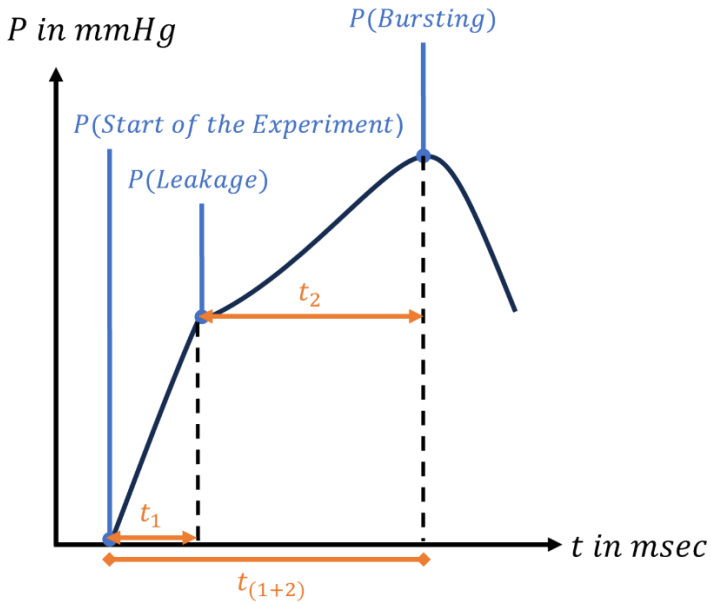

Figure 15. Analysis of key parameters during the experimental process. This figure presents key parameters of the experimental process, including start pressure, LP, BP, and time intervals. $mmHg$ = Millimeters of Mercury; P = Pressure in $mmHg$; t = Time; t_1 = Start to LP Time; t_2 = LP to BP Time; $t_{(1+2)}$ = Start to BP Time. *(Adapted from Cira et al., Langenbecks Arch Surg 2024)* [2]

3.3.5.2 Interrelated analyses derived from experimental outcomes

In the pursuit of comprehensively understanding anastomotic stability and pressure resistance within this *ex-vivo* model, a series of interrelated analyses was conducted based on the experimental outcomes. These analyses aimed to elucidate the temporal relationship between AL and bursting events, as well as to investigate the pressure and time differences associated with these critical occurrences.

The "Proportion of BP at LP" analysis involves quantifying the ratio of the BP to the LP, measured in $mmHg$. This assessment offers insights into the pressure relationship between the initiation of leakage (LP) and the peak pressure recorded during bursting (BP). By calculating the proportion of these pressure values, this analysis provides valuable information about the relative magnitude of pressures associated with these significant events. The focus for this analysis was on the absolute numerical values of the pressure measurements.

Therefore, the magnitude of the pressure increase from leakage point to the point of bursting was assessed, allowing for a direct comparison of pressure differences between groups.

The "Percentage of BP at LP" analysis involves calculating the BP as a percentage of the LP. It quantifies the proportion of the peak pressure recorded during bursting (BP) in relation to the pressure at which leakage initiates (LP). This assessment provides insights into the relative magnitude of pressure values associated with these crucial events, expressed as a percentage. To describe the relationship between the two pressure thresholds, the percentage of BP at the point of LP was calculated as a relative measure. In contrast to the previously mentioned proportion of BP at LP, this analysis considers the relative proportion of BP reached at the leakage point. By normalizing the BP based on the individual LP, it allows for a comparison of the proportion of BP achieved relative to the LP. This approach provides a standardized assessment of BP in the context of LP, enabling a comprehensive understanding of the pressure dynamics during these significant events.

The "Relative Difference of Pressure between Leakage and Bursting" analysis involves quantifying the pressure gap between leakage (LP) and bursting (BP) as percentage. It represents the relative difference in pressure values between the moment of leakage initiation and the peak pressure observed during bursting. This assessment provides information about the pressure fluctuations or variations between these two significant events, expressed as percentage.

The "Time of Leakage Occurrence Relative to Bursting Time" represents a quantitative assessment expressed as percentage characterizing the temporal relationship between leakage (LP) onset and subsequent bursting (BP). This analysis involves calculating the proportion of time elapsed from the experiment's initiation until the occurrence of leakage, relative to the total time taken until bursting happens. It provides insights into the sequence and temporal proximity of these critical events during the experimental process. In comparing the time difference in $msec$, the absolute duration between the two pressure points is directly

analyzed. This approach focuses on the temporal aspect and quantifies the precise time span required to transition from LP to the BP. It provides a numerical measure of the time interval and allows for direct comparisons between groups in terms of the absolute time taken to reach the BP after the occurrence of leakage.

Conversely, when comparing the percentage of time of BP at the time of LP, the relative proportion of time spent at the BP level in relation to the total time spent at the LP is considered. The ”Relative Difference of Time Between Leakage and Bursting Time” analysis normalizes the BP by taking into account the individual LP and provides a relative measure of the proportion of time spent at the BP. It enables comparisons between groups in terms of the relative duration of BP reached during the occurrence of leakage, relative to the total time spent at the LP. This comprehensive analysis of time intervals provides essential information regarding the temporal dynamics and interrelationship between leakage (LP) and bursting (BP) events, contributing to a thorough understanding of the experimental outcomes.

By conducting these interrelated analyses, the intricate factors influencing anastomotic behavior within the experimental model were explored.

3.3.5.3 Leakage and bursting location analysis

In order to investigate the location of leakage and bursting of the porcine small intestinal anastomoses, images from all four cameras capturing different angles of the anastomosis were correlated with the corresponding measured pressures for each experimental trial. The anastomosis was divided into eleven equal sections, numbered from -5 to 5, with 0 (or M0) representing the precise location of mesenteric attachment to the intestine. (**Figure 16 and Figure 17**)

To simplify data evaluation and presentation, these circular sections were transformed into a linear grid, with 0 positioned at the center, -5 to the far left, and 5 to the far right. The grid was further divided into two zones: the mesenteric zone (between -1 and +1) and the

peripheral zone (ranging from -2 to -5 and +2 to +5), labeled as zones M1 and P (P2 – P5) respectively. (**Figure 17**)

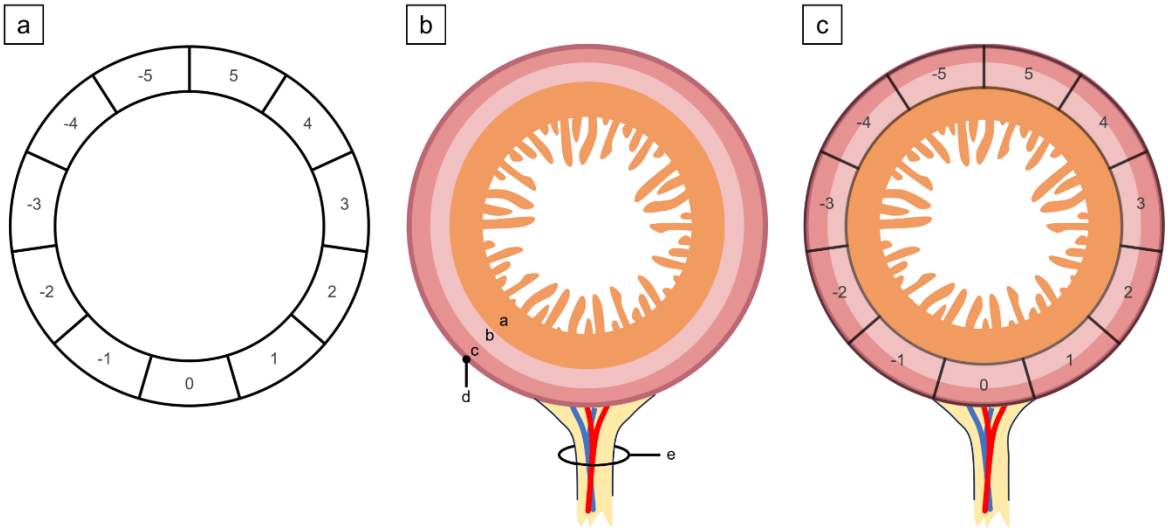

Figure 16. Location analysis of anastomotic leakage and bursting in small intestinal anastomoses. (a) The circular section model depicts the anastomoses partitioned into eleven equidistant sections, designated by numbers ranging from -5 to 5. The reference point, 0 (or M0), precisely indicates the location of the mesenteric attachment to the intestine. (b) Schematic cross-section of the small intestine. (c) The composite presentation of (a) and (b) provides insights into the spatial distribution of the eleven equidistant sections. a = Tunica mucosa; b = Tunica submucosa; c = Tunica muscularis; d = Tunica serosa; e = Mesentery. *(Adapted from Cira et al., Langenbecks Arch Surg 2024)* [2]

After marking the locations of leakage and bursting based on the corresponding images of each anastomosis, the number of occurrences per zone was assessed for each experimental trial. Comparisons were made to explore the occurrence of leakage and bursting between the mesenteric and peripheral zones within each experimental series and across different experimental groups. Additionally, a general comparison was performed to determine if leakage and bursting tended to manifest more frequently in either the mesenteric or peripheral zone across all experimental groups. (**Figure 17**)

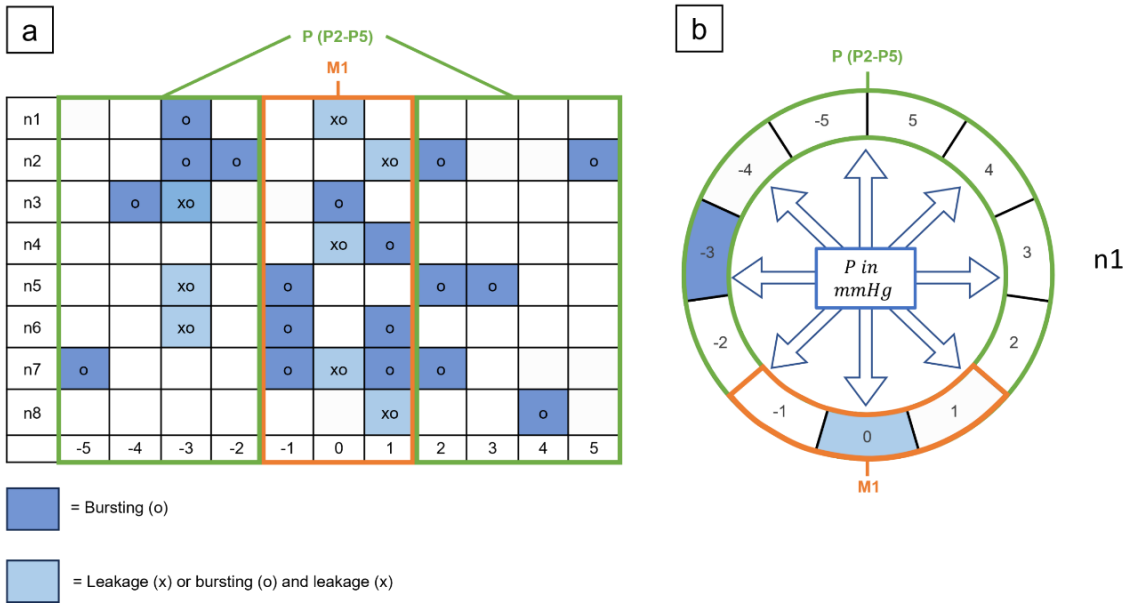

Figure 17. Location analysis: Spatial distribution of anastomotic leakage and bursting in small intestinal anastomoses. (a) To simplify data evaluation and presentation, the circular sections were transformed into a linear grid, with 0 at the center, -5 to the far left, and 5 to the far right. The grid was further divided into two zones: the mesenteric zone (between -1 and +1, labeled as zone M1) and the peripheral zone (ranging from -2 to -5 and +2 to +5, labeled as zone P (P2-P5)). Leakage points are marked with "x" and bursting points with "o". (b) The circular section model represents $n1$ on the grid. *(Adapted from Cira et al., Langenbecks Arch Surg 2024)* [2]

4. Statistical analysis

The content presented in **Chapter III.4** has been adapted and modified from the publication authored by Cira et al., 2022 [1], and Cira et al., 2024 [2]. Outcomes with a probability value (p) $p < 0.05$ in this study are considered as significant.

4.1 Meta-analyses

4.1.1 Statistical software

All statistical analyses conducted for both systematic reviews and meta-analyses were carried out using two computer software tools:

1. Review Manager (RevMan) software version 5.3. (*Nordic Cochrane Centre, Copenhagen, Denmark*) – recommended by the Cochrane Handbook for Reviews of Interventions [104]
2. JASP Team (*2021; JASP (Version 0.16) [Computer software])*

4.1.2 Meta-analysis of dichotomous outcomes

For the meta-analysis of dichotomous outcomes, the RevMan software applies the Mantel-Haenszel method [129] for both fixed-effect (FE) and random-effect (RE) model meta-analyses.

A CI of 95 % was used for all calculations. By definition,

> "A confidence interval quantifies that, if the same population is sampled on numerous occasions and interval estimates are made on each occasion, the resulting intervals would include the true population parameter in (approximately) 95 % of the cases." *Kaptein, M. and van den Heuvel, E. (2022). Statistics for Data Scientists: An Introduction to Probability, Statistics, and Data Analysis (2. Edition). Switzerland. Springer, Cham, 2022. Pp. 258.) [130]*

4.1.2.1 Odds ratio

The primary effect size used for the analyses of dichotomous outcomes included in this thesis was the OR with a CI of 95 %.

By definition,

"The *odds ratio* compares the odds for the exposed group with the odds for the unexposed group. The *odds* is a measure of how likely the outcome occurs with respect to not observing this outcome" *(Kaptein, M. and van den Heuvel, E. (2022). Statistics for Data Scientists: An Introduction to Probability, Statistics, and Data Analysis (2. Edition). Switzerland. Springer, Cham, 2022. Pp. 91.)[130]*

The OR can be calculated as follows:

$$\boldsymbol{OR} = \left(\frac{(\boldsymbol{A_E}/\boldsymbol{B_E})}{(\boldsymbol{A_C}/\boldsymbol{B_C})}\right) \qquad \text{Odds ratio (1)}$$

The numerator in equation (1) describes the odds of an event occurring in the experimental group and is calculated by dividing the number of events in the experimental group A_E by the number of non-events in the experimental group B_E. The denominator describes the odds of an event occurring in the control group and is calculated by dividing the number of events in the control group A_C by the number of non-events in the control group B_C. [131]

An OR of one ($OR = 1$) indicates that the odds for an event occurring are the same for the experimental group and control group. If the OR is greater than one ($OR > 1$), the experimental group has higher odds for an event to occur than the control group. If the OR is smaller than one ($OR < 1$), the control group has higher odds for an event to occur than the experimental group. [130, 131]

4.1.3 Meta-analysis of continuous data

Meta-analysis for continuous data was conducted by using an inverse variance method, calculating the mean difference (MD), employing the FE or RE meta-analyses, depending on the level of heterogeneity. The MD measures the absolute risk between the mean value in the experimental group and control group, estimating the amount of difference between the averages of the two groups. [131]

Since this approach can only be used when outcomes are reported on the same scale [131], the Box-Cox method proposed by McGrath et al. [132] served as a tool to estimate the sample mean and SD in cases where the data were given in the unit "median (interquartile range)" or "median (range: minimum – maximum)". This method was chosen because the authors reported overcoming several limitations of already existing methods. [132]

4.1.4 Analysis for heterogeneity

Systematic reviews and meta-analyses compare studies with a common question but may exhibit methodological or clinical diversity. Studies can differ in design, risk of bias, participants, intervention, and outcomes. This methodological and/ or clinical diversity could be responsible for discrepancies observed in study results. Statistical heterogeneity manifests as a substantial difference (variability) between the observed intervention effects (true effects) of the compared studies, and the variability between study results is not likely to be caused by a random error (chance) alone. Substantial statistical heterogeneity might influence the conclusion of systematic reviews and meta-analyses and should, therefore, be quantified. [133]

In accordance with the recommendations in the Cochrane Handbook for Reviews of Interventions [104, 134], the heterogeneity among included studies was analyzed by applying the chi squared (χ^2 or Chi^2) test and statistical I-squared I^2 – test [133]. The Chi^2-test serves as a tool to evaluate whether observed differences between studied groups are compatible with chance alone. Since this test presents reduced power with studies of a small sample size

or a small number of studies being compared in the meta-analysis, the statistical I^2 – test was conducted as well to quantify the inconsistency among the investigated studies and to assess the impact of heterogeneity on the results of the conducted meta-analysis. [104, 134]

The I^2 is calculated as follows:

$$\boldsymbol{I^2 = \left(\frac{Q - df}{Q}\right) \times 100\,\%} \qquad I^2 \text{– test (2)}$$

The numerator in equation (2) is the difference of the chi-squared statistic Q and the degree of freedom (df). This difference is then divided by Q. The resulting value is multiplied by 100 to describe the percentage of variability in effect estimates due to heterogeneity. [104, 133, 134]

A guide for the interpretation of the I^2 is given in the Cochrane Handbook for Reviews of Interventions [104, 134]:

1. The heterogeneity among included studies might not be important with an I^2 value range between 0 – 40 %.
2. The heterogeneity among included studies might be moderate with an I^2 value of 30 – 60 %.
3. The heterogeneity among included studies might be substantial with an I^2 value of 50 – 90 %.
4. The heterogeneity among included studies might be considerable with an I^2 value of 75 – 100 %.

For 2. – 4., the interpretation of the significance of observed heterogeneity requires consideration of both the magnitude and direction of effects, as well as the strength of evidence indicated by the p-value from the Chi^2-test. [104, 133, 134]

For the systematic reviews and meta-analyses included in this thesis, a statistical I^2 of ≥ 50 % or a statistically significant Chi^2-test (p-value ≤ 0.05) were considered as indicative of

substantial heterogeneity. In the presence of substantial heterogeneity, the RE meta-analysis was employed. Conversely, when the statistical I^2 was < 50 % or the Chi^2-test was statistically insignificant (p-value > 0.05) the FE meta-analysis was used.

4.1.5 Sensitivity analysis

The sensitivity analysis was conducted for all analyses, regardless of heterogeneity, to assess the stability and the robustness of observed outcomes. The effect of excluding one study at a time on the pooled OR with 95 % CI was evaluated.

4.1.6 Analysis for publication bias

Whether research results are published or not can depend on their statistical significance, as there is a chance that researchers or journals may choose to publish significant findings over non-significant ones. [134, 135] Additionally, external funding of research by government agencies or industries with potential commercial interest has been shown to influence the publication of research results. [136-141] The bias resulting from the non-reporting of specific results or entire studies could potentially introduce significant bias into reported outcomes and scientific conclusion.

A historical example illustrating how non-reporting can influence the conclusion of scientific findings was described by Kirsch et al. [142]. The authors investigated the true effect of antidepressants, specifically selective serotonin re-uptake inhibitors, in treating depression – a treatment considered effective in the 1990s after meta-analyses of published pharmacotherapy trials were conducted, comparing the effects of selective serotonin re-uptake inhibitors to placebos. Kirsch et al. [142] retrieved unpublished data from previously conducted antidepressant trials, data that were not included in the earlier published meta-analyses but were available at the FDA (provided by the pharmaceutical industry). When considering the unpublished data and re-conducting the analyses, the authors found minimal to no statistically significant differences in the effect of selective serotonin re-uptake inhibitors compared to

placebos in treating depression. The author claimed that this outcome serves as an example of how pharmaceutical companies' non-reporting of negative results, coupled with the reporting of favorable results, can impact the overall outcomes of meta-analyses and thus bias evidence. [142]

Therefore, it is crucial to assess for publication bias in the meta-analyses conducted in this thesis. To evaluate for potential publication bias, the Cochrane Handbook for Reviews of Interventions [104] recommends testing for funnel plot asymmetry, also known as the small study effect. [134, 143] The small study effect describes the tendency of small trials to differ in their estimated intervention effects from those reported in larger studies. This difference might arise, for example, from the poor methodologic quality of small studies, which can result in larger intervention effect estimates and, consequently, cause funnel plot asymmetry (plotting sample size against effect estimates). In 1997, Eggers et al. [144] proposed an approach to test for funnel plot asymmetry on the natural logarithm (log) scale of OR, using linear regression:

$$\boldsymbol{SND} = \boldsymbol{a} + \boldsymbol{bx}\,\mathbf{precision}$$

Egger's Test Formula for Funnel Plot Asymmetry on the Log Scale of Odds Rati (3)

Equation (3) displays the regression equation in which the standard normal deviate SND (OR divided by its standard error (SE)) is regressed against the estimate's precision (inverse of the SE). [144]

For meta-analyses conducted in this thesis, the Egger's test [144] was employed to assess potential publication bias, and funnel plots were graphically demonstrated. This test was used for meta-analyses of outcomes reported by ten or more studies, as the statistical power of this test would be low with fewer studies. [104, 143]

The statistical software used for conducting the Egger's test [144] was JASP Team. The effect size, represented by the log of the OR ($\log(OR)$), and the effect size SE, corresponding

to the log of the SD of the OR ($\log(SE)$), were extracted using the calculator function in RevMan software version 5.3. Subsequently, this data was transferred to a Microsoft Excel spreadsheet. The excel spreadsheet XML (xlsx) file was converted to a comma-separated values file (CSV) and uploaded in the statistical software JASP Team.

When meta-analyses were conducted using a FE model in the RevMan software, the analyses were also performed with the FE model in JASP Team. For meta-analyses conducted using the RE model in the RevMan software, the DerSimonian-Liard (RE) [134, 145] method was utilized for calculation. The software calculates a p-value and a z-value for the Egger's regression test for funnel plot asymmetry. [144]

4.1.7 Subgroup analysis

Studies investigated in meta-analyses exhibit methodological and clinical diversity, which has the potential to influence observed outcomes. Such diversities might introduce major heterogeneity among the included studies or mask significant results, especially for specific patient groups. [104, 134]

One approach to evaluating whether the different methodological or clinical methods used in the investigated studies might affect the overall outcome is to perform subgroup analyses. Study data are categorized according to defined subgroups, evaluating defined parameters such as study design, risk of bias or intervention used, among others. [134]

Careful planning of subgroup analyses is of utmost importance since conducting many different subgroup analyses carries the risk of producing false positive or false negative results, potentially leading to misleading conclusions. [134]

All subgroup analyses were conducted with the RevMan software. Subgroup differences were assessed and reported utilizing the test for subgroup differences (TSD). A subgroup difference was considered statistically significant if the p-value of the TSD was < 0.05.

Subgroup analyses for all meta-analyses conducted in this thesis were planned a priori to assess the potential effect of risk factors on postoperative outcomes and were conducted in a secondary analysis.

4.1.7.1 Systematic review and meta-analysis of human studies

For the systematic review and meta-analysis of human studies, subgroups were prespecified according to:

1. study design
    a. RCTs
    b. NRSs
    c. observational studies
    d. unknown study design
2. age group
    a. pediatric patient group
    b. adult patient group
    c. unknown age group
3. indication for surgery
    a. underlying disease
4. anatomic location of intestinal anastomoses
    a. esophagus
    b. stomach
    c. small intestine
    d. colon and/ or rectum
5. intervention used (C-BLB; FS)

4.1.7.2 Systematic review and meta-analysis of animal studies

For the systematic review and meta-analysis of animal studies, subgroups were prespecified according to:

1. animal species
2. anatomic location of intestinal anastomoses
    a. esophagus
    b. stomach
    c. small intestine
    d. colon and/ or rectum
3. anastomotic technique
    a. sutured intestinal anastomoses
    b. non-sutured intestinal anastomoses
4. sufficiency of anastomotic technique
    a. complete (sufficient) intestinal anastomoses
    b. incomplete/ partial (insufficient) intestinal anastomoses
    c. unknown sufficiency of intestinal anastomoses)

4.2 Feasibility study and functional validation of the innovative *ex-vivo* model

4.2.1 Statistical software

All statistical analyses conducted in the experimental part of this thesis were carried out using two computer software tools:

1. Microsoft Excel (*Version 2307; Microsoft, Redmond, WA*) was employed for generating descriptive statistics related to the quantitative analysis of anastomotic

performance, time intervals, and other interrelated analyses derived from experimental outcomes.

2. GraphPad Prism (*Version 8.0.2. San Diego, CA: GraphPad Software, 2020*) was utilized to create graphs representing the experimental data and to conduct the Mann-Whitney U test [146, 147] and Fisher's exact test [148] for further statistical analysis.

4.2.2 Quantitative analysis of anastomotic performance, time intervals and interrelated analyses derived from experimental outcomes

4.2.2.1 Comparison within the experimental group

The quantitative analysis of anastomotic performance and time intervals, as detailed in **Chapter III.3.3.5.1.1 – 3.3.5.1.4**, was conducted using the descriptive statistics function in Microsoft Excel. This analysis involved calculating the 95 % CI and summary statistics to provide a comprehensive assessment of the data. The statistical parameters derived from this analysis included Mean; Standard error of the mean SEM; Median; SD ; Sample Variance; Kurtosis; Skewness; Range; Minimum; Maximum; Sum; Count; Confidence Level (95.0 %). To obtain the Upper and Lower CI (95 %), the mean was added to the CI and subtracted from it, respectively.

For comparing results within an experimental series (LP, BP, analysis of time intervals), as described in the data analysis section (**Chapter III.3.3.5.2**), a subsequent comparison was conducted in Microsoft Excel. Descriptive statistics were used, and upper and lower CI were calculated. The interrelated analyses derived from the experimental data were also performed in Microsoft Excel. LP and BP within each group were presented with mean, SD, 95 % CI, upper to lower CI, as well as the calculated median and range (minimum-maximum). Additionally, the sample variance and measured distribution (Kurtosis, skewness) were provided.

For the "Proportion of BP at LP", the LP was subtracted from the BP in Microsoft Excel, and the results were presented using mean, SD, 95 % CI, median and range (minimum-maximum). The sample variance and measured distribution (Kurtosis, skewness) were also reported.

The "Percentage of BP at LP" was calculated in Microsoft Excel by dividing the LP by the BP and then multiplying the result by 100 to express it as a percentage. The "Relative Difference of Pressure between Leakage and Bursting" was also calculated in Microsoft Excel by subtracting the calculated "Percentage of BP at LP" from 100. Both results were presented with mean percentage and SD.

The time analysis was conducted using descriptive Microsoft Excel analysis (as previously described) and presented in $msec$ with mean and SD. The "Time of Leakage Occurrence Relative to Bursting Time" was calculated in Microsoft Excel by dividing the time interval (from start to LP, in $msec$) by the time interval (time from start to BP, in $msec$) and then multiplying the results by 100. The "Relative Difference of Time between Leakage and Bursting Time" was calculated by subtracting the calculated "Time of Leakage Occurrence Relative to Bursting Time" from 100. Both results were calculated using descriptive Microsoft Excel statistics and presented with mean and SD.

The graphs presenting the experimental data were generated using GraphPad Prism software.

4.2.2.2 Comparison between the experimental groups

The Mann-Whitney U test [146, 147] was employed to compare the outcomes of the quantitative analysis of anastomotic performance, time intervals, and interrelated analyses derived from experimental outcomes among the different experimental groups. This non-parametric test is suitable for comparing two independent groups when the data is not normally distributed or when the sample sizes are small.

4.2.3 Leakage and bursting location analysis

The Fisher's exact test [148], a statistical tool suitable for analyzing categorical data with small sample sizes, was employed to analyze and compare the incidence of leakage and bursting within and between areas of the anastomosis – specifically, the mesenteric zone and peripheral zone – across each of the four experimental groups.

The OR was used in this study to assess the association and quantify the strength of relationships between different aspects of anastomotic performance, with a particular focus on leakage and bursting rates at specific locations within the anastomosis.

4.2.3.1 Comparison within the experimental group

For the analysis of leakage and bursting rates, the Fisher's exact test [148] was used to determine significant differences in the occurrence of leakage or bursting at the mesenteric zone and other sections of the anastomosis (peripheral zone) within each experimental group.

4.2.3.2 Comparison between the experimental groups

The Fisher's exact test [148] was utilized to investigate and compare the incidence of leakage and bursting within specific areas of the anastomosis, namely the mesenteric zone and peripheral zone, among the different experimental series. This statistical analysis provides insights into potential variations in these rates, enabling a comprehensive assessment of anastomotic performance.

Therefore, the Fisher's exact test [148] was used to assess whether there were significant differences in the incidence of leakage or bursting at the mesenteric or peripheral zone of the anastomoses between the different experimental series.

Similarly, for the comparison of bursting rates between areas of the mesenteric zone and peripheral zone, the Fisher's exact test [148] was employed to investigate whether there were significant differences in the incidence of bursting at the mesenteric zone compared the

peripheral zone within each experimental series. The OR derived from the test offer information about the probability of bursting occurrence in the mesenteric zone compared to the peripheral zone.

IV Results

1 Systematic review and meta-analysis of human studies

The content presented in **Chapter IV.1** has been adapted and modified from the publication authored by Cira et al., 2022.[1]

1.1. Final database search on January 17, 2022

Using predefined search items, as depicted in **Supplementary Table 1**, 1,581 studies were identified through an electronic database search. Specifically, 445 search items were identified in the PubMed database, 241 in the Cochrane Library, 371 in Scopus, and 524 in Web of Science. Among these, 382 search items were removed before literature screening due to duplicates. Initially, duplicates were removed using the automation tool EndNote, and a manual duplicate removal was also undertaken. After excluding duplicates, a manual screening of titles and abstracts was performed for 1,199 studies according to predefined inclusion criteria (**Chapter III.1.1.1 – 1.1.2**), out of which 1,142 search items were excluded due to a lack of eligibility.

As a result, 57 eligible studies were acquired for full-text analysis, but 35 studies' full texts could not be retrieved. Out of the 22 eligible studies with full text available, ten studies were excluded after full-text analysis as they either lacked a control group ($n = 5$), applied other interventions ($n = 4$), or had an irrelevant endpoint ($n = 1$). The electronic database search yielded twelve eligible studies [58-64, 66-69, 149] after full-text analysis, which were included in the systematic review.

In addition to the electronic database search, another eleven studies were identified through citation searches ($n = 8$) and websites ($n = 3$) (referred to as "other methods"). Of these, eight studies were excluded as they did not include the formation of an anastomosis.

The website and citation search yielded 3 eligible full-text studies [65, 70, 71] which, after full-text analysis, were included in the systematic review.

Collectively, the electronic database search and the citation and website search yielded 15 eligible full-text studies, which were systematically reviewed, and their data were analyzed quantitatively and qualitatively for inclusion in the meta-analysis. (**Figure 18**)

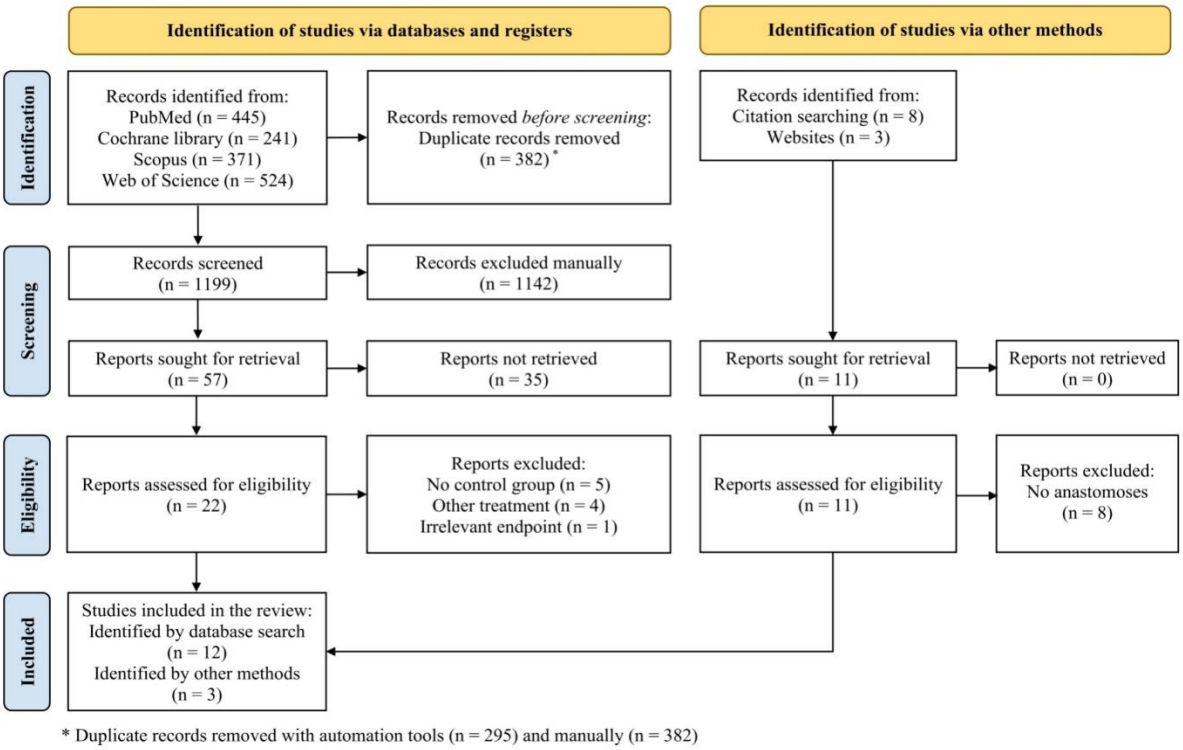

Figure 18. Study flow diagram according to the Preferred Reporting Items for Systematic Review and Meta-Analyses (PRISMA) Statement 2020 [150]. *(Adapted from the publication authored by Cira et al., Front Surg 2022)* [1]

1.2. Study characteristics

In total, five RCTs [58, 60, 62, 63, 65] and three NRSs [59, 61, 64] were identified. Among these, four studies adopted a retrospective cohort study design (RCSs) [66, 67, 69, 70], two studies employed a prospective cohort study design (PCS) [68, 71], and one abstract [149] was analyzed. The included studies spanned the period from 1997 to 2021 and were conducted in various countries, including China [67], Egypt [71], France [66], Greece [62], India [65], Italy [63, 70], Korea [68, 69], Mexico [61], Spain [58, 60, 64], Switzerland [149], and the

USA [59]. Overall, 3,630 patients were included in 15 studies [58-71, 149], with 1,387 patients receiving an intervention, while 2,243 served as controls.

Most studies reported the mean (SD) or median (range) age of included patients [58, 61, 63, 64, 66-68, 70, 71]. Only one study's [63] intervention group was significantly older compared to the control group ((mean (SD): 42.8 $\pm$ 11.7 years vs. mean (SD) 39 $\pm$ 11.6 years; $p = 0.02$). The majority of studies [58-60, 62-64, 66-71] focused on adult patients, while two studies [61, 65] examined pediatric patients.

Most included studies [58, 60-64, 67, 68, 70, 71] provided information on the sex distribution of patients, and no significant differences were found. As BMI (kg/m^2) was identified as an individual risk factor for postoperative complications, the review assessed whether there was a difference in BMI (kg/m^2) between the intervention and control groups. Five studies reported the mean (SD) BMI (kg/m^2) [63, 66-68], but no significant difference was observed between the intervention and control groups. Details of the baseline characteristics analyzed are depicted in **Table 1**.

The included studies investigated adult patients undergoing intestinal surgery for benign lesions (e.g., inflammatory bowel disease, diverticulitis, or any kind of non-malignant intestinal obstruction) [60, 66, 71], malignant tumors [58, 62, 64, 66-70, 149], or bariatric surgery due to morbid obesity [59, 63]. Pediatric patients [61, 65] underwent intestinal surgery either due to esophageal atresia with tracheoesophageal fistula [65] or caustic esophageal injury [61].

Furthermore, the included studies described different anastomotic techniques and locations in the gastrointestinal tract. Anastomoses were either located in the esophagus/ esophagogastric junction or esophagojejunal [58, 61-63, 65, 67, 70], gastro-jejunal [59, 70], small intestine [63], colon or colorectal [66, 68, 69, 71, 149], or distributed in different parts of the gastrointestinal tract [60, 64]. Moreover, open [58-62, 65, 67, 69, 71, 149] or laparoscopic

[59, 62, 63, 67, 68, 149] surgical approaches were performed. Different intestinal anastomotic techniques and suture materials were utilized [58-71, 149].

In the intervention group, C-BLBs were employed in 252 patients to cover the anastomoses [64, 66, 70], while FSs were utilized more frequently, specifically in 1,135 cases [58-63, 65, 67-69, 71, 149]. Intestinal anastomoses of patients in the intervention group were externally reinforced or covered with either C-BLBs (*Collatamp* or *TachoSil*) [64, 66, 70] or FSs (*Tisseel, Tissucol, Greenplast, Bioseal* or *Quixil*) [58-63, 65, 67-69, 71, 149]. Conversely, patients in the control group underwent the same surgical procedure as the intervention group but without covering the anastomoses. **Table 2** provides further details regarding surgical characteristics, including type and location of procedures, the number of surgeons performing surgeries on included patients, the surgical procedure in the intervention group and control group, anastomotic technique and suture material, details of intervention in the intervention group with type of collagen and/ or fibrin-based sealant, and any additional interventions in the intervention and control group.

Regarding postoperative complications, AL was most commonly assessed, as observed in a total of 14 studies [58-65, 67-71, 149]. A significantly lower AL rate was found within the intervention group compared to the control group in five studies [59, 60, 65, 67, 69]. Reoperation rates were evaluated for six studies [58-60, 63, 64, 149], out of which two studies [60, 63] found reoperations to occur significantly less commonly in patients with covered anastomoses. A significant lower Clavien-Dindo major complication (C-DMC) rate was found in the intervention group in one study [66] out of two studies [66, 67]. Mortality rates were reported by seven studies [58, 60, 61, 63, 65, 67, 70], with no significant difference between study groups described. The length of hospitalizations (days) was assessed in seven studies [58, 61, 63, 66-68, 70, 71], out of which four studies [58, 66, 67, 70] reported a significantly shorter hospitalization length in the intervention group. Further details on postoperative complications assessed in the included studies are depicted in **Table 3.**

IV Results

Table 1. Study and patient characteristics. *(Adapted from the publication authored by Cira et al., Front Surg 2022)* [1]

Table 1. Study and Patient Characteristics

Author	Year	Country	Study design	Age group	Number of patients, n		Anastomotic coating (intervention group)	Indication for surgery
					I	C		
Brehant et al. [66]	2013	France	RCS	Adult	202	404	Collatamp sponge (C-BLB)	Colorectal cancer; Benign lesions
Marano et al. [70]	2016	Italy	RCS	Adult	28	34	TachoSil (C-BLB)	Gastric cancer; Esophagogastric junction cancer
Torres-Melero et al. [64]	2016	Spain	NRS	Adult	22	27	Fibrin-coated collagen sponge (C-BLB)	Peritoneal carcinomatosis (colorectal cancer)
Fernandez et al. [58]	1996	Spain	RCT	Adult	42	44	Tissucol (FS)	Gastric adenocarcinoma
Grieder et al. [149][a]	2010	Switzerland	Pilot-Study	Adult	118	113	Fibrin glue (FS)	Colorectal cancer
Huang et al. [67]	2021	China	RCS	Adult	86	141	Bioseal (FS)	Squamous cell or adenocarcinoma of the thoracic or esophagogastric junction
Huh et al. [68]	2010	Korea	PCS	Adult	104	119	Tissucol or Greenplast (FS)	Rectal cancer
Kim et al. [69]	2013	Korea	RCS	Adult	414	734	Tissucol or Greenplast (FS)	Rectal cancer
Liu et al. [59]	2003	USA	NRS	Adult	120	360	Tisseel (FS)	Obesity (bariatric surgery)
Oliver et al. [60]	2012	Spain	RCT	Adult	52	52	Tissucol Duo (FS)	Different conditions (high-risk anastomoses)
Saldaña-Cortés et al. [61]	2009	Mexico	NRS	Pediatric	14	24	Quixil (FS)	Caustic esophageal injury
Sdralis et al. [62]	2019	Greece	RCT	Adult	35	22	Tisseel (FS)	Adenocarcinoma of distal esophagus or esophagogastric junction
Sieda et al. [71]	2015	Egypt	PCS	Adult	35	35	Commercial FS	Malignant colonic obstruction; Non-malignant colonic Obstruction
Silecchia et al. [63]	2006	Italy	RCT	Adult	93	111	Tissucol (FS)	Obesity (Bariatric Surgery)
Upadhyaya et al. [65]	2007	India	RCT	Pediatric	22	23	Tisseel (FS)	Esophageal Atresia with Tracheoesophageal Fistula

RCS = Retrospective cohort study; PCS = Prospective cohort study; RCT = Randomized controlled trial; NRS = non-randomized study; I = Intervention group (coated or reinforced anastomoses); C = Control group; C-BLB = Collagen-based laminar biomaterial; FS = Fibrin sealant; Benign lesions: Diverticulitis, inflammatory bowel disease, or other lesions; Non-malignant colonic obstruction: Perforated diverticulum, inflammatory bowel disease, volvulus, fecal fistula, bands.
[a] Abstract.

Table 2. Surgical characteristics. *(Adapted from the publication authored by Cira et al., Front Surg 2022)* [1]

Table 2. Surgical characteristics

Author	Year	Open/ laparoscopic	Surgical intervention	Site and technique of anastomosis	
				I / C	Anastomotic covering/ reinforcement (I)
Brehant et al. [66]	2013	✓/✓	Colon or colorectal resection	Intestinal anastomosis	Collatamp (10 x 10 cm)
Marano et al. [70]	2016	✓/-	Total or distal gastric resection; Distal esophagectomy and total gastrectomy	Mechanical ES esophagojejunal anastomosis (25 mm anvil head circular stapler); Mechanical SE gastrojejunal anastomosis (28 mm anvil head circular stapler)	TachoSil (9.5 x 4.8 x 0.5 cm with two seromuscular stitches)
Torres-Melero et al. [64]	2016	N/A	Debulking colon resection	Mechanical intestinal anastomosis	Fibrin-coated collagen sponge (9.5 x 4.8 cm)
Fernandez et al. [58]	1996	N/A	Curative R_2 or extended gastrectomy	Mechanical ES esophagojejunal anastomosis (Roux-en-Y jejunal loop used; Tobacco pouch formed manually)	Tissucol (applied on both surfaces during approximation of anvil to the stapler cartridge)
Grieder et al. [149][a]	2010	✓/✓	Colorectal resection	Mechanical intestinal anastomosis (approximately ten cm above anal verge)	Fibrin glue (1 ml; applied between pressure plates of stapler, fired after 2-3 min)
Huang et al. [67]	2021	✓/✓	McKeown esophagectomy	Mechanical ES esophagogastric anastomosis (inverted; Circular stapler: EEA 21 or 25 mm)	Bioseal (2.5 ml)
Huh et al. [68]	2010	-/✓	Low anterior rectal resection	Double-stapled colorectal anastomosis	Tissucol or Greenplast (1-2 ml)
Kim et al. [69]	2013	✓/✓	Low anterior rectal resection with total mesorectal excision	Double-stapled colorectal anastomosis	Tissucol or Greenplast (1-2 ml)
Liu et al. [59]	2003	✓/✓	Roux-en-Y-gastric bypass	Handsewn gastrojejunal anastomosis	Tisseel (5 ml; perivisceral fat pad glued to anterolateral part of anastomosis)
Oliver et al. [60]	2012	N/A	Esophageal resection; Roux-en-Y-gastric bypass; Gastrectomy; Rectal resection; Intestinal resection of obstructed segment	Intestinal anastomosis (according to procedure)	Tissucol
Saldaña-Cortés et al. [61]	2009	✓/-	Colon interposition for esophageal reconstruction	Handsewn, single layer, ES cervicocolic anastomosis covered (4-0 Vicryl)	Quixil (3-4 ml)
Sdralis et al. [62]	2019	✓/✓	Two-stage esophagectomy – Ivor-Lewis procedure	Intrathoracic mechanical ES esophagogastric anastomosis (Circular stapler: CDH (model number) 25 or 29 mm)	Tisseel
Sieda et al. [71]	2015	✓/-	Enterocolic resection or colectomy	Handsewn, single layer, enterocolic or colocolic anastomosis (CS, 3-0 Vicryl)	Fibrin sealant
Silecchia et al. [63]	2006	✓/-	Roux-en-Y-gastric bypass	Mechanical or handsewn gastrojejunal anastomosis (Gagner technique with circular stapler 25 EEA; Linear stapler; Two-layer CS);Jejujejunal anastomosis	Tissucol (2- or 5- ml)

Upadhyaya et al. [65]	2007	✓/-	Esophageal reconstruction	Handsewn, single layer, ES esophageal anastomosis (5-0 Vicryl)	Tisseel

N/A = not available; ✓= Yes; - = no; I = Intervention group (coated or reinforced anastomoses); C = Control group; CS = Simple continuous suture technique; ES = End-to-side; SE = Side-to-end; EEA = End-to-end anastomosis.
[a] *Abstract.*

Table 3. Postoperative outcomes. *(Adapted from the publication authored by Cira et al., Front Surg 2022)* [1]

Table 3. Postoperative outcomes.

Author	Year	Anastomotic leakage, n (%)		Reoperation, n (%)		Clavien-Dindo major complications [151], n (%)		Length of hospitalization, mean (SD) [b]; in Days		Mortality, n (%)	
		I	C	I	C	I	C	I	C	I	C
Brehant et al. [66]	2013	N/A	N/A	N/A	N/A	↓**18 (9)**	↑**67 (16.6)**	↓	↑	N/A	N/A
Marano et al. [70]	2016	0 (0)	4 (11.8)	N/A	N/A	N/A	N/A	↓ **14.7 ± 4.3**	↑ **19.9 ± 5.6**	0 (0)	0 (0)
Torres-Melero et al. [64]	2016	0 (0)	3 (11.1)	1 (4.6)	3 (11.1)	N/A	N/A	N/A	N/A	N/A	N/A
Fernandez et al. [58]	1996	0 (0)	4 (9)	0 (0)	0 (0)	N/A	N/A	N/A	N/A	0 (0)	0 (0)
Grieder et al. [149] [a]	2010	5 (4.2)	9 (8)	3(2.5)	9 (8)	N/A	N/A	N/A	N/A	N/A	N/A
Huang et al. [67]	2021	↓**4 (4.7)**	↑**28 (19.4)**	N/A	N/A	12 (14)	28 (20)	↓**12.11 ± 3.86**	↑**15.51 ± 9.54**	0 (0)	2 (1.4)
Huh et al. [68]	2010	6 (5.8)	13 (11)	N/A	N/A	N/A	N/A	9.46 ± 2.37	9.81 ± 3.03	N/A	N/A
Kim et al. [69]	2013	↓**17 (4.1)**	↑**59 (8)**	0 (0)	7 (1)	N/A	N/A	N/A	N/A	N/A	N/A
Liu et al. [59]	2003	↓**0 (0)**	↑**8 (2.2)**	↓**3 (2.5)**	↑**12 (3.3)**	N/A	N/A	N/A	N/A	N/A	N/A
Oliver et al. [60]	2012	↓**7 (13.5)**	↑**15 (28.9)**	N/A	N/A	N/A	N/A	N/A	N/A	3 (5.8)	4 (7.7)
Saldaña-Cortés et al. [61]	2009	4 (28.6)	12 (50)	N/A	N/A	N/A	N/A	12.6 ± 2.6	12.9 ± 2.6	1(7.1)	1 (4.1)
Sdralis et al. [62]	2019	5 (14.3)	3(13.7)	N/A	N/A	N/A	N/A	N/A	N/A	N/A	N/A
Sieda et al. [71]	2015	3 (8.6)	7 (20)	N/A	N/A	N/A	N/A	5 ± 1.7	7 ± 2.3	N/A	N/A
Silecchia et al. [63]	2006	0 (0)	2 (1.8)	↓**0 (0)**	↑**8 (7.2)**	N/A	N/A	7.0 ± 1.6	7.0 ± 1.8	0 (0)	0 (0)
Upadhyaya et al. [65]	2007	↓**2 (9.1)**	↑**10 (43.5)**	N/A	N/A	N/A	N/A	N/A	N/A	2 (9.1)	6 (26)

↓ *= Significantly lower;* ↑ *= Significantly higher; N/A = not available; I = Intervention group (coated or reinforced anastomoses); C = Control group.*

[a] *Abstract.*

[b] *if given in "median (interquartile range)" or "median (range: minimum-maximum)", values were converted using Box-Cox (BC) method of McGrath et al. 2020 [132] to estimate the sample mean and standard deviation.*

1.3. Risk of bias assessment

Risk of bias assessment was performed for all full-text articles [58-71, 149], excluding one abstract [152]. (**Supplementary Table 4**)

Depending on the study design, different tools for risk of bias assessment were applied in accordance with the recommendations in Cochrane Handbook for Reviews of Interventions [104]. The RoB 2 tool [107] was used to assess the risk of bias for included RCTs [58, 60, 62, 63, 65], while the ROBINS-I tool [108] was employed for assessing the risk of bias in included NRSs [59, 61, 64]. Additionally, the NOS for cohort studies [109] was used to evaluate the overall quality of included observational studies [66-71].

1.3.1 Revised Cochrane risk of bias 2 tool for randomized controlled trials

According to the RoB 2 tool [107], applied for the risk of bias assessment of RCTs, all five included RCTs [58, 60, 62, 63, 65] were rated as having some concerns (in consensus with K. C. and F. S.). The only category rated as presenting a low risk of bias in all five RCTs [58, 60, 62, 63, 65] was the subcategory "risk of bias in selection of the reported results" within the category "post-intervention" [107].

In the category “pre-intervention” and subcategory "risk of bias die to randomization process" [107], as having at least some concerns. This is justified by Fernandez et al. [58], Sdralis et al. [62], and Silecchia et al. [63] not describing the methods of allocation concealment in their studies, while Oliver et al. [60] and Upadhyaya et al. [65] did not provide any statement on whether the allocation sequence was concealed until the participants were enrolled and assigned to interventions.

For the category "post-intervention", the subcategory "risk of bias due to deviations from intended interventions" [107] showed that all studies were rated to have some concerns:

a. Fernandez et al. [58] did not used an appropriate analysis to estimate the effect of assignment to the intervention. The study did not include any statement on whether participants were aware of their assigned interventions during the trial or whether caregivers and people delivering interventions were aware of the participants' assigned intervention during the trial. [107]

b. Oliver et al. [60] did not include any statement on whether an appropriate analysis was used to estimate the effect of assignment to the intervention. Furthermore, caregivers and people delivering interventions were aware of participants' assigned interventions during the trial. [107]

c. Sdralis et al. [62] did not include any statements in their study in whether participants were aware of their assigned intervention during the trials. Furthermore, caregivers and people delivering interventions were aware of participants' assigned intervention during the trial. [107]

d. Silecchia et al. [63] did not include any statement on whether participants were aware of their assigned intervention during the trial or whether caregivers and people delivering interventions were aware of participants' assigned intervention during the trial. [107]

e. Upadhyaya et al. [65] conducted their study with caregivers and people delivering interventions being aware of participants' assigned intervention during the trial.

In the subcategory "Risk of bias due to missing outcome data" [107], all five RCTs [58, 60, 62, 63, 65] were rated with some concerns, as there was no evidence that the results were not biased by missing outcome data, which is important as missingness in the outcome could depend on its true value.

Four studies [60, 62, 63, 65] were rated with some concerns in the subcategory "risk of bias in measurement of outcomes" [107], as they did not include any statement on whether

the outcome assessor were aware of the intervention received. Therefore, the assessment of the outcomes could have been influenced by the knowledge of intervention received. Fernandez et al. [58] was rated as well with some concerns as the study did not include any statement on whether measurement or ascertainment of the outcome have differed between intervention groups or whether outcome assessors were aware of the intervention received, which is why the assessment of the outcome could have been influenced by the knowledge of intervention received. (**Supplementary Table 4**)

1.3.2 Risk of bias in non-randomized studies - of interventions tool for non-randomized controlled studies

The three NRSs [59, 61, 64] included presented with moderate risk of bias according to the ROBINS-I tool [108] assessment.

In the category "pre-intervention" including the subcategories "bias due to confounding" and "bias in selection of participants into the study" [108], all three studies [59, 61, 64] presented with low risk of bias. Similarly the risk of bias was low in the category "at intervention" and subcategory "bias in selection of classification of interventions" [108] for all three studies [59, 61, 64]. A moderate risk of bias was present for the study conducted by Liu et al. [59] in the category "post-intervention" [108]. In the subcategory "bias due to deviations from intended interventions" [108], the study was rated to present a moderate risk of bias because the test methods differentiated between the study’s intervention and control groups. No air insufflation test of the anastomoses was undertaken in the control group, while it was in the intervention group, creating a deviation from intended interventions. [59] For the other two NRSs [3, 11], no deviations from intended interventions was recognized, which is why they were rated to be at low risk for bias in the same subcategory [108].

In the subcategory "bias due to missing data" [108], the study by Liu et al. [59] was rated to present moderate risk of bias as the outcome of data were not available for all participants.

This was not the case with the studies of Saldaña-Cortés et al. [61] and Torres-Melero et al. [64], which were rated to be at low risk of bias in this subcategory [108]. Still, all three NRSs [59, 61, 64] were rated to present moderate risk of bias in the subcategory "bias in measurement of outcomes" [108], as the study conducted by Liu et al. [59] and Saldaña-Cortés et al. [61] did not include any statement on whether the outcome assessors of the study were aware of the intervention received by study participants. The study conducted by Torres-Melero et al. [64] did not include any statement on whether outcome assessors were aware of the intervention received by study participants and whether methods for outcome assessment were comparable across intervention groups.

While the study conducted by Liu et al. [59] was rated to present a moderate risk of bias in the subcategory "bias in selection of the reported results" [108], as different subgroups were included in the study, the other two NRSs [3, 11] were rated to present a low risk of bias in this subcategory [108]. (**Supplementary Table 4**)

1.3.3 Newcastle-Ottawa Scale for cohort studies

The risk of bias assessment based on the quality assessment according to the NOS for cohort studies [109] resulted in different outcomes for the six included observational studies [66-71] evaluated. The majority of studies were rated to be of moderate quality [66-70], presenting with a NOS score of six [68] or seven [67, 69, 70]. While one study [71] was rated to be of low quality with a NOS score of four, another study appeared to be of high quality with a NOS score of eight [66].

All evaluated observational studies [66-71] lost one NOS star in the category "selection" [109] as these studies weren’t able to demonstrate that the studies’ outcome of interest was not present at the start of the study. Further, two observational studies [67, 68] lost one NOS star in the category "selection" and subcategory "representativeness of exposed cohort" [109]. The study conducted by Huang et al. [67] included only patients undergoing a specific surgical

procedure, McKeown esophagectomy, instead of including other surgical procedures to treat the same condition. In the other observational cohort study conducted by Huh et al. [68], patients undergoing the same surgical procedure but with the creation of a protective stoma were excluded.

In the category "comparability" [109], Sieda et al. [71] lost two NOS stars, one in the subcategory "comparability of the cohort on the basis of the design and analysis: controlled for critical factor" and one in the subcategory "comparability of cohort on the basis of the design and analysis: controlled for additional factor" [109] because the authors did not control for any of these factors using multivariate analysis or regression method.

The study conducted by Sieda et al. [71] further lost two NOS stars in the category “outcome” and subcategory "adequacy of follow up of cohorts" [109], as no statement was given by the authors about the adequacy of follow-up for the cohorts. Marano et al. [70], Kim et al. [69], and Huh et al. [68] lost a NOS star in the exact same category for the same reason. (**Supplementary Table 4**)

1.4. Results of meta-analysis and subgroup analyses

1.4.1. Postoperative anastomotic leakage rates

Postoperative AL rates were reported by a total of 14 studies [58-65, 67-71, 149]. Overall, among 1,185 patients in the intervention group, 53 (4.5 %) experienced AL, while in the control group, 177 (9.6 %) of 1,839 patients were reported to have AL.

Using the FE meta-analysis, AL rates were significantly lower for patients with coated anastomoses ($OR, 0.37;\ 95\ \%\ CI, 0.27-0.52;\ p\ <\ 0.00001$). The studies showed homogeneity ($I^2\ =\ 0\ \%; p\ =\ 0.84$) (**Figure 19**), and no publication bias was observed (Egger’s test [144]: $p\ =\ 0.227$). (**Table 4**)

Throughout sensitivity analyses, excluding one study at a time, the observed results (pooled OR) remained stable, as depicted in **Table 4**.

Subgroup analyses were conducted to assess the potential influence of the study design, intervention used, age group, anastomotic location, indication for surgery, and its subclassification on the observed outcome. No subgroup differences were identified for subgroups stratified by study design ($TSD: p = 0.75$), intervention used ($TSD: p = 0.33$), age group ($TSD: p = 0.40$); anastomotic location ($TSD: p = 0.63$), indication for surgery ($TSD: p = 0.66$), and its subclassification ($TSD: p = 0.45$). Further details are depicted in **Table 5.**

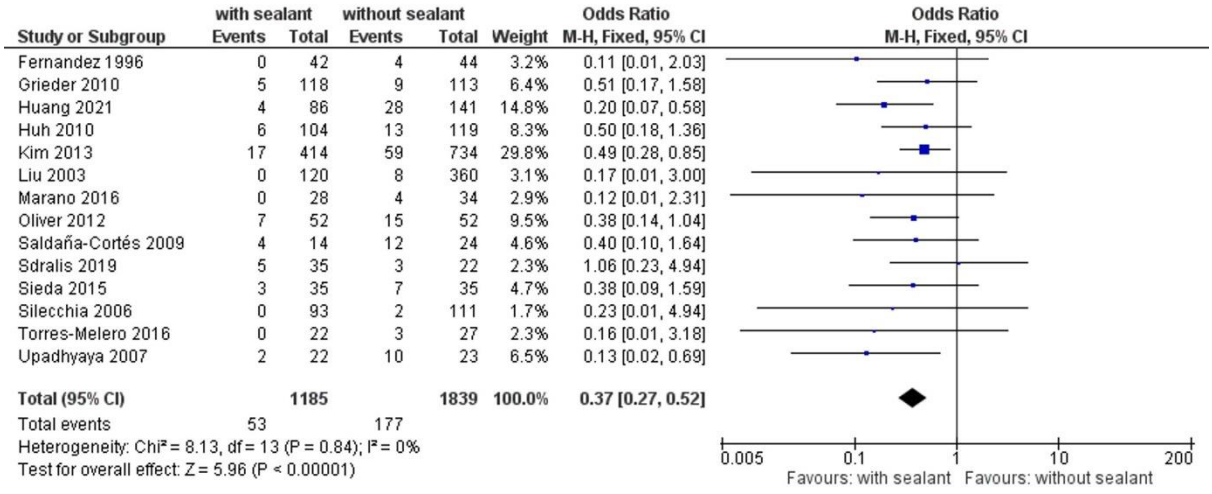

Figure 19. Fixed-effects meta-analysis for the postoperative anastomotic leakage rate in the intervention (coated or reinforced anastomoses) and control group. The forest plot of all studies is included. *(Adapted from the publication authored by Cira et al., Front Surg 2022)* [1]

1.4.2. Postoperative reoperation rates

A total of five studies [59, 60, 63, 64, 149] reported reoperation rates, occurring in seven (1.7 %) of 405 patients in the intervention group and 39 (5.9 %) of 663 patients in the control group. The reoperation rate was significantly lower for patients in the intervention group using FE model meta-analysis ($OR, 0.21;\ 95\ \%\ CI, 0.10-0.47;\ p = 0.0001$), and studies exhibited homogeneity ($I^2 = 0\ \%;\ p = 0.88$). (**Figure 20**)

IV Results

Observed results remained stable throughout sensitivity analyses, and subgroup analyses found no subgroup differences for subgroups stratified by study design ($TSD: p = 0.71$), intervention used ($TSD: p = 0.60$), anastomotic location ($TSD: p = 0.64$), and indication for surgery ($TSD: p = 0.64$). (**Table 6**)

Table 4. Fixed-effects model meta-analysis for postoperative anastomotic leakage in the intervention and control group. *(Adapted from the publication authored by Cira et al., Front Surg 2022)* [1]

Table 4. Fixed-effects model meta-analysis for postoperative anastomotic leakage in the intervention and control group.

Postoperative anastomotic leakage	**Odds ratio (OR): FE model**	**Heterogeneity**	**Egger's test**
Overall	OR, 0.37; 95 % CI, 0.27-0.52; **p < 0.00001 [↓(I); ↑(C)]**	I^2= 0 %; p = 0.84	p = 0.227
Sensitivity analyses			
Excluded Study	**OR: FE Model**	**Heterogeneity**	
Fernandez et al. [58]	OR, 0.38; 95 % CI, 0.28-0.53; **p < 0.00001 [↓(I); ↑(C)]**	I^2 = 0 %; p = 0.83	
Grieder et al. [149]	OR, 0.36; 95 % CI, 0.26-0.51; **p < 0.00001 [↓(I); ↑(C)]**	I^2 = 0 %; p = 0.79	
Huang et al. [67]	OR, 0.40; 95 % CI, 0.29-0.57; **p < 0.00001 [↓(I); ↑(C)]**	I^2 = 0 %; p = 0.90	
Huh et al. [68]	OR, 0.36; 95 % CI, 0.26-0.51; **p < 0.00001 [↓(I); ↑(C)]**	I^2 = 0 %; p = 0.79	
Kim et al. [69]	OR, 0.33; 95 % CI, 0.22-0.48; **p < 0.00001 [↓(I); ↑(C)]**	I^2 = 0 %; p = 0.84	
Liu et al. [59]	OR, 0.38; 95 % CI, 0.27-0.53; **p < 0.00001 [↓(I); ↑(C)]**	I^2 = 0 %; p = 0.80	
Marano et al. [70]	OR, 0.38; 95 % CI, 0.28-0.53; **p < 0.00001 [↓(I); ↑(C)]**	I^2 = 0 %; p = 0.82	
Oliver et al. [60]	OR, 0.37; 95 % CI, 0.27-0.53; **p < 0.00001 [↓(I); ↑(C)]**	I^2 = 0 %; p = 0.77	
Saldaña-Cortés et al. [61]	OR, 0.37; 95 % CI, 0.27-0.52; **p < 0.00001 [↓(I); ↑(C)]**	I^2 = 0 %; p = 0.77	
Sdralis et al. [62]	OR, 0.36; 95 % CI, 0.26-0.50; **p < 0.00001 [↓(I); ↑(C)]**	I^2 = 0 %; p = 0.89	
Sieda et al. [71]	OR, 0.37; 95 % CI, 0.27-0.52; **p < 0.00001 [↓(I); ↑(C)]**	I^2 = 0 %; p = 0.78	
Silecchia et al. [63]	OR, 0.38; 95 % CI, 0.27-0.52; **p < 0.00001 [↓(I); ↑(C)]**	I^2 = 0 %; p = 0.78	
Torres-Melero et al. [64]	OR, 0.37; 95 % CI, 0.27-0.53; **p < 0.00001 [↓(I); ↑(C)]**	I^2 = 0 %; p = 0.80	
Upadhyaya et al. [65]	OR, 0.39; 95 % CI, 0.28-0.54; **p < 0.00001 [↓(I); ↑(C)]**	I^2 = 0 %; p = 0.90	

↓ = Significantly lower; ↑ = Significantly higher; I = Intervention group (coated or reinforced anastomoses); C = Control group; FE = Fixed-effect.
The bold indicates significant outcomes.

Table 5. Subgroup analyses of fixed-effects model meta-analysis for postoperative anastomotic leakage. *(Adapted from the publication authored by Cira et al., Front Surg 2022)* [1]

Table 5. Subgroup analyses of fixed-effects model meta-analysis for postoperative anastomotic leakage.

Subgroup analyses		
Subgroup	**Odds ratio (OR): FE model**	**Test for subgroup difference (TSD)**
Study design		p = 0.75
RCT	OR, 0.33; 95 % CI, 0.17-0.65; **p = 0.001 [↓(I); ↑(C)]**	
NRS	OR, 0.27; 95 % CI, 0.09-0.87; **p = 0.03 [↓(I); ↑(C)]**	
OS	OR, 0.40; 95 % CI, 0.27-0.60; **p < 0.00001 [↓(I); ↑(C)]**	
Covering		p = 0.33
C-BLB	OR, 0.13; 95 % CI, 0.02-1.12; p = 0.06	
FS	OR, 0.39; 95 % CI, 0.28-0.54; **p < 0.00001 [↓(I); ↑(C)]**	
Age group		p = 0.40
Adult	OR, 0.39; 95 % CI, 0.28-0.55; **p < 0.00001 [↓(I); ↑(C)]**	
Pediatric	OR, 0.24; 95 % CI, 0.08-0.69; **p = 0.008 [↓(I); ↑(C)]**	
Anastomotic location		p = 0.63
Esophagus	OR, 0.28; 95 % CI, 0.15-0.55; **p = 0.0002 [↓(I); ↑(C)]**	
Esophagojejunal or gastrojejunal	OR, 0.28; 95 % CI I, 0.12-0.67; **p = 0.004 [↓(I); ↑(C)]**	
Gastrojejunal (bariatric surgery)	OR, 0.19; 95 % CI, 0.02-1.58; p = 0.12	
Colorectal	OR, 0.47; 95 % CI, 0.31-0.71; **p = 0.0004 [↓(I); ↑(C)]**	
Miscellaneous	OR, 0.38; 95 % CI, 0.28-0.51; p = 0.06	
Indication for surgery		p = 0.66
Malignant tumor	OR, 0.40; 95 % CI, 0.28-0.58; **p < 0.00001 [↓(I); ↑(C)]**	
Obesity (bariatric surgery)	OR, 0.19; 95 % CI, 0.02-1.58; p = 0.12	
Miscellaneous	OR, 0.31; 95 % CI, 0.15-0.63; **p = 0.001 [↓(I); ↑(C)]**	
Indication for surgery (subclassified)		p = 0.45
Upper GIT malignancy	OR, 0.26; 95 % CI, 0.12-0.56; **p = 0.0005 [↓(I); ↑(C)]**	
Lower GIT malignancy	OR, 0.47; 95 % CI, 0.31-0.71; **p = 0.0004 [↓(I); ↑(C)]**	
Obesity (bariatric surgery)	OR, 0.19; 95 % CI, 0.02-1.58; p = 0.12	
Miscellaneous	OR, 0.31; 95 % CI, 0.15-0.63; **p = 0.001 [↓(I); ↑(C)]**	

↓ = Significantly lower; ↑ = Significantly higher; RCT = Randomized controlled trial; NRS = Non-randomized study; OS = Observational study; C-BLB = Collagen-based laminar biomaterials; FS = Fibrin sealant; GIT = Gastrointestinal tract. ; I = Intervention group (coated or reinforced anastomoses); C = Control group; FE = Fixed-effect.
The bold indicates significant outcomes.

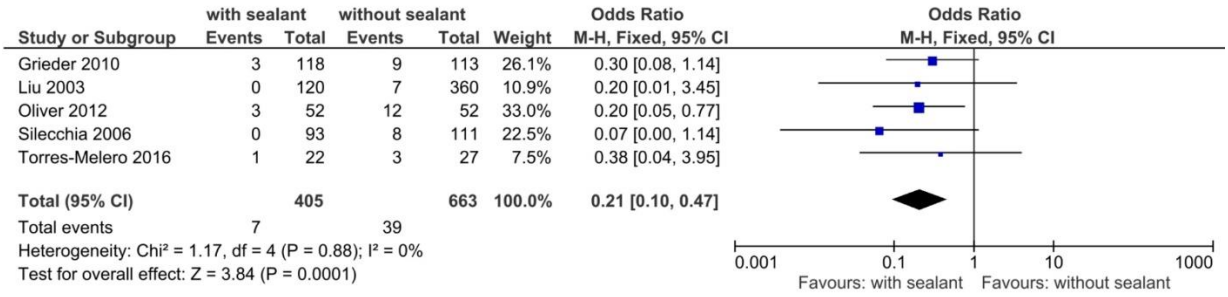

Figure 20. Fixed-effects meta-analysis for the postoperative reoperation rate in the intervention (coated or reinforced anastomoses) and control group. The forest plot of all studies is included. *(Adapted from the publication authored by Cira et al., Front Surg 2022)* [1]

1.4.3. Overall postoperative Clavien-Dindo major complication rates

A total of two studies [66, 67] reported postoperative C-DMC [153]. C-DMC developed in 30 (10.4 %) of 288 patients with anastomotic coating and 95 (17.4 %) of 545 patients in the control group.

Rates of C-DMC were significantly lower in the intervention group, as indicated by FE model meta-analysis ($OR, 0.54;\ 95\ \%\ CI, 0.35–0.84;\ p\ =\ 0.006$). The studies exhibited homogeneity ($I^2\ =\ 0\ \%;\ p\ =\ 0.54$). (**Figure 21**)

Table 6. Fixed-effects model meta-analysis for postoperative reoperation in the intervention and control group. *(Adapted from the publication authored by Cira et al., Front Surg 2022)* [1]

Table 6. Fixed-effects model meta-analysis for postoperative reoperation in the intervention and control group.

Postoperative reoperation	**Odds ratio (OR): FE model**	**Heterogeneity**
Overall	OR, 0.21; 95 % CI, 0.10-0.47; **p = 0.0001 [↓(I); ↑(C)]**	I^2 = 0 %; p = 0.88
Sensitivity analyses		
Excluded Study	**OR: FE Model**	**Heterogeneity**
Grieder et al. [149]	OR, 0.18; 95 % CI, 0.07-0.48; **p = 0.0007 [↓(I); ↑(C)]**	I^2 = 0 %; p = 0.82
Liu et al. [59]	OR, 0.21; 95 % CI, 0.09-0.48; **p = 0.0002 [↓(I); ↑(C)]**	I^2 = 0 %; p = 0.76
Oliver et al. [60]	OR, 0.21; 95 % CI, 0.08-0.57; **p = 0.002 [↓(I); ↑(C)]**	I^2 = 0 %; p = 0.76
Silecchia et al. [63]	OR, 0.25; 95 % CI, 0.11-0.58; **p = 0.001 [↓(I); ↑(C)]**	I^2 = 0 %; p = 0.96
Torres-Melero et al. [64]	OR, 0.20; 95 % CI, 0.08-0.46; **p = 0.0002 [↓(I); ↑(C)]**	I^2 = 0 %; p = 0.81
Subgroup analyses		
Subgroup	**Odds ratio (OR): FE model**	**Test for subgroup difference (TSD)**
Study design		p = 0.71
RCT	OR, 0.15; 95 % CI, 0.04-0.49; **p = 0.002 [↓(I); ↑(C)]**	
NRS	OR, 0.27; 95 % CI, 0.04-1.65; p = 0.16	
OS	OR, 0.30; 95 % CI, 0.08-1.14; p = 0.08	
Covering		p = 0.60
C-BLB	OR, 0.38; 95 % CI, 0.04-3.95; p = 0.42	
FS	OR, 0.20; 95 % CI, 0.08-0.46; **p = 0.0002 [↓(I); ↑(C)]**	
Age group (adults only)		
Anastomotic location		p = 0.64
Gastrojejunal (bariatric surgery)	OR, 0.11; 95 % CI, 0.01-0.81; **p = 0.03 [↓(I); ↑(C)]**	
Colorectal	OR, 0.32; 95 % CI, 0.10-1.02; **p = 0.05 [↓(I); ↑(C)]**	
Miscellaneous	OR, 0.20; 95 % CI, 0.05-0.77; **p = 0.02 [↓(I); ↑(C)]**	
Indication for surgery		p = 0.64
Malignant tumor	OR, 0.32; 95 % CI, 0.10-1.02; **p = 0.05 [↓(I); ↑(C)]**	
Obesity (bariatric surgery)	OR, 0.11; 95 % CI, 0.01-0.81; **p = 0.03 [↓(I); ↑(C)]**	
Miscellaneous	OR, 0.20; 95 % CI, 0.05-0.77; **p = 0.02 [↓(I); ↑(C)]**	

↓ = Significantly lower; ↑ = Significantly higher; RCT = Randomized controlled trial; NRS = Non-randomized study; OS = Observational study; C-BLB = Collagen-based laminar biomaterials; FS = Fibrin sealant; GIT = Gastrointestinal tract; I = Intervention group (coated or reinforced anastomoses); C = Control; FE = Fixed-effect.
The bold indicates significant outcomes.

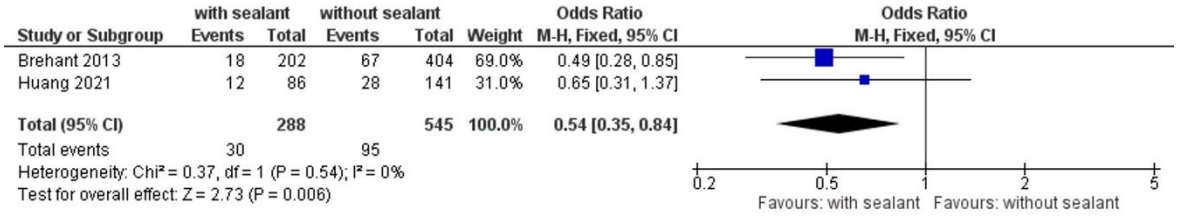

Figure 21. Fixed-effects meta-analysis for the postoperative major complication rate according to the Clavien–Dindo classification of surgical complications [153] in the intervention (coated or reinforced anastomoses) and control group. The forest plot of all studies is included. *(Adapted from the publication authored by Cira et al., Front Surg 2022)* [1]

1.4.4 Length of hospitalization

Seven studies [58, 61, 63, 67, 68, 70, 71] assessed the overall length of hospitalization. The analysis, conducted using the RE model meta-analysis, revealed a significantly shorter hospitalization period for patients in the intervention group compared to those in the control group, with a weighted MD ($WMD, -1.96$; $95\ \%\ CI, -3.21, -0.71$; $p = 0.002$). However, significant substantial heterogeneity among these studies was observed ($I^2 = 88\ \%$; $p < 0.00001$). (**Figure 22**)

The observed results demonstrated stability throughout sensitivity analyses. However, a significant subgroup difference emerged in subgroup analyses when patients were stratified based on the intervention used ($TSD: p = 0.0010$), anastomotic location ($TSD: p < 0.00001$), indication for surgery ($TSD: p = 0.001$), and its subclassification ($TSD: p = 0.001$).

Patients with coated anastomoses exhibited a significantly shorter length of hospitalization compared to the control group when undergoing intestinal surgical procedures for malignant gastrointestinal tumors ($WMD, -3.06$; $95\ \%\ CI, -4.93, -1.19$; $p = 0.001$). This effect was particularly pronounced when tumors were located in the upper gastrointestinal tract ($WMD, -4.94$; $95\ \%\ CI, -7.98, -1.90$; $p = 0.001$), and when surgeries involved the creation of an esophagojejunal or gastrojejunal anastomosis ($WMD, -2.28$; $95\ \%\ CI, -6.35, -4.31$; $p < 0.00001$). (**Figure 22 and Table 7**)

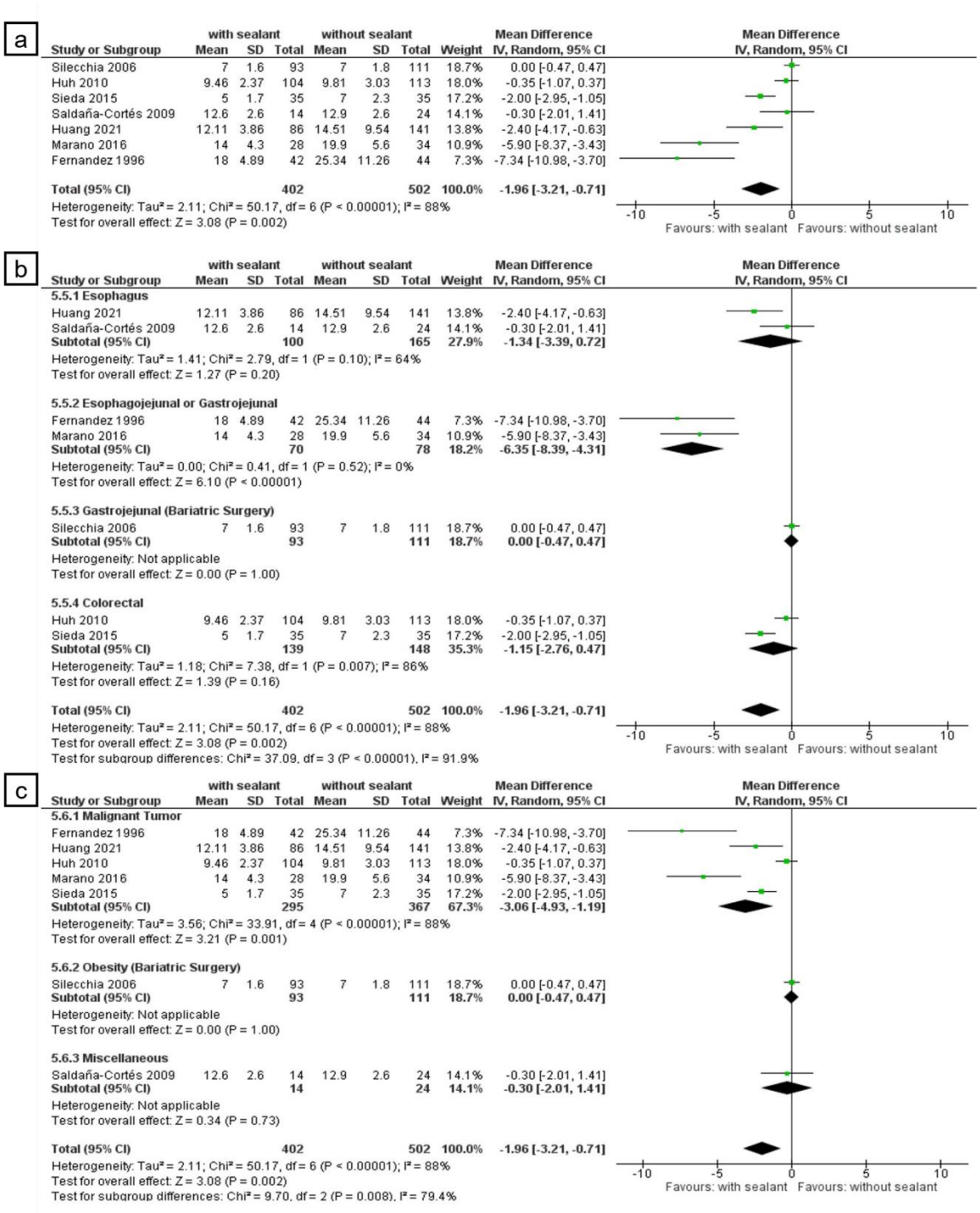

Figure 22. Random-effects meta-analysis for the length of hospitalization in the intervention (coated or reinforced anastomoses) and control group. (a) Forest plot of all studies included. (b) Forest plot of subgroup analysis stratified by location of anastomoses. (c) Forest plot of subgroup analysis stratified by indication of surgery. *(Adapted from the publication authored by Cira et al., Front Surg 2022)* [1]

Table 7 Random-effects model meta-analysis for length of hospitalization in the intervention and control group. *(Adapted from the publication authored by Cira et al., Front Surg 2022)* [1]

Table 7. Random-effects model meta-analysis for length of hospitalization in the intervention and control group.

Length of hospitalization	**Weighted mean difference (WMD): RE model**	**Heterogeneity**
Overall	WMD, -1.96; 95 % CI: -3.21, -0.71; **p = 0.002 [↓(I); ↑(C)]**	I^2 = 88 %; **p < 0.00001**
Sensitivity analyses		
Excluded study	**WMD: RE model**	**Heterogeneity**
Fernandez et al. [58]	WMD, -1.48; 95 % CI, -2.62, -0.33; **p = 0.01 [↓(I); ↑(C)]**	I^2 = 86 %; **p < 0.00001**
Huang et al. [67]	WMD, -1.90; 95 % CI, -3.24, -0.55; **p = 0.006 [↓(I); ↑(C)]**	I^2 = 89 %; **p < 0.00001**
Huh et al. [68]	WMD, -2.50; 95 % CI, -4.21, -0.79; **p = 0.004 [↓(I); ↑(C)]**	I^2 = 90 %; **p < 0.00001**
Marano et al. [70]	WMD, -1.36; 95 % CI, -2.46, -0.25; **p = 0.02 [↓(I); ↑(C)]**	I^2 = 84 %; **p < 0.00001**
Saldaña-Cortés et al. [61]	WMD, -2.28; 95 % CI, -3.68, -0.87; **p = 0.001 [↓(I); ↑(C)]**	I^2 = 90 %; **p < 0.00001**
Sieda et al. [71]	WMD, -1.99; 95 % CI, -3.41, -0.57; **p = 0.006 [↓(I); ↑(C)]**	I^2 = 88 %; **p < 0.00001**
Silecchia et al. [63]	WMD, -2.53; 95 % CI, -4.12, -0.94; **p = 0.002 [↓(I); ↑(C)]**	I^2 = 86 %; **p < 0.00001**
Subgroup analyses		
Subgroup	**WMD: RE model**	**Test for subgroup difference (TSD)**
Study design		p = *0.22*
RCT	WMD, -3.44; 95 % CI, -10.62, 3.74; p = 0.35	
NRS	WMD, -0.30; 95 % CI, -2.01, 1.41; p = 0.73	
OS	WMD, -2.36; 95 % CI, -4.10, -0.61; **p = 0.008 [↓(I); ↑(C)]**	
Covering		***p = 0.0010***
C-BLB	WMD, -5.90; 95 % CI CI:, -8.37, -3.43; **p < 0.00001 [↓(I); ↑(C)]**	
FD	WMD, -1.36; 95 % CI, -2.46, -0.25; **p = 0.02 [↓(I); ↑(C)]**	
Age group		p = 0.08
Adult	WMD, -2.28; 95 % CI, -3.68, -0.87; **p=0.001 [↓(I); ↑(C)]**	
Pediatric	WMD, -0.30; 95 % CI, -2.01, 1.41; p = 0.73	
Anastomotic location		***p < 0.00001***
Esophagus		
Esophagojejunal or gastrojejunal	WMD, -1.34; 95 % CI, -3.39, 0.72; p = 0.2	
Gastrojejunal (bariatric surgery)	WMD, -2.28; 95 % CI, -6.35, -4.31; **p < 0.00001 [↓(I); ↑(C)]**	
Colorectal	WMD, 0.0; 95 % CI, -0.47, 0.47; p = 1.0	
Miscellaneous	WMD, -1.15; 95 % CI, -2.76, 0.47; p = 0.16	
Indication for surgery		***p = 0.008***
Malignant tumor	WMD, -3.06; 95 % CI, -4.93, -1.19; **p = 0.001 [↓(I); ↑(C)]**	
Obesity (bariatric surgery)	WMD, 0.0; 95 % CI, -0.47, 0.47; p = 1.0	
Miscellaneous	WMD, -0.30; 95 % CI, -2.01, 1.41; p = 0.73	
Indication for surgery (subclassified)		***p = 0.010***
Upper GIT malignancy	WMD, -4.94; 95 % CI, -7.98, -1.90; **p = 0.001[↓(I); ↑(C)]**	
Lower GIT malignancy	WMD, -1.15; 95 % CI, -2.76, 0.47; p = 0.16	
Obesity (bariatric surgery)	WMD, 0.0; 95 % CI, -0.47, 0.47; p = 1.0	
Miscellaneous	WMD, -0.30; 95 % CI, -2.01, 1.41; p = 0.73	

↓ = Significantly lower; ↑ = Significantly higher; RCT = Randomized controlled trial; NRS = Non-randomized study; OS = Observational study; C-BLB = Collagen-based laminar biomaterials; FS = Fibrin sealant; GIT = Gastrointestinal tract; I = Intervention group (coated or reinforced anastomoses); C = Control group; RE = Random-effects.
The bold indicates significant outcomes.

1.4.5 Postoperative mortality rate

A total of four studies [60, 61, 65, 67] monitored postoperative mortality rates, occurring in six (3.4 %) of 174 patients with FS coated anastomoses and 13 (5.5 %) of 240 patients in the control group. The mortality rate showed no significant differences between the patients with FS-coated anastomoses and control group using FE meta-analysis ($OR, 0.52;\ 95\ \%\ CI, 0.20–1.39;\ p\ =\ 0.19$). Studies were homogeneous ($I^2\ =\ 0\ \%;\ p\ =\ 0.69$). (**Figure 23**)

Observed results remained stable in sensitivity analyses. No significant differences in the subgroup analyses was found for subgroups stratified by study design ($TSD: p\ =\ 0.66$), age group ($TSD: p\ =\ 0.78$), anastomotic location ($TSD: p\ =\ 0.59$), and indication for surgery ($TSD: p\ =\ 0.74$) (**Figure 23; Table 8**)

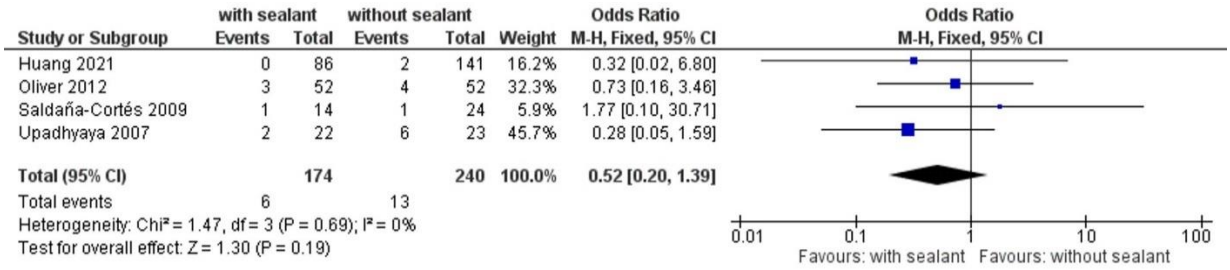

Figure 23. Fixed-effects meta-analysis for the postoperative mortality rate in the intervention (coated or reinforced anastomoses) and control group. The forest plot of all studies is included. *(Adapted from the publication authored by Cira et al., Front Surg 2022)* [1]

Table 8. Fixed-effect model meta-analysis for postoperative mortality in the intervention and control group. *(Adapted from the publication authored by Cira et al., Front Surg 2022)* [1]

Table 8. Fixed-effects model meta-analysis for postoperative mortality in the intervention and control group.

Mortality	**Odds ratio (OR): FE model**	**Heterogeneity**
Overall	OR, 0.52; 95 % CI, 0.20-1.39; p = 0.19	I^2 = 0 %; p = 0.69
Sensitivity analyses		
Excluded study	**OR: FE model**	**Heterogeneity**
Huang et al. [67]	OR, 0.56; 95 % CI, 0.20-1.59; p = 0.28	I^2 = 0 %; p = 0.51
Oliver et al. [60]	OR, 0.42; 95 % CI, 0.12-1.52; p = 0.19	I^2 = 0 %; p = 0.55
Saldaña-Cortés et al. [61]	OR, 0.44; 95 % CI, 0.15-1.28; p = 0.13	I^2 = 0 %; p = 0.70
Upadhyaya et al. [65]	OR, 0.72; 95 % CI, 0.22-2.42; p = 0.60	I^2 = 0 %; p = 0.72
Subgroup analyses		
Subgroup	**OR: FE model**	**Test for subgroup difference (TSD)**
Study design		p = 0.66
RCT	OR, 0.47; 95 % CI, 0.15-1.46; p = 0.19	
NRS	OR, 1.77; 95 % CI, 0.10-30.71; p = 0.70	
OS	OR, 0.32; 95 % CI, 0.02-6.80; p = 0.47	
Covering (FS only)		
Age group		p = 0.78
Adult	OR, 0.60; 95 % CI, 0.15-2.31; p = 0.46	
Pediatric	OR, 0.45; 95 % CI, 0.11-1.87; p = 0.27	
Anastomotic location		p = 0.59
Esophagus	OR, 0.42; 95 % CI, 0.12-1.52; p = 0.19	
…Miscellaneous	OR, 0.73; 95 % CI, 0.16-3.46; p = 0.70	
Indication for surgery		p = 0.74
Upper GIT malignancy	OR, 0.32; 95 % CI, 0.02-6.8; p = 0.47	
Miscellaneous	OR, 0.56; 95 % CI, 0.20-1.59; p = 0.28	

RCT = Randomized controlled trial; NRS = Non-randomized study; OS = Observational study; FS = Fibrin sealant; GIT = Gastrointestinal tract; FE = Fixed-effect.

2 Systematic review and meta-analysis of animal studies

2.1. Final database search on October 6, 2021

Utilizing predefined search items as outlined in **Supplementary Table 2**, 202 studies were identified through the performed electronic database search. The electronic database PubMed contributed 58 search items, the Cochrane Library provided 15 search items, Scopus included 67 search items, and Web of Science contained 62 search items. Before screening, 77 duplicate search items were removed. Initial removal of duplicates was performed using an automation tool of EndNote X9, followed by a manual review for duplicate removal. After this process, titles and abstracts of 125 search items were manually assessed according to predefined eligibility criteria (**Chapter III.2.1.1 – 2.1.2**).

Following the exclusion of 99 studies that lacked eligibility, retrieval was sought for the remaining 26 studies. Of these, 15 studies were further assessed for eligibility, as full-text reports for eleven studies could not be retrieved. Two studies were excluded due to the absence of a control group, and one study lacked sufficient data presentation.

Additionally, seven studies were identified through manual screening of the reference lists of included studies, referred to as "other methods". All seven studies were retrieved for full-text analysis. Out of these seven studies, six were excluded for the following reasons:

1. One study was excluded due to a lack of a control group.
2. One study was excluded due to insufficient data presentation.
3. Two studies were excluded because they included human study groups.
4. One study was excluded because it presented a systematic review.
5. One study was excluded because non-transmural defect closures were investigated.

Overall, the electronic database search and reference list search yielded 13 studies with 15 discrete data sets [45-57], which were qualitatively and quantitatively analyzed for this

systematic review. Ten studies with eleven discrete data sets [46, 47, 50-57] were eligible to be included in the meta-analysis. (**Figure 24**)

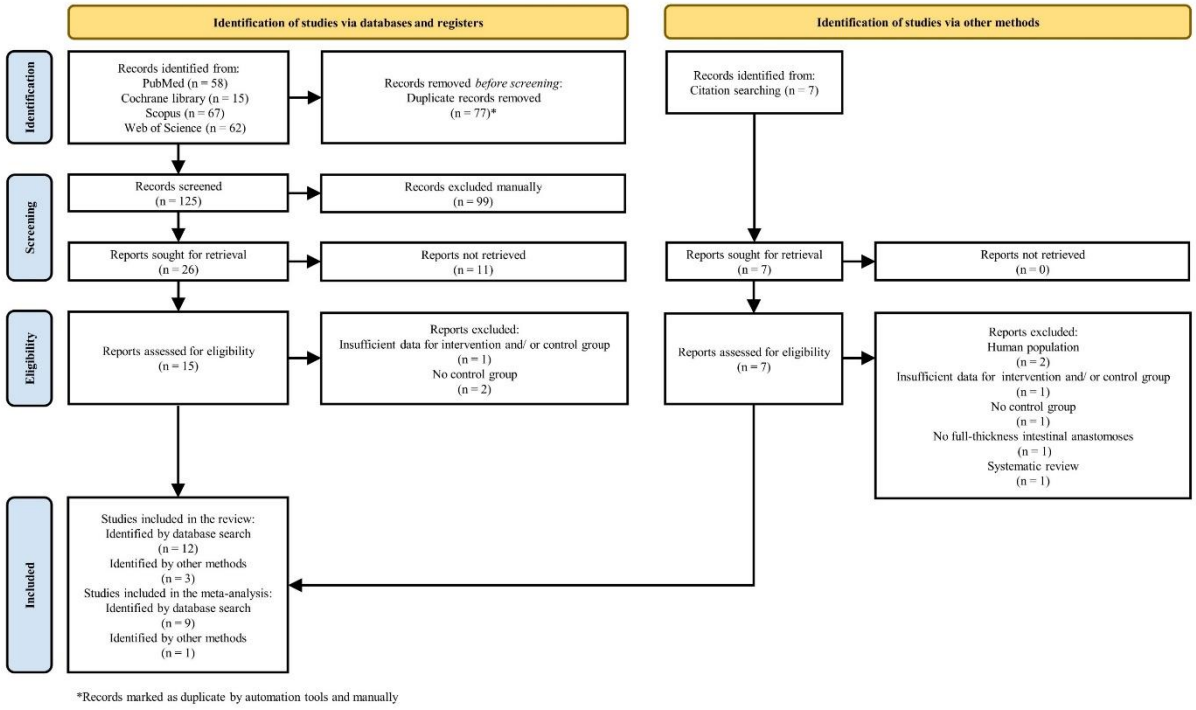

Figure 24. Study flow diagram according to the Preferred Reporting Items for Systematic Review and Meta-Analyses (PRISMA) Statement 2020 [150].

2.2. Study characteristics

Overall, 13 prospective *in-vivo* animal studies (comprising 15 discrete data sets) [45-57], published between 2000 and 2017, were analyzed for this review. The majority of studies were conducted in European countries, including Belgium [56], Denmark [48, 51], Germany [45, 47, 50, 54], the Netherlands [53, 57], and Spain [46, 55]. Only two studies were performed outside of Europe, in Brazil [52] and Turkey [49].

In total, 569 animals were included in 13 studies (15 discrete data sets) [45-57], with 290 (51 %) receiving intestinal anastomoses coated with C-BLBs (intervention group) and 279 (49 %) receiving intestinal anastomoses without any coating (control group). Rodents were the most commonly studied animals [45-47, 49, 52, 53, 55-57], including 309 rats (60 males from the genus Sprague-Dawley [45, 46], 249 males and/ or females from the genus Wistar [47, 49,

52, 53, 55-57]), and 208 mice (male C57BL/6) [50, 51]. Additionally, 52 pigs were investigated by two studies [48, 54], with 20 being female Göttingen Minipigs [48].

Anastomoses were located most frequently in the proximal [49-51, 55] and distal [47, 52, 53, 56] colon, followed by the small intestine [45, 48, 54], esophagus [56] and the esophagogastric junction [46].

In the majority of studies, the utilized C-BLB was TachoSil (*Fibrin Sealant Patch; Takeda Pharma A/S*) [45-48, 50-52, 55, 57]. Further applied biomaterials included: TachoComb (*Fibrin Sealant Patch; Takeda Pharma A/S*) in two studies [49, 54], TissuFleece (*Baxter Healthcare*) in one study [53], and an unspecified collagen sponge in one study [56]. (**Table 9**)

Suture techniques included SBS techniques [45, 46, 48-52, 55, 56] for either complete (sufficient) [45, 52, 56] or incomplete/ partial (insufficient) [46, 50, 51, 55] anastomoses, CS techniques [57], as well as sutureless anastomoses [47, 49, 53, 54]. Additional details on anastomotic techniques and interventions are presented in **Table 10**.

All studies, except one [49], reported postoperative AL and mortality rates. Significance in outcomes was only observed in three of these: two studies found a significantly lower postoperative AL rate in the intervention group compared to the control group [50, 51], and one discrete data set from a study found a significantly reduced postoperative mortality rate in the intervention group [50]. The results of BP measurements were reported by eleven studies, comprising 13 discrete data sets [45-50, 52-54, 56, 57]. (**Table 11**)

The presence of postoperative adhesions was examined in six studies (involving seven discrete data sets) [45, 48, 49, 52, 54, 55]. Additionally, postoperative anastomotic stenosis was assessed in four studies [48, 51-53], while postoperative weight loss was investigated in three studies [45, 51, 52]. Postoperative anastomotic collagen content was determined in four studies [45, 49, 53, 56], and other studies examined the anastomotic collagen type 1 and 3 expression [47, 50, 54] or measured fibroblast activity [49, 56]. (**Table 12**)

Table 9. Study characteristics.

Table 9. Study characteristics.

Author	Year	Country	Animal		Number of animals, n		Anastomoses	
			Animal (species)	Sex	I	C	Location	Covering biomaterial (I)
Chmelnik et al. [45]	2011	Germany	Rats (Sprague-Dawley)	M	5	5	SI	TachoSil
Garcia-Perez et al. [46]	2017	Spain	Rats (Sprague-Dawley)	M	25	25	E-G	TachoSil
Holmer et al. [47]	2014	Germany	Rats (Wistar)	M	18	24	DC	TachoSil
Nordentoft et al. [48]	2007	Denmark	Pigs (Göttingen Minipigs)	F	10	10	SI	TachoSil
Ozel et al. *(1)* [49] [a]	2006	Turkey	Rats (Wistar; albino)	U	12	12	PC	TachoComb
Ozel et al. *(2)* [49] [a]					12			
Pantelis et al. *(4)* [50] [a]	2010	Germany	Mice (C57BL/6)	M	34	30	PC	TachoSil
Pantelis et al. *(8)* [50] [a]					32	32		
Pommergaard et al. [51]	2014	Denmark	Mice (C57BL/6)	M	40	40	PC	TachoSil
Sabino et al. [52]	2014	Brazil	Rats (Wistar)	M	10	10	DC	TachoSil
Schreinemacher et al. [53]	2011	Netherlands	Rats (Wistar)	M	21	20	DC	TissuFleece
Stumpf et al. [54]	2009	Germany	Pigs	M	16	16	SI	TachoComb
Suárez-Grau et al. [55]	2016	Spain	Rats (Wistar; white)	M/F	28	28	PC	TachoSil
Vaneerdeweg et al. [56]	2000	Belgium	Rats (Wistar)	M	10	10	DC	Collagen sponge
Verhage et al. [57]	2012	Netherlands	Rats (Wistar)	M	17	17	E	TachoSil

M = Male; F = Female; U = Unknown; E = Esophagus; E-G = Esophagogastric junction; PI = Proximal intestine; SI = Small intestine; PC = Proximal colon; DC = Distal colon; I = Intervention group (intestinal anastomosis coated with collagen-based laminar biomaterial); C = Control group.

[a] *Ozel et al. [49] and Pantelis et al. [50] include two discrete data sets.*

Table 10. Surgical characteristics.

Table 10. Surgical characteristics.

Author	Year	Number of animals, n		Anastomoses								Additional intervention	
				Technique		Layers, n		Stitches, n		Suture material			
		I	C	I	C	I	C	I	C	I	C	I	C
Chmelnik et al. [45]	2011	5	5	IS	IS	1	1	9	9	R	R	RT-R (caecal incision; closed with 2 IS)	-
Garcia-Perez et al. [46]	2017	25	25	IS	IS	1	1	3	3	NR	NR	-	-
Holmer et al. [47]	2014	18	24	NS	CS	N/A	1	N/A	CS	N/A	NR	a) High risk anastomoses: induced peritonitis b) Postoperative antibiosis	
Nordentoft et al. [48]	2007	10	10	IS	IS	1	1	N/A	N/A	R	R	-	-
Ozel et al. *(1)* [49] [a]	2006	12	12	IS	IS	1	1	N/A	N/A	NR	NR	-	-
Ozel et al. *(2)* [49] [a]		12		NS		N/A		N/A		N/A			
Pantelis et al. *(4)* [50] [a]	2010	34	30	IS	IS	1	1	4	4	R	R	-	-
Pantelis et al. *(8)* [50] [a]		32	32	IS	IS	1	1	8	8	R	R	Induced peritonitis or sepsis	
Pommergaard et al. [51]	2014	40	40	IS	IS	N/A	N/A	4	4	R	R	-	-
Sabino et al. [52]	2014	10	10	IS	IS	N/A	N/A	10-12	10-12	NR	NR	5-FU administration POD 0 to 3	
Schreinemacher et al. [53]	2011	21	20	NS	IS	N/A	N/A	N/A	4	N/A	NR	Fibrin glue administration (TisseelDuo)	
Stumpf et al. [54]	2009	16	16	NS	IS	N/A	1	N/A	N/A	N/A	R	Fibrin glue administration	
Suárez-Grau et al. [55]	2016	28	28	IS	IS	N/A	N/A	2	2	R	R	-	-
Vaneerdeweg et al. [56]	2000	10	10	IS	IS	1	1	8	8	N/A	N/A	Collagen sponge fixed with 2 IS	
Verhage et al. [57]	2012	17	17	CS	CS	1	1	CS	CS	NR	NR	-	-

N/A = Not available; I = Intervention group (intestinal anastomosis coated with collagen-based laminar biomaterial); C = Control group; IS = Interrupted suture; CS = Continuous suture; NS = No suture; R = Resorbable suture material; NR = Non-resorbable suture material; RT-R = Rubber-tube removal; 5-FU = 5-Fluorouracil, POD = Postoperative day.
[a] Ozel et al. [49] and Pantelis et al. [50] include two discrete data sets.

Table 11. Postoperative complications and bursting pressure measurements.

Table 11. Postoperative complications and bursting pressure measurements.

Author	Year	Number of animals, n		Postoperative complications				Postoperative bursting pressure measurement, mean (SD), in $mmHg$	
				Mortality, n		Anastomotic leakage, n			
		I	C	I	C	I	C	I	C
Chmelnik et al. [45]	2011	5	5	0	0	0	0	↔POD 0: 131 ± 31.3 ↔POD 2: 71.0 ± 32.5 ↓**POD 10: 140 ± 73.5**	↔POD 0: 97.0 ± 21.1 ↔POD 2: 69.0 ± 10.2 ↑**POD 10: 242 ± 6.5**
Garcia-Perez et al. [46]	2017	25	25	2	9	0	7	↑**119.5 ± 22.0**	↓**93.5 ± 30.0**
Holmer et al. [47]	2014	18	24	0	0	4	0	↔POD 1 ↔POD 3 ↔POD 5	↔POD 1 ↔POD 3 ↔POD 5
Nordentoft et al. [48]	2007	10	10	0	0	0	0	↔157 ± 56.53	↔156 ± 40.77
Ozel et al. *(1)* [49] [a]	2006	12	12	N/A	N/A	N/A	N/A	↑**POD 3: 87.3 ±38.1** ↓**POD 7: 134.8 ± 33.25**	↓***(1)***; ↔*(2)* **POD 3: 41.8 ± 20.42** ↑**POD 7: 174.8 ± 70.32**
Ozel et al. *(2)* [49] [a]		12		N/A		N/A		↔POD 3: 71.8 ± 24.59 ↓**POD 7: 127.0 ± 39.49**	
Pantelis et al. *(4)* [50] [a]	2010	34	30	↓**3**	↑**12**	↓**2**	↑**11**	↑**POD2: 17.7 ± 2.0** ↑**POD 5: 18.8 ± 2.1** ↑**POD 14: 18.2 ± 1.9**	↓**POD2: 8.3 ± 4.8** ↓**POD 5: 6.4 ± 8.9** ↓**POD 14: 0 ± 0**
Pantelis et al. *(8)* [50] [a]		32	32	5	4	0	1	↔POD 2: 11.2 ± 3.4 ↔POD 5: 14.5 ± 2.7 ↔POD 14: 19.1 ± 2.5	↔POD 2: 11.2 ± 3.4 ↔POD 5: 14.5 ± 2.7 POD 14: 19.1 ± 2.5
Pommergaard et al. [51]	2014	40	40	N/A	N/A	↓**10**	↑**20**	N/A	N/A
Sabino et al. [52]	2014	10	10	0	1	0	0	↔POD 4: 67 ± 24	↔POD 4: 73 ± 24
Schreinemacher et al. [53]	2011	21	20	1	3	0	3	↔POD 3: 50.7 ± 15.5 ↔POD 7: 114.8 ± 27.5	↔POD 3: 60.5 ± 11.3 ↔POD 7: 199 ± 27.9
Stumpf et al. [54]	2009	16	16	0	0	1	1	↔POD 7 and 30	↔POD 7 and 30
Suárez-Grau et al. [55]	2016	28	28	6	10	6	10	N/A	N/A
Vaneerdeweg et al. [56]	2000	10	10	0	0	0	1	↑**POD 0: 102 ± 7.3** ↑**POD 3: 34.6 ± 4.9** ↔POD 5: 53.4 ± 6.6 ↔POD 7: 97.2 ± 8.3	↓**POD 0: 55.1 ± 4.6** ↓**POD 3: 19.7 ± 3.3** ↔POD 5: 60.9 ± 18.2 ↔POD 7: 118.8 ± 20.2
Verhage et al. [57]	2012	17	17	2	2	9	N/A	↓**POD 4**	↑**POD 4**

↓ = Significantly lower; ↔ = No difference; ↑ = Significantly higher; N/A = Not available; I = Intervention group (intestinal anastomoses coated with collagen-based laminar biomaterial); C = Control group; $mmHg$ = Millimetre of mercury; mean (SD) = Mean (standard deviation); POD = Postoperative day; SEM values of Ozel et al., 2006 [49] were converted to SD by calculating: $SD = SEM \; x \; \sqrt[2]{sample\ size}$.

The bold indicates significant outcomes.

[a] *Ozel et al. [49] and Pantelis et al. [50] include two discrete data sets.*

Table 12. Other postoperative outcomes.

Table 12. Other postoperative outcomes.

Author	Year	Other postoperative outcomes	
		I	C
Chmelnik et al. [45]	2011	↑**POD 2 and 10: weight loss** ↔adhesion ↔POD 2 and 10: collagen content	↓**POD 2 and 10: weight loss** ↔adhesion ↔POD 2 and 10: collagen content
Garcia-Perez et al. [46]	2017	N/A	N/A
Holmer et al. [47]	2014	↔POD 1: col-1 and col-3 mRNA ↑**POD 3: col-1 mRNA** ↔POD 3 and 5: col-3 mRNA ↔VEGF mRNA; MMP-13	↔ POD 1: col-1 and col-3 mRNA ↓**POD 3: col-1 mRNA** ↔POD 3 and 5: col-3 mRNA ↔VEGF mRNA; MMP-13
Nordentoft et al. [48]	2007	↔adhesion ↔abscess formation; peritonitis ↔stenosis; histology	↔adhesion ↔abscess formation; peritonitis ↔stenosis; histology
Ozel et al. *(1)* [49] [a]	2006	↓**POD 7: collagen deposition** ↓**neovascularity of anastomoses** ↑**inflammatory cell infiltration** ↓**fibroblastic activity** ↔adhesion	↑**POD 7: collagen deposition** ↑**neovascularity of anastomoses** ↓**inflammatory cell infiltration** ↑**fibroblastic activity** ↔ *(1)*; ↓ ***(2)*** **adhesion**
Ozel et al. *(2)* [49] [a]		↑**adhesion**	
Pantelis et al. *(4)* [50] [a]	2010	↑**POD 1: col-3 expression** ↓**POD 5: induction col-1 expression** ↑**hydroxyproline concentration** ↔POD 2: anastomotic healing score ↑**POD 5 and 10: anastomotic healing score**	↓**POD 1: col-3 expression** ↑**POD 5: induction col-1 expression** ↓**hydroxyproline concentration** ↔POD 2: anastomotic healing score ↓**POD 5 and 10: anastomotic healing score**
Pantelis et al. *(8)* [50] [a]		↑**POD 1: col-1 and col-3 expression** ↑**POD 5: induction col-1 expression** ↓**POD 5: col-3 expression** ↑**hydroxyproline concentration** ↔ POD 5 and 14: anastomotic healing score	↓**POD 1: col-1 and col-3 expression** ↓**POD 5: induction col-1 expression** ↑**POD 5: col-3 expression** ↓**hydroxyproline concentration** ↔POD 5 and 14: anastomotic healing score
Pommergaard et al. [51]	2014	↔anastomotic breaking strength ↑**stenosis** ↑**weight loss** ↑**wellness score**	↔anastomotic breaking strength ↓**stenosis** ↓**weight loss** ↓**wellness score**
Sabino et al. [52]	2014	↔adhesion; stenosis; inflammation ↔neoangiogenesis; weight loss	↔adhesion; stenosis; inflammation ↔neoangiogenesis; weight loss
Schreinemacher et al. [53]	2011	↔ POD 3 and 7: collagen content ↑**POD 3 and 7: stenosis**	↔ POD 3 and 7: collagen content ↓**POD 3 and 7: stenosis**
Stumpf et al. [54]	2009	↔POD 7 and 30: col-1/ col-3 ratio ↔adhesion; MMP-13 ↔POD 3: MMP-1 ↓**POD 7: MMP-1** ↑**POD 30: MMP-1; massive scar around collagen fleece**	↔POD 7 and 30: col-1/ col-3 ratio ↔adhesion; MMP-13 ↔POD 3: MMP-1 ↑**POD 7: MMP-1** ↓**POD 30: MMP-1; massive scar around collagen fleece**
Suárez-Grau et al. [55]	2016	↔POD 15 and 60: adhesion	↔POD 15 and 60: adhesion
Vaneerdeweg et al. [56]	2000	↔POD 3 and 7: collagen content ↔POD 3: fibroblastic activity (α-SMA) ↓**POD 3: collagen (Sirius Red)** ↔POD 7: collagen (Sirius Red) ↑**POD 7: fibroblastic activity (α-SMA)** ↔ macrophage activity ↔ inflammatory response	↔POD 3 and 7: collagen content ↔POD 3: fibroblastic activity (α-SMA) ↑**POD 3: collagen (Sirius Red)** ↔POD 7: collagen (Sirius Red) ↓**POD 7: fibroblastic activity (α-SMA)** ↔ macrophage activity ↔ inflammatory response
Verhage et al. [57]	2012	↑**weight loss**	↓**weight loss**

↓ = Significantly lower; ↔ = No difference; ↑ = Significantly higher; ; N/A = Not available; I = Intervention group (coated with collagen-based laminar biomaterial); C = Control group; POD = Postoperative day; Sirius red = Histologic staining score collagen; α-SMA = Histologic staining scores for fibroblastic activity; col-1 = Collagen type 1; col-3 = Collagen type 3; mRNA = Messenger ribonucleic acid; MMP = Matrix metalloproteinase; VEGF = Vascular endothelial growth factor.
The bold indicates significant outcomes.
[a] *Ozel et al. [49] and Pantelis et al. [50] include two discrete data sets.*

2.3. Risk of bias assessment

All full-text articles underwent a comprehensive risk of bias assessment. This systematic evaluation encompassed the entire set of included studies [45-57], employing SYRCLE's risk of bias tool specifically designed for animal studies [110]. Additionally, the quality of reporting was evaluated in accordance with the ARRIVE guidelines for animal research [111].

2.3.1 Risk of bias assessment using the Systematic Review Centre for Laboratory Animal Experimentation tool

According to the SYRCLE’s risk of bias tool for animal studies [110] and in consensus with K. C. and F. S., four studies [49, 54, 55, 57] were rated as having an overall high risk of bias. However, the majority of studies were assessed to have some concerns [45-48, 50-53, 56].

In the category of "selection bias" and subcategory "sequence generation" [110], all included studies [45-57] exhibited an unclear risk of bias. Within the subcategory “baseline characteristics” [110], Ozel et al. [49] and Suárez-Grau et al. [55] were rated as having a high risk of bias, given that baseline characteristics were not matched in the included study groups. Conversely, all other studies [45-48, 50-54, 56, 57] were rated to be at low risk of bias in this subcategory. The subcategory "allocation concealment" [110] indicated that two studies [53, 57] were rated as presenting a low risk of bias, while all other studies [45-52, 54-56] were rated as having an unclear risk of bias.

In the category of "performance bias" and subcategories "random housing" and "blinding" [110], all studies [45-57] were rated to present with unclear risk of bias. Similarly, in the category of "detection bias" and subcategories "random outcome assessment" and "blinding" [110], all studies [45-57] were rated to present with unclear risk of bias.

In the category of "attribution bias" and subcategory "incomplete outcome data", as well as the category of "reporting bias" and subcategory "selective outcome reporting" [110], all

included studies [45-57] were rated as presenting a low risk of bias. In the category of "others" and subcategory "other source of bias" [110]:

1. Stumpf et al. [54] was rated as presenting a high risk of bias due to an unit of analysis error, in which interventions to different parts of the body within one animal were undertaken.
2. Suárez-Grau et al. [55] was rated as presenting a high risk of bias in this category because the experimental unit was not clear.
3. Verhage et al. [57] was rated as presenting a high risk of bias in this subcategory due to an unrestricted grant which was provided by Nycomed BV (The Netherlands).
4. Three studies [45, 47, 49] were rated as presenting an unclear risk of bias.
5. Seven studies [46, 48, 50-53, 56] were rated as presenting with low risk of bias.

Additional information regarding the risk of bias assessment using SYRCLE's tool for animal studies is provided in **Supplementary Table 5**.

2.3.2 Quality of reporting assessment using the Animal Research: Reporting of In Vivo Experiments tool

Adhering to the ARRIVE guidelines for reporting animal research, the assessment of reporting quality revealed a considerable range among the included studies, aligning with the consensus of K. C. and F. S.. (**Supplementary Table 6**)

2.4 Results of meta-analysis and subgroup analyses

2.4.1 Postoperative anastomotic leakage

Postoperative events of AL were reported by nine studies (ten discrete data sets) [46, 47, 50, 51, 53-55, 57], occurring in 23 of 231 (10 %) animals in the intervention group and 54 of 238 (22.7 %) animals in the control group. Significantly lower AL rates were evident for animals in

the intervention group based on FE model meta-analysis ($OR, 0.36;\ 95\ \%\ CI, 0.22 - 0.62;\ p = 0.0002$). These studies exhibited homogeneity ($I^2 = 29\ \%;\ p = 0.18$). (**Figure 25**)

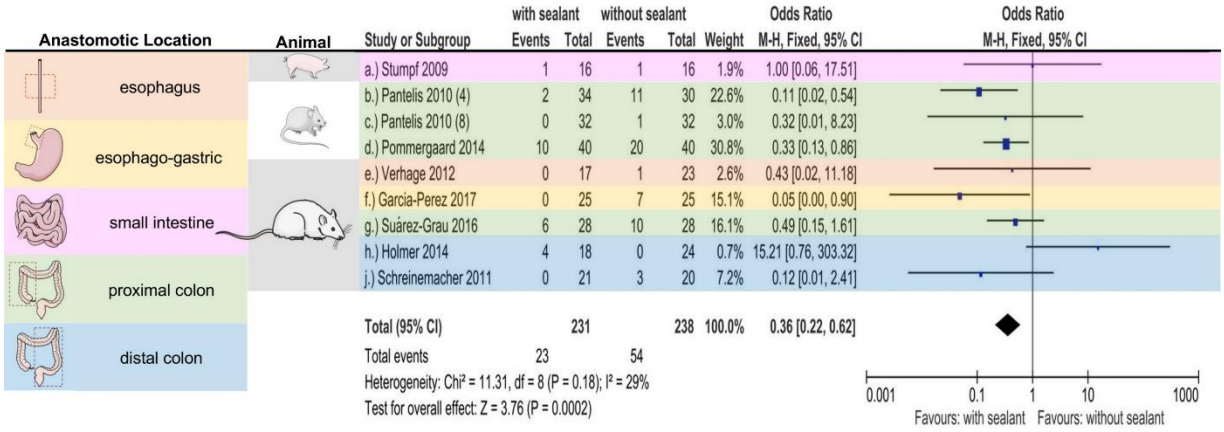

Figure 25. Fixed-effects model meta-analysis for postoperative anastomotic leakage in intervention (coated anastomoses) and control group. Forest plot of all studies included. *Elements in Figure 25 were modified from SMART (Servier Medical Art), licensed under a Creative Common Attribution 3.0 Generic License. http://smart.servier.com/.* [154]

Excluding one study at a time, observed results remained stable throughout sensitivity analyses. (**Table 13**)

Table 13. Fixed-effects model meta-analysis for postoperative anastomotic leakage in the intervention and control group.

Table 13. Fixed-effects model meta-analysis for postoperative anastomotic leakage in the intervention and control group.		
Postoperative anastomotic leakage	**Odds ratio (OR): FE model**	**Heterogeneity**
Overall	OR, 0.36; 95 % CI, 0.22-0.62; **p = 0.0002 [↓(I); ↑(C)]**	I^2 = 29 %; p = 0.18
Sensitivity analyses		
Excluded study	**OR: FE model**	**Heterogeneity**
Garcia-Perez et al. [46]	OR, 0.42; 95 % CI, 0.24-0.73; **p = 0.002 [↓(I); ↑(C)]**	I^2 = 27 %; p = 0.21
Holmer et al. [47]	OR, 0.26; 95 % CI, 0.15-0.47; **p < 0.00001 [↓(I); ↑(C)]**	I^2 = 0 %; p = 0.66
Pantelis et al. *(4)* [50] [a]	OR, 0.44; 95 % CI, 0.25-0.77; **p = 0.004 [↓(I); ↑(C)]**	I^2 = 22 %; p = 0.25
Pantelis et al. *(8)* [50] [a]	OR, 0.37; 95 % CI, 0.21-0.62; **p = 0.0002 [↓(I); ↑(C)]**	I^2 = 38 %; p = 0.13
Pommergaard et al. [51]	OR, 0.38; 95 % CI, 0.20-0.71; **p = 0.003 [↓(I); ↑(C)]**	I^2 = 38 %; p = 0.13
Stumpf et al. [54]	OR, 0.35; 95 % CI, 0.21-0.60; **p = 0.0001 [↓(I); ↑(C)]**	I^2 = 35 %; p = 0.15
Schreinemacher et al. [53]	OR, 0.38; 95 % CI, 0.22-0.66; **p = 0.0005 [↓(I); ↑(C)]**	I^2 = 35 %; p = 0.15
Suárenz-Grau et al. [55]	OR, 0.34; 95 % CI, 0.19-0.61; **p = 0.0003 [↓(I); ↑(C)]**	I^2 = 36 %; p = 0.14
Verhage et al. [57]	OR, 0.36; 95 % CI, 0.21-0.62; **p = 0.0002 [↓(I); ↑(C)]**	I^2 = 38 %; p = 0.13
↓ = Significantly lower; ↑ = Significantly higher; I = Intervention group (intestinal anastomoses coated with collagen-based laminar biomaterial); C = Control group; FE = Fixed-effect.		
The bold indicates significant outcomes.		
[a] *Pantelis et al. [50] includes two discrete data sets.*		

Subgroup analyses were conducted to assess the potential influence of the studied animal species, location of anastomoses, anastomotic technique, and its sufficiency on the observed outcomes. These analyses revealed a significant difference between subgroups stratified by sufficiency of the anastomotic suture techniques ($TSD: p = 0.05$), the type of suture material utilized ($TSD: p = 0.04$), and the type of anastomotic technique applied ($TSD: p = 0.02$) Animals with incomplete/ partial (insufficient) anastomoses presented significantly lower leakage rates when anastomoses were coated with C-BLBs ($OR, 0.25;\ 95\ \%\ CI, 0.13 - 0.47;\ p < 0.0001$). (**Figure 26**)

Despite the significant TSD for subgroups stratified by type of suture material utilized, AL was significantly lower in the intervention group, regardless of whether resorbable ($OR, 0.37;\ 95\ \%\ CI, 0.16 - 0.57;\ p = 0.0002$) or non-resorbable ($OR, 0.10;\ 95\ \%\ CI, 0.01 - 0.89;\ p < 0.03$) suture materials were used. (**Figure 26**) Animals with sutured and coated anastomoses using collagen-based laminar biomaterials showed significantly lower leakage rates compared to those with suture-free anastomoses and coating ($OR, 0.26;\ 95\ \%\ CI, 0.14 - 0.48;\ p < 0.0001$).

No subgroup differences were demonstrable for subgroups stratified by animal species animal species ($TSD: p = 0.33$)**,** or anastomotic location ($TSD: p = 0.36$) (**Figure 26**).

IV Results

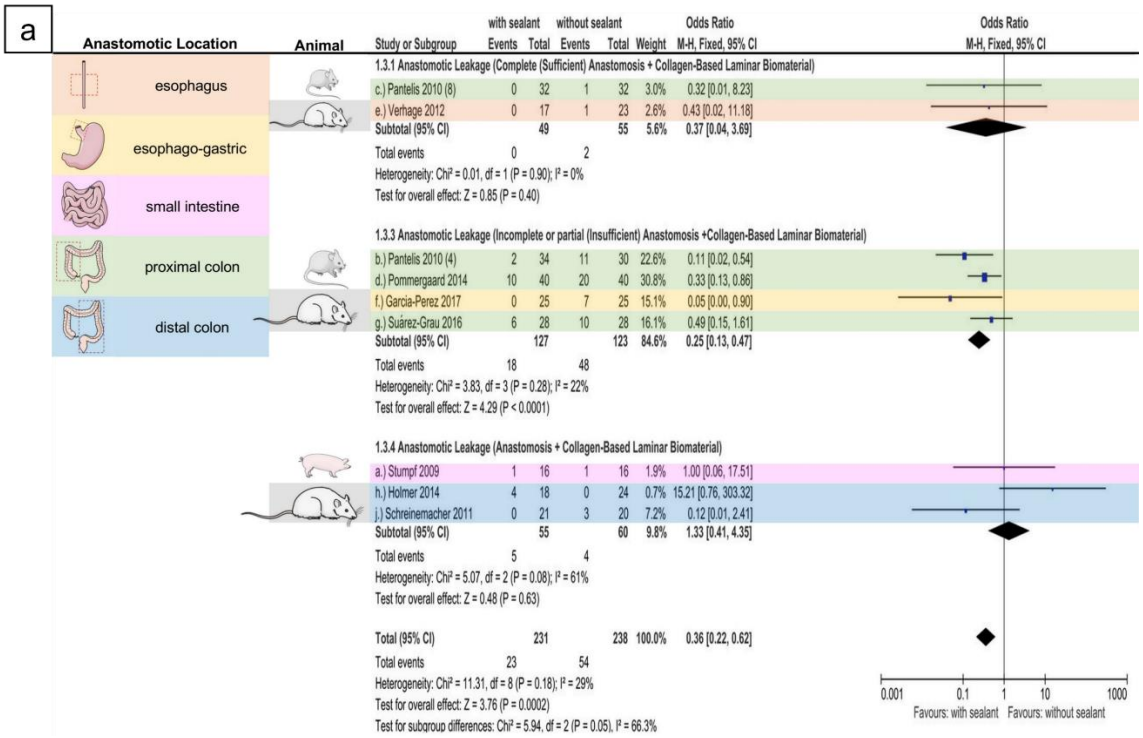
a
Anastomotic Location
Animal
esophagus
esophago-gastric
small intestine
proximal colon
distal colon
with sealant
without sealant
Odds Ratio
Odds Ratio
Study or Subgroup Events Total Events Total Weight M-H, Fixed, 95% CI
M-H, Fixed, 95% CI
1.3.1 Anastomotic Leakage (Complete (Sufficient) Anastomosis + Collagen-Based Laminar Biomaterial)
c.) Pantelis 2010 (8) 0 32 1 32 3.0% 0.32 [0.01, 8.23]
e.) Verhage 2012 0 17 1 23 2.6% 0.43 [0.02, 11.18]
Subtotal (95% CI) 49 55 5.6% 0.37 [0.04, 3.69]
Total events 0 2
Heterogeneity: Chi² = 0.01, df = 1 (P = 0.90); I² = 0%
Test for overall effect: Z = 0.85 (P = 0.40)
1.3.3 Anastomotic Leakage (Incomplete or partial (Insufficient) Anastomosis +Collagen-Based Laminar Biomaterial)
b.) Pantelis 2010 (4) 2 34 11 30 22.6% 0.11 [0.02, 0.54]
d.) Pommergaard 2014 10 40 20 40 30.8% 0.33 [0.13, 0.86]
f.) Garcia-Perez 2017 0 25 7 25 15.1% 0.05 [0.00, 0.90]
g.) Suárez-Grau 2016 6 28 10 28 16.1% 0.49 [0.15, 1.61]
Subtotal (95% CI) 127 123 84.6% 0.25 [0.13, 0.47]
Total events 18 48
Heterogeneity: Chi² = 3.83, df = 3 (P = 0.28); I² = 22%
Test for overall effect: Z = 4.29 (P < 0.0001)
1.3.4 Anastomotic Leakage (Anastomosis + Collagen-Based Laminar Biomaterial)
a.) Stumpf 2009 1 16 1 16 1.9% 1.00 [0.06, 17.51]
h.) Holmer 2014 4 18 0 24 0.7% 15.21 [0.76, 303.32]
j.) Schreinemacher 2011 0 21 3 20 7.2% 0.12 [0.01, 2.41]
Subtotal (95% CI) 55 60 9.8% 1.33 [0.41, 4.35]
Total events 5 4
Heterogeneity: Chi² = 5.07, df = 2 (P = 0.08); I² = 61%
Test for overall effect: Z = 0.48 (P = 0.63)
Total (95% CI) 231 238 100.0% 0.36 [0.22, 0.62]
Total events 23 54
Heterogeneity: Chi² = 11.31, df = 8 (P = 0.18); I² = 29%
Test for overall effect: Z = 3.76 (P = 0.0002)
Test for subgroup differences: Chi² = 5.94, df = 2 (P = 0.05), I² = 66.3%
0.001 0.1 1 10 1000
Favours: with sealant Favours: without sealant

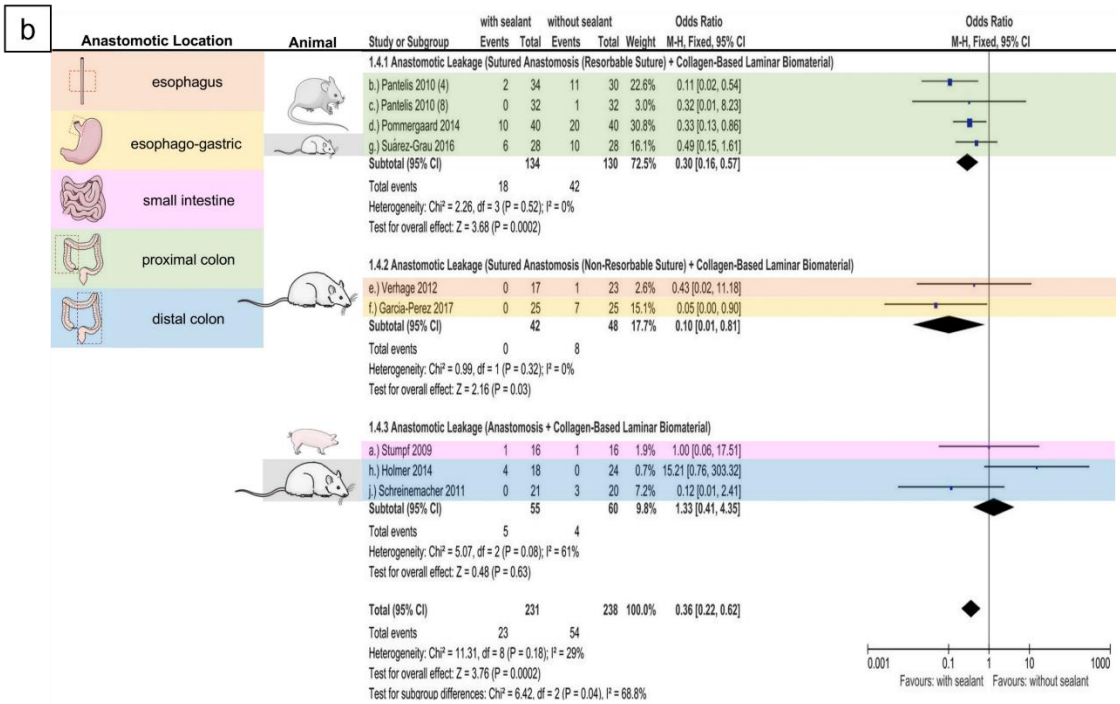
b
Anastomotic Location
Animal
esophagus
esophago-gastric
small intestine
proximal colon
distal colon
with sealant
without sealant
Odds Ratio
Odds Ratio
Study or Subgroup Events Total Events Total Weight M-H, Fixed, 95% CI
M-H, Fixed, 95% CI
1.4.1 Anastomotic Leakage (Sutured Anastomosis (Resorbable Suture) + Collagen-Based Laminar Biomaterial)
b.) Pantelis 2010 (4) 2 34 11 30 22.6% 0.11 [0.02, 0.54]
c.) Pantelis 2010 (8) 0 32 1 32 3.0% 0.32 [0.01, 8.23]
d.) Pommergaard 2014 10 40 20 40 30.8% 0.33 [0.13, 0.86]
g.) Suárez-Grau 2016 6 28 10 28 16.1% 0.49 [0.15, 1.61]
Subtotal (95% CI) 134 130 72.5% 0.30 [0.16, 0.57]
Total events 18 42
Heterogeneity: Chi² = 2.26, df = 3 (P = 0.52); I² = 0%
Test for overall effect: Z = 3.68 (P = 0.0002)
1.4.2 Anastomotic Leakage (Sutured Anastomosis (Non-Resorbable Suture) + Collagen-Based Laminar Biomaterial)
e.) Verhage 2012 0 17 1 23 2.6% 0.43 [0.02, 11.18]
f.) Garcia-Perez 2017 0 25 7 25 15.1% 0.05 [0.00, 0.90]
Subtotal (95% CI) 42 48 17.7% 0.10 [0.01, 0.81]
Total events 0 8
Heterogeneity: Chi² = 0.99, df = 1 (P = 0.32); I² = 0%
Test for overall effect: Z = 2.16 (P = 0.03)
1.4.3 Anastomotic Leakage (Anastomosis + Collagen-Based Laminar Biomaterial)
a.) Stumpf 2009 1 16 1 16 1.9% 1.00 [0.06, 17.51]
h.) Holmer 2014 4 18 0 24 0.7% 15.21 [0.76, 303.32]
j.) Schreinemacher 2011 0 21 3 20 7.2% 0.12 [0.01, 2.41]
Subtotal (95% CI) 55 60 9.8% 1.33 [0.41, 4.35]
Total events 5 4
Heterogeneity: Chi² = 5.07, df = 2 (P = 0.08); I² = 61%
Test for overall effect: Z = 0.48 (P = 0.63)
Total (95% CI) 231 238 100.0% 0.36 [0.22, 0.62]
Total events 23 54
Heterogeneity: Chi² = 11.31, df = 8 (P = 0.18); I² = 29%
Test for overall effect: Z = 3.76 (P = 0.0002)
Test for subgroup differences: Chi² = 6.42, df = 2 (P = 0.04), I² = 68.8%
0.001 0.1 1 10 1000
Favours: with sealant Favours: without sealant

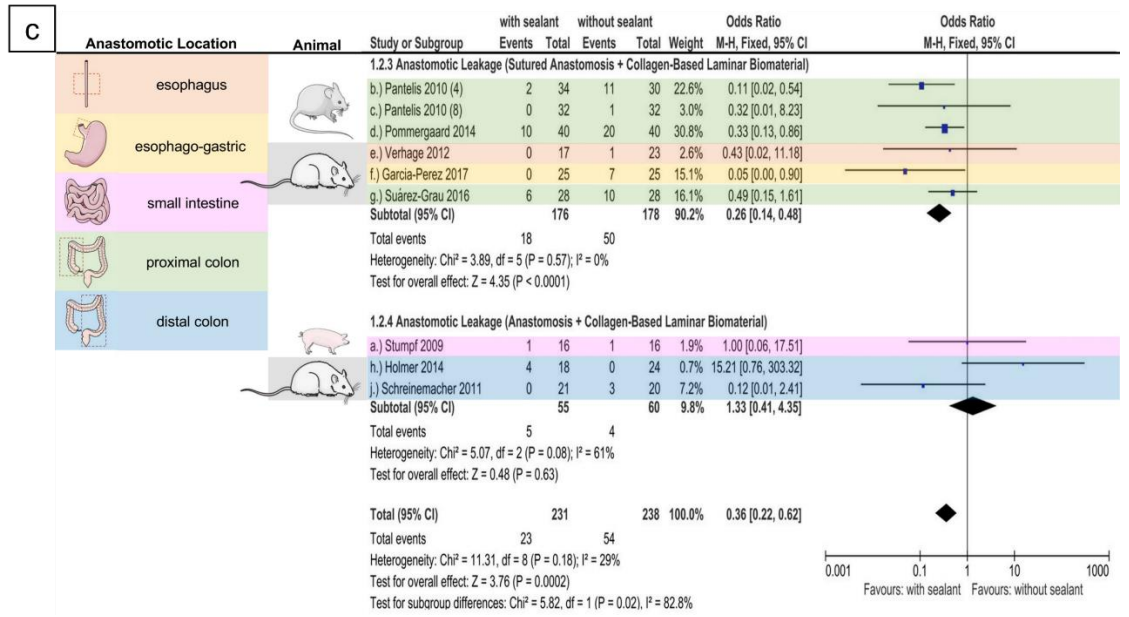
c
Anastomotic Location
Animal
esophagus
esophago-gastric
small intestine
proximal colon
distal colon
with sealant
without sealant
Odds Ratio
Odds Ratio
Study or Subgroup Events Total Events Total Weight M-H, Fixed, 95% CI
M-H, Fixed, 95% CI
1.2.3 Anastomotic Leakage (Sutured Anastomosis + Collagen-Based Laminar Biomaterial)
b.) Pantelis 2010 (4) 2 34 11 30 22.6% 0.11 [0.02, 0.54]
c.) Pantelis 2010 (8) 0 32 1 32 3.0% 0.32 [0.01, 8.23]
d.) Pommergaard 2014 10 40 20 40 30.8% 0.33 [0.13, 0.86]
e.) Verhage 2012 0 17 1 23 2.6% 0.43 [0.02, 11.18]
f.) Garcia-Perez 2017 0 25 7 25 15.1% 0.05 [0.00, 0.90]
g.) Suárez-Grau 2016 6 28 10 28 16.1% 0.49 [0.15, 1.61]
Subtotal (95% CI) 176 178 90.2% 0.26 [0.14, 0.48]
Total events 18 50
Heterogeneity: Chi² = 3.89, df = 5 (P = 0.57); I² = 0%
Test for overall effect: Z = 4.35 (P < 0.0001)
1.2.4 Anastomotic Leakage (Anastomosis + Collagen-Based Laminar Biomaterial)
a.) Stumpf 2009 1 16 1 16 1.9% 1.00 [0.06, 17.51]
h.) Holmer 2014 4 18 0 24 0.7% 15.21 [0.76, 303.32]
j.) Schreinemacher 2011 0 21 3 20 7.2% 0.12 [0.01, 2.41]
Subtotal (95% CI) 55 60 9.8% 1.33 [0.41, 4.35]
Total events 5 4
Heterogeneity: Chi² = 5.07, df = 2 (P = 0.08); I² = 61%
Test for overall effect: Z = 0.48 (P = 0.63)
Total (95% CI) 231 238 100.0% 0.36 [0.22, 0.62]
Total events 23 54
Heterogeneity: Chi² = 11.31, df = 8 (P = 0.18); I² = 29%
Test for overall effect: Z = 3.76 (P = 0.0002)
Test for subgroup differences: Chi² = 5.82, df = 1 (P = 0.02), I² = 82.8%
0.001 0.1 1 10 1000
Favours: with sealant Favours: without sealant

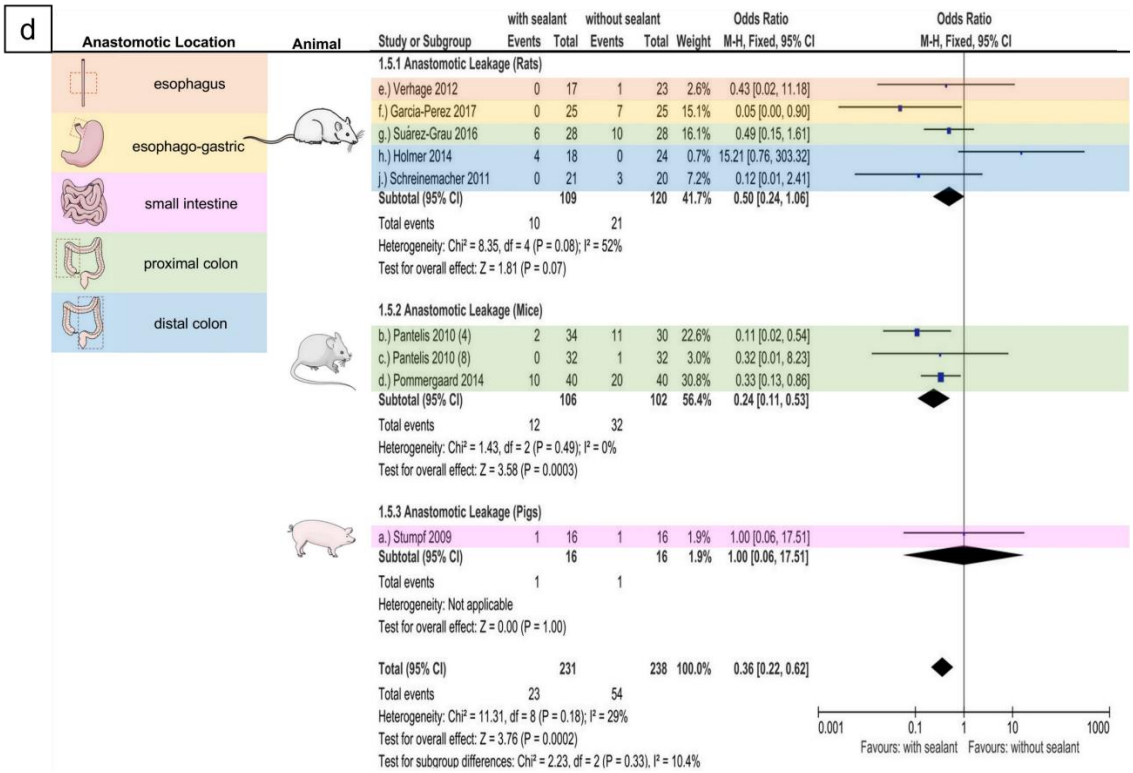
d
Anastomotic Location
Animal
esophagus
esophago-gastric
small intestine
proximal colon
distal colon
with sealant
without sealant
Odds Ratio
Odds Ratio
Study or Subgroup Events Total Events Total Weight M-H, Fixed, 95% CI
M-H, Fixed, 95% CI
1.5.1 Anastomotic Leakage (Rats)
e.) Verhage 2012 0 17 1 23 2.6% 0.43 [0.02, 11.18]
f.) Garcia-Perez 2017 0 25 7 25 15.1% 0.05 [0.00, 0.90]
g.) Suárez-Grau 2016 6 28 10 28 16.1% 0.49 [0.15, 1.61]
h.) Holmer 2014 4 18 0 24 0.7% 15.21 [0.76, 303.32]
j.) Schreinemacher 2011 0 21 3 20 7.2% 0.12 [0.01, 2.41]
Subtotal (95% CI) 109 120 41.7% 0.50 [0.24, 1.06]
Total events 10 21
Heterogeneity: Chi² = 8.35, df = 4 (P = 0.08); I² = 52%
Test for overall effect: Z = 1.81 (P = 0.07)
1.5.2 Anastomotic Leakage (Mice)
b.) Pantelis 2010 (4) 2 34 11 30 22.6% 0.11 [0.02, 0.54]
c.) Pantelis 2010 (8) 0 32 1 32 3.0% 0.32 [0.01, 8.23]
d.) Pommergaard 2014 10 40 20 40 30.8% 0.33 [0.13, 0.86]
Subtotal (95% CI) 106 102 56.4% 0.24 [0.11, 0.53]
Total events 12 32
Heterogeneity: Chi² = 1.43, df = 2 (P = 0.49); I² = 0%
Test for overall effect: Z = 3.58 (P = 0.0003)
1.5.3 Anastomotic Leakage (Pigs)
a.) Stumpf 2009 1 16 1 16 1.9% 1.00 [0.06, 17.51]
Subtotal (95% CI) 16 16 1.9% 1.00 [0.06, 17.51]
Total events 1 1
Heterogeneity: Not applicable
Test for overall effect: Z = 0.00 (P = 1.00)
Total (95% CI) 231 238 100.0% 0.36 [0.22, 0.62]
Total events 23 54
Heterogeneity: Chi² = 11.31, df = 8 (P = 0.18); I² = 29%
Test for overall effect: Z = 3.76 (P = 0.0002)
Test for subgroup differences: Chi² = 2.23, df = 2 (P = 0.33), I² = 10.4%
0.001 0.1 1 10 1000
Favours: with sealant Favours: without sealant

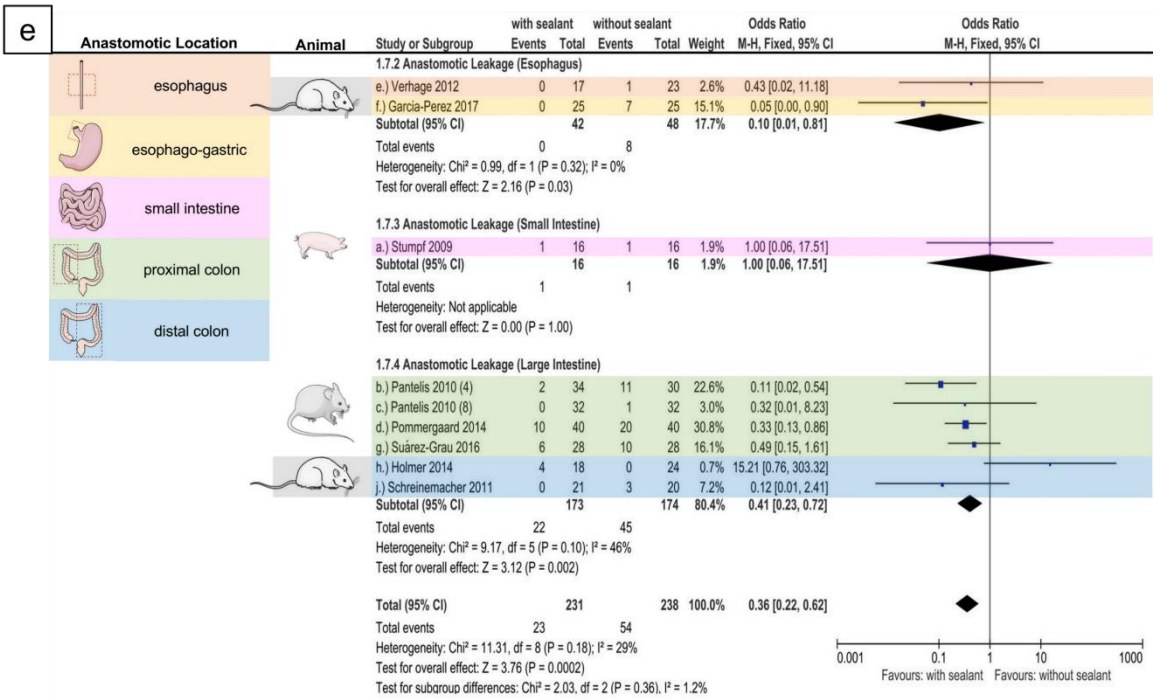

Figure 26. **Fixed-effects model meta-analysis for postoperative anastomotic leakage in intervention (coated anastomoses) and control group.** (a) Forest plot of subgroup analysis stratified by sufficiency of anastomoses. (b) Forest plot of subgroup analysis stratified by utilized suture material. (c) Forest plot of subgroup analysis stratified by anastomotic technique. (d) Forest plot of subgroup analysis stratified by animal species. (e) Forest plot of subgroup analysis stratified by anastomotic location.

Elements in Figure 26 were modified from SMART (Servier Medical Art), licensed under a Creative Common Attribution 3.0 Generic License. http: //smart.servier.com/. [154]

2.4.2 Postoperative mortality rate

Overall, six studies (seven discrete data sets) [46, 50, 52, 53, 55, 56] reported the incidence of postoperative mortality, occurring in 18 of 160 (11.3 %) animals in the intervention group and 42 of 155 (27 %) in the control group. Using the FE model meta-analysis, the overall postoperative mortality rate was significantly lower for animals with coated anastomoses compared to animals in the control group ($OR, 0.34$; $95\ \%\ CI, 0.19 - 0.63$; $p = 0.0005$). The studies were homogeneous ($I^2 = 0\ \%$; $p = 0.56$). (**Figure 27**) Observed results remained stable throughout sensitivity analyses. (**Table 14**)

Subgroup analyses found no differences between subgroups stratified by animal species (TSD: $p = 0.83$), location of anastomoses (TSD: $p = 0.30$), anastomotic techniques (TSD: $p = 0.87$), anastomotic sufficiency ($TSD\ p = 0.28$), or type of suture material utilized ($TSD\ p = 0.62$). (**Figure 28**)

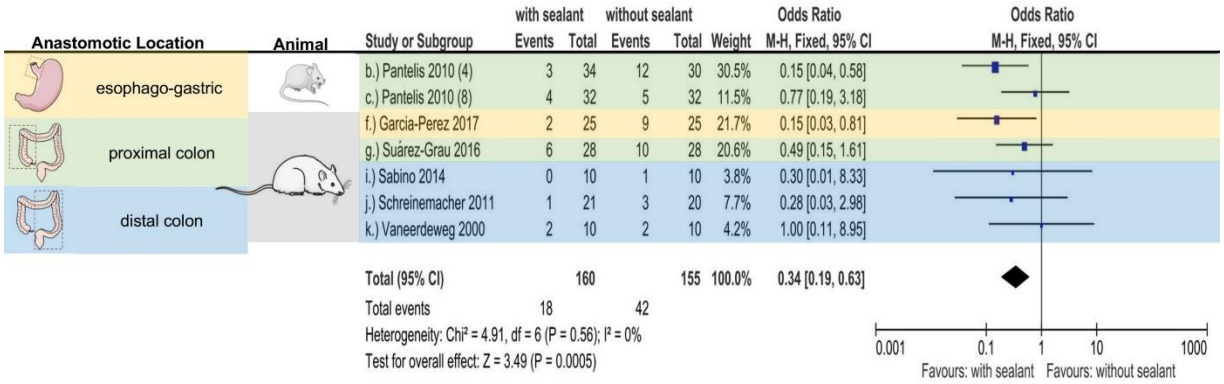

Figure 27. Fixed-effects model meta-analysis for postoperative mortality in intervention (coated anastomoses) and control group. Forest plot of all studies included. *Elements in Figure 27 were modified from SMART (Servier Medical Art), licensed under a Creative Common Attribution 3.0 Generic License. http: //smart.servier.com/.* [154]

Table 14 Fixed-effects model meta-analysis for postoperative mortality in the intervention and control group.

Table 14. Fixed-effects model meta-analysis for postoperative mortality in the intervention and control group.

Postoperative mortality	**Odds ratio (OR): FE model**	**Heterogeneity**
Overall	OR, 0.34; 95 % CI, 0.19-0.63; **p = 0.0005 [↓(I); ↑(C)]**	I^2 = 0 %; p = 0.56
Sensitivity analyses		
Excluded study	**OR: FE model**	**Heterogeneity**
Garcia-Perez et al. [46]	OR, 0.40; 95 % CI, 0.21-0.76; **p = 0.005 [↓(I); ↑(C)]**	I^2 = 0 %; p = 0.58
Pantelis et al. *(4)* [50] [a]	OR, 0.43; 95 % CI, 0.22-0.85; **p = 0.01 [↓(I); ↑(C)]**	I^2 = 0 %; p = 0.72
Pantelis et al. *(8)* [50] [a]	OR, 0.29; 95 % CI, 0.15-0.56; **p = 0.003 [↓(I); ↑(C)]**	I^2 = 0 %; p = 0.63
Sabino et al. [52]	OR, 0.34; 95 CI, 0.19-0.63; **p = 0.0006 [↓(I); ↑(C)]**	I^2 = 0 %; p = 0.43
Schreinemacher et al. [53]	OR, 0.35; 95 % CI, 0.19-0.65; **p = 0.0009 [↓(I); ↑(C)]**	I^2 = 0 %; p = 0.43
Suárenz-Grau et al. [55]	OR, 0.30; 95 % CI, 0.15-0.61; **p = 0.0009 [↓(I); ↑(C)]**	I^2 = 0 %; p = 0.48
Vaneerdeweg et al. [56]	OR, 0.31; 95 % CI, 0.17-0.59; **p = 0.0005 [↓(I); ↑(C)]**	I^2 = 0 %; p = 0.55

↓ = Significantly lower; ↑ = Significantly higher; I = Intervention group (intestinal anastomoses coated with collagen-based laminar biomaterial); C = Control group; FE = Fixed-effect.
The bold indicates significant outcomes.
[a] *Pantelis et al. [50] includes two discrete data sets.*

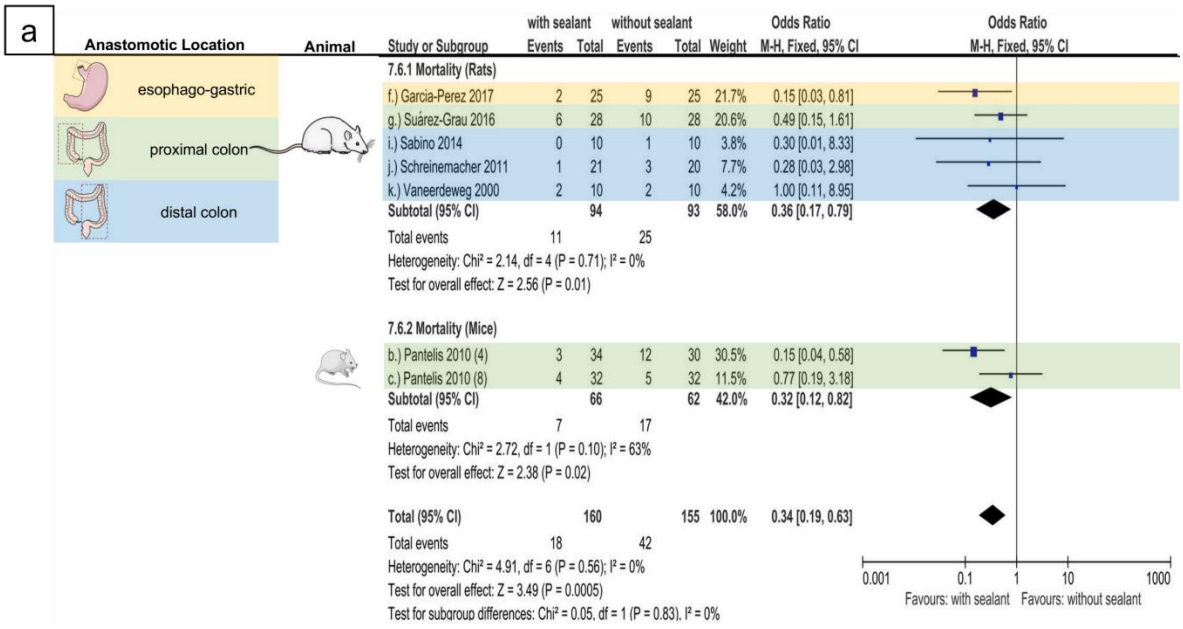

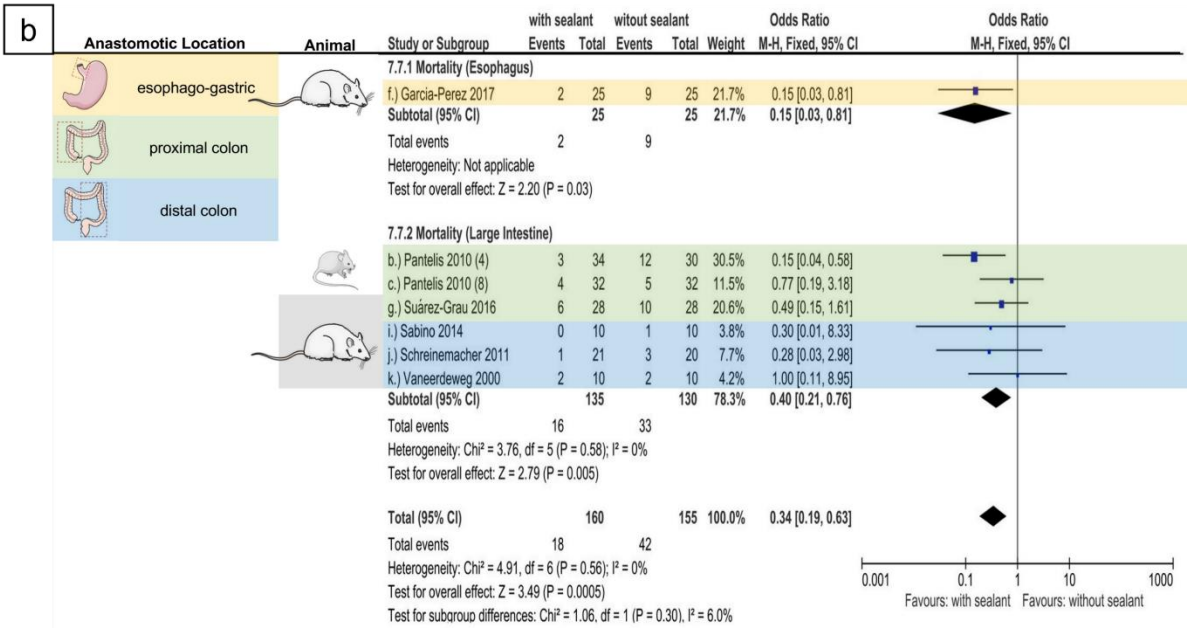
b
Anastomotic Location
Animal
esophago-gastric
proximal colon
distal colon
with sealant
witout sealant
Odds Ratio
Odds Ratio
Study or Subgroup Events Total Events Total Weight M-H, Fixed, 95% CI
M-H, Fixed, 95% CI
7.7.1 Mortality (Esophagus)
f.) Garcia-Perez 2017 2 25 9 25 21.7% 0.15 [0.03, 0.81]
Subtotal (95% CI) 25 25 21.7% 0.15 [0.03, 0.81]
Total events 2 9
Heterogeneity: Not applicable
Test for overall effect: Z = 2.20 (P = 0.03)
7.7.2 Mortality (Large Intestine)
b.) Pantelis 2010 (4) 3 34 12 30 30.5% 0.15 [0.04, 0.58]
c.) Pantelis 2010 (8) 4 32 5 32 11.5% 0.77 [0.19, 3.18]
g.) Suárez-Grau 2016 6 28 10 28 20.6% 0.49 [0.15, 1.61]
i.) Sabino 2014 0 10 1 10 3.8% 0.30 [0.01, 8.33]
j.) Schreinemacher 2011 1 21 3 20 7.7% 0.28 [0.03, 2.98]
k.) Vaneerdeweg 2000 2 10 2 10 4.2% 1.00 [0.11, 8.95]
Subtotal (95% CI) 135 130 78.3% 0.40 [0.21, 0.76]
Total events 16 33
Heterogeneity: Chi² = 3.76, df = 5 (P = 0.58); I² = 0%
Test for overall effect: Z = 2.79 (P = 0.005)
Total (95% CI) 160 155 100.0% 0.34 [0.19, 0.63]
Total events 18 42
Heterogeneity: Chi² = 4.91, df = 6 (P = 0.56); I² = 0%
Test for overall effect: Z = 3.49 (P = 0.0005)
Test for subgroup differences: Chi² = 1.06, df = 1 (P = 0.30), I² = 0%
0.001 0.1 1 10 1000
Favours: with sealant Favours: without sealant

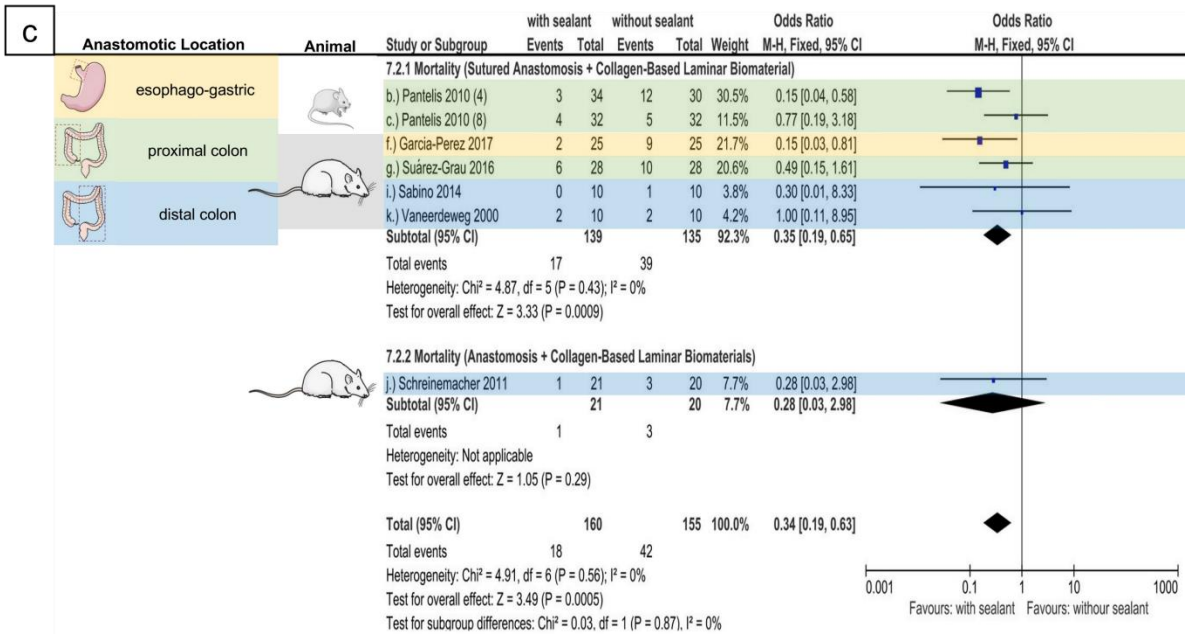
c
Anastomotic Location
Animal
esophago-gastric
proximal colon
distal colon
with sealant
without sealant
Odds Ratio
Odds Ratio
Study or Subgroup Events Total Events Total Weight M-H, Fixed, 95% CI
M-H, Fixed, 95% CI
7.2.1 Mortality (Sutured Anastomosis + Collagen-Based Laminar Biomaterial)
b.) Pantelis 2010 (4) 3 34 12 30 30.5% 0.15 [0.04, 0.58]
c.) Pantelis 2010 (8) 4 32 5 32 11.5% 0.77 [0.19, 3.18]
f.) Garcia-Perez 2017 2 25 9 25 21.7% 0.15 [0.03, 0.81]
g.) Suárez-Grau 2016 6 28 10 28 20.6% 0.49 [0.15, 1.61]
i.) Sabino 2014 0 10 1 10 3.8% 0.30 [0.01, 8.33]
k.) Vaneerdeweg 2000 2 10 2 10 4.2% 1.00 [0.11, 8.95]
Subtotal (95% CI) 139 135 92.3% 0.35 [0.19, 0.65]
Total events 17 39
Heterogeneity: Chi² = 4.87, df = 5 (P = 0.43); I² = 0%
Test for overall effect: Z = 3.33 (P = 0.0009)
7.2.2 Mortality (Anastomosis + Collagen-Based Laminar Biomaterials)
j.) Schreinemacher 2011 1 21 3 20 7.7% 0.28 [0.03, 2.98]
Subtotal (95% CI) 21 20 7.7% 0.28 [0.03, 2.98]
Total events 1 3
Heterogeneity: Not applicable
Test for overall effect: Z = 1.05 (P = 0.29)
Total (95% CI) 160 155 100.0% 0.34 [0.19, 0.63]
Total events 18 42
Heterogeneity: Chi² = 4.91, df = 6 (P = 0.56); I² = 0%
Test for overall effect: Z = 3.49 (P = 0.0005)
Test for subgroup differences: Chi² = 0.03, df = 1 (P = 0.87), I² = 0%
0.001 0.1 1 10 1000
Favours: with sealant Favours: withour sealant

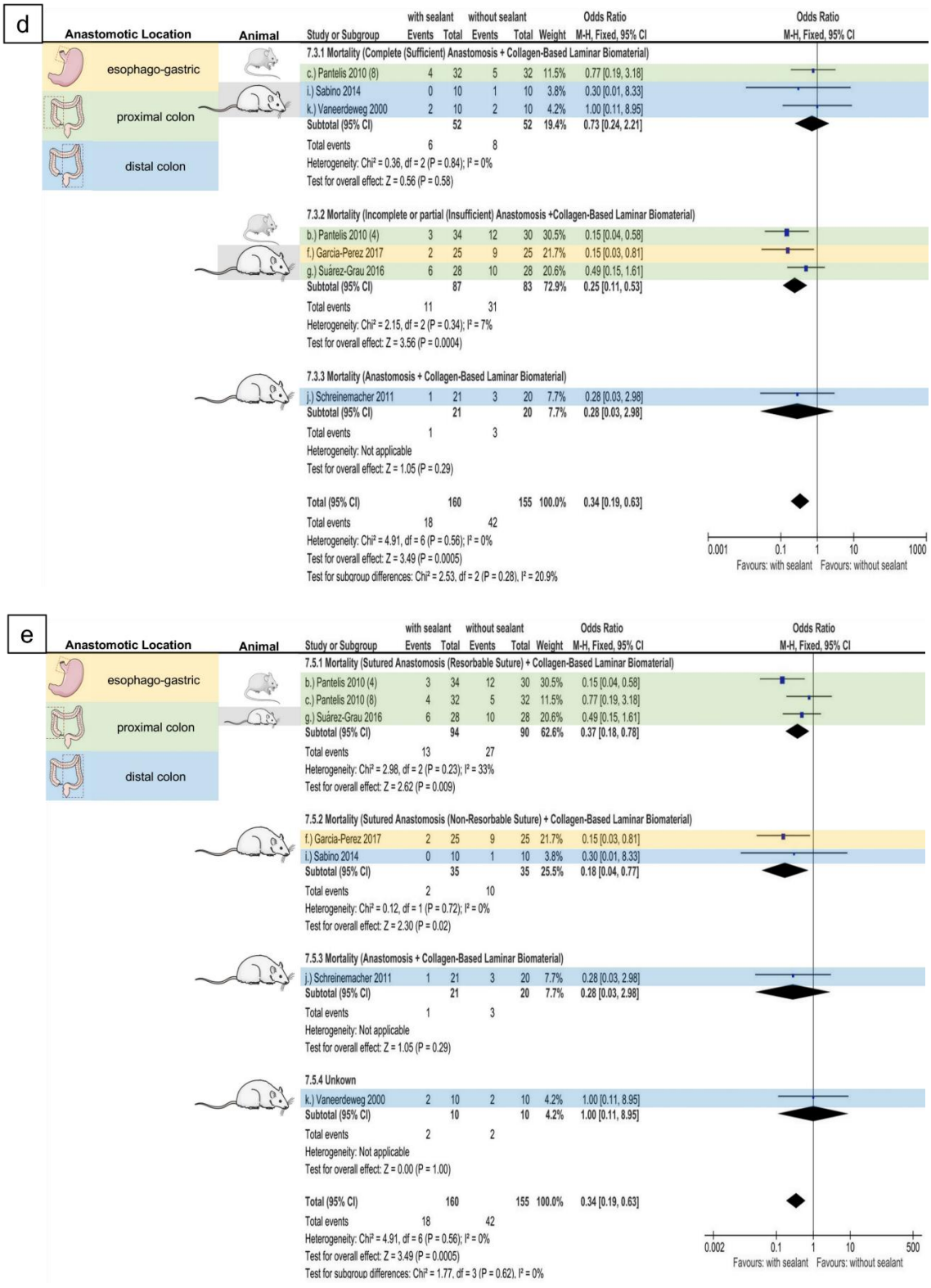

Figure 28 Fixed-effects model meta-analysis for postoperative mortality in intervention (coated anastomoses) and control group. (a) Forest plot of subgroup analysis stratified by animal species. (b) Forest plot of subgroup analysis stratified by anastomotic location. (c) Forest plot of subgroup analysis stratified by anastomotic technique. (d) Forest plot of subgroup analysis stratified by sufficiency of anastomoses. (e) Forest plot of subgroup analysis stratified by suture material. *Elements in Figure 28 were modified from SMART (Servier Medical Art), licensed under a Creative Common Attribution 3.0 Generic License. http: //smart.servier.com/*. [154]

3. Feasibility study and functional validation of the innovative *ex-vivo* model

The content presented in **Chapter IV.3** has been adapted and modified from the publication authored by Cira et al., 2024 [2].

3.1. Descriptive statistics

3.1.1 Experimental series 1: Handsewn small intestinal end-to-end anastomosis using interrupted suture technique in the low-flow group

In total, eight handsewn sufficient small intestinal EEAs using the SBS technique were tested in the LF model. After preparing the anastomoses according to the technique describe in **Chapter III.3.3.4.2**, every individual anastomosis was tested according to the test protocol. (**Figure 29**)

3.1.1.1 Quantitative analysis of anastomotic performance and time intervals

3.1.1.1.1 Leakage pressure analysis

All eight SBS-CON-LF anastomoses had a mean LP of 16.98 $mmHg$ with a SD of $\pm$ 14.88 $mmHg$ (95 % CI, 4.54 – 29.41 $mmHg$; SEM of 5.26). The calculated median LP corresponded to 13.45 $mmHg$. The measured values showed a range of 42.6 $mmHg$ (-0.4 – 42.2 $mmHg$), and a sample variance of 221.35. The distribution of the measured values presented with negative kurtosis (-0.61) and a positive skewness (0.61). (**Table 15**)

3.1.1.1.2 Bursting pressure analysis

For evaluated BPs, anastomoses presented a mean BP of 89.74 $mmHg$ with a SD of $\pm$ 58.37 $mmHg$ (95 % CI, 40.94 – 138.53 $mmHg$; SEM of 20.64). The calculated median BP corresponded to 83.75 $mmHg$. The measured values showed a range of 170.4 $mmHg$ (8.9 –

179.3 $mmHg$), and a sample variance of 3,406.53. The distribution of the measured values presented with negative kurtosis (-1.13) and a positive skewness (0.21). (**Table 15**)

3.1.1.1.3 Analysis of time intervals

The mean time interval from the first measurement (actual start of the experiment) until BP amounted 129,109.88 $msec$ with an SD of $\pm$ 104,506.61 $msec$. Breaking it down, the time needed from the first measurement to reach the LP had a mean of 25,271.13 $msec$ (SD $\pm$ 13,337.71 $msec$), and from LP to BP, the mean was 103,838.75 $msec$ (SD $\pm$ 100,388.24 $msec$). Additional values evaluated in the descriptive statistics are presented in **Table 16**.

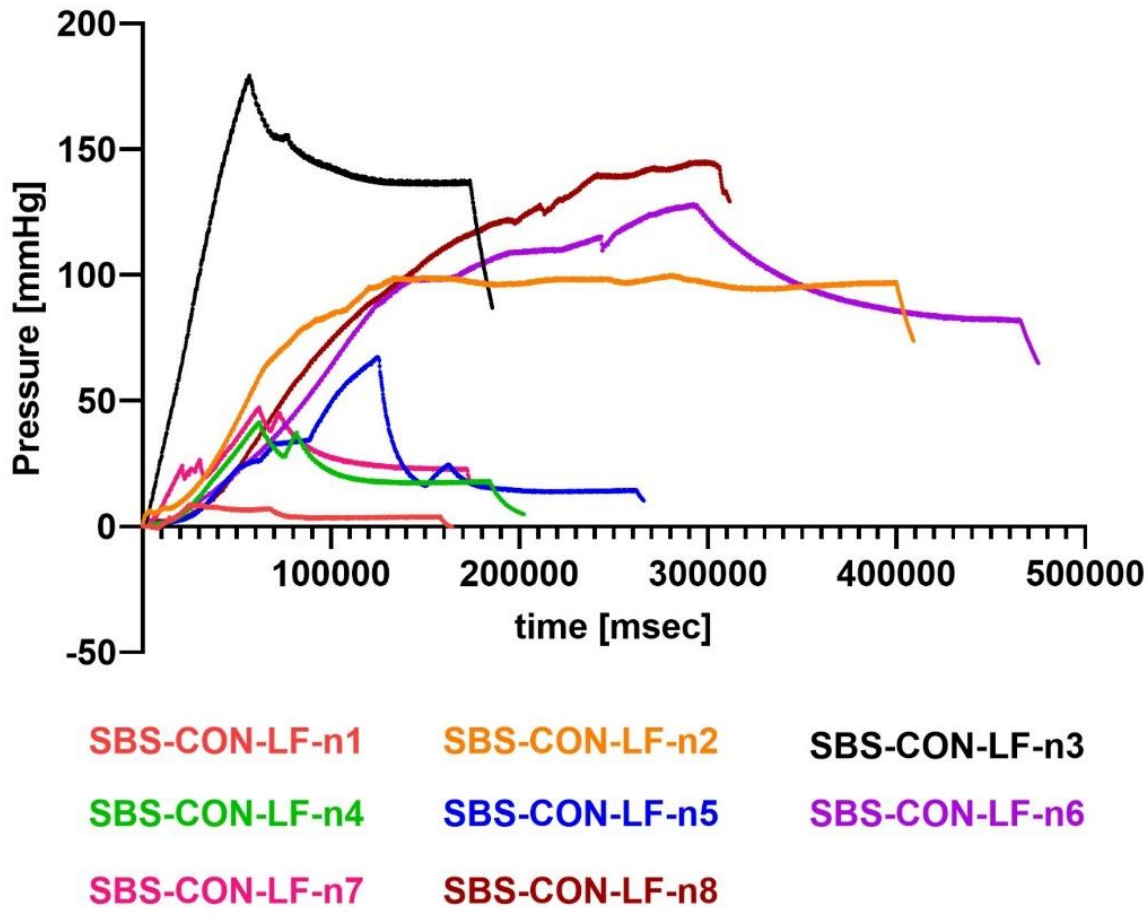

Figure 29 Pressure-time profiles of all eight SBS-CON-LF anastomoses. *SBS-CON-LF = Handsewn sufficient small intestinal end-to-end anastomoses using interrupted suture technique, tested in the low-flow model; $mmHg$ = Millimeters of mercury; $msec$ = Milliseconds. (Adapted from Cira et al., Langenbecks Arch Surg 2024)* [2]

3.1.1.2 Interrelated analyses derived from experimental outcomes

3.1.1.2.1 Proportion of bursting pressure at leakage pressure

The mean pressure difference between measured LP and BP was calculated to be 72.76 $mmHg$ with a SD of $\pm$ 52.53 $mmHg$ (95 % CI, 28.85 – 116.68 $mmHg$; SEM 18.57). The calculated median pressure difference between measured LP and BP corresponded to 61.2 $mmHg$. The measured values showed a range of 134.2 $mmHg$ (9.3 – 143.5 $mmHg$), and sample variance of 2,759.04. The distribution of the measured values presented with negative kurtosis (-1.74) and a positive skewness (0.32). (**Table 16**)

3.1.1.2.2 Percentage of bursting pressure at leakage pressure and relative difference of pressure between leakage and bursting

The mean pressure difference between measured LP and BP corresponded to 19.38 % with a SD of $\pm$ 17.61 %. Therefore, the LP was reached at a mean of 80.62 % of the BP with a SD of $\pm$ 17.61 %. (**Table 16**)

3.1.1.2.3 Time of leakage occurrence relative to bursting time and relative difference of time between leakage and bursting time

The mean time difference between measured LP and BP corresponded to 26.33 % with a SD of $\pm$11.77 %. Therefore, the LP was reached at a mean time of 73.67 % of BP with a SD of $\pm$ 11.77 %. (**Table 16**)

Table 15. Quantitative analysis of anastomotic performance: Evaluation of leakage pressure and bursting pressure. Summary of descriptive statistics for the SBS-CON-LF experimental series. *(Adapted from Cira et al., Langenbecks Arch Surg 2024)* [2]

Table 15. Quantitative analysis of anastomotic performance: Evaluation of leakage pressure and bursting pressure. Summary of descriptive statistics for the SBS-CON-LF experimental series.		
Anastomosis (name)	**Leakage pressure in $mmHg$**	**Bursting pressure in $mmHg$**
SBS-CON-LF-n1	-0.4	8.9
SBS-CON-LF-n2	32.3	100.1
SBS-CON-LF-n3	42.2	179.3
SBS-CON-LF-n4	8.9	41.5
SBS-CON-LF-n5	12.8	67.4
SBS-CON-LF-n6	14.1	128.2
SBS-CON-LF-n7	24.2	47.3
SBS-CON-LF-n8	1.7	145.2
Summary of descriptive statistics		
Mean	16.98	89.74
Standard error of the mean (SEM)	5.26	20.64
Median	13.45	83.75
Mode	N/A	N/A
Standard deviation (SD)	14.88	58.37
Sample variance	221.35	3,406.53
Kurtosis	-0.61	-1.13
Skewness	0.61	0.21
Range	42.6	170.4
Minimum	-0.4	8.9
Maximum	42.2	179.3
Sum	135.8	717.9
Count	8	8
Confidence level (CI) (95 %)	12.44	48.80
Upper CI (95 %)	29.41	138.53
Lower CI (95 %)	4.54	40.94
SBS-CON-LF = Handsewn sufficient small intestinal end-to-end anastomoses using interrupted suture technique, tested in the low flow model; $mmHg$ = Millimeters of mercury; N/A = Not available.		

Table 16. Quantitative analysis of anastomotic performance in the SBS-CON-LF experimental series: Time interval analysis. Interrelated analyses derived from experimental outcomes. *(Adapted from Cira et al., Langenbecks Arch Surg 2024)* [2]

Table 16. Quantitative analysis of anastomotic performance in the SBS-CON-LF experimental series: Time interval analysis. Interrelated analyses derived from experimental outcomes.

Anastomosis (name)	Time (start to leakage pressure), in $msec$	Time (start to bursting pressure), in $msec$	Time (LP to BP), in $msec$	Proportion of BP at LP, in $mmHg$	Percentage of BP at LP, in %	Relative difference of pressure between LP and BP, in %	Time of leakage occurrence relative to bursting time, in %	Relative difference of time between leakage and bursting time, in %
SBS-CON-LF-n1	6,800	25,300	18,500	9.30	-4.49	104.49	26.88	73.12
SBS-CON-LF-n2	43,169	279,869	236,700	67.80	32.27	67.73	15.43	84.58
SBS-CON-LF-n3	14,249	56,700	42,451	137.10	23.54	76.46	25.13	74.87
SBS-CON-LF-n4	26,729	62,002	35,273	32.60	21.45	78.55	43.11	56.89
SBS-CON-LF-n5	38,302	124,805	86,503	54.60	18.99	81.01	30.69	69.31
SBS-CON-LF-n6	37,513	124,099	86,586	114.10	11.00	89.00	30.23	69.77
SBS-CON-LF-n7	21,304	61,802	40,498	23.10	51.16	48.84	34.47	65.53
SBS-CON-LF-n8	14,103	2,983,020	284,199	143.50	1.17	98.83	4.73	95.27
Summary of descriptive statistics								
Mean	25,271.13	129,109.88	103,838.75	72.76	19.39	80.62	26.33	73.67
Standard error of the mean (SEM)	4,715.59	36,948.67	35,492.60	18.57	6.23	6.23	4.16	4.16
Median	24,016.5	93,050.5	64,477	61.2	20.22	79.78	28.55	71.45
Mode	N/A	N/A	N/A	N/A	N/A	N/A	N/A	N/A
Standard deviation (SD)	13,337.71	104,506.61	100,388.24	52.53	17.61	17.61	11.77	11.77
Sample variance	177,894,475.8	10,921,632,403	10,077,798,275	2,759.04	309.96	309.96	138.48	138.48
Kurtosis	-1.64	-0.53	0.08	-1.74	0.41	0.41	0.75	0.75
Skewness	0.06	1.03	1.28	0.32	0,49	-0.49	-0.70	0.70
Range	36,369	273,002	265,699	134.2	55.66	55.66	38.38	38.38
Minimum	6,800	25,300	18,500	9.3	-4.49	48.84	4.73	56.89

Maximum	43,169	298,302	284,199	143.5	51.16	104.49	43.11	95.27
Sum	202,169	1,032,879	830,710	582.1	155.08	644.92	210.66	589.34
Count	8	8	8	8	8	8	8	8
Confidence level (CI) (95 %)	11,150.60	87,369.72	83,926.67	43.91	14.72	14.72	9.84	9.84
Upper CI (95 %)	36,421.73	216,479.59	187,765.42	116.68	34.10	95.33	36.17	83.51
Lower CI (95 %)	14,120.52	41,740.16	19,912.08	28.85	4.67	65.90	16.49	63.83

SBS-CON-LF = Handsewn sufficient small intestinal end-to-end anastomoses using interrupted suture technique, tested in the low-flow model; $mmHg$ *= Millimeters of mercury;* $\boldsymbol{msec}$ *= Milliseconds; % = Percent; N/A = Not available.*

3.1.2 Experimental series 2: Handsewn small intestinal end-to-end anastomosis using interrupted suture technique in the high-flow group

In total, eight handsewn sufficient small intestinal EEAs using SBS were tested in the HF model. After preparing the anastomoses according to the technique describe in **Chapter III.3.3.4.2**, every individual anastomosis was tested according to the test protocol. (**Figure 30**)

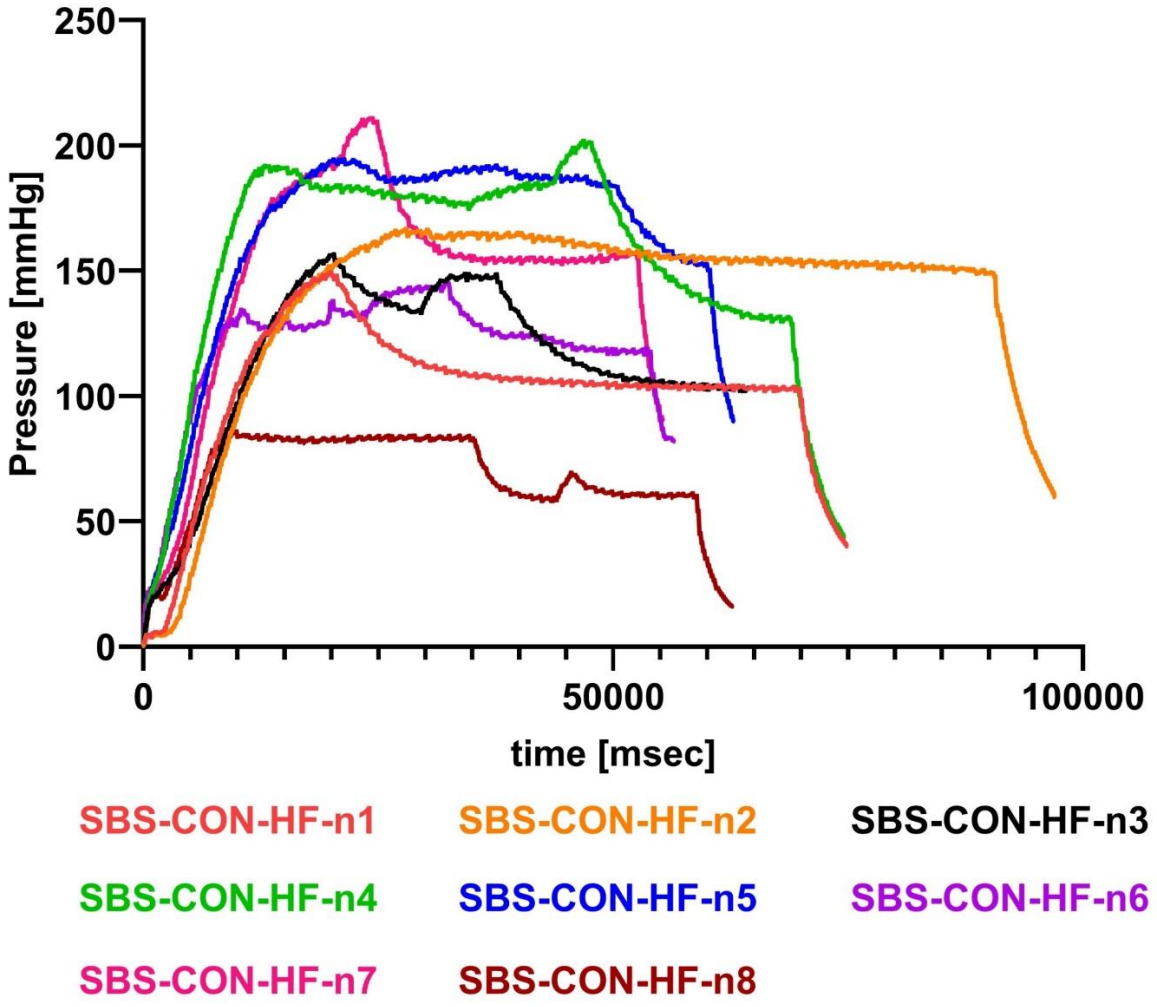

Figure 30. Pressure-time profiles of all eight SBS-CON-HF anastomoses. *SBS-CON-HF = Handsewn sufficient small intestinal end-to-end anastomoses using interrupted suture technique, tested in the high-flow model;* $mmHg$ *= Millimeters of mercury;* $msec$ *= Milliseconds. (Adapted from Cira et al., Langenbecks Arch Surg 2024)* [2]

3.1.2.1 Quantitative analysis of anastomotic performance and time intervals

3.1.2.1.1 Leakage pressure analysis

All eight SBS-CON-HF anastomoses had a mean LP of 62.35 $mmHg$ with a SD of $\pm$ 49.78 $mmHg$ (95 % CI, 20.74 – 103.98 $mmHg$; SEM of 17.6). The calculated median LP corresponded to 55.05 $mmHg$. The measured values showed a range of 148.3 $mmHg$ (5.9 – 154.2 $mmHg$) and a sample variance of 2,478.41. The distribution of the measured values presented with positive kurtosis (0.12) and a positive skewness (0.82). (**Table 17**)

3.1.2.1.2 Bursting pressure analysis

For evaluated BP, a mean BP of 163.88 $mmHg$ with a SD of $\pm$ 40.15 $mmHg$ (95 % CI, 130.31 – 197.44 $mmHg$; SEM of 14.20) was observed. The calculated median BP corresponded to 161.6 $mmHg$. The measured values showed a range of 124.9 $mmHg$ (86 – 210.9 $mmHg$) and a sample variance of 1,611.89. The distribution of the measured values presented with positive kurtosis (1.01) and a negative skewness (-0.87). (**Table 17**)

3.1.2.1.3 Analysis of time intervals

The mean time interval from the first measurement (actual start of the experiment) until bursting was 25,091 $msec$ with a SD of $\pm$ 10,989.51 $msec$. Splitting it up, the time needed from the first measurement to reaching the LP was a mean time of 5,057.88 $msec$ (SD $\pm$ 3,516.90 $msec$), and from LP to BP was a mean of 20,033.13 $msec$ (SD $\pm$ 11,762.89 $msec$). Further values evaluated in the descriptive statistics are depicted in **Table 18**.

3.1.2.2 Interrelated analyses derived from experimental outcomes

3.1.2.2.1 Proportion of bursting pressure at leakage pressure

The mean pressure difference between measured LP and BP was calculated to be 101.51 $mmHg$ with a SD of $\pm$ 19.54 $mmHg$ (95 % CI, 55.31 – 147.71 $mmHg$; SEM of 18.57). The

calculated median pressure difference between measured LP and BP corresponded to 87.65 $mmHg$. The measured values showed a range of 145.7 $mmHg$ (40.3 – 186 $mmHg$) and sample variance of 3,053.68. The distribution of the measured values presented with negative kurtosis (-1.46) and a positive skewness (0.4). (**Table 18**)

3.1.2.2.2 Percentage of bursting pressure at leakage pressure and relative difference of pressure between leakage and bursting

The mean pressure difference between measured LP and BP corresponded to 37.74 % with a SD of $\pm$ 27.74 %. Therefore, the LP was reached at a mean of 62.26 % of the BP with a SD of $\pm$ 27.74 %. (**Table 18**)

3.1.2.2.3 Time of leakage occurrence relative to bursting time and relative difference of time between leakage and bursting time

The mean time difference between measured LP and BP corresponded to 22.68 % with a SD of $\pm$ 16.93 %. Therefore, the LP was reached at a mean time of 77.32 % of BP with a SD of $\pm$ 16.93 %.(**Table 18**)

Table 17. Quantitative analysis of anastomotic performance: Evaluation of leakage pressure and bursting pressure. Summary of descriptive statistics for the SBS-CON-HF experimental series. *(Adapted from Cira et al., Langenbecks Arch Surg 2024)* [2]

Table 17. Quantitative analysis of anastomotic performance: Evaluation of leakage pressure and bursting pressure. Summary of descriptive statistics for the SBS-CON-HF experimental series.

Anastomosis (name)	Leakage pressure in $mmHg$	Bursting pressure in $mmHg$
SBS-CON-HF-n1	5.9	149.3
SBS-CON-HF-n2	66.8	166.7
SBS-CON-HF-n3	81.1	156.5
SBS-CON-HF-n4	43.3	201.9
SBS-CON-HF-n5	154.2	194.5
SBS-CON-HF-n6	103.7	145.2
SBS-CON-HF-n7	24.9	210.9
SBS-CON-HF-n8	19	86
Summary of descriptive statistics		
Mean	62.36	163.88
Standard error of the mean (SEM)	17.60	14.20
Median	55.05	161.6
Mode	N/A	N/A
Standard deviation (SD)	49.78	40.15
Sample variance	2,478.41	1,611.89
Kurtosis	0.12	1.01
Skewness	0.82	-0.87
Range	148.3	124.9
Minimum	5.9	86
Maximum	154.2	210.9
Sum	4,989	1,311
Count	8	8
Confidence level (CI) (95 %)	41.62	33.57
Upper CI (95 %)	103.98	197.44
Lower CI (95 %)	20.74	130.31

SBS-CON-HF = Handsewn sufficient small intestinal end-to-end anastomoses using interrupted suture technique, tested in the high-flow model; $mmHg$ = Millimeters of mercury; N/A = Not available.

Table 18. Quantitative analysis of anastomotic performance in the SBS-CON-HF experimental series: Time interval analysis. Interrelated analyses derived from experimental outcomes. *(Adapted from Cira et al., Langenbecks Arch Surg 2024)* [2]

Table 18. Quantitative analysis of anastomotic performance in the SBS-CON-HF experimental series: Time interval analysis. Interrelated analyses derived from experimental outcomes.

Anastomosis (name)	Time (start to leakage pressure (LP), in $msec$	Time (start to bursting pressure (BP), in $msec$	Time (LP to BP), in $msec$	Proportion of BP at LP, in $mmHg$	Percentage of BP at LP, in %	Relative difference of pressure between LP and BP, in %	Time of leakage occurrence relative to bursting time, in %	Relative difference of time between leakage and bursting time, in %
SBS-CON-HF-n1	2,004	19,900	17,896	143.40	3.95	96.05	10.07	89.93
SBS-CON-HF-n2	7,712	27,899	20,187	99.90	40.07	59.93	27.64	72.36
SBS-CON-HF-n3	8,401	20,200	11,799	75.40	51.82	48.18	41.59	58.41
SBS-CON-HF-n4	2,499	46,799	44,300	158.60	21.45	78.55	5.34	94.66
SBS-CON-HF-n5	10,585	20,184	9,599	40.30	79.28	20.72	52.44	47.56
SBS-CON-HF-n6	5,704	32,098	26,394	41.50	71.42	28.58	17.77	82.23
SBS-CON-HF-n7	1,688	24,088	22,400	186.00	11.81	88.19	7.01	92.99
SBS-CON-HF-n8	1,870	9,560	7,690	67.00	22.09	77.91	19.56	80.44
Summary of descriptive statistics								
Mean	5,057.88	25,091	5,057.88	101.51	37.74	62.26	22.68	77.32
Standard error of the mean (SEM)	1,243.41	3,885.38	1,243.41	19.54	9.81	9.81	5.99	5.99
Median	4,101.5	22,144	4,101.5	87.65	31.08	68.92	18.67	81.33
Mode	N/A	N/A	N/A	N/A	N/A	N/A	N/A	N/A
Standard deviation (SD)	3,516.90	10,989.5090	3,516.90	55.26	27.74	27.75	16.93	16.93
Sample variance	12,368,578.7	120,769,308.3	12,368,578.7	3,053.68	769.72	769.72	286.73	286.73
Kurtosis	-1.61	1.7901	-1.61	-1.46	-1.32	-1.32	-0.36	-0.36
Skewness	0.48	0.93	0.49	0.40	0.43	-0.43	0.87	-0.87
Range	8,897	37,239	8,897	145.7	75.33	75.33	47.10	47.10
Minimum	1,688	9,560	1,688	40.3	3.95	20.72	5.34	47.56

IV Results

Maximum	10,585	46,799	10,585	186	79.28	96.05	52.44	94.66
Sum	40,463	200,728	40,463	812.1	301.89	498.11	181.42	618.58
Count	8	8	8	8	8	8	8	8
Confidence level (CI) (95 %)	2,940.20	9,187.46	2,940.20	46.20	23.20	23.20	14.16	14.16
Upper CI (95 %)	7,998.08	34,278.46	7,998.08	147.71	60.93	85.46	36.83	91.48
Lower CI (95 %)	2,117.67	15,903.54	2,117.67	55.31	14.54	39.07	8.52	63.17

SBS-CON-HF = Handsewn sufficient small intestinal end-to-end anastomoses using interrupted suture technique, tested in the high-flow model; $mmHg$ = Millimeters of mercury; $msec$ = Milliseconds; % = Percent; N/A = Not available.

3.1.3 Experimental Series 3: Handsewn small intestinal end-to-end anastomosis using continuous suture technique in the low-flow group

Overall, eight handsewn sufficient small intestinal EEAs using CS technique were tested in the LF model. After preparing the anastomoses according to the technique describe in **Chapter III.3.3.4.2**, every individual anastomosis was tested according to the test protocol. (**Figure 31**)

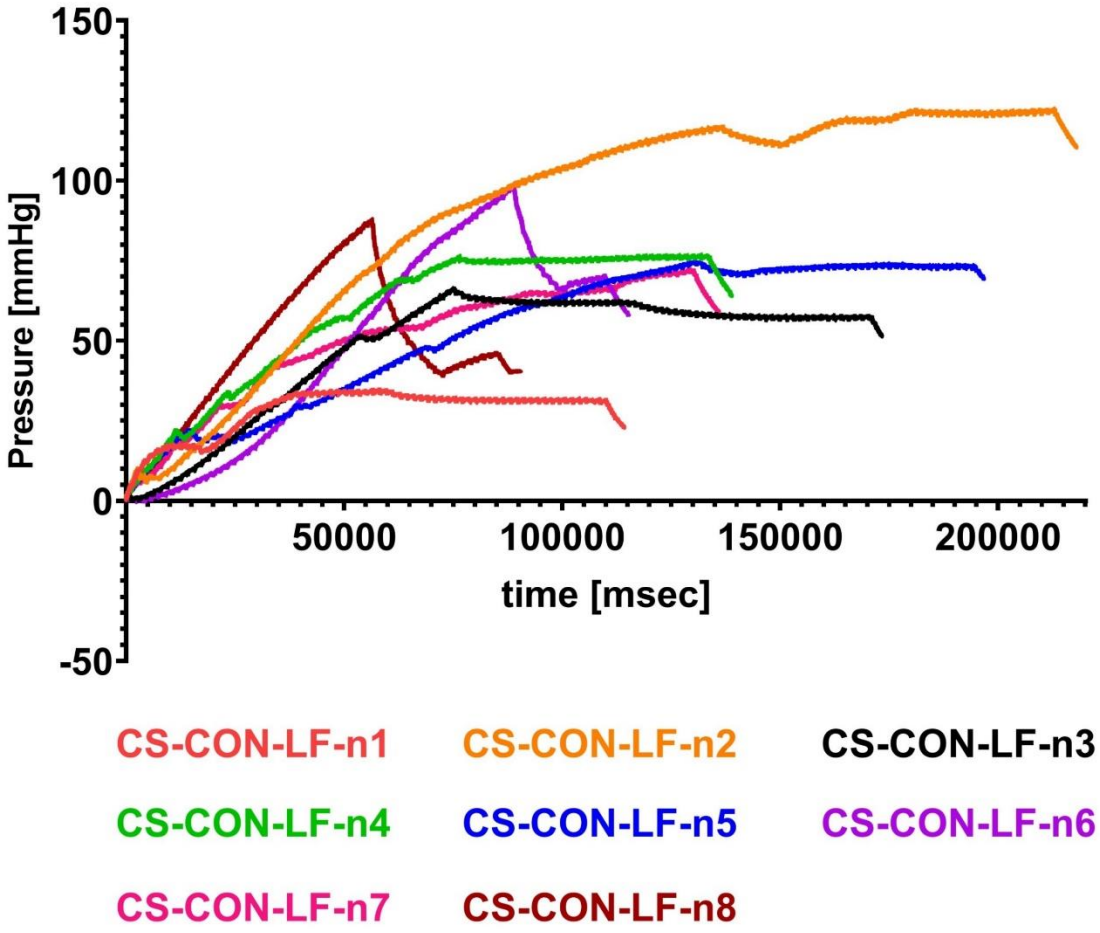

Figure 31. Pressure-time profiles of all eight CS-CON-LF anastomoses. *CS-CON-LF = Handsewn sufficient small intestinal end-to-end anastomoses using simple continuous suture technique, tested in the low-flow model;* $mmHg$ *= Millimeters of mercury;* $msec$ *= Milliseconds. (Adapted from Cira et al., Langenbecks Arch Surg 2024)* [2]

3.1.3.1 Quantitative analysis of anastomotic performance and time intervals

3.1.3.1.1 Leakage pressure analysis

All eight CS-CON-LF anastomoses had a mean LP of 34.88 $mmHg$ with a SD of $\pm$ 21.8 $mmHg$ (95 % CI, 16.63 – 53.15 $mmHg$; SEM of 7.72). The calculated median LP corresponded to 37.35 $mmHg$. The measured values showed a range of 65.4 $mmHg$ (7.6 – 73 $mmHg$) and a sample variance of 476.92. The distribution of the measured values presented with negative kurtosis (-0.351) and a positive skewness (0.43). (**Table 19**)

3.1.3.1.2 Bursting pressure analysis

For evaluated BP, a mean BP of 79.11 $mmHg$ with a SD of $\pm$ 25.42 $mmHg$ (95 % CI, 57.87 – 100.36 $mmHg$; SEM of 8.99) was observed. The calculated median BP corresponded to 75.65 $mmHg$. The measured values showed a range of 87.6 $mmHg$ (34.7 – 122.3 $mmHg$) and a sample variance of 645.93. The distribution of the measured values presented with positive kurtosis (1.30) and a negative skewness (-0.02). (**Table 19**)

3.1.3.1.3 Analysis of time intervals

The mean time interval from the first measurement (actual start of the experiment) until bursting was 110,254.75 $msec$ with a SD of $\pm$ 52,210.8 of $msec$. The time needed from the first measurement to reaching the LP was a mean time of 33,568.63 $msec$ (SD $\pm$ 20,879.14 $msec$), and from LP to BP a mean time of 76,686.13 $msec$ (SD $\pm$ 44,833.58 $msec$). Further values evaluated in the descriptive statistics are depicted in **Table 20**.

3.1.3.2 Interrelated analyses derived from experimental outcomes

3.1.3.2.1 Proportion of bursting pressure at leakage pressure

The mean pressure difference between measured LP and BP was calculated to be 44.23 $mmHg$ with a SD of $\pm$ 21.80 $mmHg$ (95 % CI, 26.0 – 62.45 $mmHg$; SEM of 7.71). The calculated median pressure difference between measured LP and BP corresponded to 38.95

$mmHg$. The measured values showed a range of 67.4 $mmHg$ (17.5 – 84.9 $mmHg$) and sample variance of 475.12. The distribution of the measured values presented with positive kurtosis (0.47) and a positive skewness (0.91). (**Table 20**)

3.1.3.2.2 Percentage of bursting pressure at leakage pressure and relative difference of pressure between leakage and bursting

The mean pressure difference between measured LP and BP corresponded to 44.12 % with a SD of $\pm$ 20.56 %. Therefore, the LP was reached at a mean of 55.88 % of the BP with a SD of $\pm$ 20.56 %. (**Table 20**)

3.1.3.2.3 Time of leakage occurrence relative to bursting time and relative difference of time between leakage and bursting time

The mean time difference between measured LP and BP corresponded to 32.40 % with a SD of $\pm$ 15.90 %. Therefore, the LP was reached at a mean time of 67.60 % of BP with a SD of $\pm$ 15.90 %. (**Table 20**)

Table 19. Quantitative analysis of anastomotic performance: Evaluation of leakage pressure and bursting pressure. Summary of descriptive statistics for the CS-CON-LF experimental series. *(Adapted from Cira et al., Langenbecks Arch Surg 2024)* [2]

Table 19. Quantitative analysis of anastomotic performance: Evaluation of leakage pressure and bursting pressure. Summary of descriptive statistics for the CS-CON-LF experimental series.		
Anastomosis (name)	**Leakage pressure in $mmHg$**	**Bursting pressure in $mmHg$**
CS-CON-LF-n1	17.2	34.7
CS-CON-LF-n2	73	122.3
CS-CON-LF-n3	30.9	66.3
CS-CON-LF-n4	43.8	76.7
CS-CON-LF-n5	47.9	74.6
CS-CON-LF-n6	13.5	98.4
CS-CON-LF-n7	7.6	72.2
CS-CON-LF-n8	45.2	87.7
Summary of descriptive statistics		
Mean	34.89	79.11
Standard error of the mean (SEM)	7.73	8.99
Median	37.35	75.65
Mode	N/A	N/A
Standard deviation (SD)	21.84	25.42
Sample variance	476.92	645.93
Kurtosis	-0.35	1.30
Skewness	0.43	-0.02
Range	65.4	87.6
Minimum	7.6	34.7
Maximum	73	122.3
Sum	279.1	632.9
Count	8	8
Confidence level (CI) (95 %)	18.26	21.25
Upper CI (95 %)	53.15	100.36
Lower CI (95 %)	16.63	57.87
CS-CON-LF = Handsewn sufficient small intestinal end-to-end anastomoses using simple continuous technique, tested in the low-flow model; $mmHg$ = Millimeters of mercury; N/A = Not available.		

Table 20. Quantitative analysis of anastomotic performance in the CS-CON-LF experimental series: Time interval analysis. Interrelated analyses derived from experimental outcomes. *(Adapted from Cira et al., Langenbecks Arch Surg 2024)* [2]

Table 20. Quantitative analysis of anastomotic performance in the CS-CON-LF experimental series: Time interval analysis. Interrelated analyses derived from experimental outcomes.

Anastomosis (name)	Time (start to leakage pressure (LP), in $msec$	Time (start to bursting pressure (BP), in $msec$	Time (LP to BP), in $msec$	Proportion of BP at LP, in $mmHg$	Percentage of BP at LP, in %	Relative difference of pressure between LP and BP, in %	Time of leakage occurrence relative to bursting time, in %	Relative difference of time between leakage and bursting time, in %
CS-CON-LF-n1	14,941	57,941	43,000	17.5	49.57	50.43	25.79	74.21
CS-CON-LF-n2	56,502	212,706	156,204	49.3	59.69	40.31	26.56	73.44
CS-CON-LF-n3	35,300	75,002	39,702	35.4	46.61	53.39	47.07	52.94
CS-CON-LF-n4	34,700	131,702	97,002	32.9	57.11	42.89	26.35	73.65
CS-CON-LF-n5	69,300	130,510	61,210	26.7	64.21	35.79	53.10	46.90
CS-CON-LF-n6	25,893	88,680	62,787	84.9	13.72	86.28	29.20	70.80
CS-CON-LF-n7	5,508	129,200	123,692	64.6	10.53	89.47	4.26	95.74
CS-CON-LF-n8	26,405	56,297	29,892	42.5	51.54	48.46	46.90	53.10
Summary of descriptive statistics								
Mean	33,568.63	110,254.75	76,686.13	44.23	44.12	55.88	32.40	67.60
Standard error of the mean (SEM)	7,381.89	18,459.34	15,851.06	7.71	7.27	7.27	5.62	5.62
Median	30,552.5	108,940	61,998.5	38.95	50.55	49.45	27.88	72.12
Mode	N/A	N/A	N/A	N/A	N/A	N/A	N/A	N/A
Standard deviation (SD)	20,879.14	52,210.88	44,833.58	21.80	20.56	20.56	15.90	15.90
Sample variance	435,938,335.4	2,725,976,322	2,010,049,469	475.12	422.61	422.61	252.89	252.89
Kurtosis	-0.1	1.03	-0.40	0.47	-0.33	-0.33	-0.05	-0.05
Skewness	0.59	0.9987	0.88	0.91	-1.13	1.13	-0.38	0.38
Range	63,792	156,409	126,312	67.4	53.68	53.68	48.84	48.84
Minimum	5,508	56,297	29,892	17.5	10.53	35.79	4.26	46.90

Maximum	69,300	212,706	156,204	84.9	64.21	89.47	53.10	95.74
Sum	268,549	882,038	613,489	353.8	352.96	447.04	259.23	540.77
Count	8	8	8	8	8	8	8	8
Confidence level (CI) (95 %)	17,455.40	43,649.39	37,481.81	18.22	17.19	17.19	13.30	13.30
Upper CI (95 %)	51,024.02	153,904.14	114,167.93	62.45	61.31	73.07	45.70	80.89
Lower CI (95 %)	16,113.23	66,605.36	39,204.32	26.00	26.93	38.69	19.11	54.30

CS-CON-LF = Handsewn sufficient small intestinal end-to-end anastomoses using simple continuous suture technique, tested in the low-flow model; $\mathrm{mm}Hg$ = Millimeters of mercury; $msec$ = Milliseconds; % = Percent; N/A = Not available.

3.1.4 Experimental Series 4: Handsewn small intestinal end-to-end anastomosis using continuous suture technique in the high-flow group

In total, eight handsewn sufficient small intestinal EEAs using CS technique were tested in the HF model. After preparing the anastomoses according to the technique describe in **Chapter III.3.3.4.2**, every individual anastomosis was tested according to the test protocol. (**Figure 32**)

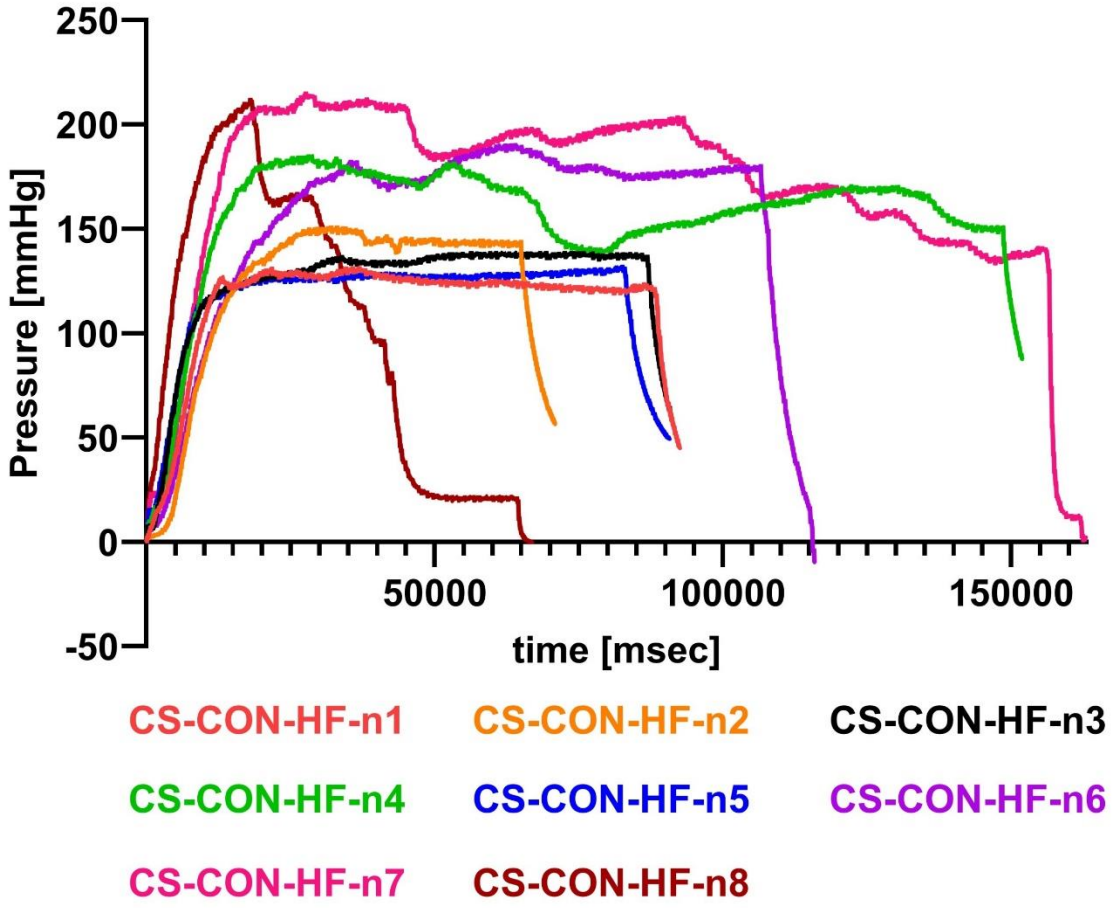

Figure 32 Pressure-time profiles of all eight CS-CON-HF anastomoses. CS-CON-HF = Handsewn sufficient small intestinal end-to-end anastomoses using simple continuous suture technique, tested in the high-flow model; $mmHg$ = Millimeters of mercury; $msec$ = Milliseconds. *(Adapted from Cira et al., Langenbecks Arch Surg 2024)* [2]

3.1.4.1 Quantitative analysis of anastomotic performance and time intervals

3.1.4.1.1 Leakage pressure analysis

All eight CS-CON-HF anastomoses had a mean LP of 36.59 $mmHg$ with a SD of $\pm$ 31.02 $mmHg$ (95 % CI, 10.65 – 62.52 $mmHg$; SEM of 10.97). The calculated median LP corresponded to 23.35 $mmHg$. The measured values showed a range of 91.1 $mmHg$ (7.6 – 98.7 $mmHg$) and a sample variance of 962.44. The distribution of the measured values presented with positive kurtosis (1.40) and skewness (1.53). (**Table 21**)

3.1.4.1.2 Bursting pressure analysis

For evaluated BP, a mean BP of 169.13 $mmHg$ with a SD of $\pm$ 35.24 $mmHg$ (95 % CI, 139.67 – 198.59 $mmHg$; SEM of 12.46) was observed. The calculated median BP corresponded to 167.6 $mmHg$. The measured values showed a range of 83.5 $mmHg$ (131.2 – 214.7 $mmHg$) and a sample variance of 1,241.49. The distribution of the measured values presented with negative kurtosis (-2.037) and a positive skewness (0.19). (**Table 21**)

3.1.4.1.3 Analysis of time intervals

The mean time interval from the first measurement (actual start of the experiment) until bursting was 45,334.13 $msec$ with an SD of $\pm$ 24,307.65 of $msec$. The time needed from the first measurement to reaching the LP was a mean time of 3,756.5 $msec$ (SD $\pm$ 2,878.53 $msec$), and from LP to BP a mean time of 41,577.63 $msec$ (SD $\pm$ 24,960.04 $msec$). Further values evaluated in the descriptive statistics are depicted in **Table 22.**

3.1.4.2 Interrelated analyses derived from experimental outcomes

3.1.4.2.1 Proportion of bursting pressure at leakage pressure

The mean pressure difference between measured LP at BP was calculated to be 132.54 $mmHg$ with a SD of $\pm$ 48.15 $mmHg$ (95 % CI, 92.29 – 172.79 $mmHg$; SEM 17.02). The

calculated median pressure difference between measured LP and BP corresponded to 113.55 $mmHg$. The measured values showed a range of 123.6 $mmHg$ (80.5 – 204.1 $mmHg$) and sample variance of 2,318.20. The distribution of the measured values presented with negative kurtosis (-1.57) and a positive skewness (0.55). (**Table 22**)

3.1.4.2.2 Percentage of bursting pressure at leakage pressure and relative difference of pressure between leakage and bursting

The mean pressure difference between measured LP and BP corresponded to 22.38 % with a SD of $\pm$ 17.87 %. Therefore, the LP was reached at a mean of 77.62 % of the BP with a SD of $\pm$ 17.87 %. (**Table 22**)

3.1.4.2.3 Time of leakage occurrence relative to bursting time and relative difference of time between leakage and bursting time

The mean time difference between measured LP and BP corresponded to 10.28 % with a SD of $\pm$ 10.59 %. Therefore, the LP was reached at a mean time of 89.72 % of BP with a SD of $\pm$ 10.59 %.(**Table 22**)

Table 21. Quantitative analysis of anastomotic performance: Evaluation of leakage pressure and bursting pressure. Summary of descriptive statistics for the CS-CON-HF experimental series. *(Adapted from Cira et al., Langenbecks Arch Surg 2024)* [2]

Table 21. Quantitative analysis of anastomotic performance: Evaluation of leakage pressure and bursting pressure. Summary of descriptive statistics for the CS-CON-HF experimental series.

Anastomosis (name)	Leakage pressure in $mmHg$	Bursting pressure in $mmHg$
CS-CON-HF-n1	22.5	131.2
CS-CON-HF-n2	70	150.5
CS-CON-HF-n3	20	138.4
CS-CON-HF-n4	98.7	184.7
CS-CON-HF-n5	28	131.8
CS-CON-HF-n6	21.7	190
CS-CON-HF-n7	24.2	214.7
CS-CON-HF-n8	7.6	211.7
Summary of descriptive statistics		
Mean	36.59	169.13
Standard error of the mean (SEM)	10.97	12.46
Median	23.35	167.6
Mode	N/A	N/A
Standard deviation (SD)	31.02	35.24
Sample variance	962.44	1,241.49
Kurtosis	1.40	-2.04
Skewness	1.53	0.19
Range	91.1	83.5
Minimum	7.6	131.2
Maximum	98.7	214.7
Sum	292.7	1353
Count	8	8
Confidence level (CI) (95 %)	25.94	29.46
Upper CI (95 %)	62.52	198.58
Lower CI (95 %)	10.65	139.67

CS-CON-HF = Handsewn sufficient small intestinal end-to-end anastomoses using simple continuous technique, tested in the high-flow model; $mmHg$ = Millimeters of mercury; N/A = Not available.

Table 22. Quantitative analysis of anastomotic performance in the CS-CON-LF experimental series: Time interval analysis. Interrelated analyses derived from experimental outcomes. *(Adapted from Cira et al., Langenbecks Arch Surg 2024)* [2]

Table 22. Quantitative analysis of anastomotic performance in the CS-CON-HF experimental series: Time interval analysis. Interrelated analyses derived from experimental outcomes.

Anastomosis (name)	Time (start to leakage pressure (LP), in $msec$	Time (start to bursting pressure (BP), in $msec$	Time (LP to BP), in $msec$	Proportion of BP at LP, in $mmHg$	Percentage of BP at LP, in %	Relative difference of pressure between LP and BP, in %	Time of leakage occurrence relative to bursting time, in %	Relative difference of time between leakage and bursting time, in %
CS-CON-HF-n1	33,602	36,893	33,602	108.7	17.15	82.85	8.92	91.08
CS-CON-HF-n2	23,699	31,956	23,699	80.5	46.51	53.49	25.84	74.16
CS-CON-HF-n3	71,400	73,593	71,400	118.4	14.45	85.55	2.98	97.02
CS-CON-HF-n4	20,328	28,129	20,328	86	53.44	46.56	27.73	72.27
CS-CON-HF-n5	80,089	82,499	80,089	103.8	21.24	78.76	2.92	97.08
CS-CON-HF-n6	60,001	64,001	60,001	168.3	11.42	88.58	6.25	93.75
CS-CON-HF-n7	25,500	27,600	25,500	190.5	11.27	88.73	7.61	92.39
CS-CON-HF-n8	18,002	18,002	18,002	204.1	3.59	96.41	0	100
Summary of descriptive statistics								
Mean	3,756.5	45,334.13	41,577.63	132.54	22.39	77.62	10.28	89.72
Standard error of the mean (SEM)	1,017.71	8,594.05	8,824.71	17.02	6.32	6.32	3.74	3.74
Median	2,850.5	34,424.5	29,551	113.55	15.80	84.20	6.93	93.07
Mode	N/A	N/A	N/A	N/A	N/A	N/A	N/A	N/A
Standard deviation (SD)	2,878.53	24,307.65	24,960.04	48.15	17.87	17.87	10.59	10.59
Sample variance	8,285,906	590,861,652.1	623,003,330	2,318.20	319.29	319.29	112.15	112.15
Kurtosis	-0.44	-1.51	-1.55	-1.57	-0.10	-0.10	-0.30	-0.30
Skewness	0.75	0.61	0.70	0.56	1.14	-1.14	1.14	-1.14
Range	8,257	64,497	62,087	123.6	49.85	49.85	27.73	27.73
Minimum	0	18,002	18,002	80.5	3.59	46.56	0	72.27

IV Results

Maximum	8,257	82,499	80,089	204.1	53.44	96.41	27.73	100
Sum	30,052	362,673	332,621	1,060.3	179.08	620.92	82.25	717.75
Count	8	8	8	8	8	8	8	8
Confidence level (CI) (95 %)	2,406.5071	20,321.70	20,867.11	40.25	14.94	14.94	8.85	8.85
Upper CI (95 %)	6,163.01	65,655.83	62,444.74	172.79	37.32	92.55	19.13	98.57
Lower CI (95 %)	1,349.99	25,012.42	20,710.51	92.29	7.45	62.68	1.43	80.87

CS-CON-HF = Handsewn sufficient small intestinal end-to-end anastomoses using simple continuous suture technique, tested in the high-flow model; $mmHg$ *= Millimeters of mercury;* $msec$ *= Milliseconds; % = Percent; N/A = Not available.*

3.2 Quantitative analysis of anastomotic performance and time intervals: Comparison between the experimental series

The Mann-Whitney U test [146, 147] was employed for conducting the following statistical analyses.

3.2.1 Leakage pressure analysis

A significant difference was observed between the LP of the SBS-CON-LF and SBS-CON-HF groups ($p = 0.0281$), with an exact 95.01 % CI for the difference ranging from 4.200 to 81.50 $mmHg$. This indicates that the HF model had higher LP compared to the LF model when examining SBS-anastomoses. (**Figure 33)**

No significant difference in LP was found between the CS-CON-LF and CS-CON-HF groups ($p = 0.9043$; exact 95.01 % CI of difference -23.8 to 24.80 $mmHg$), suggesting that there was no difference in LP between the two flow models when testing CS-anastomoses. (**Figure 33**) Similarly, there was no significant difference in LP between the SBS-CON-LF and CS-CON-LF groups ($p = 0.0830$; exact 95.01 % CI of difference -1.300 to 39.00 $mmHg$) (**Figure 33**), as well as the SBS-CON-HF and CS-CON-HF groups ($p = 0.3823$; exact 95.01 % CI of difference -73.50 to 15.80 $mmHg$) (**Figure 33**), indicating no difference in LP when comparing the two studied suture techniques. (**Figure 33**)

3.2.2 Bursting pressure analysis

A statistically significant difference was observed between the SBS-CON-LF and SBS-CON-HF groups ($p = 0.0115$), indicating that the SBS-anastomoses in the HF model reached a significantly higher BP compared to the LF model. (**Figure 34**) The exact 95.01 % CI for the difference in BP between groups ranged from 18.60 to 136.3 $mmHg$. Similarly, a significant difference in BP was seen between the CS-CON-LF and CS-CON-HF groups ($p = 0.0002$),

with an exact 95.01 % CI of difference of 56.60 to 124.0 $mmHg$, suggesting that the CS-anastomoses in the HF model reached a higher BP than those in the LF model. (**Figure 34**)

On the other hand, no significant difference in BP was found between the SBS-CON-LF and CS-CON-LF groups ($p = 0.7984$; exact 95.01 % CI of difference -65.40 to 40.40 $mmHg$) (**Figure 34**), as well as the SBS-CON-HF and CS-CON-HF groups ($p > 0.9999$; exact 95.01 % CI of difference -34.90 to 45.80 $mmHg$) (**Figure 34**), indicating that there was no difference in BP between the two different suture techniques tested.

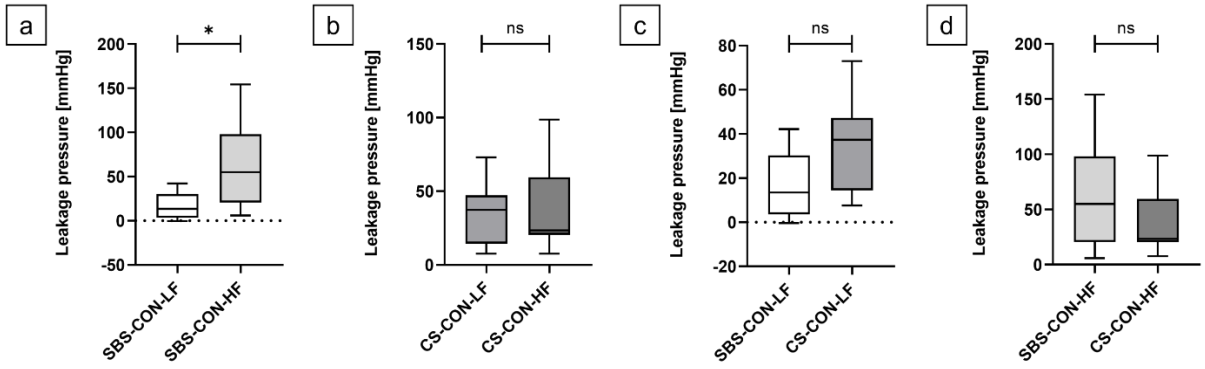

Figure 33 Leakage pressure (LP) comparison among experimental series. Box plots of anastomotic LP values ($mmHg$) comparing SBS-CON-LF with SBS-CON-HF anastomoses, CS-CON-LF with CS-CON-HF anastomoses, SBS-CON-LF with CS-CON-LF anastomoses and SBS-CON-HF with CS-CON-HF anastomoses. (a) SBS-CON-HF anastomoses had a statistically significantly higher LP compared to SBS-CON-LF anastomoses ($p = 0.0281$). (b) No significant difference in LP was seen between CS-CON-LF and CS-CON-HF ($p = 0.9043$), (c) SBS-CON-LF and CS-CON-LF ($p = 0.0830$), and (d) SBS-CON-HF and CS-CON-HF ($p = 0.3823$) anastomoses. Significance was assessed using Mann-Whitney U tests. $* \ p < 0.05$; *ns = non-significant. (Adapted from Cira et al., Langenbecks Arch Surg 2024)* [2]

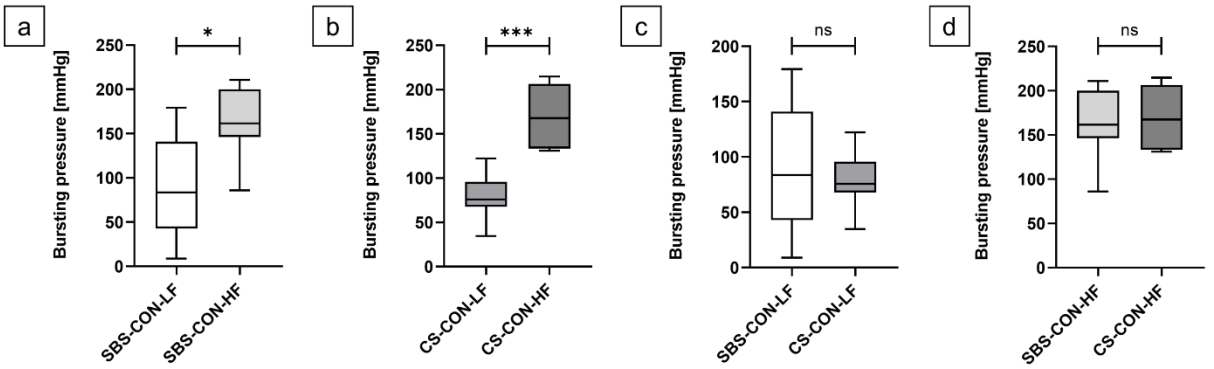

Figure 34. Bursting pressure (BP) comparison among experimental series. Box plots of anastomotic BP values ($mmHg$) comparing SBS-CON-LF with SBS-CON-HF anastomoses, CS-CON-LF with CS-CON-HF anastomoses, SBS-CON-LF with CS-CON-LF anastomoses and SBS-CON-HF with CS-CON-HF anastomoses. (a) SBS-CON-HF anastomoses had a statistically significantly higher BP compared to SBS-CON-LF anastomoses ($p = 0.0115$). (b) CS-CON-HF anastomoses had a statistically significantly higher BP compared to CS-CON-LF anastomoses ($p = 0.0002$). No significant difference in BP was seen between (c) SBS-CON-LF and CS-CON-LF ($p = 0.7984$) and (d) SBS-CON-HF and CS-CON-HF ($p > 0.9999$) anastomoses. Significance was assessed using Mann-Whitney U tests. $* p < 0.05$; $*** p < 0.001$*; ns = non-significant. (Adapted from Cira et al., Langenbecks Arch Surg 2024)* [2]

3.2.3 Time interval analysis

3.2.3.1 Time from start to leakage

The time interval ($msec$) from the initiation of the experiment until the attainment of LP was assessed and compared among the various experimental groups using the Mann-Whitney U test [146, 147]. A statistically significant difference was observed between the SBS-CON-LF and SBS-CON-HF groups ($p = 0.0011$, exact 95.01 % CI of difference ranging from -35,014 to -6,537 $msec$) (**Figure 35**), as well as between the CS-CON-LF and CS-CON-HF groups ($p = 0.0006$, exact 95.01 % CI of difference ranging from -52,502 to -12,748 $msec$) (**Figure 35**). These results imply that the HF model demonstrated a notably shorter duration to reach LP compared to the LF model.

However, no statistically significant difference was found between the SBS-CON-LF and CS-CON-LF groups ($p = 0.6454$, exact 95.01 % CI of difference ranging from -11,620 to 27,900 $msec$) (**Figure 35**), nor between the SBS-CON-HF and CS-CON-HF groups ($p = 0.7984$, exact 95.01 % CI of difference ranging from -5,519 to 1,603 $msec$) (**Figure 35**). These

findings indicate that there was no significant disparity in the time required to reach LP when comparing the different anastomotic techniques within both the LF and the HF flow models.

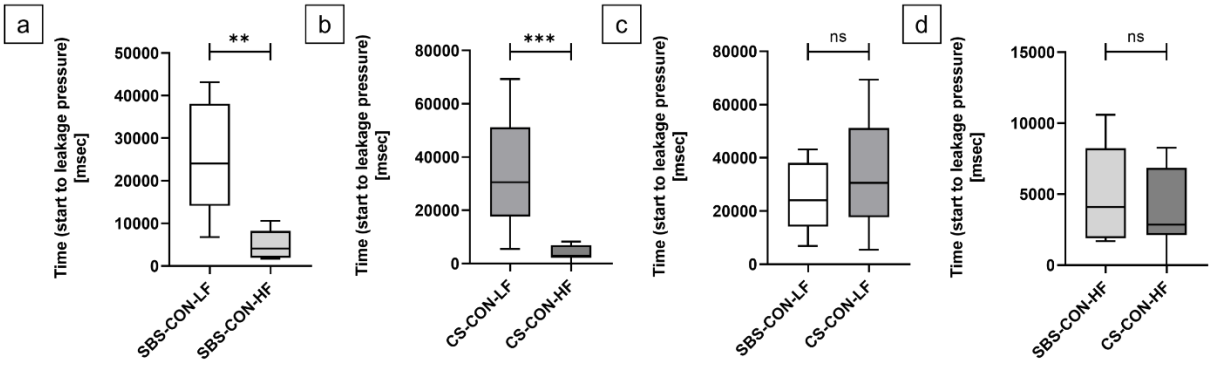

Figure 35. Comparison of time interval assessment for attainment of leakage pressure (LP) in the experimental series. Box plots illustrating the time interval (in $msec$) for achieving LP comparing SBS-CON-LF with SBS-CON-HF anastomoses, CS-CON-LF with CS-CON-HF anastomoses, SBS-CON-LF with CS-CON-LF anastomoses and SBS-CON-HF with CS-CON-HF anastomoses. (a) SBS-CON-HF anastomoses had a statistically significantly shorter duration to reach LP compared to SBS-CON-LF anastomoses ($p = 0.0011$). (b) CS-CON-HF anastomoses had a statistically significantly shorter duration to reach LP compared to CS-CON-LF anastomoses ($p = 0.0006$). No significant difference in time required to reach LP was seen between (c) SBS-CON-LF and CS-CON-LF ($p = 0.6454$) and (d) SBS-CON-HF and CS-CON-HF ($p = 0.7984$) anastomoses. Significance was assessed using Mann-Whitney U tests. $** \; p < 0.01; *** \; p =< 0.001$*; ns = non-significant. (Adapted from Cira et al., Langenbecks Arch Surg 2024)* [2]

3.2.3.2 Time from start to bursting

The time from the start of the experiment until reaching BP (in $msec$) was compared using the Mann-Whitney U test [146, 147] among the different experimental groups. A significant difference was observed between the SBS-CON-LF and SBS-CON-HF groups ($p = 0.0011$, exact 95.01 % CI of difference of -251,503 to -29,704 $msec$) (**Figure 36**), as well as between the CS-CON-LF and CS-CON-HF groups ($p = 0.0070$, exact 95.01 % CI of difference of -102,910 to -24,341 $msec$) (**Figure 36**). These findings indicate that the HF model resulted in significantly faster attainment of BP compared to the LF model.

No significant difference was found between the SBS-CON-LF and CS-CON-LF groups ($p = 0.7984$, exact 95.01 % CI of difference of -148,167 to 69,700 $msec$) (**Figure 36**), as well

as between the SBS-CON-HF and CS-CON-HF groups ($p = 0.0830$, exact 95.01 % CI of difference of -299.0 to 45,694 $msec$) (**Figure 36**). This suggests that there was no significant difference in the time until bursting when comparing the different anastomotic techniques in both the LF and HF models.

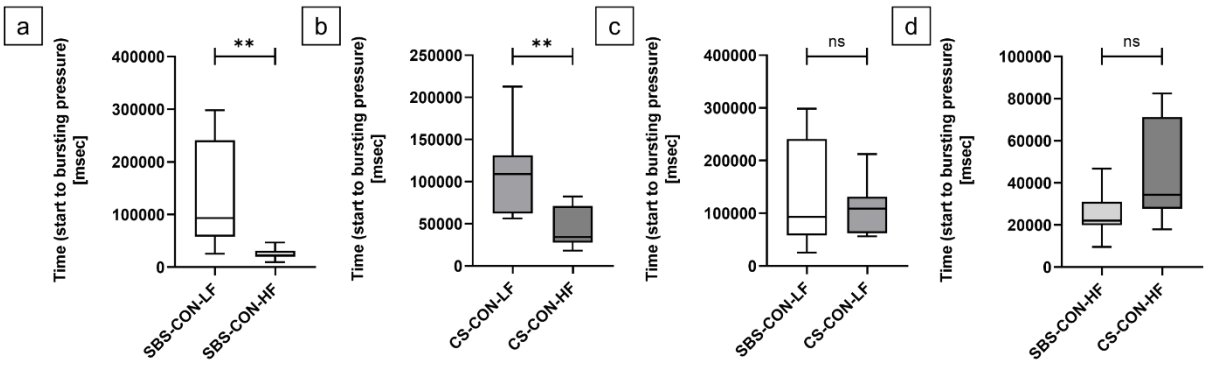

Figure 36. Comparison of time interval assessment for attainment of bursting pressure (BP) in the experimental series. Box plots illustrating the time interval (in $msec$) for achieving BP comparing SBS-CON-LF with SBS-CON-HF anastomoses, CS-CON-LF with CS-CON-HF anastomoses, SBS-CON-LF with CS-CON-LF anastomoses and SBS-CON-HF with CS-CON-HF anastomoses. (a) SBS-CON-HF anastomoses attained statistically significantly faster BP compared to SBS-CON-LF anastomoses ($p = 0.0011$). (b) CS-CON-HF anastomoses attained statistically significantly faster BP compared to CS-CON-LF anastomoses ($p = 0.0070$). No significant difference in time required to reach BP was seen between (c) SBS-CON-LF and CS-CON-LF ($p = 0.7984$) and (d) SBS-CON-HF and CS-CON-HF ($p = 0.0830$) anastomoses. Significance was assessed using Mann-Whitney U tests. $* p < 0.05$; $** p < 0.01$*; ns = non-significant. (Adapted from Cira et al., Langenbecks Arch Surg 2024)* [2]

3.2.3.3 Time from leakage to bursting

The time duration ($msec$), between the occurrence of LP and the attainment of BP was evaluated and compared among the different experimental groups using the Mann-Whitney U [146, 147] test. A statistically significant difference was observed between the SBS-CON-LF and SBS-CON-HF groups ($p = 0.0070$, exact 95.01 % CI of difference ranging from -214,300 to -14,104 $msec$) (**Figure 37**), indicating that the SBS-anastomoses reached the BP more rapidly after leakage in the HF model. Similarly, a significant difference was observed between the SBS-CON-HF and CS-CON-HF groups ($p = 0.0379$, exact 95.01 % CI of difference ranging from 141.0 to 50,402 $msec$) (**Figure 37**), suggesting that bursting occurred significantly

sooner after leakage in the SBS-anastomoses compared to the CS-anastomoses in the HF model compared to the LF model.

However, no statistically significant difference was observed between the CS-CON-LF and CS-CON-HF groups ($p = 0.0650$, exact 95.01 % CI of difference ranging from -76,674 to 3,710 $msec$) (**Figure 37**), indicating that there was no significant disparity in the time required to reach bursting after leakage when comparing the CS-anastomoses in the HF model. Similarly, no significant difference was observed between the SBS-CON-LF and CS-CON-LF groups ($p = 0.9591$, exact 95.01 % CI of difference ranging from -127,995 to 54,551 $msec$) (**Figure 37**), indicating that there was no significant difference in the time needed to reach bursting after leakage between the two different suture techniques in the LF model.

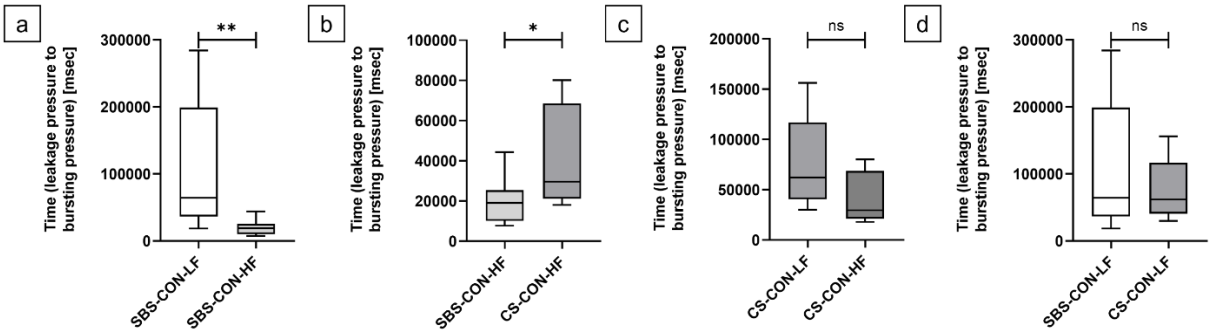

Figure 37 Comparison of time interval assessment for attainment of bursting pressure (BP) in the experimental series. Box plots illustrating the time interval (in $msec$) for achieving BP after LP comparing SBS-CON-LF with SBS-CON-HF anastomoses, SBS-CON-HF with CS-CON-HF anastomoses, CS-CON-LF with CS-CON-HF anastomoses and SBS-CON-LF with CS-CON-LF anastomoses. (a) SBS-CON-HF anastomoses attained statistically significantly faster BP after LP compared to SBS-CON-LF anastomoses ($p = 0.0070$). (b) SBS-CON-HF anastomoses attained statistically significantly faster BP after LP compared to CS-CON-HF anastomoses ($p = 0.0379$). (c) No significant difference in time required to reach BP after LP was seen between (c) CS-CON-LF and CS-CON-HF ($p = 0.0650$) and (d) SBS-CON-LF and CS-CON-LF ($p = 0.9591$) anastomoses. Significance was assessed using Mann-Whitney U tests. $* p < 0.05$; $** p < 0.01$*; ns = non-significant. (Adapted from Cira et al., Langenbecks Arch Surg 2024)* [2]

3.3 Interrelated analyses derived from experimental outcomes

The Mann-Whitney U test [146, 147] was employed for conducting the following statistical analyses.

3.3.1 Proportion of bursting pressure at leakage pressure

The results indicated a significant difference between the CS-CON-LF and CS-CON-HF groups ($p = 0.0003$, with an exact 95.01 % CI of 45.10 to 141.2 $mmHg$). (**Figure 38**) This suggests that, for CS-anastomoses after leakage, the anastomoses in the HF model experienced a significantly higher increase in intraluminal pressure until bursting compared to those in the LF model.

On the other hand, no significant difference was found between the SBS-CON-LF and SBS-CON-HF groups ($p = 0.2786$, with exact 95.01 % CI of difference -37.2 to 90.60 $mmHg$). (**Figure 38**) This indicates that BP occurred after a similar increase in pressure following LP in both groups. Similarly, no significant difference was observed between the SBS-CON-LF and CS-CON-LF groups ($p = 0.4418$, with exact 95.01 % CI of difference -87.40 to 17.40 $mmHg$) (**Figure 38**), as well as between the SBS-CON-HF and CS-CON-HF groups ($p = 0.1605$, with exact 95.01 % CI of difference -34.70 to 90.60 $mmHg$) (**Figure 38**). These findings suggest that there was no significant difference in the pressure increase after leakage until bursting between the different suture techniques tested in both the LF and HF flow models.

3.3.2 Percentage of bursting pressure at leakage pressure and relative difference of pressure between leakage and bursting

There was a significant difference in the percentage of BP at LP when comparing the SBS-CON-LF and CS-CON-LF groups ($p = 0.0499$, with an exact 95.01 % CI of difference of 0.3793 to 46.11 %) (**Figure 39**). This finding suggests that CS-anastomoses in the LF model had a lower percentage of BP at the leakage point compared to SBS-anastomoses in the LF model.

Therefore, with CS-anastomoses, there was a relatively higher increase in pressure after leakage before reaching the point of bursting.

No significant difference was observed between the SBS-CON-LF and SBS-CON-HF groups ($p = 0.1691$, exact 95.01 % CI of difference -9.640 to 47.88 %) (**Figure 39**), as well as between the CS-CON-LF and CS-CON-HF groups ($p = 0.0830$, exact 95.01 % CI of difference -45.24 to 0.7452 %) (**Figure 39**), indicating that there was no difference in the percentage of BP at the leakage point when comparing the two flow models. Furthermore, no significant difference was found between the SBS-CON-HF and CS-CON-HF groups ($p = 0.1949$, exact 95.01 % CI of difference -40.55 to 7.471 %) (**Figure 39**). This indicates that there was no difference in the suture technique used when considering the HF model.

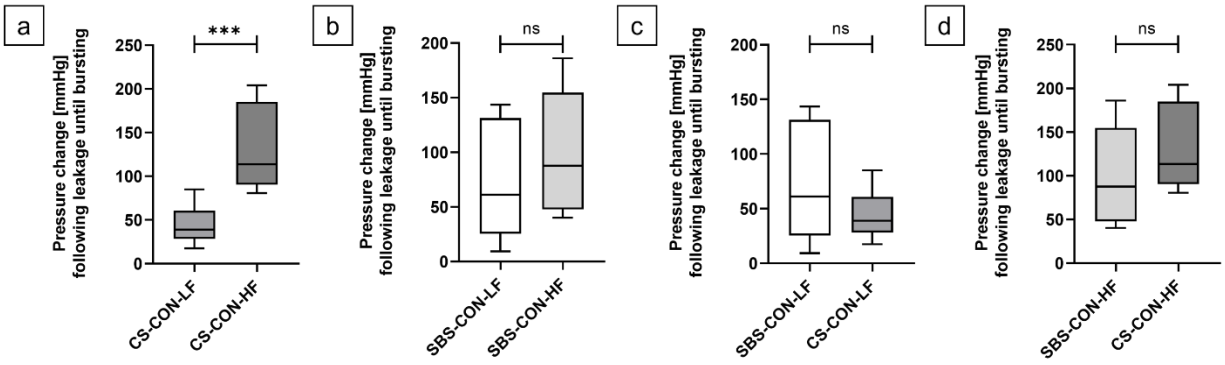

Figure 38. **Comparison of the proportion of bursting pressure (BP) at leakage pressure (LP) (in $mmHg$) between the experimental series. Box plots illustrating the pressure change (in $msec$) following LP until BP comparing CS-CON-LF with CS-CON-HF anastomoses, SBS-CON-LF with SBS-CON-HF anastomoses, SBS-CON-LF with CS-CON-LF anastomoses and SBS-CON-HF with CS-CON-HF anastomoses.** (a) After reaching LP, CS-CON-HF anastomoses had a statistically significantly higher increase in intraluminal pressure until BP compared to CS-CON-LF anastomoses ($p = 0.0003$). No significant difference in intraluminal pressure increase after LP until BP was observed between (b) SBS-CON-LF and SBS-CON-HF anastomoses ($p = 0.2786$), (c) SBS-CON-LF and CS-CON-LF anastomoses ($p = 0.4418$), and (d) SBS-CON-HF and CS-CON-HF anastomoses ($p = 0.1605$). Significance was assessed using Mann-Whitney U tests. $*** p =< 0.001$*; ns = non-significant. (Adapted from Cira et al., Langenbecks Arch Surg 2024)* [2]

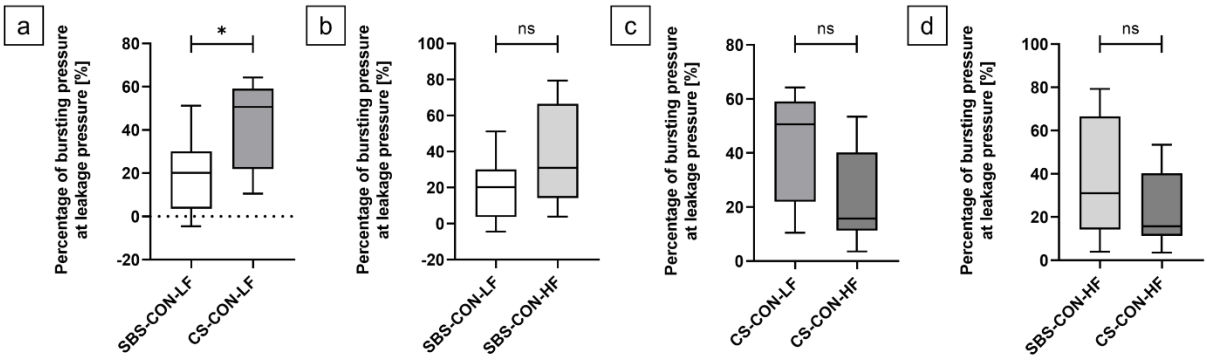

Figure 39. Comparison of the percentage of bursting pressure (BP) at leakage pressure (LP) (in %) between the experimental series. Box plots illustrating the percentage of BP at LP (in %) comparing SBS-CON-LF with CS-CON-LF anastomoses, SBS-CON-LF with SBS-CON-HF anastomoses, CS-CON-LF with CS-CON-HF anastomoses and SBS-CON-HF with CS-CON-HF anastomoses. (a) CS-CON-HF anastomoses showed a statistically significantly relatively higher increase in intraluminal pressure after LP before reaching the point of bursting compared to SBS-CON-LF anastomose ($p = 0.0499$). No significant difference in the percentage of BP at LP were seen between (b) SBS-CON-LF and SBS-CON-HF anastomoses ($p = 0.1691$), (c) CS-CON-LF and CS-CON-HF anastomoses ($p = 0.0830$) and (d) SBS-CON-HF and CS-CON-HF anastomoses ($p = 0.1949$). Significance was assessed using Mann-Whitney U tests. $* p < 0.05$*; ns = non-significant. (Adapted from Cira et al., Langenbecks Arch Surg 2024)* [2]

3.3.3 Time of leakage occurrence relative to bursting time and relative difference of time between leakage and bursting time

There was a significant difference between CS-CON-LF and CS-CON-HF when comparing the percentage of time of BP at time of LP ($p = 0.0148$, exact 95.01 % CI of difference ranging from -1.465 to 40.65 %) (**Figure 40**), indicating that for CS-anastomoses the HF group reached BP faster after leakage compared to the LF group.

No significant differences were observed for SBS-CON-LF vs. SBS-CON-HF groups ($p = 0.5737$, exact 95.01 % CI of difference ranging from -13.04 to 20.62 %) (**Figure 40**) indicating that there was no difference between the two flow models in terms of the percentage of time of BP at the time of LP for SBS-anastomoses. Similarly, no significant differences were observed between SBS-CON-LF and CS-CON-LF groups ($p = 0.6454$, exact 95.01 % CI of difference ranging from -21.77 to 7.908 %) (**Figure 40**) and the SBS-CON-HF and CS-CON-HF groups ($p = 0.1049$, exact 95.01 % CI of difference ranging from -0.999 to 26.60 %)

(**Figure 40**). This indicates that there was no difference in the suture technique used when considering the LF or the HF model.

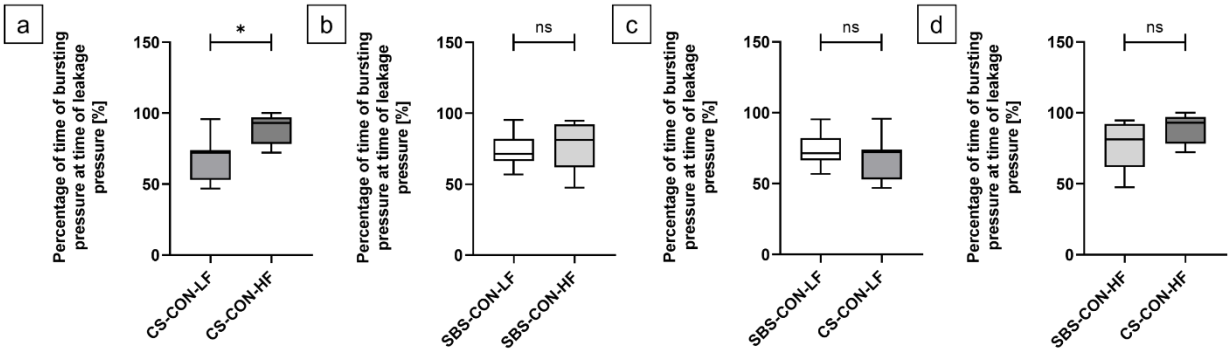

Figure 40. Comparison of the time of leakage occurrence relative to the bursting time (in %) between the experimental series. Box plots illustrating the percentage of time of BP at the time of LP (in %) comparing CS-CON-LF with CS-CON-HF anastomoses, SBS-CON-LF with SBS-CON-HF anastomoses, SBS-CON-LF with CS-CON-LF anastomoses and SBS-CON-HF with CS-CON-HF anastomoses. (a) CS-CON-HF anastomoses statistically significantly reached BP faster after LP compared to CS-CON-LF ($p = 0.0148$). No significant difference in the percentage of time of BP at the time of LP were seen between (b) SBS-CON-LF and SBS-CON-HF anastomoses ($p = 0.5737$), (c) SBS-CON-LF and CS-CON-LF anastomoses ($p = 0.6454$), and (d) SBS-CON-HF and CS-CON-HF anastomoses ($p = 0.1049$). Significance was assessed using Mann-Whitney U tests. $* p < 0.05$ *; ns = non-significant. (Adapted from Cira et al., Langenbecks Arch Surg 2024)* [2]

3.4 Leakage and bursting location analysis

To investigate the precise sites of leakage and bursting, a comprehensive approach was employed that involved correlating images obtained from all four cameras, each capturing distinct angles of the anastomosis, with the corresponding pressure measurements obtained during each experimental trial. The initial detection of a leak in one image from a specific camera angle prompted the extraction of the corresponding pressure differential from the provided dataset, utilizing the associated time stamp for precise reference.

Subsequently, when dealing with images from alternative camera perspectives, those with time stamps that were closest to the previously determined reference point were opted to be selected. This approach ensured a comprehensive analysis of the event. Moreover, the time stamp that aligned with the measurement of BP enabled identifying the corresponding image captured from one of the camera angles. Following the same methodology, images from the remaining camera perspectives were selected with time stamps that were proximate to this reference value. This rigorous process was implemented to facilitate meticulous analysis and validation of the findings. For illustrative purposes, an exemplary figure is presented below to offer a visual representation of our methodology and its application. (**Figure 41**)

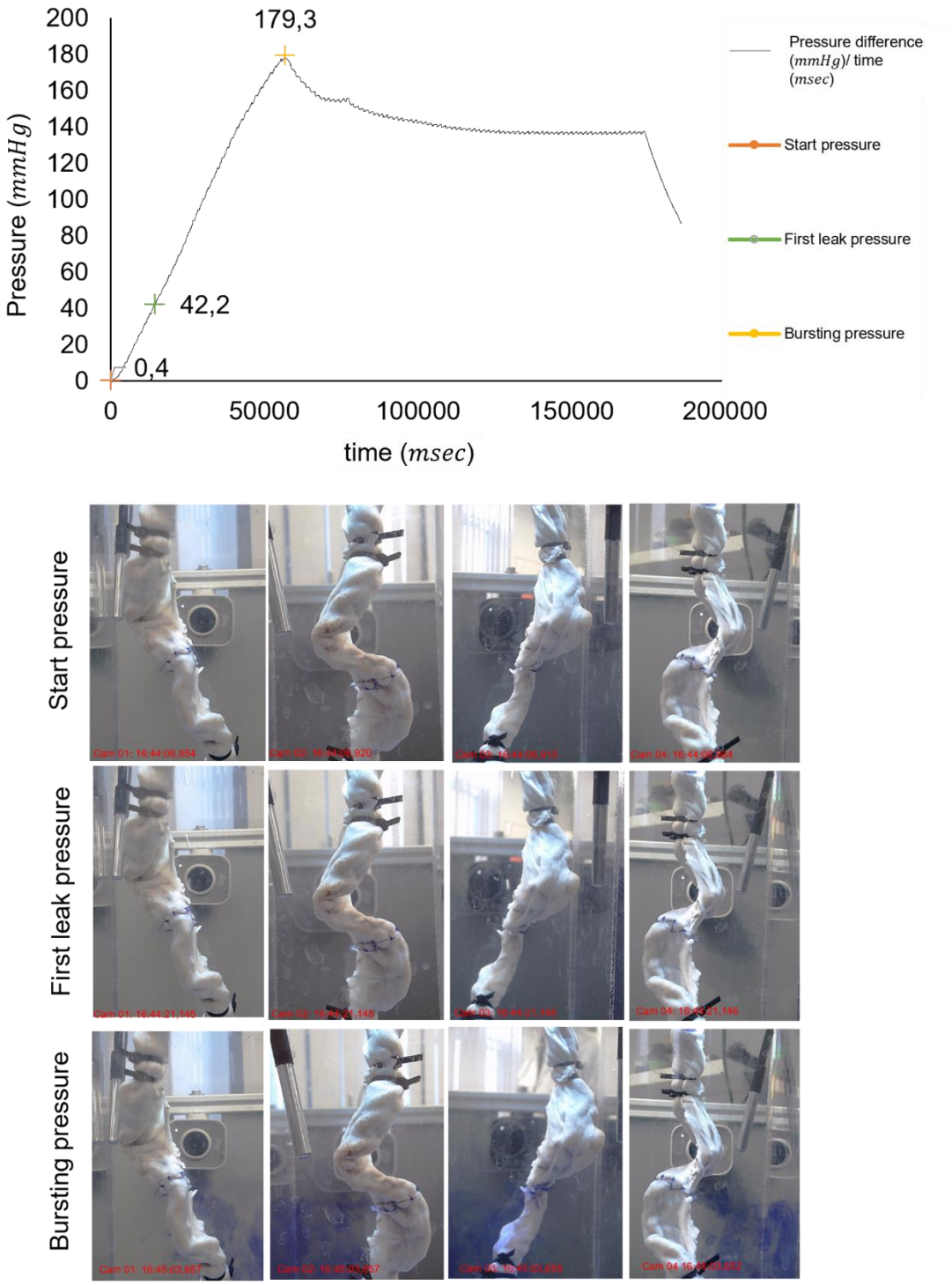

Figure 41. Methodology for precise localization of leakage and bursting sites in the experimental series. This figure illustrates the methodology using the example of the SBS-CON-LF-$n3$ anastomosis.

3.4.1 Leakage location analysis

For the SBS-CON-LF group, a total of eight anastomotic locations with leakage in the mesenteric zone were observed, while 16 anastomotic locations in the mesenteric zone did not exhibit leakage. In the peripheral zone, seven anastomotic locations displayed leakage, while 57 anastomotic locations remained free from leakage.

In the SBS-CON-HF group, eight anastomotic locations with leakage in the mesenteric zone were observed, while 16 anastomotic locations in the mesenteric zone did not exhibit leakage. In the peripheral zone, only two anastomotic locations displayed leakage, while 62 anastomotic locations remained free from leakage.

For the CS-CON-LF group, seven anastomotic locations exhibited leakage in the mesenteric zone, while 17 anastomotic locations in the mesenteric zone did not show leakage. In the peripheral zone, two anastomotic locations displayed leakage, while 62 anastomotic locations remained free from leakage.

In the CS-CON-HF group, seven anastomotic locations showed leakage in the mesenteric zone, while 17 anastomotic locations in the mesenteric zone did not exhibit leakage. Similarly, only two anastomotic locations in the peripheral zone displayed leakage, while 62 anastomotic locations remained free from leakage. (**Figure 42**)

3.4.2 Bursting location analysis

For the SBS-CON-LF group, 18 anastomotic locations with bursting in the mesenteric zone were observed, while six anastomotic locations in the mesenteric zone did not show bursting. In the peripheral zone, twelve anastomotic locations displayed bursting, while 52 anastomotic locations remained without bursting.

In the SBS-CON-HF group, 16 anastomotic locations exhibited bursting in the mesenteric zone, while eight anastomotic locations in the mesenteric zone did not show bursting. In the

peripheral zone, 13 anastomotic locations displayed bursting, while 51 anastomotic locations remained without bursting.

For the CS-CON-LF group, we observed 20 anastomotic locations with bursting in the mesenteric zone, while four anastomotic locations in the mesenteric zone did not show bursting. In the peripheral zone, 20 anastomotic locations displayed bursting, while 44 anastomotic locations remained without bursting.

In the CS-CON-HF group, 22 anastomotic locations showed bursting in the mesenteric zone, while two anastomotic locations in the mesenteric zone did not show bursting. Similarly, 22 anastomotic locations in the peripheral zone displayed bursting, while 42 anastomotic locations remained without bursting. (**Figure 42**)

3.4.3 Association between leakage and bursting locations

Among all cases of leakage observed in the study, with the exception of one, it was found that the anastomoses at the leakage location side also exhibited bursting. This consistent pattern suggests a strong association between leakage occurrence and the risk of bursting at the same location within the anastomosis.

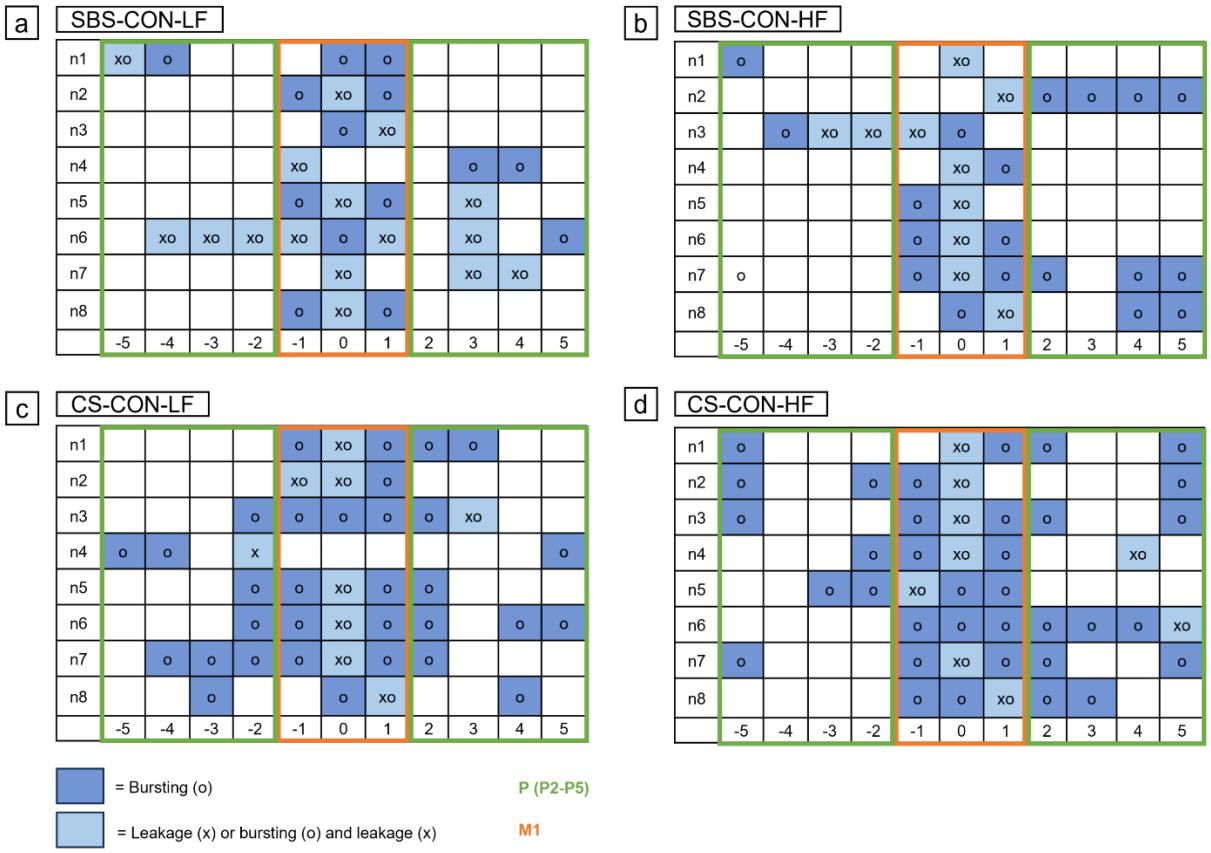

Figure 42. Location analysis: Spatial distribution of anastomotic leakage and bursting in the experimental series. The figure illustrates a linear grid, distinguishing between two zones: the mesenteric zone (between -1 and +1, labeled as zone M1) and the peripheral zone (ranging from -2 to -5 and +2 to +5, labeled as zone P (P2-P5)). Leakage points are marked with "x" and bursting points with "o". (a) SBS-CON-LF anastomoses. (b) SBS-CON-HF anastomoses. (c) CS-CON-LF anastomoses. (d) CS-CON-HF anastomoses. *(Adapted from Cira et al., Langenbecks Arch Surg 2024)* [2]

3.5 Leakage and bursting location analysis: Comparison within and between the experimental series

The Fisher's exact test [148] was employed for conducting the following statistical analyses.

3.5.1 Differences in anastomotic leakage rates between areas of the mesenteric and the peripheral zone

The incidence of leakage in the SBS-CON-LF anastomoses was significantly higher in the mesenteric zone compared to the peripheral zone ($p = 0.0230$; $OR, 4.071$). (**Figure 43**) Similarly, SBS-CON-HF anastomoses exhibited a significantly higher incidence of leakage at the mesenteric zone compared to the peripheral zone ($p = 0.0003$; $OR, 15.50$). (**Figure 43**)

Furthermore, CS-CON-LF anastomoses showed a significantly higher incidence of leakage at the mesenteric zone compared to the peripheral zone ($p = 0.0013$; $OR, 12.76$). (**Figure 43**) Similarly, CS-CON-HF anastomoses exhibited a significantly higher incidence of leakage at the mesenteric zone compared to the peripheral zone ($p = 0.0013$; $OR, 12.76$). (**Figure 43**)

Therefore, irrespective of the anastomotic technique or flow rate model utilized, anastomoses exhibited a significantly higher incidence of leakage at the mesenteric entry side compared to other sections of the anastomosis.

3.5.2 Differences in anastomotic bursting rates between areas of the mesenteric and the peripheral zone

Significantly higher incidences of bursting in the SBS-CON-LF anastomoses were observed in the mesenteric zone compared to the peripheral zone ($p < 0.0001$; $OR, 13.00$). (**Figure 44**) Similarly, SBS-CON-HF anastomoses exhibited a significantly higher incidence of bursting at the mesenteric zone compared to the peripheral zone ($p < 0.0001$; $OR, 7.846$). (**Figure 44**)

Furthermore, CS-CON-LF anastomoses showed a significantly higher incidence of bursting at the mesenteric zone compared to the peripheral zone ($p < 0.0001$; $OR, 11.00$). (**Figure 44**) Similarly, CS-CON-HF anastomoses exhibited a significantly higher incidence of bursting at the mesenteric zone compared to the peripheral zone ($p < 0.0001$; $OR, 21.00$). (**Figure 44**)

Therefore, irrespective of the experimental series or anastomotic technique used, anastomoses exhibited a significantly higher incidence of bursting at the mesenteric entry side compared to other sections of the anastomosis.

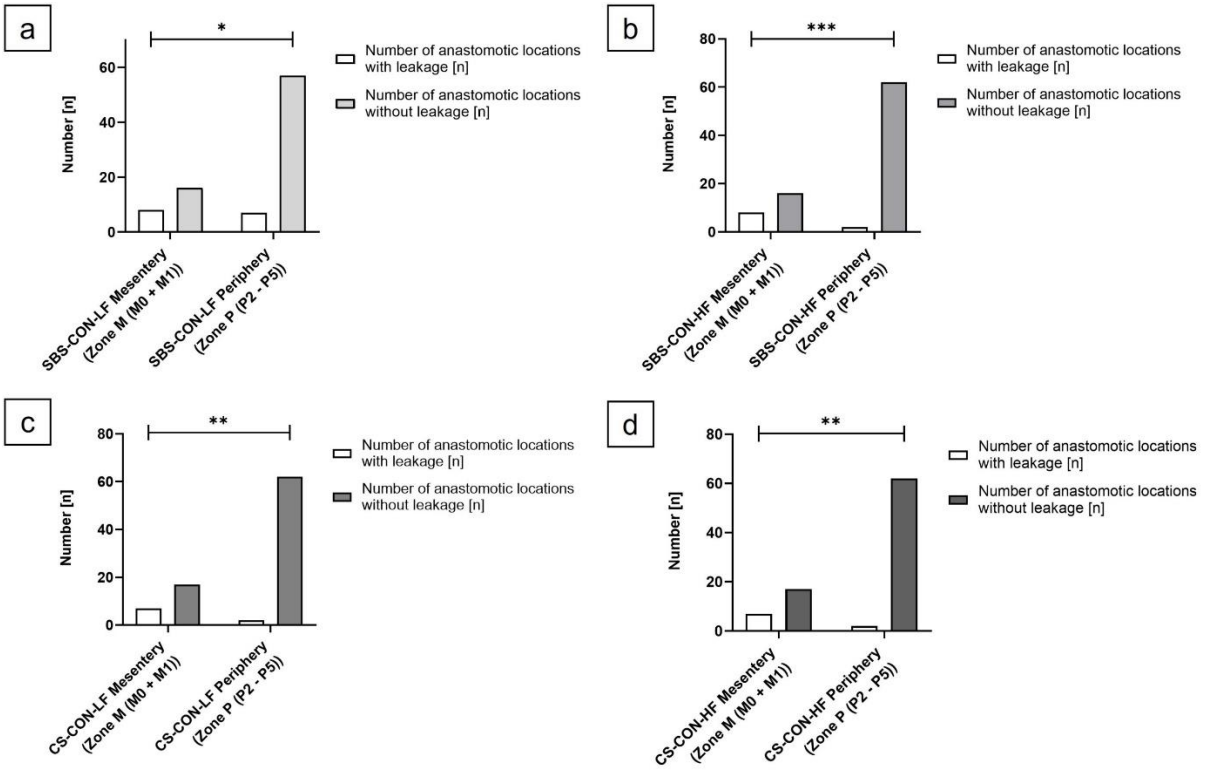

Figure 43. Differences in anastomotic leakage rates between the areas of the mesenteric and the peripheral zone. (a) SBS-CON-LF anastomoses ($p = 0.0230$), (b) SBS-CON-HF anastomoses ($p = 0.0003$), (c) CS-CON-LF anastomoses ($p = 0.0013$), and (d) CS-CON-HF anastomoses ($p = 0.0013$) exhibited a statistically significantly higher incidence of leakage at the mesenteric zone compared to the peripheral zone. Significance was assessed using Fisher's exact test. $* p < 0.05; ** p < 0.01; *** p =< 0.001$. *(Adapted from Cira et al., Langenbecks Arch Surg 2024)* [2]

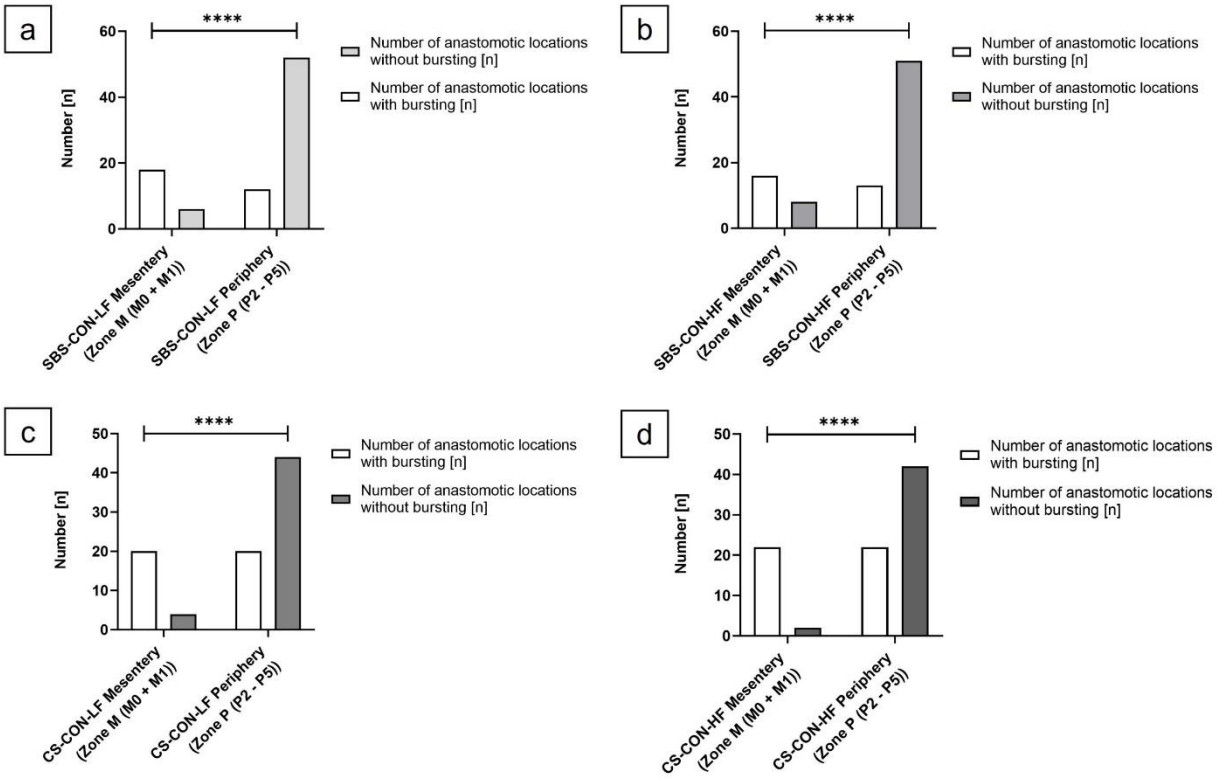

Figure 44 Differences in anastomotic bursting rates between the areas of the mesenteric and the peripheral zone. (a) SBS-CON-LF anastomoses ($p < 0.0001$), (b) SBS-CON-HF anastomoses ($p < 0.0001$), (c) CS-CON-LF anastomoses ($p < 0.0001$), and (d) CS-CON-HF anastomoses ($p < 0.0001$) exhibited a statistically significantly higher incidence of bursting at the mesenteric zone compared to the peripheral zone. Significance was assessed using Fisher's exact test. $* p < 0.05; ** p < 0.01; *** p =< 0.001; **** p < 0.0001$. *(Adapted from Cira et al., Langenbecks Arch Surg 2024)* [2]

3.5.3 Differences in anastomotic leakage rates of areas within the mesenteric zone among compared experimental series

There were no significant differences in the incidence of leakage at the mesenteric zone between SBS-CON-LF anastomoses and SBS-CON-HF anastomoses ($p > 0.9999; OR, 1.000$) (**Figure 45**), or between SBS-CON-LF anastomoses and CS-CON-LF anastomoses ($p > 0.9999; OR, 1.214$) (**Figure 45**).

Similarly, there were no significant differences in the incidence of leakage at the mesenteric zone between SBS-CON-HF anastomoses and CS-CON-HF anastomoses ($p >$

0.9999; $OR, 1.214$) (**Figure 45**), or between CS-CON-LF anastomoses and CS-CON-HF anastomoses ($p > 0.9999$; $OR, 1.000$) (**Figure 45**).

Therefore, no significant variations in leakage incidence were observed at the mesenteric entry side among the compared experimental series.

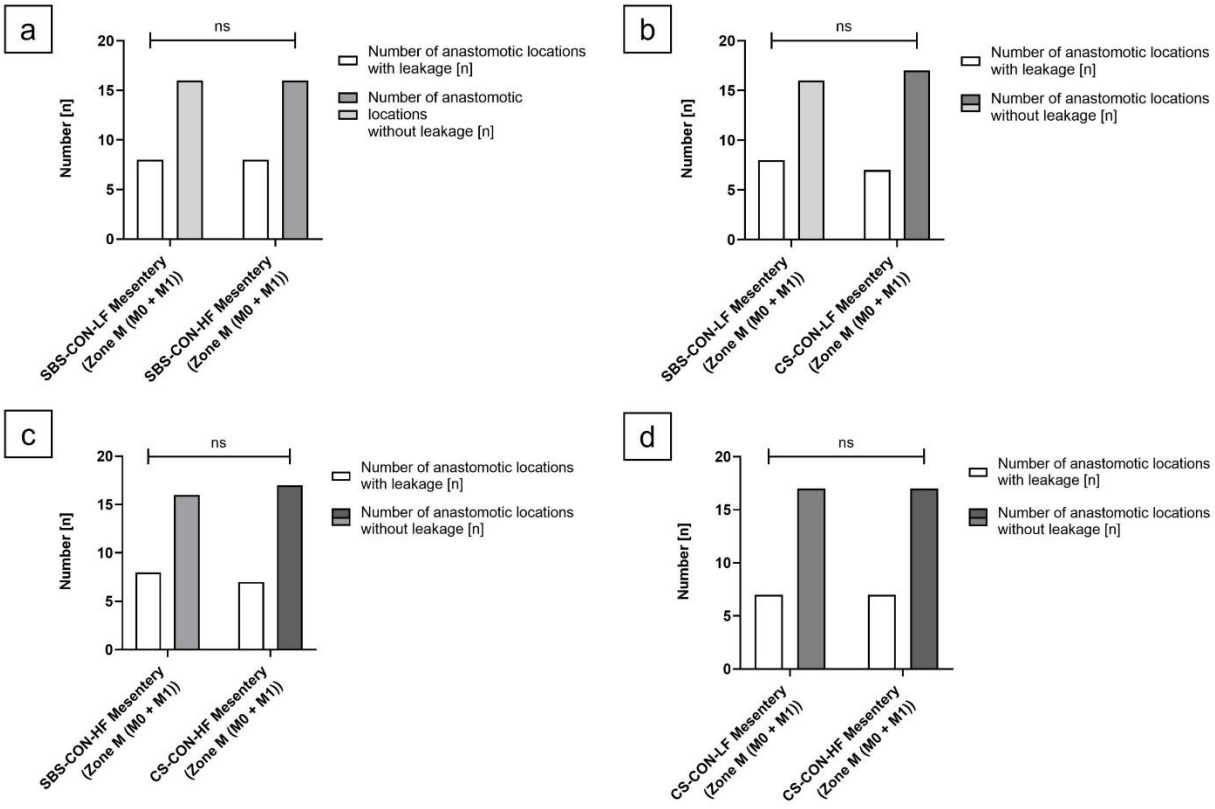

Figure 45. Differences in anastomotic leakage rates of areas within the mesenteric zone among compared experimental series. There were no statistically significant differences in the incidence of leakage at the mesenteric zone between (a) SBS-CON-LF and SBS-CON-HF anastomoses ($p > 0.9999$), (b) SBS-CON-LF and CS-CON-LF anastomoses ($p > 0.9999$), (c) SBS-CON-HF and CS-CON-HF anastomoses ($p > 0.9999$), and (d) CS-CON-LF and CS-CON-HF anastomoses ($p > 0.9999$). Significance was assessed using Fisher's exact test. *ns = non-significant. (Adapted from Cira et al., Langenbecks Arch Surg 2024)* [2]

3.5.4 Differences in anastomotic leakage rates of areas within the peripheral zone among compared experimental series

The incidence of leakage at the peripheral zone of the anastomoses did not show significant differences among the compared experimental series. This was observed between SBS-CON-

LF anastomoses and SBS-CON-HF anastomoses ($p = 0.1640$; $OR, 3.807$) (**Figure 46**) and between SBS-CON-LF anastomoses and CS-CON-LF anastomoses ($p = 0.1640$; $OR, 3.807$) (**Figure 46**). Similarly, no significant differences were found in leakage incidence at the peripheral zone between SBS-CON-HF anastomoses and CS-CON-HF anastomoses ($p > 0.9999$; $OR, 1.000$) (**Figure 46**) or between CS-CON-LF anastomoses and CS-CON-HF anastomoses ($p > 0.9999$; $OR, 1.000$) (**Figure 46**).

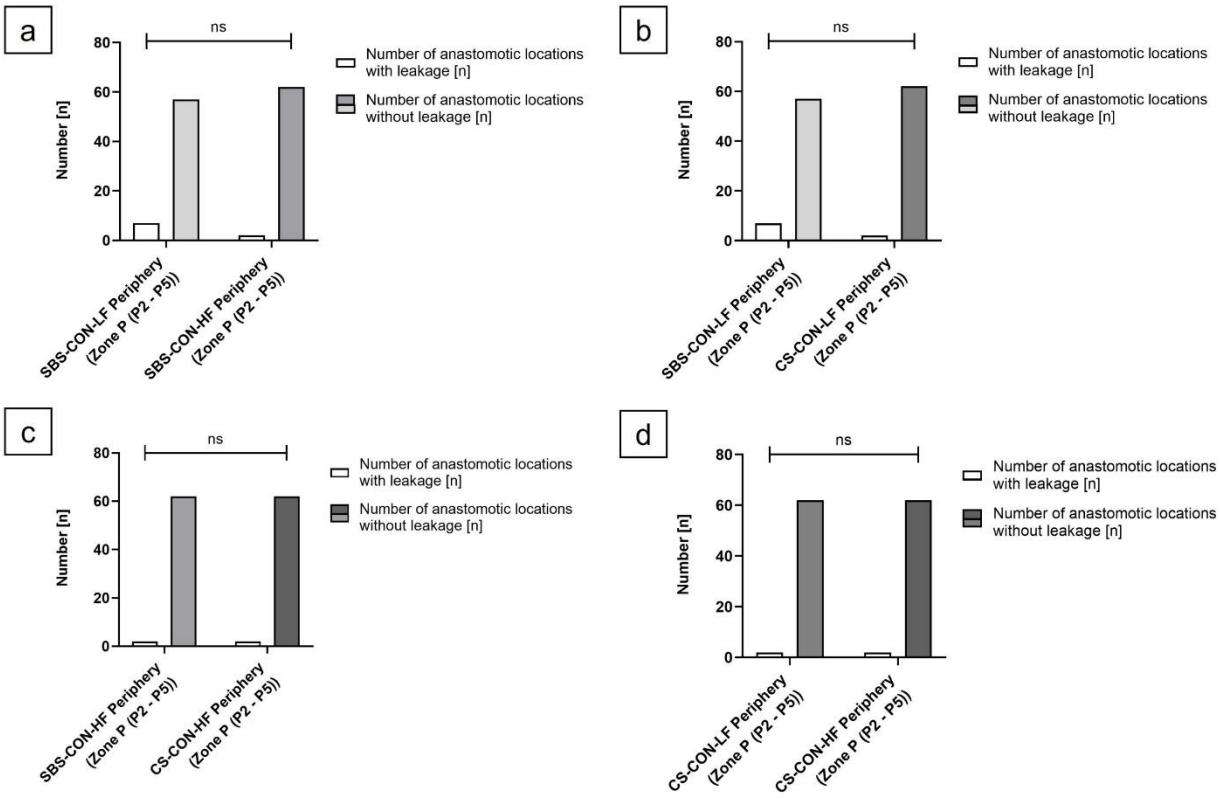

Figure 46. Differences in anastomotic leakage rates of areas within the peripheral zone among compared experimental series. There were no statistically significant differences in the incidence of leakage at the peripheral zone between (a) SBS-CON-LF and SBS-CON-HF anastomoses ($p = 0.1640$), (b) SBS-CON-LF and CS-CON-LF anastomoses ($p = 0.1640$), (c) SBS-CON-HF and CS-CON-HF anastomoses ($p > 0.9999$), and (d) CS-CON-LF and CS-CON-HF anastomoses ($p > 0.9999$). Significance was assessed using Fisher's exact test. *ns = non-significant. (Adapted from Cira et al., Langenbecks Arch Surg 2024)* [2]

These findings suggest a lack of significant variations in leakage incidence between the peripheral zones in the compared experimental series.

3.5.5 Differences in anastomotic bursting rates of areas within the mesenteric zone among compared experimental series

The incidence of bursting at the mesenteric zone did not exhibit significant differences among the compared experimental series. This was observed between SBS-CON-LF anastomoses and SBS-CON-HF anastomoses ($p = 0.7516$; $OR, 1.500$) (**Figure 47**) and between SBS-CON-LF anastomoses and CS-CON-LF anastomoses ($p = 0.6662$; $OR, 0.4545$) (**Figure 47**).

Similarly, no significant differences were found in bursting incidence at the mesenteric entry side between SBS-CON-HF anastomoses and CS-CON-HF anastomoses ($p = 0.0723$; $OR, 0.1818$) (**Figure 47**), or between CS-CON-LF anastomoses and CS-CON-HF anastomoses ($p = 0.6662$; $OR, 0.4545$) (**Figure 47**).

Therefore, no significant variations in bursting incidence were observed at the mesenteric entry side among the compared experimental series.

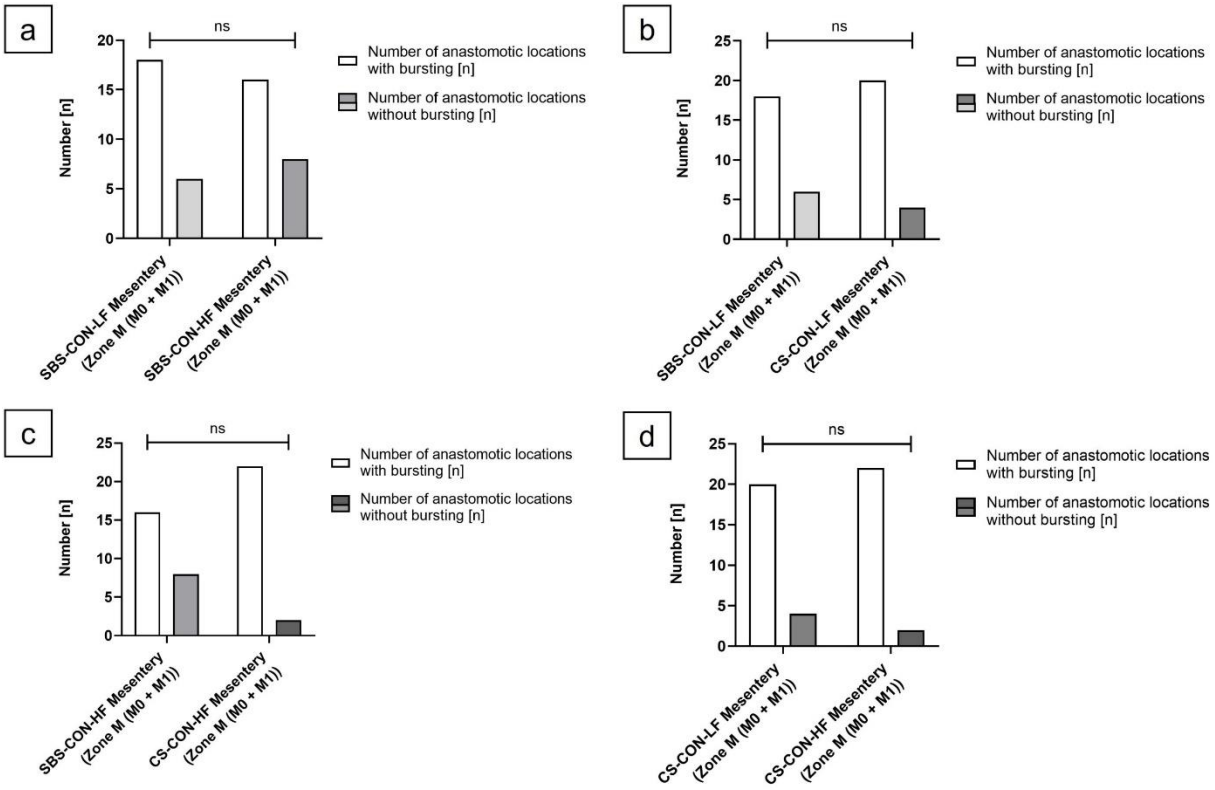

Figure 47. Differences in anastomotic bursting rates of areas within the mesenteric zone among compared experimental series. There were no statistically significant differences in the incidence of leakage at the mesenteric zone between (a) SBS-CON-LF and SBS-CON-HF anastomoses ($p = 0.7516$), (b) SBS-CON-LF and CS-CON-LF anastomoses ($p = 0.6662$), (c) SBS-CON-HF and CS-CON-HF anastomoses ($p = 0.0723$), and (d) CS-CON-LF and CS-CON-HF anastomoses ($p = 0.6662$). Significance was assessed using Fisher's exact test. *ns = non-significant. (Adapted from Cira et al., Langenbecks Arch Surg 2024)* [2]

3.5.6 Differences in anastomotic bursting rates of areas within the peripheral zone among compared experimental series

No significant differences were observed in the incidence of bursting at the peripheral zone of the anastomoses among the compared experimental series. This was found between SBS-CON-LF anastomoses and SBS-CON-HF anastomoses ($p > 0.9999$; $OR, 0.9053$) (**Figure 48**) and between SBS-CON-LF anastomoses and CS-CON-LF anastomoses ($p = 0.1524$; $OR, 0.5077$) (**Figure 48**).

Similarly, no significant differences were found in bursting incidence at the peripheral zone between SBS-CON-HF anastomoses and CS-CON-HF anastomoses ($p = 0.1119$; $OR, 0.4866$) (**Figure 48**) or between CS-CON-LF anastomoses and CS-CON-HF anastomoses ($p = 0.8508$; $OR, 0.8678$) (**Figure 48**).

These findings suggest a lack of significant variations in bursting incidence between the peripheral zone in the compared experimental series.

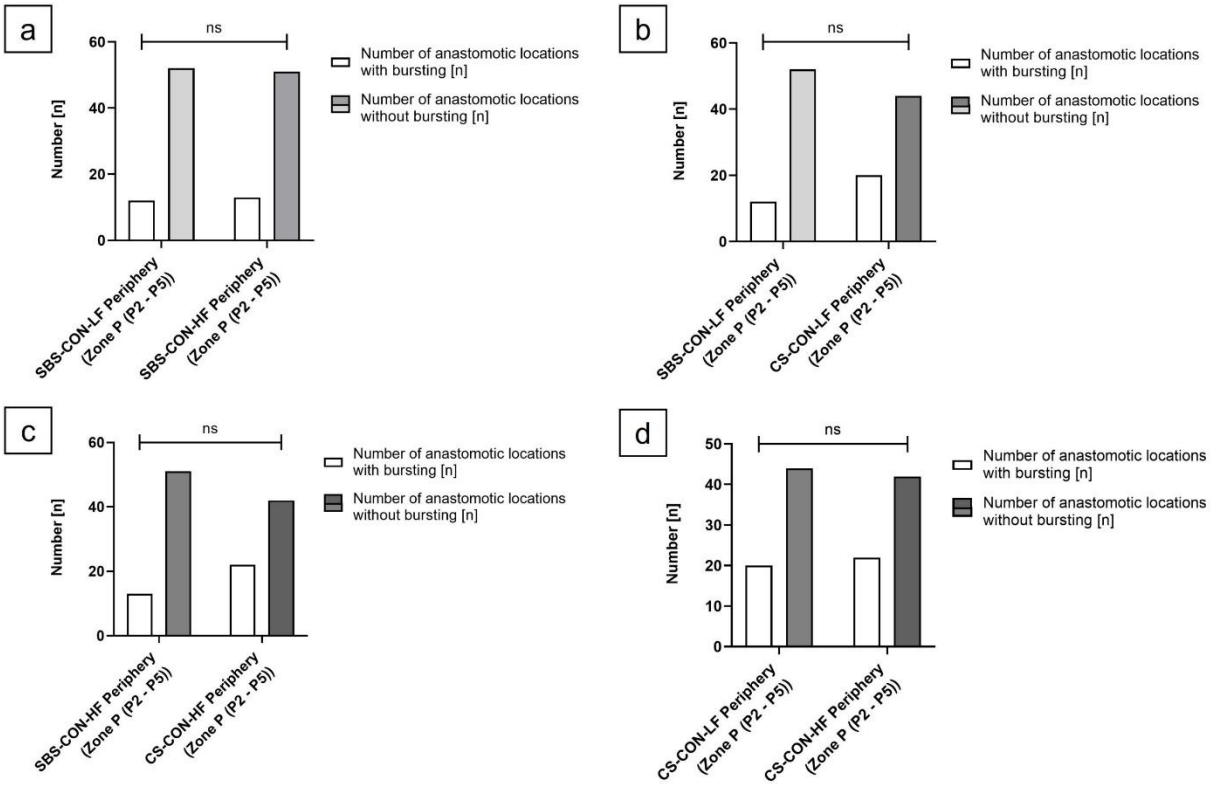

Figure 48. Differences in anastomotic bursting rates of areas within the peripheral zone among compared experimental series. There were no statistically significant differences in the incidence of leakage at the peripheral zone between (a) SBS-CON-LF and SBS-CON-HF anastomoses ($p > 0.9999$), (b) SBS-CON-LF and CS-CON-LF anastomoses ($p = 0.1524$), (c) SBS-CON-HF and CS-CON-HF anastomoses ($p = 0.4866$), and (d) CS-CON-LF and CS-CON-HF anastomoses ($p = 0.8508$). Significance was assessed using Fisher's exact test. *ns = non-significant. (Adapted from Cira et al., Langenbecks Arch Surg 2024)* [2]

V Discussion

Intestinal anastomosis formation belongs to one of the most frequently performed procedures in abdominal surgery and is often accompanied by insufficient wound healing, resulting in the development of AL. [15, 16] Despite improvements of surgical techniques, the incidence of postoperative AL and its sequelae remains considerably high. [19, 21-23, 28] Consequently, affected patients endure significant personal suffering, and the healthcare system bears a substantial socio-economic burden. [35]

In attempt to address this significant complication and reduce or even prevent the postoperative occurrence of ALs, coating of intestinal anastomoses with synthetic or genuine adhesive biomaterials has been studied previously in an experimental setting. [38, 39] As both collagen and/ or fibrin-based adhesive biomaterials show high potential in reducing leakage rates, there is limited true evidence on their effect on anastomotic healing. Therefore, the primary aim of this thesis was to systematically evaluate the effect of coating various types of intestinal anastomoses, regardless of location and underlying disease, with collagen- and/ or fibrin-based adhesive biomaterials on postoperative AL rates, its accompanying complications, and mortality rates. Given the considerable number of evaluable animal studies and human trials [1] in the literature, a systematic review and meta-analysis, including thorough sensitivity and subgroup analyses, were conducted for each.

During the evaluation of the systematic review and meta-analysis of animal studies, another scientific question arose that needed addressing in this thesis. The analysis of various *ex-vivo* models studying gastrointestinal anastomotic stability and pressure resistance revealed a lack of comparability and reproducibility of scientific data. [45-50, 52-54, 56, 57] Therefore, the secondary aim to this thesis was to develop an innovative *ex-vivo* test-setup to determine gastrointestinal anastomotic quality quantitatively and precisely in terms of its

stability and pressure resistance with high comparability, reproducibility, and user-independence. This approach aimed to increase the understanding of the biomechanics of intestinal anastomoses and therefore AL.

In the following, the results of the three parts of this thesis will be discussed critically in the context of the current literature.

1. Systematic review and meta-analysis of human studies

The first part of this thesis presented a systematic review and meta-analysis on the efficacy of externally coating intestinal anastomoses with C-BLBs or FSs in reducing postoperative AL rates and its accompanying sequelae for patients undergoing surgery with the formation of an intestinal anastomosis. Since this analysis was the first systematic review and meta-analysis conducted on this subject, it provides a comprehensive synthesis of the current evidence. [1]

The content presented in **Chapter V.1** has been adapted and modified from the publication authored by Cira et al., 2022. [1].

1.1. Summary of outcomes and interpretation

Overall, 15 studies [58-71, 149] and therefore 1,387 patients in the intervention group and 2,243 patients in the control group were identified according to the predetermined eligibility criteria (**Chapter III.1.1.1 – 1.1.2**). Given the expected significant differences among the included studies, predefined subgroups were established for a secondary analysis to assess subgroup differences. These subgroups were stratified by study design, intervention used (C-BLB and/or FS), age group (adult or pediatric), location of anastomoses (esophagus, stomach, small intestine, colon, and/ or rectum), and indication for surgery.

Despite variations among the included studies, all patients in the intervention group, irrespective of anastomotic location or technique, had their intestinal anastomosis reinforced or covered with either a C-BLB (*Collatamp* or *TachoSil*) [64, 66, 70] or a FS (*Tisseel, Tissucol,*

Greenplast, Bioseal or Quixil) [58-63, 65, 67-69, 71, 149]. In contrast, patients in the control group did not receive any substance coverage after undergoing the same procedure.

The risk of bias varied among the included studies. The included RCTs [58, 60, 62, 63, 65] raised some concerns, the included NRSs [59, 61, 64] showed a moderate risk of bias, and the cohort studies were of were of moderate quality (n = 5; NOS score 6–7) [66-70] or low quality (NOS < 5) [71]. The interpretation of the outcomes of these risk of bias assessments will be crucial when discussing the limitations of this study. (**Supplementary Table 4**)

To evaluate whether significant differences in postoperative AL rates or its accompanying sequelae exist between the studied groups, a meta-analysis was conducted, ensuring its quality through sensitivity and subgroup analyses. For all complications analyzed, except for the mortality rate (**Table 8**), significant differences between the examined groups were found by the conducted meta-analysis. (**Figure 19, Figure 20, Figure 21, Table 4, Table 5, Table 6, and Table 7)**

Postoperative AL (FE: $OR, 0.37;\ 95\ \%\ CI, 0.27-0.52;\ p < 0.00001$) (**Figure 19, Table 4, and Table 5)** and reoperation rates (FE: $OR, 0.21;\ 95\ \%\ CI, 0.10-0.47;\ p = 0.0001$) (**Figure 20 and Table 6**) were shown to be significantly lower for patients in the intervention group. The stability of these results was confirmed by sensitivity analyses. Subgroup analyses showed outcomes remained significant regardless of the biomaterial used for anastomotic coating, study design, age group studied, location of anastomoses, or indication of surgery. (**Table 4 and Table 6**) Furthermore, according to the Clavien–Dindo classification for surgical complications [151], patients in the intervention group appeared to have significantly lower major complication rates (FE: $OR, 0.54;\ 95\ \%\ CI, 0.35-0.84;\ p = 0.006$). (**Figure 21**) Neither sensitivity nor subgroup analyses could be conducted, as only two studies [66, 67] reported complications, categorized by this classification [151].

The length of hospitalization, monitored by seven studies [58, 61, 63, 67, 68, 70, 71], was significantly shorter for patients in the intervention group ($WMD, -1.96;\ 95\ \%\ CI: -$

$3.21, -0.71;\ p\ = 0.002$). (**Figure 22 and Table 7**) Sensitivity analyses confirmed the stability of these findings. Subgroup analyses showed no differences between studies stratified by study design, intervention used, or age group. However, subgroups stratified by location of anastomoses and the indication for surgery presented significant subgroup differences. Regarding the location of anastomoses, patients in the intervention group undergoing intestinal surgery with esophagojejunal or gastrojejunal anastomoses were significantly shorter hospitalized compared to those with anastomoses performed more distally. Similarly, with reference to the indication for surgery, the length of hospitalization was shorter for patients in the intervention group undergoing surgery for a malignant tumor. Further analysis allowed stating that anatomically, malignancies of the upper gastrointestinal tract are responsible for the observed outcome. (**Table 7**)

No significant difference between the intervention and control group was found for the postoperative mortality rate ($OR, 0.52;\ 95\ \%\ CI, 0.20 – 1.39;\ p\ =\ 0.19$). (**Figure 23 and Table 8**) These results remained stable during sensitivity analyses. Even subgroup analyses found no difference between the subgroups studied. (**Table 8**) Since only four [60, 61, 65, 67] out of 14 studies [58-65, 67-71, 149] reporting AL rate also reported postoperative mortality rates, the outcome of the meta-analysis should be interpreted with caution.

1.2 Discussion in the context of literature and clinical implication

AL accompanies a significant proportion of intestinal surgical procedures [19, 21-23, 28] and still presents itself as a commonly occurring and potentially devastating postoperative complication. [15, 16] In attempt to reduce this complication, human trials and animal studies have been utilizing FSs to coat intestinal anastomoses. Human trials report mostly positive effects, while animal studies [45-48, 50-55, 155, 156] present ambiguous outcomes.

Interestingly, FSs have already been used successfully to treat postoperative ALs endoscopically and appear to be a safe option for managing this complication. [157-159] These

successful therapeutic outcomes should be attributed to reduced exudation from the AL site, thereby decreasing the systemic inflammatory response and reducing clinical symptoms of treated patients. [157]

The surgical application of C-BLBs and FSs and their efficacy in preventing AL were previously systematically reviewed. When applied to esophageal anastomoses, which are particularly prone to leakage, the authors concluded, for the most part, that this treatment demonstrated positive effects in preventing AL [160] Similar effects were observed for colorectal procedures, after staple-line reinforcement with a FS. [161] These results coincide mainly with the findings of the conducted meta-analysis (**Figure 19, Table 4, and Table 5)** and therefore present an important summarizing interpretation of current literature and evidence.

Reflecting the indication of surgery once again, two studies [59, 63] included in this meta-analysis evaluated the effect of anastomotic reinforcement with FSs on postoperative anastomotic complication rates in patients undergoing bariatric surgery.

Patients undergoing bariatric surgery, such as laparoscopic sleeve gastrectomy or Roux-en-Y-gastric bypass, for morbid obesity were previously evaluated for a potential reduction of the incidence of postoperative AL upon staple-line and anastomotic reinforcement with FSs. Chen et al. [162] conducted a meta-analysis of six RCTs in 2021, demonstrating no significant difference in postoperative AL rates between the intervention and control group. These results generally coincide with findings of the respective subgroup analysis (subgroups stratified by indication for surgery) performed in this meta-analysis. (**Table 5**) Still, a major difference to the study conducted by Chen et al. [162] can be demonstrated by the fact that this meta-analysis excluded any surgical procedure without the formation of an intestinal anastomosis. Therefore, precautions should be taken when comparing these results.

Turning attention to the economic aspects of anastomotic complications and their sequelae, the study of Panda et al. [163] is particularly striking. The authors conducted a comparative cost analysis of patients undergoing colorectal surgery with anastomosis to

evaluate the differences in economic burden upon covering the anastomoses with a FS. Focusing on resource expenses provided by the healthcare system, authors were able to conduct the analysis using a potential model. Upon reinforcing colorectal anastomoses with a FS, the authors demonstrated that the observed reduction in AL rates contributed to cost savings of roughly 22 %. Furthermore, the authors specified the origin of these cost savings, which appeared to emerge mainly due to shorter hospitalization lengths, influenced primarily by differences in postoperative reoperations, radiological interventions, and/or transfusions. [163] The meta-analysis conducted in this part of this thesis was able to show significantly shorter hospitalization lengths for patients in the intervention group. (**Figure 22 and Table 7**) Therefore, to some extent, these findings correlate with the observed outcomes of study conducted by Panda et al. [163]

Although, coating intestinal anastomoses with C-BLBs or FSs resulted in significantly reduced postoperative rates of ALs, reoperations and C-DMCs, there is still room for improvement. (**Figure 19, Figure 20, Figure 21, Table 4, Table 5, and Table 6)**

One aspect of improvement focuses on the function and composition of collagen- and or fibrin-based adhesive biomaterials. In this context it is substantial to reflect the physiology of anastomotic wound healing and the pathophysiological mechanisms of the evolution of AL, specifically the role of infections.

Adequate collagen deposition plays a crucial role in the physiology of anastomotic healing [37]. If collagenase enzyme activities exceed the physiological levels needed for proper wound healing, as is the case with anastomotic infections, anastomotic failure can occur. [164, 165] In a recently conducted study by Anderson et al. [166], it appeared that a large proportion of postoperatively occurring ALs were associated with anastomotic infections. The authors investigated cultures of 19 patients with AL, seven patients with stump leaks and 16 patients with a deep infection not associated with a staple-line. The presence of the Enterococcus faecalis (24 % of all infections) appeared to be significantly associated with the development

of AL ($p = 0.029$). Furthermore, authors found 74 % of patients' ALs to be colonized with collagenase-producing microorganisms. [166] It can thus be assumed that the risk of anastomotic wound failure corresponds to the activity of collagenase enzymes. [164]

Therefore, anastomotic infections also have the potential to compromise the functionality of collagen-based anastomotic coatings. Collagenase-producing microorganisms would have a destructive effect on the basic framework of the adhesive biomaterial, thereby destroying its functional integrity.

One possible approach to improving the function of collagen-based adhesive biomaterials, enhancing resistance to infection, and ensuring complete functionality, might involve incorporating healing-supporting collagen fibrils and antimicrobial substances into the sealants. This would effectively protect the anastomosis and the adhesive from collagenase-producing microorganisms. Theoretically, this could lead to a much higher efficacy in further reducing postoperative anastomotic complications.

1.3 Limitations

In the following, certain limitations of this analysis need to be addressed and discussed. The main limitations to this systematic review and meta-analysis include variable study designs, a broad range of publication years (1996-2021), and mainly moderate study quality (according to the risk of bias assessment performed) (**Supplementary Table 4Error! Reference source not found.**). Studies older than 15 years [58, 59, 63, 65] were included for analysis due to the comparability of interventions and the similarity of adhesive biomaterials used in more recent studies.

Additionally, potential biases may have been introduced to the analysis since included studies exhibited variability in patient characteristics (such as age groups and surgical indications), surgical characteristics (anastomotic location), and interventional characteristics (type and material of adhesive biomaterial used to cover the anastomoses of the intervention

group). To address this limitation, thorough subgroup analyses were performed, with predefined subgroups stratified by potential confounding factors, as mentioned in **Chapter III.4.1.6.1**. Sensitivity analyses were conducted to further minimize the impact of individual biases on meta-analytic results, evaluating the impact of excluding one study at a time on the pooled OR, regardless of observed heterogeneity.

To be more specific about the type of anastomosis performed, this study intentionally excluded all types of anastomoses other than upper or lower gastrointestinal anastomoses. This decision was based on the fact that corresponding anastomoses, such as biliodigestive or pancreaticointestinal anastomoses, involve a distinct surgical technique compared to intestinal anastomoses. Furthermore, the specific risks for AL and associated morbidities are assumed to differ significantly from those observed with intestinal anastomoses. While this exclusion may have reduced the risk of bias in the outcomes of this meta-analysis, it is recommended for future research to conduct a separate systematic review and meta-analysis assessing the effect of coating these distinct types of anastomoses with adhesive biomaterials on postoperative complications.

The relevance of the risk of bias assessment becomes apparent when discussing the limitations of this study, as potential bias might have been introduced by a lack of adequate blinding of studies. Comments on the outcome assessor's awareness of the intervention or a possible influence the manufacturer (adhesive biomaterial utilized) might have had by funding the study were not provided in any of the RCTs [58, 60, 62, 63, 65] and three NRSs [59, 61, 64]. Since this study evaluates the efficacy of a medical product in reducing postoperative AL rates and its accompanying sequelae, it is reasonable to consider that potential bias might have been introduced by the manufacturer of the studied adhesive biomaterials by funding the study. A careful examination of the funding situations of each included study revealed that, based on current knowledge, the manufacturer of any studied adhesive biomaterial in any of

the included studies did not play a funding role. Additionally, no author was identified as a representative for the manufacturer.

Despite these presented limitations, the strength of this study lies in its uniqueness as the first systematic review with a meta-analysis conducted to investigate the efficacy of coating intestinal anastomoses with C-BLBs or FSs, presenting the most frequently utilized absorbable adhesive biomaterials [167, 168], in reducing or preventing the occurrence of postoperative AL and its accompanying sequelae.

1.4 Outlook and Conclusion

The outcomes of this systematic review and meta-analysis carry significant clinical implications, emphasizing the necessity for future research to consolidate findings. Moreover, larger RCTs examining the effects of the studied adhesives across various surgical indications and patient groups should be undertaken. The question arises as to why the coating of intestinal anastomoses with C-BLBs and/or FSs has not yet become established in everyday clinical practice. Potential reasons could include the challenging and user-unfriendly application forms, leading to additional time expenditure, or the relatively low adhesive strength of these biomaterials on intestinal surfaces. Despite these challenges, given the significant efficacy demonstrated by these adhesive biomaterials in reducing postoperative morbidity after intestinal surgery, future research and innovative developments should address these unfavorable factors.

In conclusion, current evidence suggests that covering intestinal anastomoses with either a C-BLB or a FS significantly reduces postoperative rates of AL, reoperation, and C-DMC. Furthermore, a notable reduction in the length of hospitalization can be observed, particularly for patients undergoing surgery for upper gastrointestinal malignancies. Nevertheless, it is crucial to address the risk of anastomotic and potential adhesive failure associated with anastomotic infection. This can be achieved by investigating the efficacy of antimicrobial

collagen-based sealants in protecting intestinal anastomoses from the deleterious effects of collagenase-producing microorganisms.

To consolidate findings, further large RCTs are needed to examine the effects of coating intestinal anastomoses with the studied adhesives on postoperative leakage. Moreover, future studies should explore the effects of coating other types of anastomoses commonly performed in abdominal surgery on postoperative complications. Finally, there is a need to develop a simple and user-friendly application form for a somewhat stronger adhesive C-BLB and/ or FS. This would establish the possibility of routine use in surgical practice.

2 Systematic review and meta-analysis of animal studies

The second part of this thesis comprised a review and meta-analysis providing a systematic overview of the effect of coating intestinal anastomoses with collagen-based biomaterials on postoperative AL rates and healing for animals undergoing intestinal surgery.

In the review section, assumptions were made on the intervention's impact on postoperative anastomotic stability (BP measurements), anastomotic healing process (evaluated by collagen content) and other general outcomes, such as adhesions; stenosis and weight loss. The conducted meta-analysis was designed to ensure a reliable assessment of the intervention's impact on postoperative AL and mortality rates.

2.1 Summary of outcomes and interpretation

A significant reduction in AL and mortality rates was observed for animals in the intervention group [46, 47, 50, 51, 53-55, 57] (**Figure 25, Figure 26, Figure 27, Figure 28, Table 13, and Table 14**). Subgroup analyses focusing on postoperative AL revealed a significant reduction in this complication for animals with coated but incomplete anastomoses. (**Figure 26**) Postoperative mortality rates were significantly lower for animals with coated anastomoses [46, 50, 52, 53, 55, 56], irrespective of animal species, anastomotic technique or sufficiency, utilized suture material or anastomotic location. (**Figure 27 and Figure 28**) The importance of these outcomes is underscored by its stability demonstrated in sensitivity analyses excluding one study at a time. **(Supplementary Figure 1 and Supplementary Figure 2)**

Results of BP measurements were reported by eleven studies (13 discrete data sets) [45-50, 52-54, 56, 57], which conducted these measures between postoperative days (POD) zero to 30. The majority of included studies did not find a significant difference in BP between the compared groups. [45, 47-50, 52-54, 57] Significantly higher [46, 49, 50, 57] or lower [45, 49, 56] postoperative BPs in the intervention group were evenly distributed among the included studies. (**Table 11**)

The outcomes of BP measurements were decided not to be included in the meta-analysis for the following reasons: First, intestinal organs of differently sized animals evidently have different physiologic working and BP properties; second, the included studies used different techniques to assess the BPs; and third, the BPs were measured on different PODs. Statistical evaluation of the available data in the form of a meta-analysis was not possible due to incomparability of these outcomes.

To systematically evaluate the impact of coating anastomoses with C-BLBs, future prospective animal studies should be recommended to use both a standardized and reproducible technique for the measurement of postoperative BP and a defined postoperative point in time for it to be measured.

2.2 Discussion in the context of literature and clinical implication

The formation of a stable collagen network within the anastomosis is considered a crucial factor in regaining near-preoperative tensile and mechanical strength. [50, 169] Interestingly, one study's discrete dataset [50] demonstrated significantly higher induction of collagen type 3 expression within the intervention group at POD one. Similar results were report for collagen type 1 expression in the other discrete data set [50]. Holmer et al. [47], found no difference in collagen type 1 and 3 messenger ribonucleic acid (mRNA) expression between the investigated groups at POD 1. However, at POD 3, significantly increased collagen type 1 mRNA was detected in the intervention group [47]. These findings suggest that animals' intestinal anastomosis may benefit from C-BLBs coverage by inducing higher tensile and mechanical strength in the early phases of anastomotic healing.

Haverkamp et al. [170], urged caution using C-BLBs after conducting a technical feasibility study of *TachoSil* covering esophageal anastomoses in humans, citing its potential to cause postoperative anastomotic stenosis. The author described long-term (nine months) anastomotic stenosis as a complication possibly resulting from a *TachoSil*-induced surplus in

reinforcing stimulation that may increase fibrotic processes. [170] Data presented in this review either showed significantly higher anastomotic stenosis rates within the intervention group [51, 53] or found no differences between the intervention and control groups [48, 52]. Becker et al. [171], found fibrin glue, *in-vitro*, to increase both the proliferation of fibroblasts and the accumulation of vascular endothelial growth factor within the anastomotic region. [171] Based on these observations, an elevated risk of developing postoperative anastomotic stenosis within the intervention group could therefore have arisen or at least been potentiated by the fibrinous coating of the utilized C-BLB. Against this background, future research on anastomotic coating could be recommended to focus on adhesive collagen-based biomaterials without - or at least with reduced - fibrinous content.

Since the sealing of intestinal anastomoses with commercially available C-BLBs to reduce postoperative AL is not approved for this indication, an inconvenient, time-consuming, and user-unfriendly application process could limit the implementation of this potentially very effective method into surgical practice. Therefore, future research should focus on improving collagen-based biomaterials by developing adhesives specifically for coating intestinal anastomoses. To enhance future collagen-based biomaterials, efforts should focus on increasing adhesive strength and ensuring the ability to withstand mechanical stress caused by physiological bowel movements, thus preventing dislodgement from the anastomotic site. Moreover, the application process or technique should be designed for user-independent handling to minimize its influence on the outcome.

2.3 Limitations

This study has some limitations worth noting. Firstly, the included studies involved animals of different species, limiting the generalization of observed outcomes and their transferability to humans. However, over the past decade, numerous feasibility studies in humans have reported that *TachoSil* covering of intestinal anastomoses is safe and well-tolerated. [170, 172-174] Furthermore, one NRS [175] and two observational human studies [66, 70] explored the

effect of coating intestinal anastomoses with C-BLBs on various outcomes such as postoperative AL [70, 175], mortality [175], surgical-site infections [66], reoperation rate [175], and length of hospitalization [66, 70, 175]. Both observational studies found the intervention group to have significantly lower postoperative complication rates and shorter length of hospitalization [66, 70]. Nevertheless, further experimental studies investigating the effect of coating intestinal anastomoses with C-BLBs on postoperative AL and mortality need to be conducted in larger animals of mammalian origin to evaluate the long-term effects of this intervention and the transferability of these results to humans.

The strength of this study lies in its uniqueness, as, to our knowledge, it is the first systematic review and meta-analysis of prospective animal studies investigating the effect of coating intestinal anastomoses with C-BLBs on postoperative complications, including AL, mortality, or anastomotic healing processes. This study minimized the risk of reporting biased outcomes primarily through thorough sensitivity analyses, excluding one study at a time, demonstrating the stability of the results. (**Table 13 and Table 14**). The risk of biased outcome reporting resulting from comparison of different animal species, anastomotic locations, types of suture material used, anastomotic techniques and their sufficiency was diminished through detailed subgroup analyses.

2.4 Outlook and Conclusion

This study emphasizes the necessity to evaluate the impact of coating intestinal anastomoses with C-BLBs on postoperative AL and mortality in future research. It is crucial to conduct prospective studies involving larger mammals, such as pigs, to assess the consistency of outcomes identified in this review and to evaluate its long-term effects and transferability to humans. To determine the effect size of this intervention on reducing postoperative AL and mortality in humans, RCTs should be conducted utilizing commercially available C-BLBs. Coating intestinal anastomoses with C-BLBs could represent an effective and sustainable approach in reducing AL after intestinal surgery. Subsequent studies need to explore whether

coating intestinal anastomoses with C-BLBs should be established as a standard procedure for defined indications in surgical practice.

Furthermore, this study has demonstrated that to compare the quality of different anastomoses in an experimental setting, it is essential to assess their stability through BP measurement. Consequently, there is a need to develop a standardized and reproducible technique for measuring BP to ensure data comparability. For this purpose, a prototype of an innovative *ex-vivo* model for evaluating the stability and pressure resistance of gastrointestinal anastomoses was developed, and a more detailed discussion on this was provided in the third part of this thesis.

In conclusion, the coating of intestinal anastomoses with C-BLBs significantly decreased the incidence of postoperative AL, particularly for incomplete anastomoses, and mortality in animal species. This novel approach proved to be an effective and sustainable measure against postoperative AL. However, the potential risk of fibrin-containing C-BLBs contributing to postoperative anastomotic stenosis was considered. Therefore, future prospective animal studies, particularly those involving larger mammals (e.g., pigs), are needed to evaluate the long-term effects of this intervention and its transferability to humans. Finally, the development of a strongly adhesive collagen-based biomaterial with a more convenient, time-saving, and user-friendly application method is required to establish this innovative method of AL prevention in everyday surgical practice.

3. Innovative *ex-vivo* model for evaluation of stability and pressure resistance of gastrointestinal anastomoses

The third part of this thesis evaluated the innovative *ex-vivo* test-setup that was developed to determine the gastrointestinal anastomotic quality quantitatively and precisely in terms of its stability and pressure resistance. The goal was to ensure high comparability, reproducibility and user-independence. This aimed to enhance the understanding of the biomechanics of intestinal anastomoses and, consequently, AL. It is crucial to emphasize that the objective was not to replicate *in vivo* intestinal stress with precision; instead, the aim was to induce stress on the tissue wall in a manner that reflects the observed human stress situations. This approach enables the analysis of biomechanical behavior, particularly focusing on stretching and stiffness.

The content presented in **Chapter V.3** has been partially adapted and modified from the publication authored by Cira et al., 2024 [2].

3.1 Summary of outcomes and interpretation

An innovative *ex-vivo* model was developed to assess the quality and stability of gastrointestinal anastomoses precisely and quantitatively, adhering to the 3R principles (reduction, refinement, replacement) as closely as possible. [114] The innovation resides in the comprehensive evaluation of the anastomosis, extending beyond conventional BP measurements. Instead, it is subjected to controlled pressure and temperature conditions to observe its response in stress experiments.

The *ex-vivo* model, as illustrated in **Figure 3**, has been widely employed in various studies [45, 47-50, 52-54, 56, 57] for measuring BP of anastomosed intestinal segments. Despite its widespread use, this model faces significant challenges related to user-dependence and irreproducibility. Inconsistencies arise from variations in the injection speed of the fluid during experiments, external disturbances impacting the pressure sensor, and inadequate

visualization of the entire anastomosis due to the setup's limitations. Additionally, the positioning of the anastomosis may hinder the detection of initial leaks, potentially compressing them under the weight of the anastomosis. The absence of a physiologically simulated environment and the potential temperature discrepancies of the injected fluid further restrict the applicability of this model. Moreover, the orientation of the anastomosis in a lying position introduces pressure disparities, with higher pressure observed at the inferior part compared to the superior part of the anastomosis. These factors collectively contribute to the limitations of the *ex-vivo* model in measuring BP in anastomotic evaluations.

The innovative *ex-vivo* model presented in this thesis is based on a modified perfusion bioreactor and incorporating an open fluid circulation system. This model utilized an HMI interface to transport colored PBS solution at a constant temperature (35 – 39 °C) and flow rate (about 20 ml/min ; LF model, simulating physiological intraabdominal pressure) or 200 ml/min (HF model, simulating an increased intraabdominal pressure) intraluminal into the porcine small intestinal anastomosis. All anastomoses, freely floating vertically in 35 – 39 °C PBS solution with a distal counterweight attached, are subjected to pressure measurements using a pressure probe. (**Figure 4, Figure 5, Figure 6, Figure 7, Figure 8, and Figure 9**)

Throughout the experiment, the increase in intraluminal pressure and the temperature of the surrounding PBS solution were measured. Four different cameras recorded the experiment from various angles of the anastomosis with full HD and 25 frames per second (two frames per pressure reading). (**Figure 4, Figure 5, Figure 6, Figure 9, Figure 29, Figure 30, Figure 31, and Figure 32**)

3.1.1 Quantitative analysis of anastomotic performance, time intervals and interrelated analyses derived from experimental outcome

Overall, 32 EEAs were performed on formalin-fixed small intestinal tissue obtained from the cadaver of two pigs. Among these, 16 were formed by using the SBS technique, while the

remaining were created using the CS technique. These anastomoses were performed by one surgical resident (K. C.). Subsequently, the anastomoses underwent testing with two different flow rates (LF and HF), leading to their classification in SBS-CON-LF, SBS-CON-HF, CS-CON-LF, and CS-CON-HF groups. (**Figure 10, Figure 11, Figure 12, Figure 13, and Figure 14)**

The feasibility trial and functional validation compared LP, BP; proportion of BP at LP, and time intervals in different experimental series. The results revealed significant differences in certain parameters based on flow models and anastomotic techniques.

Regarding LP, the HF model demonstrated significantly higher LP than the LF model for SBS-anastomoses ($p = 0.0281$), while no significant difference was observed between the flow models for CS-anastomoses. The suture technique did not significantly affect leakage pressure. (**Figure 33**)

For BP, both SBS-anastomoses ($p = 0.0115$) and CS-anastomoses ($p = 0.0002$) in the HF model reached higher BPs compared to the LF model. No significant difference in BP was observed between the two different suture techniques tested. (**Figure 34**)

Proportional analysis demonstrated that CS-anastomoses in the HF model reached significantly higher BP levels after leakage compared to the LF model ($p = 0.0003$). However, no significant differences were observed between SBS-anastomoses in both flow models. Comparing suture techniques within flow models did not reveal significant differences. (**Figure 38**)

Since the percentage of BP at LP was used to compare the relative proportion of BP achieved at the point of LP, the experiments revealed that CS-anastomoses in the LF model had a lower percentage of BP at the leakage point compared to SBS-anastomoses in LF ($p = 0.0499$). Consequently, with CS-anastomoses, there was a relatively higher increase in pressure after leakage before reaching the point of bursting. However, no significant

differences were found when comparing SBS-CON-LF and SBS-CON-HF groups , CS-CON-LF and CS-CON-HF, and SBS-CON-HF and CS-CON-HF groups. (**Figure 39**)

In terms of time intervals, the HF model resulted in significantly faster attainment of LP and BP compared to the LF model for both SBS-anastomoses ($p = 0.0011$ and $p = 0.0011$) and CS-anastomoses ($p = 0.0006$ and $p = 0.0070$). However, there were no significant differences in the time until bursting or leakage when comparing different anastomotic techniques within both the LF and HF models. (**Figure 35 and Figure 36**)

Interestingly, bursting occurred significantly sooner after leakage in the SBS-anastomoses of the HF model compared to the LF model ($p = 0.007$). Similarly, bursting occurred significantly sooner after leakage in the SBS-CON-HF groups compared to the CS-CON-HF groups ($p = 0.0379$). However, this was not the case when comparing CS-anastomoses in the HF and LF model, as well as SBS-CON-LF and CS-CON-LF groups. (**Figure 37**)

When analyzing the percentage of time at BP at the time of LP, it was found that CS-anastomoses in the HF group reached BP faster after leakage compared to the LF group ($p = 0.0148$). No significant differences were observed for SBS-anastomoses in both flow models or between different suture techniques in the LF and HF models. (**Figure 40**)

3.1.2 Leakage and bursting location analysis

The four experimental groups exhibited leakage and bursting in both the mesenteric zone and peripheral zone. The number of anastomotic locations with leakage varied among the groups. In all cases of leakage, except one, anastomoses at the leakage location also exhibited bursting, indicating a strong association between the occurrence of leakage and the risk of bursting at the same location within the anastomosis. (**Figure 42**)

Anastomoses at the mesenteric zone exhibited significantly higher leakage and bursting incidents compared to the peripheral zone in all experimental groups (SBS-CON-LF: $p = 0.023$ and $p < 0.0001$; SBS-CON-HF: $p = 0.0003$ and $p < 0.0001$; CS-CON-LF: $p = 0.0013$; CS-CON-HF: $p = 0.0013$ and $p < 0.0001$). (**Figure 43 and Figure 44**) No significant differences in leakage and bursting rates were found at the mesenteric entry side among the compared experimental series. (**Figure 45 and Figure 47**) Similarly, no significant differences in leakage and bursting rates were observed in the peripheral zone among the compared experimental series. (**Figure 46, Figure 47, and Figure 48**)

These findings suggest that the occurrence of leakage and bursting in anastomoses is associated with the location within the anastomosis, specifically the mesenteric entry side.

3.2 Discussion in the context of literature and clinical implication

3.2.1 Quantitative analysis of anastomotic performance, time intervals and interrelated analyses derived from experimental outcome

The observed phenomena can be attributed to the viscoelastic properties of biologic tissues, describing their response to mechanical stress and strain. Viscoelastic materials possess both elastic and viscous characteristics, allowing them to store and release energy when subjected to stress and strain. [72-75]

When tissue is suddenly subjected to stress, the elastic component of viscoelastic materials rapidly responds by storing energy, while the viscous component responds more slowly, absorbing and dissipating energy. The stretching and realignment of cellular structures take time to adapt to the new load. [176-178]

Consequently, a sudden increase in pressure within the small intestine requires time for the tissue to stretch and adjust, leading to an increase in intraluminal pressure. This time-dependent stress-strain response implies that the tissue needs to fully stretch and accommodate the stress. [72-75]

The viscous behavior results from fluid movement within the tissue, causing a time-dependent response to deformation. Elastic behavior, on the other hand, stems from the stretching and recoiling of the tissue, leading to an immediate response to deformation. In cases of high influx rate, the tissue experiences a sudden pressure increase due to its immediate elastic response. However, the viscous behavior causes a time-dependent response, resulting in continuous stretching over time and a subsequent pressure increase until the tissue ultimately bursts. [72-75, 179-181]

These characteristics align with expectations during activities such as the Valsalva maneuver, coughing, jumping, or strenuous exercise. [122]

On the other hand, when tissue is subjected to slow loading, the viscous component has more time to respond, resulting in a gradual stress-strain response. Consequently, upon stress removal, the tissue experiences faster relaxation. In the case of a slow increase in pressure, the tissue has sufficient time to adapt gradually, leading to a lesser increase in intraluminal pressure. When the intraluminal fluid influx rate is low, the tissue undergoes a gradual pressure increase, allowing its viscous behavior to keep pace with deformation. As a result, a lower final pressure is reached before bursting. [72-75, 179-181]

These characteristics align with the behavior observed in a paralytic ileus, a condition characterized by the impaired intestinal motility due to factors such as nerve damage, muscle dysfunction, or inflammation. In a paralytic ileus, slow movement of intestinal contents leads to a gradual increase in intraluminal pressure, enabling the tissue to respond and accommodate the deformation without experiencing a rapid rise in pressure. [182]

The observed behavior in biological tissues supports the fundamental principle that they possess characteristics of both elastic solids and viscous fluids. This means that the stress experienced by tissues depends not only on the applied strain, as seen in solids, but also on the rate at which the strain is applied, similar to viscous fluids. In other words, the response of tissues is time-dependent, and the stress-strain relationship does not occur instantaneously. When the tissue is suddenly strained, and the strain is maintained at a constant level, the induced stresses in the tissue gradually decrease over time. This phenomenon is known as stress relaxation, reflecting the tissues' ability to adapt and alleviate applied stress. [72-75]

Notably, no differences were observed between the suture techniques in terms of LP and BP. (**Figure 33 and Figure 34**) This suggests that the choice of suture technique may not have a significant impact on the stability and pressure resistance of EEAs.

3.2.2 Leakage and bursting location analysis

The observed findings emphasize the association between leakage and bursting and the specific location within the anastomosis, particularly the insertion site of the mesentery. This supports the assumption that the insertion site of the mesentery represents a vulnerable point where AL can develop.

The insertion site of the mesentery serves as a potential weak spot due to its role as a transition area between the mobile and fixed parts of the intestine. Here, the mesentery, responsible for blood supply and nerve innervation, attaches to the intestinal wall, creating a point of stress concentration that increases the susceptibility to mechanical failure or disruption. [183]

Anastomoses performed at the insertion site of the mesentery during surgical procedures compound the risk as they weaken the tissue and elevate the likelihood of complications such as AL. However, factors such as suture quality, tissue healing response, and mechanical stress also contribute to the risk of leakage in this specific anatomical location. [86, 87, 184-186]

Given the clinical significance of anastomotic complications, careful evaluation and management of the insertion site of the mesentery during surgical procedures are crucial. Surgeons should exercise caution and employ appropriate techniques to ensure secure and reliable anastomoses at this critical location. Exploring advancements in surgical techniques, including reinforcement methods or innovative approaches to strengthen the anastomotic site, is essential to mitigate the risk of complications and improve patient outcomes.

By gaining a better understanding of potential weak spots in anastomoses, such as the insertion site of the mesentery, surgeons can make informed decisions and implement strategies to minimize the occurrence of AL. Collaborative efforts between surgeons and researchers, along with future research endeavors, are warranted to refine surgical techniques, develop novel interventions, and enhance patient safety in the context of anastomotic procedures.

3.3 Limitations

The test-setup exhibits certain limitations that require attention. *Ex-vivo* models generally fall short in replicating the intricate physiological conditions encountered in the *in-vivo* setting. Factors such as blood flow, tissue perfusion, and the presence of surrounding organs are inadequately simulated in *ex-vivo* models, impacting the accuracy and relevance of the obtained results. Additionally, most models fail to account for variations in surrounding body temperature and intraluminal intestinal pressure.

3.3.1 Tissue temperature

Tissue temperature holds significant importance in biomechanical testing for multiple reasons. Firstly, maintaining a physiological temperature during testing ensures that the mechanical properties of the tissue remain representative of *in-vivo* conditions. Tissues are sensitive to temperature deviations, and alterations from the normal physiological range can modify their viscoelastic behavior, thereby affecting their response to mechanical stress. [187-189] Moreover, tissue temperature influences the rate of enzymatic reactions and cellular metabolic activity, thereby impacting the tissue's mechanical behavior. [190] By controlling the temperature, a standardized testing environment can be established, reducing variability introduced by temperature fluctuations.

While it is challenging to fully replicate factors such as blood flow and tissue perfusion, conducting gastrointestinal anastomotic stability and pressure resistance testing in near physiological environment is applicable. Consequently, in this innovative *ex-vivo* model, when using PBS solution for transport into or around the anastomosis, the solution was heated to a range of 35–39 $°C$. Furthermore, prior rehydration of the intestinal tissue was performed to maintain a near physiological environment.

3.3.2 Intraluminal intestinal pressure and flow models

Intraluminal intestinal pressure can vary depending on physiological states and external factors. During periods of rest, the intraluminal intestinal pressure remains relatively low, within a range that allows for proper digestion and nutrient absorption. Resting intraabdominal pressure typically ranges from 2 – 4 $mmHg$ but can fluctuate depending on different activities. For example, jumping can elevate intraabdominal pressure to 170 $mmHg$, coughing to 100 $mmHg$, the Valsalva maneuver to 40 $mmHg$, and simply standing to 20 $mmHg$. [122]

In the small intestine, resting intraluminal pressure varies in the literature and is estimated to range from 6 – 13 $mmHg$. [123-125] However, with various peristaltic movements, it is estimated to reach 20 – 30 $mmHg$. [126] Under normal physiological conditions, the fluid flow rate in the proximal small intestine exhibits variations based on whether it is measured during fasting or after meals. During fasting, a fluid flow rate of approximately 2.5 ml/min has been observed [115, 116], while after meals, the fluid flow rate can increase to approximately 20 ml/min [117-121].

To simulate a physiological increase in intraluminal intestinal pressure under normal conditions, a fluid flow rate of about 20 ml/min was selected and designated as the LF model. To simulate a sudden increase in intraluminal pressure, as experienced during the Valsalva maneuver, coughing, or jumping, an intraluminal intestinal fluid flow rate of 200 ml/min, ten times the rate of the LF model, was chosen and designated as the HF model.

3.3.3 Fixation methods

The viability and preservation of tissue in *ex-vivo* models pose significant challenges. Over time, tissue degradation and loss of biomechanical properties can occur, introducing potential inaccuracies and unreliability in the obtained results. Consistently maintaining tissue quality and functionality throughout the testing process is particularly challenging.

In this study, formalin-fixed porcine intestinal tissue was utilized as a preservation method. However, this fixation method has known disadvantages that can impact tissue properties and cellular structures. Formalin fixation, commonly used in histology and pathology for tissue preservation, induces cross-linking between proteins, resulting in changes in the tissue's mechanical properties. This can lead to a stiffer and more brittle tissue compared to fresh tissue. [191, 192]

Future research should focus on exploring the biomechanical characteristics of intestinal tissue using alternative fixation methods, such as fresh, frozen or ethanol-fixed intestinal tissue. It is crucial to investigate whether these different fixation approaches have any impact on tissue biomechanics. This line of investigation will provide valuable insights into the suitability of different tissue preservation techniques for *ex-vivo* models.

3.3.4 Preconditioning of biological tissue

It is also recommended to incorporate preconditioning protocols when testing soft biological tissues. Preconditioning, involving subjecting soft biological tissues to repeated load cycles, is a well-established practice in mechanical testing. The purpose of preconditioning is to obtain a consistent and repeatable mechanical response from the tissue. The concept of preconditioning effects was initially introduced in the context of uniaxial tensile testing of skin tissue, describing the phenomenon of the mechanical response evolving over time as a result of repeated loading. [193] Therefore, preconditioning helps minimize the influence of initial tissue variability and ensure a more reliable and reproducible assessment of mechanical

properties. By subjecting the tissue to repeated loading cycles prior to the actual testing, the tissue undergoes a conditioning process that allows it to reach a stable mechanical state. This approach improves the accuracy and consistency of the obtained mechanical measurements.

3.3.5 Dynamic physiological forces

Currently, *ex-vivo* models are unable to faithfully replicate the dynamic physiological forces experienced by anastomoses *in-vivo*, including peristalsis, pulsatile blood flow, and changes in intraabdominal pressure. These dynamic conditions are crucial for assessing anastomotic stability and pressure resistance.

To overcome this limitation, modifications can be implemented in the *ex-vivo* test setup to incorporate tissue perfusion, blood flow, and peristalsis, thereby achieving a more realistic simulation of the *in-vivo* environment. Tissue perfusion could be accomplished by integrating a perfusion system that delivers oxygenated blood or an appropriate perfusate to the tissue. This approach ensures tissue viability, simulates nutrient supply, and establishes a physiologically relevant environment for investigating anastomotic quality.

Simulating blood flow could be achieved by introducing a vascular network into the *ex-vivo* model, capable of replicating the flow dynamics and pressure characteristics of blood vessels. This could enable the evaluation of anastomoses under realistic hemodynamic conditions. By further implementing a pulsatile flow or controlling flow rates, the influence of blood flow on anastomotic stability and healing could be systematically examined.

To account for peristalsis, enhancements could be made to the *ex-vivo* model by incorporating mechanisms that emulate the rhythmic contractions and relaxations of the gastrointestinal tract. Extensive data obtained from human imaging studies can be employed to incorporate diverse peristaltic movement patterns into the virtual model. This may involve programmable actuators or devices that accurately mimic the movements and forces exerted during peristalsis. By subjecting anastomoses to controlled peristaltic motions, it becomes

possible to assess their mechanical properties and leakage resistance in a more representative manner.

By integrating tissue perfusion, blood flow, and peristalsis into the *ex-vivo* test setup, a more comprehensive and physiologically relevant model can be achieved to investigate anastomotic quality and wound healing. This approach would yield insights into the behavior of anastomoses under conditions closely resembling the *in-vivo* environment, thereby enhancing the translational potential of *ex-vivo* models in the field of biomedical research.

3.3.6 Inter-individual and intra-individual variability

Biological tissues exhibit notable inter-individual and intra-individual variability in their biomechanical properties. However, *ex-vivo* models commonly employ a restricted number of tissue samples that may not encompass the full heterogeneity observed in clinical settings. Consequently, the generalizability and applicability of the findings can be compromised by this limited representation of tissue variability.

To improve upon this limitation, future studies should strive to incorporate larger and more diverse sample populations, encompassing a broader range of demographic and physiological characteristics. This approach will enhance the representativeness of *ex-vivo* models, enabling a more comprehensive understanding of the biomechanical properties of the tissues under investigation.

Furthermore, it is crucial to expand the scope of research by incorporating human tissue samples, such as remnants from the operating theatre, in addition to animal tissue. This shift will facilitate a closer alignment between the experimental models and the clinical scenario. By addressing these considerations, the robustness and translational potential of *ex-vivo* models can be enhanced in the field of biomechanics, ultimately leading to improved clinical relevance and applicability in understanding tissue behavior and its implications for medical interventions.

3.3.7 Tissue healing and advanced tissue engineering

Moreover, the current *ex-vivo* test setup faces the limitation of not being able to fully simulate the intricate process of tissue healing that occurs after an anastomosis. Tissue healing involves complex remodeling and collagen deposition over time, which directly influences the long-term stability and durability of anastomoses. [85]

Consequently, the insights gained from *ex-vivo* models may not fully reflect the clinical scenario, where the healing process plays a critical role in the success of anastomotic procedures. To overcome this limitation, it is crucial to develop strategies that enable a more realistic simulation of tissue healing in *ex-vivo* models.

One approach is to incorporate advanced tissue engineering techniques, such as biomimetic scaffolds or tissue constructs, which can facilitate tissue remodeling and provide a more physiologically relevant environment for studying anastomotic healing. Additionally, *ex-vivo* models can be modified to include sequential testing of anastomoses at different stages of healing. Animal models can be employed to investigate anastomoses at various time points post-surgery, allowing for the assessment of the impact of tissue healing on anastomotic stability and durability. This approach provides valuable insights into the progression of tissue healing and its correlation with mechanical properties and clinical outcomes.

Furthermore, advanced imaging techniques like laser profilometry or laser scanning can be utilized to collect data on the surface morphology of the anastomosis, including shape changes and roughness. This data can be processed and analyzed using artificial intelligence algorithms to extract significant features and detect temporal changes. By comparing scans taken at different time intervals, the algorithm can quantify relevant parameters related to the anastomosis, such as dimensional alterations, surface deformation, and variations in roughness. These measurements offer insights into the dynamic behavior and stability of the anastomosis during the healing process or under diverse conditions. Moreover, the acquired laser scanning data can be used to generate a virtual model of the anastomosis, which can be

integrated into a simulation setup. By simulating the test environment and applying known mechanical properties to the virtual model, it becomes possible to predict and evaluate the response of the anastomosis to various forces or conditions. This comprehensive approach incorporating tissue engineering techniques, advanced imaging, and virtual modelling enhances our understanding of tissue healing and its influence on anastomotic behavior, contributing to improved clinical outcomes in the field of biomedical research.

While *ex-vivo* models excel in evaluating mechanical parameters, such as BP and tensile strength, they may have limitations in fully capturing clinically relevant outcomes, particularly AL. The relationship between mechanical properties and clinical outcomes is intricate, and other critical factors, including tissue inflammation, infection, and healing response, can significantly influence the success of anastomotic healing and therefore the biomechanical outcomes. To address this limitation, it is crucial for future developments to integrate more comprehensive and clinically relevant assessment parameters into the *ex-vivo* test setup.

3.3.8 User-dependence and reproducibility

Ex-vivo models strongly rely on skilled operators to perform the tests accurately and consistently. However, the inherent variability among operators, in terms of technique and experience, can introduce inconsistencies in the results obtained. This user-dependence may hinder the reproducibility and reliability of the findings. To mitigate this limitation, efforts should be made to standardize the testing procedures and provide comprehensive training for operators. Implementing strict protocols and guidelines will help reduce operator-related variability and enhance the overall reliability of the *ex-vivo* test results. Additionally, the use of automated testing systems and advanced robotic technologies can further minimize operator influence, leading to more robust and reproducible outcomes. In this specific test system, which is predominantly automated, operator independence is achieved, leading to highly reproducible and comparable data. This automation ensures consistent and precise execution of the test procedures, resulting in reliable and reproducible measurements. By minimizing

operator-related variability, this innovative test setup offers enhanced reliability and the ability to generate robust data for comparative analysis.

3.4 Outlook

In future developments, there are several possibilities to enhance the capabilities of this innovative *ex-vivo* test setup. Firstly, it is crucial to address the limitations associated with replicating physiological conditions encountered in the *in vivo* setting. Efforts should be made to simulate factors such as blood flow, tissue perfusion, and variations in surrounding body temperature and intraluminal intestinal pressure. While full replication may be challenging, creating a near-physiological environment by incorporating a perfusion system, a vascular network, and mechanisms to emulate peristalsis can significantly improve the relevance and accuracy of the test results.

Standardizing testing procedures and providing comprehensive training for operators is essential to mitigate the variability introduced by skilled operators. Implementing strict protocols, guidelines, and automated testing systems can reduce operator influence, leading to more reproducible and comparable data.

Additionally, future research should focus on exploring alternative fixation methods for tissue preservation in *ex-vivo* models, such as fresh, frozen, ethanol-fixed, or other suitable techniques. Comparing the biomechanical characteristics of tissues preserved using different methods will provide valuable insights into their impact on tissue behavior. Furthermore, the application of repeated loading cycles to the tissue before conducting the actual testing initiates a conditioning process, enabling the tissue to attain a stable mechanical state. By subjecting the tissue to repeated loading cycles prior to the actual testing, as a part of the testing protocol, the tissue undergoes a conditioning process that allows it to reach a stable mechanical state. This approach, when implemented in the testing protocol, improves the accuracy and consistency of the obtained mechanical measurements.

Collaborative efforts with clinicians and surgeons are crucial in refining the ex-vivo model to better align with the challenges encountered in clinical practice. By incorporating their expertise and insights, the *ex-vivo* test setup can become a valuable tool for investigating anastomotic performance and optimizing surgical outcomes.

Overall, by addressing these limitations and incorporating advancements in imaging techniques, artificial intelligence algorithms, tissue engineering, and collaboration with clinicians, the *ex-vivo* test setup holds great potential for providing more accurate, clinically relevant data, leading to improved understanding of anastomotic behavior and enhanced surgical outcomes. With the aim of completely eliminating the need for animal testing, the data derived from this innovative *ex-vivo* model will be leveraged for the future development of a digital simulation encompassing the biomechanical behavior and healing processes of intestinal anastomoses or tissue. Comparable to the established predictive assessment and classification of abdominal aortic aneurysms through virtual simulations [194-196], the advancements in the current *ex-vivo* model are anticipated to yield data for predictive risk assessment and classification of AL using simulation and artificial intelligence, with substantial scientific and medical impact.

Additionally, the *ex-vivo* test setup enables the determination and visualization of leakage and BP, allowing for the analysis of weak spots in an anastomosis. This capability opens up future implications for studying the mechanical strengthening of biologic adhesives used to coat intestinal anastomoses. By assessing the degree of reinforcement provided by these adhesives, researchers can explore novel approaches to enhance anastomotic stability and reduce the risk of leakage.

Furthermore, the *ex-vivo* test setup provides a platform for reproducibly comparing different suture or anastomotic staple techniques. This comparative analysis can offer valuable insights into the performance and effectiveness of various techniques, guiding surgeons in selecting the optimal approach for anastomosis.

3.5 Conclusion

In conclusion, the innovative *ex-vivo* model for quantitively precise determination of the gastrointestinal anastomotic quality in terms of stability and pressure resistance presented a high comparability, reproducibility, user-independence and showed to be a feasible method.

The experimental results revealed significant differences in LP, BP, and time intervals based on the flow models and anastomotic techniques tested. The HF model demonstrated higher LP for SBS-anastomoses, and a higher BP for SBS- and CS anastomoses. The observed phenomena can be attributed to the viscoelastic properties of biologic tissues, which exhibit time-dependent stress-strain responses. The choice of suture technique did not significantly affect leakage and BP, suggesting that it may not have a substantial impact on anastomotic stability and pressure resistance.

Anastomoses at the insertion site of the mesentery exhibited significantly higher rates of leakage and bursting compared to other sections of the anastomosis. This observation suggests that the insertion site of the mesentery serves as a potential weak spot where AL is more prone to occur. Given that surgical procedures frequently involve anastomoses at this location, there is an increased risk of complications associated with AL. These findings underscore the importance of careful consideration and appropriate management of the mesenteric insertion site during surgical interventions to minimize the likelihood of anastomotic complications. Further investigations and refinements in surgical techniques may be warranted to optimize outcomes in this critical area of anastomotic procedures.

VI List of figures, tables, supplementary tables and equations

1. Figure legend

2. Table legend

3. Supplementary table legend

4. Equation Legend

VII Supplementary Material

1. Supplementary Table 1

Supplementary Table 1. Search strategy. Final database search (January 17, 2022). *(Adapted from the publication authored by Cira et al., Front Surg 2022)* [1]

Supplementary Table 1. Search strategy. Final database search (January 17, 2022).

Database	Predefined search Terms	Number of results, n
PubMed (MEDLINE)		
Search 1:	(anastomo* AND (bowel[tiab] OR intestin*[tiab] OR enter*[tiab] OR ile*[tiab] OR colo*[tiab] OR colorect*[tiab] OR rect*[tiab] OR rectal[tiab] OR pancrea*[tiab] OR "intestines"[Mesh] OR "intestine, large" [Mesh] OR "intestine, small") OR "Colon"[Mesh] OR "Ileum"[Mesh] OR "Rectum"[Mesh] OR "Pancreas"[Mesh])	299,677
Search 2:	("collagen patch" OR "collagen fleece" OR "collagen mesh" OR "collagen dressing" OR "collagen coating" OR avitene[tiab] OR hemopatch[tiab] OR permacol*[tiab] OR tacho*[tiab] OR "bovine pericard*"[tiab] OR (collag*[tiab] AND matri*[tiab]) "tachosil"[tiab] OR tachocomb[tiab] OR lyostypt[tiab] OR tissuefleece[tiab] OR "collagen sponge"[tiab] OR "fibrin tissue patch"[tiab] OR "collagen matrix"[tiab] OR ("collageneous"[Title/Abstract] AND "matrices"[Title/Abstract]) OR "bovine pericard*"[tiab] OR "fibrin glue"[tiab] OR glue*[tiab] OR "fibrin sealant"[tiab] OR artiss[tiab] OR tisseel[tiab] OR floseal[tiab] OR coseal[tiab] OR beriplast[tiab] OR evicel[tiab] OR "thrombin-JMI"[tiab] OR quixil[tiab] OR vistaseal[tiab] OR dermabond[tiab] OR actifoam[tiab])	23,912
Final search:	Search 1 AND Search 2	445

VII Supplementary Material

Web of Science		
Search 1:	TS=(anastomo* AND TS=(bowel OR 235ermacol235* OR enter* OR ile* OR colo* OR colorect* OR rect* OR rectal OR permacol*)	31,249
Search 2:	TS= (collagen patch OR collagen fleece OR collagen mesh OR collagen dressing OR collagen coating OR avitene OR hemopatch OR 235ermacol* OR tacho* OR bovine pericard OR collagen matrix OR collag* matri* OR tachosil OR tachocomb OR lyostypt OR tissuefleece OR collagen sponge OR fibrin tissue patch OR fibrin glue OR glue* OR fibrin sealant OR artiss OR tisseel OR flosea OR coseal OR beriplast OR evicel OR thrombin-JMI OR quixil OR vistaseal OR dermabond OR actifoam)	1,319,993
Final search:	Search 1 AND Search 2	524
Scopus		
Search 1:	TITLE ((anastomo* AND bowel) OR (anastomo* AND intestin*) OR (antastomo* AND enter*) OR (anastomo AND ile*) OR (anastomo* AND colo*) OR (anastomo* AND colorect*) OR (anastomo* AND rect*) OR (anastomo* AND rectal) OR (anastomo* OR pancrea*) OR (anastomo* W/2 bowel) OR (anastomo* W/2 intestin*) OR (antastomo* W/2 enter*) OR (anastomo W/2 ile*) OR (anastomo* W/2 colo*) OR (anastom* W/2 colorect*) OR (anastomo* W/2 rect*) OR (anastomo* W/2 rectal) OR (anastomo* W/2 pancrea*))	251,645
Search 2:	TITLE ((((((((((((((((((((collagen AND patch) OR (collagen AND fleece) OR (collagen AND mesh) OR (collagen AND dressing) OR (collagen AND coating) OR (bovine AND pericard*) OR (collage* AND matr*) OR (collagen AND sponge) OR (thrombin AND jmi) OR (fibrin AND tissue AND patch) OR (fribrin AND glue) OR (fibrin AND seal*)) OR tachosil) OR tacho*) OR avitene) OR hemopatch) OR permacol*) OR tachocomb) OR lyostypt) OR tissuefleece) OR glue*) OR artiss) OR tisseel) OR floseal) OR coseal) OR beriplast) OR evicel) OR quixil) OR vistaseal) OR dermabond) OR actifoam)	19,483
Final search:	Search 1 AND Search 2	371
Cochrane Library		

VII Supplementary Material

Search 1:	(anastomo*):ti,ab,kw AND (bowel):ti,ab,kw OR (intesin*):ti,ab,kw OR (enter*):ti,ab,kw OR (ile*):ti,ab,kw OR (colo*):ti,ab,kw OR (colorect*):ti,ab,kw OR (rect*):ti,ab,kw	126,984
Search 2:	(collagen patch):ti,ab,kw OR (colalgen fleece):ti,ab,kw OR (collagen mesh):ti,ab,kw OR (collagen dressing):ti,ab,kw OR (collagen coating):ti,ab,kw OR (avitene):ti,ab,kw OR (hemopathc):ti,ab,kw OR (permacol*):ti,ab,kw OR (tacho*):ti,ab,kw OR (bovine pericard*):ti,ab,kw OR (collagen sponge):ti,ab,kw OR (collagen matrix):ti,ab,kw OR (collag* AND matri*):ti,ab,kw OR (tachosil):ti,ab,kw OR (tachocomb):ti,ab,kw OR (lyostypt):ti,ab,kw OR (tissuefleece):ti,ab,kw OR (fibrin tissue patch):ti,ab,kw OR (fibrin glue):ti,ab,kw OR (fibrin sealant):ti,ab,kw OR (artiss):ti,ab,kw OR (tisseel):ti,ab,kw OR (floseal):ti,ab,kw OR (coseal):ti,ab,kw OR (beriplast):ti,ab,kw OR (evicel):ti,ab,kw OR (thrombin JMI):ti,ab,kw OR (quixil):ti,ab,kw OR (vistaseal):ti,ab,kw OR (dermabond):ti,ab,kw OR (actifoam):ti,ab,kw	3,244
Final Search:	Search 1 AND Search 2	241
Additional data sets identified		
Citation searching		8
Website		3

2. Supplementary Table 2

Supplementary Table 2. Search strategy. Final database search (October 6, 2021).

Supplementary Table 2. Search strategy. Final database search (October 6, 2021).		
Database	**Predefined search terms**	**Number of results, *n***
PubMed (MEDLINE)		
Search 1:	((("collagen fleece") OR "tachosil") OR "tachocomb") AND anastomo*	
Search 2:	(anastomo* AND (bowel[tiab] OR intestin*[tiab] OR enter*[tiab] OR ile*[tiab] OR colo*[tiab] OR colorect*[tiab] OR rect*[tiab] OR rectal[tiab] OR pancrea*[tiab] OR "intestines"[Mesh] OR "intestine, large" [Mesh] OR "intestine, small") OR "Colon"[Mesh] OR "Ileum"[Mesh] OR "Rectum"[Mesh] OR "Pancreas"[Mesh]) AND ("collagen patch" OR "collagen fleece" OR "collagen mesh" OR "collagen dressing" OR "collagen coating" OR avitene[tiab] OR hemopatch[tiab] OR permacol*[tiab] OR tacho*[tiab])	
Final search:	**Search 1 OR Search 2**	**58**
Web of Science		
Search 1:	TS= (collagen fleece OR tachosil OR tachocomb) AND TS=anastomo*	
Search 2:	TS= (anastomo* AND TS= (bowel OR intestin* OR enter* OR ile* OR colo* OR colorect* OR rect* OR rectal OR pancrea*) AND TS= ("collagen patch" OR "collagen fleece" OR "collagen mesh" OR "collagen dressing" OR "collagen coating" avitene OR hemopatch OR permacol* OR tacho*))	
Final search:	**Search 1 OR Search 2**	**62**
Scopus		
Search 1:	TITLE (((collagen fleece) OR tachosil) OR tachocomb) AND anastomo*	
Search 2:	((TITLE((anastomo* AND bowel) OR (anastomo* AND intestin*) OR (antastomo* AND enter*) OR (anastomo AND ile*) OR (anastomo* AND colo*) OR (anastomo* AND colorect*) OR (anastomo* AND rect*) OR (anastomo* AND rectal) OR (anastomo* OR pancrea*) OR (anastomo* W/2 bowel) OR (anastomo* W/2 intestin*) OR (antastomo* W/2 enter*) OR (anastomo W/2 ile*) OR (anastomo* W/2 colo*) OR (anastom* W/2 colorect*) OR (anastomo* W/2 rect*) OR (anastomo* W/2 rectal) OR (anastomo* W/2 pancrea*))) AND (TITLE((collagen* AND patch) OR (collagen* AND fleece) OR (collagen* AND mesh) OR (collagen* AND dressing) OR (collagen* AND coating) OR (collagen* W/2 patch) OR (collagen* W/2 fleece) OR (collagen* W/2 mesh) OR (collagen* W/2 dressing) OR (collagen* W/2 coating) OR (avitene) OR (hemopathy) OR (permacol) OR (tacho*)))) AND NOT (TITLE((pancreatectomy) OR (pancreatic AND fistula))) AND NOT (TITLE((vasc* AND anastomo*))) AND PUBYEAR > 1900	
Final search:	**Search 1 OR Search 2**	**67**
Cochrane Library		
Final search:	((("collagen fleece") OR "tachosil") OR "tachocomb") AND anastomo*	**15**
	Additional data sets identified	

Reference list search	7

3. Supplementary Table 3

Supplementary Table 3. Innovative *ex-vivo* model. Chemicals, reagents, surgical and consumable materials, laboratory equipment, hardware and software. *(Adapted from Cira et al., Langenbecks Arch Surg 2024)* [2]

Supplementary Table 3. Innovative *ex-vivo* model. Chemicals, reagents, surgical and consumable materials, laboratory equipment, hardware and software.

Type of material	Name	Brand and supplier (postal code, city, country)
Reagents	Distilled water	SAV Liquid Production GmbH (83126 Flintsbach am Inn, Germany)
	Formaldehyde solution (PN: 252549)	Sigma-Aldrich Chemie GmbH (82024 Taufkirchen, Germany)
	Methyl green (C. I. 42590)	Carl Roth GmbH & Co. KG (76185 Karlsruhe, Germany)
	Phosphate-buffered solution tablets	EMD Millipore Corporation; Sigma-Aldrich Chemie GmbH (82024 Taufkirchen, Germany)
Parent solution	A 3.7 % formaldehyde solution (1:9 ratio) was prepared by diluting 100 ml of ACS reagent (37 wt. %) in water with 10-15 % methanol as a stabilizer, in 900 ml of water.	See brand and supplier in reagents
	A methyl green solution was prepared by dissolving one g of methyl green, one phosphate-buffered solution tablet, in one liter of distilled water.	
	A phosphate-buffered solution was made using one phosphate-buffered solution tablet and one liter of distilled water.	
Surgical instruments and suture material	Anatomical forceps (14.5 cm, ClinaStar)	Entrhal Medical GmbH (47638 Straelen, Germany)
	Disposable Scalpel (Category number 11, 100 mm length)	FEATHER; SOCOREX ISBA SA (1024 Ecublens/Lausanne, Switzerland)
	Iris scissors (11 cm, ClinaStar)	Entrhal Medical GmbH (47638 Straelen, Germany)
	Needle holder (PN : 56127, Hegar-Mayo, MF: BM065R, 150 mm, wire 5/0 from Aesculap)	B. Braun SE (34212 Melsungen, Germany)
	Needle holder (Mayo-Hegar, 12 cm, ClinaStar)	Entrhal Medical GmbH (47638 Straelen, Germany)
	PDS II (violet monofilament, with needle SH-1 PLUS (22 mm 1/2c and VISI-BLACK, USP 4-0, 70 cm thread length))	Ethicon Deutschland Johnson & Johnson Medical GmbH (22851 Norderstedt, Germany)
Other consumable materials	Cable ties (150 mm 2.50 mm Black UV-proof)	TRU COMPONENTS; Conrad Electronic SE (1923 Berlin, Germany)

	Connecting tubes: - Tubing system with pressure converter (cut to size): Reduced roller pump tubing with connector AR-6411, Arthrex, no information on ID and WD, Self-measurement: ID = 4.8 mm, WD = 1 mm Pump tubing: Tubing R-3603, TYGON, ID = 3.2 mm, WD = 1.6 mm (now replaced by model E-3603)	Arthrex GmbH (81249 München, Germany) TYGON (Saint-Gobain Performance Plastics) (50769 Köln, Germany)
	Custom-made Framework (Aluminum strut profiles of type 5 with 20 x 20 mm cross-section): - Profile 5 20 x 20, natural, length: 58 mm; Article number: 0.0.370.03 - Profile 5 20 x 20, natural, length: 180 mm; Article number: 0.0.370.03 - Profile 5 20 x 20, natural, length: 210 mm; Article number: 0.0.370.03 - Profile 5 20 x 20, natural, length: 400 mm; Article number: 0.0.370.03 - Profile 5 20 x 20, natural, length: 450 mm; Article number: 0.0.370.03 - Profile 5 20 x 20, natural, length: 368 mm; Article number: 0.0.370.03 - Cover cap 5 20 x 20, black; Article number: 0.0.370.09 - Clamping lever Pi 50 M 5 x 20, white; Article number: 0.0.678.50 - T-slot nut 5 M5, galvanized; Article number: 0.0.370.01 - Automatic connection set 5, galvanized; Article number: 0.0.391.60 - Angle set 5 20 x 20; Article number: 0.0.425.02 - Joint 5 20 x 20 with clamping lever; Article number: 0.0.464.43 - Angle 5 20, white aluminum; Article number: 0.0.677.77 - Mounting set 5 2 – 4 mm with countersunk M5; Article number: 0.0.680.92 - Half-round screw M 5 x 16, galvanized; Article number: 8.0.000.07 - Half-round screw M 5 x 12, galvanized; Article number: 8.0.005.45 - Angle 40 x 40 x 20 galvanized zinc; Article number: 0.0.474.60 - Clamping lever Pi 50 M5 x 16; Article number: 0.0.684.60 - Profile bar 5 St galvanized; Article number: 0.0.370.56 - Angle set 5 20 x 20; Article number: 0.0.425.02	Item Industrietechnik GmbH (42651 Solingen, Germany)
	Custom-made scaffolding walls (gray twin-wall sheet, ITEM (custom cut))	
	Cutting mat (FINFÖRDELA – cutting mat, flexible, dark gray/ dark turquoise, 28 x 36 cm)	IKEA Deutschland GmbH & Co. KG (Germany)
	Discofix C Three-Way Stopcock	B. Braun SE (34212 Melsungen, Germany)
	Disposable pipettes (Transfer Pipets)	Avantor, Inc; VWR International GmbH (64295 Darmstadt, Germany)

	Duran Laboratory Bottle with Closure - (1000 ml capacity, Borosilicate glass 3.3, polypropylene cap)	DURAN Schott; Avantor, Inc; VWR International GmbH (64295 Darmstadt, Germany)
	Flasks: - Large: Duran Erlenmeyer flask, wide neck (2000 ml) - Small: Duran beaker (600 ml, borosilicate glass 3.3.)	DURAN Schott; Avantor, Inc; VWR International GmbH (64295 Darmstadt, Germany)
	Inject Luer-Solo Syringe (5 ml, 10 ml, 20 ml, 60 ml)	B. Braun SE (34212 Melsungen, Germany)
	Laboratory Lifting Platform	JUCHHEIM Laborgeräte GmbH (79224 Umkirch, Germany)
	Luer-Lock adapter: - Adapter from male Luer-Lock to metric fitting PTFE-, PE for less elastic hoses / PC; ID 1.6 mm; rct-online; Thomafluid - Adapter from female Luer-Lock to metric fitting for less elastic hoses / PC; ID 1.6 mm; rct-online; Thomafluid - Adapter from male Luer-Lock to metric fitting PTFE-, PE for less elastic hoses / PC; ID 3.2 mm; rct-online; Thomafluid - Adapter from female Luer-Lock to metric fitting for less elastic hoses / PC; ID 3.2 mm; rct-online; Thomafluid - Adapter from male Luer-Lock to metric fitting PTFE-, PE for less elastic hoses / PC; ID 4.8 mm; rct-online; Thomafluid - Adapter from female Luer-Lock to metric fitting for less elastic hoses / PC; ID 4.8 mm; rct-online; Thomafluid	RCT Reichelt Chemietechnik GmbH + Co. (69126 Heidelberg, Germany)
	MoliNea E Water Absorbing Sheets	Paul Hartmann AG (89522 Heidenheim, Germany)
	Mounting for temperature probe, and different holder (made with 3D printer, Hose Center T1 v5, Hose Center T2 v4, Hose Holder I v2, Temperature Rod Holder Block v3, printed material from resin)	
	Materials for the perfusion bioreactor	The materials were adopted from Micheler et al., 2017 [98-102]
	Ruler	
	Screw with a weight of 16,8 g	
	Specimen container (Wide-mouth container, clear PVC, 500 ml)	Kautex Textron GmbH & Co KG (80807 Munich, Germany)
	LED ring light 60	Omegon.de (86899 Landsberg am Lech, Germany)
	StreamCam webcam	Logitech Europe S.A. (1015 Lausanne, Switzerland)
	USB-C hub 4 port	SITECOM Europe B.V. (81274 CJ Huizen, The Netherlands)
	NI-myRIO	National Instruments (11500 Austin, USA)
Laboratory equipment	Digital heating plate (HP-20D Set)	Witeg Labortechnik GmbH (97877 Wertheim, Germany)
	GTH 175 Pt Digital Thermometer	Freisinger Electronic GmbH (82031 Grünwald, Germany)

	Magnetic stirrer with ceramic heating plate (180 x 180 mm, Professional Series	Avantor, Inc; VWR International GmbH (64295 Darmstadt, Germany)
	Peristaltic pump (Ecoline VC-380/1, Ismatec)	Ismatec; VWR International GmbH (64295 Darmstadt, Germany)
	Pressure sensor (AMS 5812-0150-D)	Amsys GmbH & Co. KG (55124 Mainz, Germany)
	Temperature sensor	Conrad Electronic SE (1923 Berlin, Germany)
Software Tools	LabView: LabVIEW 2021 SP1 f2 (16. February 2022)	National Instruments (11500 Austin, USA)
	Office-Programs: Word, Excel, PowerPoint (Version 8.0.2)	Microsoft Corporation (San Diego, USA)
	Endnote X9.3.1 (Build 13578) Endnote 20.1 (Build 15341) Endnote 21.2 (Build 17387)	Clarivate Analytics (19130 Philadelphia, USA)
	GraphPad Prism Software Version 8.0.2	GraphPad Software, Inc. (92108 San Diego, USA)
	PhotoScape X 3.0.3	MOOII TECH (94111 San Francisco, USA)

3D = Three-dimensional; ACS = American Chemical Society; C. I. = Color index; cm = Centimeter; g = Gram; ID = Inner diameter; LED = Light-emitting diode; M5 = Metric thread size designation (5 mm diameter); MF = Manufacturer number; ml = Milliliter; mm = Millimeter; NI-myRIO = NI-myRIO Controller; PC = Polycarbonate; PE = Polyethylene; PDS = Polydioxanone; PN = Product number; PTFE = Polytetrafluoroethylene; PVC = Polyvinyl chloride; USB-C = Universal serial bus connector C; USP = United states pharmacopeia; UV = Ultraviolet; WD = Wall thickness; wt. = Weight.

4. Supplementary Table 4

Supplementary Table 4. Risk of bias assessment for included studies (abstracts excluded). *(Adapted from the publication authored by Cira et al., Front Surg 2022)* [1]

Supplementary Table 4. Risk of bias assessment for included studies (abstracts excluded).

Study		Risk of bias in NRSs (ROBINS-I) [108]							
		Pre-intervention		At intervention	Post-intervention				Overall risk of bias
Author	Year	Bias due to confounding	Bias in selection of participants into the study	Bias in selection of classification of interventions	Bias due to deviations from intended Interventions	Bias due to missing data	Bias in measurement of outcomes	Bias in selection of the reported results	Low/ moderate/ serious/ critical
Liu et al. [59]	2003	L	L	L	M[1]	M[2]	M[3]	M[4]	Moderate
Saldaña-Cortés et al. [61]	2009	L	L	L	L	L	M[3]	L	Moderate
Torres-Melero et al.[64]	2016	L	L	L	L	L	M[5]	L	Moderate
		Risk of bias 2 (RoB 2) for RCTs [107]							
		Pre-intervention	Post-intervention						Overall risk of bias
		Risk of bias due to randomization process	Risk of bias due to deviations from intended interventions		Risk of bias due to missing outcome data		Risk of bias in measurement of outcomes	Risk of bias in selection of the reported results	Low/ some concerns/ high
Fernandez et al. [58]	1996	SC[6]	SC[8]		SC[9]		SC[10]	L	Some concerns
Oliver et al. [60]	2012	SC[7]	SC[11]		SC[9]		SC[12]	L	Some concerns
Sdralis et al. [62]	2019	SC[6]	SC[13]		SC[9]		SC[12]	L	Some concerns
Silecchia et al. [63]	2006	SC[6]	SC[14]		SC[9]		SC[12]	L	Some concerns
Upadhyaya et al. [65]	2007	SC[7]	SC[15]		SC[9]		SC[12]	L	Some concerns
		NOS Assessment to assess quality of included cohort studies (out of a total of nine stars) [109]							
		Selection [a]				Comparability [b]		Outcome [c]			Overall quality
		A	B	C	D	E	F	G	H	I	Low/ moderate/ high NOS-Score (stars, n)
Brehant et al. [66]	2013	★	★	★	-[16]	★	★	★	★	★	High (8)
Huang et al. [67]	2021	-[17]	★	★	-[16]	★	★	★	★	★	Moderate (7)
Huh et al. [68]	2012	-[18]	★	★	-[16]	★	★	★	★	-[16]	Moderate (6)
Kim et al. [69]	2013	★	★	★	-[16]	★	★	★	★	-[16]	Moderate (7)
Marano et al. [70]	2016	★	★	★	-[16]	★	★	★	★	-[16]	Moderate (7)

Sieda et al. [71]	2015	★	★	★	-[16]	-[19]	-[19]	-[16]	★	-[16]	Low (4)

L = Low risk; M = Moderate risk; SC = Some concerns; NRS = Non-randomized controlled study; RCT = Randomized controlled trial; NOS = Newcastle-Ottawa-Quality Scale.

[a] A = Representativeness of the exposed cohort; B = Selection of the non-exposed cohort; C = Ascertainment of exposure; D= Demonstration that outcome of interest was not present at start of study.

[b] E = Comparability of cohort based on the design and analysis: Controlled for critical factor; F= Comparability of cohort based on the design and analysis: Controlled for additional factor.

[c] G = Assessment of outcome; H = Was the follow up long enough for outcomes to occur; I = Adequacy of follow up of cohorts.

[1] No air insufflation test of the anastomoses in the control group;

[2] Outcome data were not available for all or nearly all participants;

[3] No statement whether outcome assessors were aware of the intervention received by study participants;

[4] Bias in selection of reported result due to different subgroups;

[5] No statement whether outcome assessors were aware of the intervention received by study participants and whether methods for outcome assessment were comparable across intervention groups;

[6] No description of the methods of allocation concealment;

[7] No statement whether allocation sequence was concealed until participants were enrolled and assigned to interventions;

[8] No appropriate analysis used to estimate the effect of assignment to intervention; no statement whether participants were aware of their assigned interventions during the trial; no statement whether carers and people delivering interventions were aware of participants' assigned intervention during the trial;

[9] No evidence that the results were not biased by missing outcome data and missingness in the outcome could depend on its true value;

[10] No statement whether measurement or ascertainment of the outcome have differed between intervention groups or whether outcome assessors were aware of the intervention received; assessment of the outcome could have been influenced by the knowledge of intervention received;

[11] Carers and people delivering interventions were aware of participants' assigned intervention during the trial; no statement whether an appropriate analysis was used to estimate the effect of assignment to intervention;

[12] No statement whether outcome assessors were aware of the intervention received; assessment of the outcome could have been influenced by the knowledge of intervention received;

[13] No statement whether participants were aware of their assigned intervention during the trial; carers and people delivering interventions were aware of participants' assigned intervention during the trial;

[14] No statement whether participants were aware of their assigned intervention during the trial or whether carers and people delivering interventions were aware of participants' assigned intervention during the trial;

[15] Carers and people delivering interventions were aware of participants' assigned intervention during the trial;

[16] No statement;

[17] Just patients undergoing McKeown esophagectomy were included, other operative procedure for the same condition were not included;

[18] Patients with the same procedure but with a protective stoma were excluded;

[19] Did not controlled for any factor using multivariate analysis or regression methods.

5. Supplementary Table 5

Supplementary Table 5. Risk of Bias Assessment using the Systematic Review Centre for Laboratory Animal Experimentation (SYRCLE) tool for animal studies [109]

Supplementary Table 5.	Risk of Bias Assessment using the Systematic Review Centre for Laboratory Animal Experimentation (SYRCLE) tool for animal studies. **[110]**										
Author	**Year**	**Selection bias**			**Performance bias**		**Detection bias**		**Attribution bias**	**Reporting bias**	**Others**	**Overall judgment**
		SG	**BC**	**AC**	**RH**	**B**	**RAS**	**B**	**IOD**	**SOR**	**OSB**	
Chmelnik et al. [45]	2011	U	L	U	U	U	U	U	L	L	U	Some concerns
Garcia-Perez et al. [46]	2017	U	L	U	U	U	U	U	L	L	L	Some concerns
Holmer et al. [47]	2014	U	L	U	U	U	U	U	L	L	U	Some concerns
Nordentoft et al. [48]	2007	U	L	U	U	U	U	U	L	L	L	Some concerns
Ozel et al. [49]	2006	U	H[a]	U	U	U	U	U	L	L	U	High risk of bias
Pantelis et al. [50]	2010	U	L	U	U	U	U	U	L	L	L	Some concerns
Pommergaard et al. [51]	2014	U	L	U	U	U	U	U	L	L	L	Some concerns
Sabino et al. [52]	2014	U	L	U	U	U	U	U	L	L	L	Some concerns
Schreinemacher et al. [53]	2011	U	L	L	U	U	U	U	L	L	L	Some concerns
Stumpf et al. [54]	2009	U	L	U	U	U	U	U	L	L	H[b]	High risk of bias
Suárez-Grau et al. [55]	2016	U	H[a]	U	U	U	U	U	L	L	H[c]	High risk of bias
Vaneerdeweg et al. [56]	2000	U	L	U	U	U	U	U	L	L	L	Some concerns
Verhage et al. [57]	2012	U	L	L	U	U	U	U	L	L	H[d]	High risk of bias

L = Low risk of bias; H = High risk of bias; U = Unclear risk of bias; SG = Sequence generation; BC = Baseline characteristics; AC = Allocation concealment; RH = Random housing; B = Blinding; ROA = Random outcome assessment; IOD = Incomplete outcome data; SOR = Selective outcome reporting; OSB = Other source of bias.

[a] *Baseline characteristics were not matched.*

[b] *Unit of analysis errors: intervention to parts of the body within one participant.*
[c] Experimental unit not clear.
[d] Unrestricted grant was provided by Nycomed BV (The Netherlands).

6. Supplementary Table 6

Supplementary Table 6. Quality of Reporting Assessment according to the Animals in Research: Reporting In Vivo Experiments (ARRIVE) guidelines [110]

Supplementary Table 6. Quality of Reporting Assessment according to the Animals in Research: Reporting *In Vivo* Experiments (ARRIVE) guidelines. [111]

Author and Year	Item																				
	1	2	3	4	5	6	7	8	9	10	11	12	13	14	15	16	17	18	19	20	Total[a]
Chmelnik et al., 2011 [45]	Y	Y	Y	Y	N	Y	Y	Y	N	Y	N	Y	Y	N	Y	Y	Y	N	Y	N	**14**
Garcia-Perez et al., 2017 [46]	Y	Y	Y	N	Y	Y	Y	Y	N	N	N	Y	N	N	Y	N	Y	N	N	N	**10**
Holmer et al., 2014 [47]	Y	Y	Y	N	Y	Y	Y	Y	Y	Y	N	Y	Y	Y	Y	Y	Y	Y	Y	Y	**18**
Nordentoft et al., 2007 [48]	Y	Y	N	N	Y	N	Y	Y	Y	Y	N	Y	Y	N	Y	Y	Y	Y	Y	Y	**15**
Ozel et al., 2006 [49]	Y	Y	N	Y	N	Y	Y	N	N	N	N	Y	Y	N	Y	Y	N	Y	Y	N	**11**
Pantelis et al., 2010 [50]	Y	Y	Y	N	Y	Y	Y	Y	Y	Y	Y	Y	Y	N	Y	Y	Y	Y	Y	Y	**18**
Pommergaard et al., 2014 [51]	Y	Y	Y	Y	Y	Y	Y	Y	N	Y	N	Y	Y	Y	Y	Y	Y	Y	Y	Y	**18**
Sabino et al., 2014 [52]	N	Y	Y	N	Y	Y	Y	Y	Y	Y	N	Y	Y	Y	Y	Y	Y	Y	Y	N	**16**
Schreinemacher et al., 2011 [53]	Y	Y	Y	Y	Y	Y	Y	Y	N	Y	Y	Y	Y	Y	Y	Y	Y	Y	Y	N	**18**
Stumpf et al., 2009 [54]	Y	Y	Y	Y	Y	Y	Y	N	N	Y	Y	Y	Y	N	Y	Y	Y	N	Y	Y	**16**
Suárez-Grau et al., 2016 [55]	Y	N	Y	Y	Y	Y	Y	N	N	N	N	Y	Y	N	N	Y	Y	N	Y	Y	**12**
Vaneerdeweg et al., 2000 [56]	Y	Y	N	N	N	Y	Y	Y	N	Y	N	Y	Y	Y	Y	Y	Y	N	N	N	**12**
Verhage et al., 2012 [57]	N	Y	Y	Y	Y	Y	Y	Y	Y	Y	Y	Y	Y	Y	Y	Y	Y	Y	Y	Y	**19**

Y = Indicates adequate reporting; N = Indicates inadequate reporting.
[a] Number of adequately reported items (out of 20)

1 =	Title	"Provide as accurate and concise a description of the content of the article as possible."
2 =	Abstract	"Provide an accurate summary of the background, research objectives, including details of the species or strain of animal used, key methods, principal findings and conclusions of the study."
3 =	Background	"a. Include sufficient scientific background (including relevant references to previous work) to understand the motivation and context for the study and explain the experimental approach and rationale. b. Explain how and why the animal species and model being used can address the scientific objectives and, where appropriate, the study's relevance to human biology."
4 =	Objectives	"Clearly describe the primary and any secondary objectives of the study, or specific hypotheses being tested."
5 =	Ethical statement	"Indicate the nature of the ethical review permissions, relevant licences (e.g. Animal [Scientific Procedures] Act 1986), and national or institutional guidelines for the care and use of animals, that cover the research."

6 =	Study design	“For each experiment, give brief details of the study design including a. The number of experimental and control groups. b. Any steps taken to minimise the effects of subjective bias when allocating animals to treatment (e.g. randomisation procedure) and when assessing results (e.g. if done, describe who was blinded and when). c. The experimental unit (e.g. a single animal, group or cage of animals). A time-line diagram or flow chart can be useful to illustrate how complex study designs were carried out.”
7 =	Experimental procedures	“For each experiment and each experimental group, including controls, provide precise details of all procedures carried out. For example: a. How (e.g. drug formulation and dose, site and route of administration, anaesthesia and analgesia used [including monitoring], surgical procedure, method of euthanasia). Provide details of any specialist equipment used, including supplier(s). b. When (e.g. time of day) c. Where (e.g. home cage, laboratory, water maze). d. Why (e.g. rationale for choice of specific anaesthetic, route of administration, drug dose used.”
8 =	Experimental animals	“a. Provide details of the animals used, including species, strain, sex, developmental stage (e.g. mean or median age plus age range) and weight (e.g. mean or median weight plus weight range). b. Provide further relevant information such as the source of animals, international strain nomenclature, genetic modification status (e.g. knock-out or transgenic), genotype, health/immune status, drug or test naïve, previous procedures, etc.”
9 =	Housing and husbandry	“Provide details of: a. Housing (type of facility e.g. specific pathogen free [SPF]; type of cage or housing; bedding material; number of cage companions; tank shape and material etc. for fish). b. Husbandry conditions (e.g. breeding programme, light/dark cycle, temperature, quality of water etc for fish, type of food, access to food and water, environmental enrichment). c. Welfare-related assessments and interventions that were carried out prior to, during, or after the experiment.”
10 =	Sample size	“a. Specify the total number of animals used in each experiment, and the number of animals in each experimental group. b. Explain how the number of animals was arrived at. Provide details of any sample size calculation used. c. Indicate the number of independent replications of each experiment, if relevant.”
11 =	Allocating animals to experimental groups	“a. Give full details of how animals were allocated to experimental groups, including randomisation, or matching if done. b. Describe the order in which the animals in the different experimental groups were treated and assessed.”
12 =	Experimental outcomes	“Clearly define the primary and secondary experimental outcomes assessed (e.g. cell death, molecular markers, behavioural changes.”
13 =	Statistical methods	“a. Provide details of the statistical methods used for each analysis. b. Specify the unit of analysis for each dataset (e.g. single animal, group of animals, single neuron). c. Describe any methods used to assess whether the data met the assumptions of the statistical approach.”
14 =	Baseline data	“For each experimental group, report relevant characteristics and health status of animals (e.g. weight, microbiological status, and drug or test naïve) prior to treatment or testing. (This information can often be tabulated.”
15 =	Numbers analysed	“a. Report the number of animals in each group included in each analysis. Report absolute numbers (e.g. 10/20, not 50%). b. If any animals or data were not included in the analysis, explain why.”
16 =	Outcomes and estimation	“Report the results for each analysis carried out, with a measure of precision (e.g. standard error or confidence interval”
17 =	Adverse events	“a. Give details of all important adverse events in each experimental group. b. Describe any modifications to the experimental protocols made to reduce adverse events.”
18 =	Interpretation/ scientific implications	“a. Interpret the results, taking into account the study objectives and hypotheses, current theory and other relevant studies in the literature. b. Comment on the study limitations including any potential sources of bias, any limitations of the animal model, and the imprecision associated with the results. c. Describe any implications of your experimental methods or findings for the replacement, refinement or reduction (the 3Rs) of the use of animals in research.”

19 =	Generalizability/ translation	“Comment on whether, and how, the findings of this study are likely to translate to other species or systems, including any relevance to human biology.”
20 =	Funding	“List all funding sources (including grant number) and the role of the funder(s) in the study.”

VIII Appendix

1. List of publications and conference proceedings

1.1 List of Publications

1.1.1 Complete List of Publications

1. **Cira, K.**; Weber, M.-C.; Wilhelm, D.; Friess, H.; Reischl, S.; Neumann, P.-A. The Effect of Anti-Tumor Necrosis Factor-Alpha Therapy within 12 Weeks Prior to Surgery on Postoperative Complications in Inflammatory Bowel Disease: A Systematic Review and Meta-Analysis. J. Clin. Med. 2022, 11, 6884. https://doi.org/10.3390/jcm11236884

2. **Cira K**, Janett SN, Friess H, Neumann P-A. Neue Anastomosentechniken in Der Chirurgie Bei Morbus Crohn. Gastro-News (2023) 10(1):39-43. doi: 10.1007/s15036-023-3189-z. 4. Cira K, Janett SN, Friess H, Neumann P-A. Neue Anastomosentechniken in Der Chirurgie Bei Morbus Crohn. Gastro-News (2023) 10(1):39-43. doi: 10.1007/s15036-023-3189-z.

1.1.2 Thesis-related publications

1. **Cira K**, Stocker F, Reischl S, Obermeier A, Friess H, Burgkart R and Neumann P (2022) Coating of Intestinal Anastomoses for Prevention of Postoperative Leakage: A Systematic Review and Meta-Analysis. Front. Surg. 9:882173. doi: 10.3389/fsurg.2022.882173

2. **Cira, K**., Janett, S.N., Micheler, C. et al. The mesenteric entry site as a potential weak point in gastrointestinal anastomoses – findings from an *ex-vivo* biomechanical analysis. Langenbecks Arch Surg 409, 124 (2024). https://doi.org/10.1007/s00423-024-03318-8

1.2 List of thesis-related conference proceedings

1. **Cira K**, Micheler C, Janett SN, Friess H, Obermeier A, Burgkart RH, et al. 1282 Development of an Innovative Ex-Vivo Model for the Evaluation of Stability and Pressure Resistance of Gastrointestinal Anastomoses. Gastroenterology (2023) 164(6):S-1518-S-9. doi: 10.1016/S0016-5085(23)04611-5. *Digestive Disease Week 2023*

2. **Cira K**, Janett SN, Micheler C, Obermeier A, Burgkart RH, Friess H and Neumann P. Usage of an Innovative Ex-Vivo Model for Evaluation of Anastomotic Leakage Location in Handsewn End-to-End Anastomoses. *Chirurgische Forschungstage 2023*

2. Published material and reprint permission

Figure 1 and **Figure 2** were previously published in: **Cira K**, Janett SN, Friess H, Neumann P-A. Neue Anastomosentechniken in Der Chirurgie Bei Morbus Crohn. Gastro-News (2023) 10(1):39-43. doi: 10.1007/s15036-023-3189-z. 4. No written electronic form for permission to reproduce is needed, as Springer Medizin Verlag GmbH states:

> "Ownership of copyright in original research articles remains with the Author, and provided that, when reproducing the contribution or extracts from it or from the Supplementary Information, the Author acknowledges first and reference publication in the Journal, the Author retains the following non-exclusive rights:
>
> To reproduce the contribution in whole or in part in any printed volume (book or thesis) of which they are the author(s). The author and any academic institution, where they work, at the time may reproduce the contribution for the purpose of course teaching. To reuse figures or tables created by the Author and contained in the Contribution in oral presentations and other works created by them. To post a copy of the contribution as accepted for publication after peer review (in locked Word processing file, of a PDF version thereof) on the Author's own web site, or the Author's institutional repository, or the Author's funding body's archive, six months after publication of the printed or online edition of the Journal, provided that they also link to the contribution on the publisher's website.
>
> Authors wishing to use the published version of their article for promotional use or on a web site must request in the normal way."
>
> (*https://s100.copyright.com/AppDispatchServlet?title=Neue%20Anastomosentechniken%20in%20der%20Chirurgie%20bei%20Morbus%20Crohn&author=Kamacay%20Cira%20et%20al&contentID=10.1007%2Fs15036-023-3189-z&copyright=Springer%20Medizin%20Verlag%20GmbH%2C%20ein%20Teil%20von*

%20Springer%20Nature&publication=1869-1005&publicationDate=2023-02-16&publisherName=SpringerNature&orderBeanReset=true; webpage last accessed January 31, 2024)

Figure 5, **Figure 6**, **Figure 7**, **Figure 8**, **Figure 9**, **Figure 10**, **Figure 11**, **Figure 13** ,**Figure 14**, **Figure 15**, **Figure 16**, **Figure 17**, **Figure 29**, **Figure 30**, **Figure 31**, **Figure 32**, **Figure 33**, **Figure 34**, **Figure 35**, **Figure 36**, **Figure 37**, **Figure 38**, **Figure 39**, **Figure 40**, **Figure 41**, **Figure 42**, **Figure 43**, **Figure 44**, **Figure 45**, **Figure 46**, **Figure 47**, **Figure 48**, **Table 15**, **Table 16**, **Table 17**, **Table 18**, **Table 19**, **Table 20**, **Table 21**, **Table 22**, and **Supplementary Table 3** were previously published in: **Cira, K.**, Janett, S.N., Micheler, C. et al. The mesenteric entry site as a potential weak point in gastrointestinal anastomoses – findings from an ex-vivo biomechanical analysis. Langenbecks Arch Surg 409, 124 (2024). https://doi.org/10.1007/s00423-024-03318-8. No written electronic form for permission to reproduce is needed, as Springer Nature Limited states:

" Authors have the right to reuse their article's Version of Record, in whole or in part, in their own thesis. Additionally, they may reproduce and make available their thesis, including Springer Nature content, as required by their awarding academic institution. Authors must properly cite the published article in their thesis according to current citation standards. Material from: 'AUTHOR, TITLE, JOURNAL TITLE, published [YEAR], [publisher - as it appears on our copyright page] *(*https://www.springer.com/gp/rights-permissions/obtaining-permissions/882*; webpage last accessed April 4, 2024)*

Figure 18, **Figure 19**, **Figure 20**, **Figure 21**, **Figure 22**, **Figure 23**, **Table 2**, **Table 3**, **Table 4**, **Table 5**, **Table 6**, **Table 7**, **Table 8**, **Supplementary Table 1**, and **Supplementary Table 4** were previously published in: **Cira K**, Stocker F, Reischl S, Obermeier A, Friess H, Burgkart R and Neumann P (2022) Coating of Intestinal Anastomoses for Prevention of Postoperative Leakage: A Systematic Review and Meta-Analysis. Front. Surg. 9:882173. doi:

10.3389/fsurg.2022.882173. No written electronic form for permission to reproduce is needed, as Frontiers Media S.A. states:

> "Copyright © 2022 Cira, Stocker, Reischl, Obermeier, Friess, Burgkart and Neumann. This is an open-access article distributed under the terms of the Creative Commons Attribution License (CC BY). The use, distribution or reproduction in other forums is permitted, provided the original author(s) and the copyright owner(s) are credited and that the original publication in this journal is cited, in accordance with accepted academic practice. No use, distribution or reproduction is permitted which does not comply with these terms."

Figure 18, **Figure 19**, **Figure 20**, **Figure 21**, **Figure 22**, **Figure 23**, **Table 2**, **Table 3**, **Table 4**, **Table 5**, **Table 6**, **Table 7**, **Table 8**, **Supplementary Table 1**, and **Supplementary Table 4** are adapted from "**Cira K**, Stocker F, Reischl S, Obermeier A, Friess H, Burgkart R and Neumann P (2022) Coating of Intestinal Anastomoses for Prevention of Postoperative Leakage: A Systematic Review and Meta-Analysis. Front. Surg. 9:882173. doi: 10.3389/fsurg.2022.882173. © 2022 Cira, Stocker, Reischl, Obermeier, Friess, Burgkart and Neumann. This work is licensed under a Creative Commons Attribution (CC BY) https://creativecommons.org/licenses/by/4.0/ International License (CC BY 4.0)" without modifications.

3. Acknowledgements

With sincere gratitude and profound respect, I express my appreciation to those who have played a pivotal role in the successful completion of my thesis. This achievement reflects collaborative efforts fueled by the steadfast support and commitment of many individuals and groups. I extend my heartfelt thanks to:

Univ.-Prof. Dr. H. Friess, my esteemed doctoral advisor and a respected authority in surgical discipline. His unwavering support, encouragement, and trust in my academic pursuits have been pivotal. Moreover, his role as my supervisor at Klinikum rechts der Isar has greatly contributed to my professional and academic growth.

Prof. Dr. R. Burgkart, who has not only been an invaluable mentor but also a driving force behind the refinement and advancement of my research. His dedicated research team, Dr. Obermeier and C. Micheler, along with his engaging and insightful contributions, has been instrumental. Their expertise and mentorship have greatly enhanced the quality of my work.

PD Dr. P-A. Neumann, a longstanding supervisor, mentor, and very good friend, has been invaluable. His erudition, expert guidance, and inspirational direction have profoundly influenced the trajectory of my scholarly journey. In 2019, Dr. Neumann graciously welcomed me into his research group, granting me the autonomy to work independently and providing me the space to grow. Countless projects and opportunities, including my position as a surgical resident at the Klinikum rechts der Isar (Technical University of Munich), owe their inception to his guidance. Our journey culminated in the formation of a formidable partnership and genuine friendship.

S. N. Janett, a valued collaborator and friend, I want to express my sincere gratitude for your unwavering dedication and shared sense of purpose. Our joint efforts on this academic journey have not only significantly contributed to this research but have also created a collection of memorable and often delightful moments that I will always cherish.

Dr. S. Reischl, my mentor, has been an invaluable source of guidance and expertise. I want to express my special appreciation for his consistent support and mentorship.

Prof. Dr. Dr. h.c. K. A. Lamers significantly influenced my academic and professional journey with consistent encouragement, mentorship, and support in forging valuable connections. Beyond his roles in politics and law, his impact has been a steady presence since my youth, shaping my path. His support and guidance have played a crucial role in my personal development. **Monika Becker**, through her insightful guidance, has imparted to me not only the essential skill of assertiveness but has also emphasized the particular significance of navigating and succeeding as a strong woman in academia. I sincerely and profoundly appreciate her counselling and support.

I want to express my deep gratitude to my family - my beloved brother, **Uçkunbay Çıra**, mother, **Leyla Çıra**, father, **Durmuş Çıra**, grandparents **Roswitha** and **Ismail Çıra**, as well as **Şadiye** and **Hüseyin Aksoy**, along with my **aunts** and **uncles**. Your support has been my anchor, inspiring and encouraging me to strive for academic excellence with love and steadfast encouragement.

Finally, I acknowledge the financial support of the Bavarian Research Association in carrying out this research.

4. Funding

The research conducted in this thesis and its associated publications was generously supported by the Bavarian Research Foundation under Grant No. AZ-1508-21. We express our gratitude for their financial assistance and commitment to advancing scientific inquiry.

The publication of "**Cira K**, Janett SN, Micheler C, Obermeier A, Burgkart RH, Friess H and Neumann P (2024) The Mesenteric Entry Site as a Potential Weak Point in Gastrointestinal Anastomoses – Findings from an Ex-Vivo Biomechanical Analysis. Accepted in Langenbeck's Arch. Surg. 04/2024." was made possible through funding provided by the DEAL agreement with the publishing group Springer Nature of the Technical University of Munich. We appreciate their support in making this research accessible and contributing to the dissemination of knowledge.

IX Bibliography

[1] K. Cira *et al.*, "Coating of Intestinal Anastomoses for Prevention of Postoperative Leakage: A Systematic Review and Meta-Analysis," (in eng), *Front Surg,* vol. 9, p. 882173, 2022, doi: 10.3389/fsurg.2022.882173.

[2] K. Cira *et al.*, "The mesenteric entry site as a potential weak point in gastrointestinal anastomoses - findings from an ex-vivo biomechanical analysis," (in eng), *Langenbecks Arch Surg,* vol. 409, no. 1, p. 124, Apr 13 2024, doi: 10.1007/s00423-024-03318-8.

[3] R. M. Kirk and M. C. Winslet, *Essential general surgical operations*, 2nd ed. ed. Edinburgh New York: Elsevier/Churchill Livingstone, 2007.

[4] C. Chen, "The Art of Bowel Anastomosis," *Scandinavian Journal of Surgery,* vol. 101, no. 4, pp. 238-240, 2012/12/01 2012, doi: 10.1177/145749691210100403.

[5] N. Senn, "Enterorrhaphy: its history, technique and present status," *The Journal of the American Medical Association,* pp. 21: 215–235, 1893.

[6] K. J. Hardy, "A view of the development of intestinal suture. Part II. Principles and techniques," (in eng), *Aust N Z J Surg,* vol. 60, no. 5, pp. 377-84, May 1990, doi: 10.1111/j.1445-2197.1990.tb07388.x.

[7] "Classic articles in colonic and rectal surgery. Nicholas Senn 1844-1908. Enterorrhaphy; its history, technique and present status. III--Recent methods," (in eng), *Dis Colon Rectum,* vol. 28, no. 3, pp. 204-14, Mar 1985.

[8] M. M. Ravitch, "Development of intestinal anastomotic devices," (in eng), *South Med J,* vol. 75, no. 12, pp. 1520-4, Dec 1982, doi: 10.1097/00007611-198212000-00016.

[9] M. L. Corman, E. D. Prager, T. G. Hardy, Jr., and M. P. Bubrick, "Comparison of the Valtrac biofragmentable anastomosis ring with conventional suture and stapled anastomosis in colon surgery. Results of a prospective, randomized clinical trial," (in eng), *Dis Colon Rectum,* vol. 32, no. 3, pp. 183-7, Mar 1989, doi: 10.1007/bf02554523.

[10] D. L. Dyess, P. W. Curreri, and J. J. Ferrara, "A new technique for sutureless intestinal anastomosis. A prospective, randomized, clinical trial," (in eng), *Am Surg,* vol. 56, no. 2, pp. 71-5, Feb 1990.

[11] T. G. Hardy, Jr. *et al.*, "Initial clinical experience with a biofragmentable ring for sutureless bowel anastomosis," (in eng), *Dis Colon Rectum,* vol. 30, no. 1, pp. 55-61, Jan 1987, doi: 10.1007/bf02556926.

[12] T. G. Hardy, Jr., W. G. Pace, J. W. Maney, A. R. Katz, and A. L. Kaganov, "A biofragmentable ring for sutureless bowel anastomosis. An experimental study," (in eng), *Dis Colon Rectum,* vol. 28, no. 7, pp. 484-90, Jul 1985, doi: 10.1007/bf02554090.

[13] O. Kaidar-Person, R. J. Rosenthal, S. D. Wexner, S. Szomstein, and B. Person, "Compression anastomosis: history and clinical considerations," *The American Journal of Surgery,* vol. 195, no. 6, pp. 818-826, 2008, doi: 10.1016/j.amjsurg.2007.10.006.

[14] M. P. Bubrick, M. L. Corman, C. J. Cahill, T. G. Hardy, Jr., F. C. Nance, and C. H. Shatney, "Prospective, randomized trial of the biofragmentable anastomosis ring. The BAR Investigational Group," (in eng), *Am J Surg,* vol. 161, no. 1, pp. 136-42; discussion 142-3, Jan 1991, doi: 10.1016/0002-9610(91)90374-m.

[15] E. P. Weledji, "Is patient factor more important than surgeon-related factor in sepsis prevention in colorectal surgery?," *International Journal of Surgery Open,* vol. 12, pp. 29-36, 2018/01/01/ 2018, doi: https://doi.org/10.1016/j.ijso.2018.07.001.

[16] M. Sartelli, E. A. Griffiths, and M. Nestori, "The challenge of post-operative peritonitis after gastrointestinal surgery," (in eng), *Updates Surg,* vol. 67, no. 4, pp. 373-81, Dec 2015, doi: 10.1007/s13304-015-0324-1.

[17] T. Akasu, M. Takawa, S. Yamamoto, T. Yamaguchi, S. Fujita, and Y. Moriya, "Risk factors for anastomotic leakage following intersphincteric resection for very low rectal adenocarcinoma," (in eng), *J Gastrointest Surg,* vol. 14, no. 1, pp. 104-11, Jan 2010, doi: 10.1007/s11605-009-1067-4.

[18] F. G. Bader, M. Schröder, P. Kujath, E. Muhl, H. P. Bruch, and C. Eckmann, "Diffuse postoperative peritonitis -- value of diagnostic parameters and impact of early indication for relaparotomy," (in eng), *Eur J Med Res,* vol. 14, no. 11, pp. 491-6, Nov 3 2009, doi: 10.1186/2047-783x-14-11-491.

[19] A. Doeksen, P. J. Tanis, B. C. Vrouenraets, J. A. Gooszen, J. J. van Lanschot, and W. F. van Tets, "Outcome of rectal cancer surgery after the introduction of preoperative radiotherapy in a low-volume hospital," (in eng), *J Gastrointest Cancer,* vol. 38, no. 2-4, pp. 63-70, 2007, doi: 10.1007/s12029-008-9018-y.

[20] E. R. C. Hagens, M. A. Reijntjes, M. C. J. Anderegg, W. J. Eshuis, M. I. van Berge Henegouwen, and S. S. Gisbertz, "Risk Factors and Consequences of Anastomotic Leakage After Esophagectomy for Cancer," *The Annals of Thoracic Surgery,* vol. 112, no. 1, pp. 255-263, 2021/07/01/ 2021, doi: 10.1016/j.athoracsur.2020.08.022.

[21] C. Y. Kang *et al.*, "Risk factors for anastomotic leakage after anterior resection for rectal cancer," (in eng), *JAMA Surg,* vol. 148, no. 1, pp. 65-71, Jan 2013, doi: 10.1001/2013.jamasurg.2.

[22] M. F. J. Seesing *et al.*, "A Propensity Score Matched Analysis of Open Versus Minimally Invasive Transthoracic Esophagectomy in the Netherlands," (in eng), *Ann Surg,* vol. 266, no. 5, pp. 839-846, Nov 2017, doi: 10.1097/sla.0000000000002393.

[23] T. Akasu, M. Takawa, S. Yamamoto, T. Yamaguchi, S. Fujita, and Y. Moriya, "Risk Factors for Anastomotic Leakage Following Intersphincteric Resection for Very Low Rectal Adenocarcinoma," *Journal of Gastrointestinal Surgery,* vol. 14, no. 1, pp. 104-111, 2010/01/01 2010, doi: 10.1007/s11605-009-1067-4.

[24] K. Lindner, M. Fritz, C. Haane, N. Senninger, D. Palmes, and R. Hummel, "Postoperative complications do not affect long-term outcome in esophageal cancer patients," (in eng), *World J Surg,* vol. 38, no. 10, pp. 2652-61, Oct 2014, doi: 10.1007/s00268-014-2590-3.

[25] H. M. Schmidt *et al.*, "Defining Benchmarks for Transthoracic Esophagectomy: A Multicenter Analysis of Total Minimally Invasive Esophagectomy in Low Risk Patients," (in eng), *Ann Surg,* vol. 266, no. 5, pp. 814-821, Nov 2017, doi: 10.1097/sla.0000000000002445.

[26] F. van Workum *et al.*, "Improved Functional Results After Minimally Invasive Esophagectomy: Intrathoracic Versus Cervical Anastomosis," (in eng), *Ann Thorac Surg,* vol. 103, no. 1, pp. 267-273, Jan 2017, doi: 10.1016/j.athoracsur.2016.07.010.

[27] B. Struecker *et al.*, "Evaluation of Anastomotic Leak after Esophagectomy for Esophageal Cancer: Typical Time Point of Occurrence, Mode of Diagnosis, Value of Routine Radiocontrast Agent Studies and Therapeutic Options," (in eng), *Dig Surg,* vol. 35, no. 5, pp. 419-426, 2018, doi: 10.1159/000480357.

[28] E. R. C. Hagens, M. A. Reijntjes, M. C. J. Anderegg, W. J. Eshuis, M. I. van Berge Henegouwen, and S. S. Gisbertz, "Risk Factors and Consequences of Anastomotic Leakage After Esophagectomy for Cancer," (in eng), *Ann Thorac Surg,* vol. 112, no. 1, pp. 255-263, Jul 2021, doi: 10.1016/j.athoracsur.2020.08.022.

[29] M. Watanabe *et al.*, "Total gastrectomy risk model: data from 20,011 Japanese patients in a nationwide internet-based database," (in eng), *Ann Surg,* vol. 260, no. 6, pp. 1034-9, Dec 2014, doi: 10.1097/sla.0000000000000781.

[30] P. Michelet *et al.*, "Perioperative Risk Factors for Anastomotic Leakage After Esophagectomy: Influence of Thoracic Epidural Analgesia," *Chest,* vol. 128, no. 5, pp. 3461-3466, 2005/11/01/ 2005, doi: https://doi.org/10.1378/chest.128.5.3461.

[31] M. Thornton *et al.*, "Management and outcome of colorectal anastomotic leaks," *International Journal of Colorectal Disease,* vol. 26, no. 3, pp. 313-320, 2011/03/01 2011, doi: 10.1007/s00384-010-1094-3.

[32] B. P. Whooley, S. Law, A. Alexandrou, S. C. Murthy, and J. Wong, "Critical appraisal of the significance of intrathoracic anastomotic leakage after esophagectomy for cancer," (in eng), *Am J Surg,* vol. 181, no. 3, pp. 198-203, Mar 2001, doi: 10.1016/s0002-9610(01)00559-1.

[33] A. Mirnezami, R. Mirnezami, K. Chandrakumaran, K. Sasapu, P. Sagar, and P. Finan, "Increased local recurrence and reduced survival from colorectal cancer following anastomotic leak: systematic review and meta-analysis," (in eng), *Ann Surg,* vol. 253, no. 5, pp. 890-9, May 2011, doi: 10.1097/SLA.0b013e3182128929.

[34] P. M. Krarup, A. Nordholm-Carstensen, L. N. Jorgensen, and H. Harling, "Anastomotic leak increases distant recurrence and long-term mortality after curative resection for colonic cancer: a nationwide cohort study," (in eng), *Ann Surg,* vol. 259, no. 5, pp. 930-8, May 2014, doi: 10.1097/SLA.0b013e3182a6f2fc.

[35] J. Hammond, S. Lim, Y. Wan, X. Gao, and A. Patkar, "The burden of gastrointestinal anastomotic leaks: an evaluation of clinical and economic outcomes," (in eng), *J Gastrointest Surg,* vol. 18, no. 6, pp. 1176-85, Jun 2014, doi: 10.1007/s11605-014-2506-4.

[36] K. L. Guyton, N. H. Hyman, and J. C. Alverdy, "Prevention of Perioperative Anastomotic Healing Complications: Anastomotic Stricture and Anastomotic Leak," (in eng), *Adv Surg,* vol. 50, no. 1, pp. 129-41, Sep 2016, doi: 10.1016/j.yasu.2016.03.011.

[37] P. A. Neumann *et al.*, "Assessment of MMP-2/-9 expression by fluorescence endoscopy for evaluation of anastomotic healing in a murine model of anastomotic leakage," (in eng), *PLoS One,* vol. 13, no. 3, p. e0194249, 2018, doi: 10.1371/journal.pone.0194249.

[38] A. Anders, T. Bodemann, U. Baer, K. J. Bauknecht, and J. U. Lawerenz, "Are fibrin adhesive and collagen fleece additional protective measures for colon anastomoses?," *Langenbecks Archiv fur Chirurgie,* Article vol. Suppl. 1981, pp. 175-180, 1981, doi: 10.1007/978-3-642-68016-8_35.

[39] J. Scheele, J. Herzog, and E. Muehe, "Fibrin glue protection of digestive anastomoses," *Zentralblatt fur Chirurgie,* Article vol. 103, no. 20, pp. 1325-1336, 1978. [Online]. Available: https://www.scopus.com/inward/record.uri?eid=2-s2.0-0018210392&partnerID=40&md5=b4ccf8f90f068a390b7314bca0ba0cba.

[40] V. B. Aleksandrov, L. L. Kapuller, A. M. Poliakova, V. I. Baranchikov, and M. Slavin Iu, "[The reaction of intestinal wall tissue to several types of cyacrin glue and its combined use with mechanical tantalum suture in anterior resection of the rectum (experimental study)]," (in rus), *Eksp Khir Anesteziol,* vol. 16, no. 2, pp. 46-50, Mar-Apr 1971. Reaktsiia tkaneĭ stenki kishki na nekotorye vidy tsiakrinovogo kleia i na kombinirovannoe ego primenie s mekhanicheskim tantalovym shvom pri peredneĭ reazektsii priamoĭ kishki (ėksperimental'noe issledovanie.

[41] A. A. Vishnevskiĭ, Jr., "[An instrument for intestinal anastomosis with the use of glue]," (in rus), *Eksp Khir Anesteziol,* vol. 11, no. 5, pp. 21-2, Sep-Oct 1966. Instrument dlia nalozheniia kishechnogo anastomoza pri pomoshchi kleia.

[42] J. A. Rusca, G. H. Bornside, and I. Cohn, Jr., "Everting versus inverting gastrointestinal anastomoses: bacterial leakage and anastomotic disruption," (in eng), *Annals of surgery,* vol. 169, no. 5, pp. 727-735, 1969, doi: 10.1097/00000658-196905000-00010.

[43] A. Toro, M. Mannino, G. Reale, and I. Di Carlo, "TachoSil use in abdominal surgery: a review," (in eng), *J Blood Med,* vol. 2, pp. 31-6, 2011, doi: 10.2147/jbm.S13061.

[44] W. D. Spotnitz, "Fibrin Sealant: The Only Approved Hemostat, Sealant, and Adhesive-a Laboratory and Clinical Perspective," (in eng), *ISRN surgery,* vol. 2014, pp. 203943-203943, 2014, doi: 10.1155/2014/203943.

[45] M. Chmelnik, L. Lasch, S. Weih, E. Wink, P. Romero, and S. Holland-Cunz, "Anastomotic sealing with a fibrin-coated collagen patch in small-diameter bowel," (in eng), *Langenbecks Arch Surg,* vol. 396, no. 5, pp. 685-91, Jun 2011, doi: 10.1007/s00423-011-0750-6.

[46] R. Garcia-Perez *et al.*, "Histopathological and Immunohistochemical Analysis of the Use of Collagen Dressing as a Reinforcement of Esophagic Anastomosis in a Rat Experimental Model," (in eng spa), *Cir Esp,* vol. 95, no. 10, pp. 588-593, Dec 2017, doi: 10.1016/j.ciresp.2017.08.008. Análisis histopatológico e inmunohistoquímico del uso del apósito de colágeno como refuerzo de anastomosis esofágica en un modelo experimental en rata.

[47] C. Holmer, C. Praechter, L. Mecklenburg, M. Heimesaat, H. Rieger, and U. Pohlen, "Anastomotic stability and wound healing of colorectal anastomoses sealed and sutured with a collagen fleece in a rat peritonitis model," (in eng), *Asian J Surg,* vol. 37, no. 1, pp. 35-45, Jan 2014, doi: 10.1016/j.asjsur.2013.07.008.

[48] T. Nordentoft, J. Rømer, and M. Sørensen, "Sealing of gastrointestinal anastomoses with a fibrin glue-coated collagen patch: a safety study," (in eng), *J Invest Surg,* vol. 20, no. 6, pp. 363-9, Nov-Dec 2007, doi: 10.1080/08941930701772173.

[49] S. K. Ozel, A. Kazez, and N. Akpolat, "Does a fibrin-collagen patch support early anastomotic healing in the colon? An experimental study," (in eng), *Tech Coloproctol,* vol. 10, no. 3, pp. 233-6, Oct 2006, doi: 10.1007/s10151-006-0285-y.

[50] D. Pantelis, A. Beissel, P. Kahl, S. Wehner, T. O. Vilz, and J. C. Kalff, "The effect of sealing with a fixed combination of collagen matrix-bound coagulation factors on the healing of colonic anastomoses in experimental high-risk mice models," (in eng), *Langenbecks Arch Surg,* vol. 395, no. 8, pp. 1039-48, Nov 2010, doi: 10.1007/s00423-010-0703-5.

[51] H. C. Pommergaard, M. P. Achiam, J. Burcharth, and J. Rosenberg, "Decreased leakage rate of colonic anastomoses by tachosil coating: an experimental study," (in eng), *Int Surg,* vol. 99, no. 4, pp. 359-63, Jul-Aug 2014, doi: 10.9738/intsurg-d-13-00093.1.

[52] F. D. Sabino, C. F. F. Campos, C. E. R. Caetano, M. N. S. Trotte, A. V. Oliveira, and R. G. Marques, "Effects of TachoSil and 5-fluorouracil on colonic anastomotic healing," (in English), *J. Surg. Res.,* Article vol. 192, no. 2, pp. 375-382, Dec 2014, doi: 10.1016/j.jss.2014.05.067.

[53] M. H. Schreinemacher, J. G. Bloemen, S. J. van der Heijden, M. J. Gijbels, C. H. Dejong, and N. D. Bouvy, "Collagen fleeces do not improve colonic anastomotic strength but increase bowel obstructions in an experimental rat model," (in eng), *Int J Colorectal Dis,* vol. 26, no. 6, pp. 729-35, Jun 2011, doi: 10.1007/s00384-011-1158-z.

[54] M. Stumpf, K. Junge, R. Rosch, C. Krones, U. Klinge, and V. Schumpelick, "Suture-free small bowel anastomoses using collagen fleece covered with fibrin glue in pigs," (in eng), *J Invest Surg,* vol. 22, no. 2, pp. 138-47, Mar-Apr 2009, doi: 10.1080/08941930802713001.

[55] J. M. Suárez-Grau *et al.*, "Fibrinogen-thrombin collagen patch reinforcement of high-risk colonic anastomoses in rats," (in eng), *World J Gastrointest Surg,* vol. 8, no. 9, pp. 627-633, Sep 27 2016, doi: 10.4240/wjgs.v8.i9.627.

[56] W. Vaneerdeweg, J. M. Hendriks, P. R. Lauwers, M. Ieven, and E. J. Eyskens, "Effect of gentamicin-containing sponges on the healing of colonic anastomoses in a rat model of peritonitis," (in eng), *Eur J Surg,* vol. 166, no. 12, pp. 959-62, Dec 2000, doi: 10.1080/110241500447137.

[57] R. J. Verhage, A. Ruiz, A. Verheem, R. Goldschmeding, I. H. Borel Rinkes, and R. van Hillegersberg, "Fibrin-thrombin coated sealant increases strength of esophagogastric anastomoses in a rat model," (in eng), *J Surg Res,* vol. 176, no. 2, pp. e57-63, Aug 2012, doi: 10.1016/j.jss.2011.12.028.

[58] L. Fernandez Fernandez, E. Tejero, and A. Tieso, "Randomized trial of fibrin glue to seal mechanical oesophagojejunal anastomosis," *British Journal of Surgery,* Article vol. 83, no. 1, pp. 40-41, 1996, doi: 10.1002/bjs.1800830111.

[59] C. D. Liu, G. J. Glantz, and E. H. Livingston, "Fibrin glue as a sealant for high-risk anastomosis in surgery for morbid obesity," (in eng), *Obes Surg,* vol. 13, no. 1, pp. 45-8, Feb 2003, doi: 10.1381/096089203321136575.

[60] J. L. Oliver *et al.*, "Use of fibrin based biological adhesives in the prevention of anastomotic leaks in the high risk digestive tract: preliminary results of the multicentre, prospective, randomised, controlled, and simple blind phase IV clinical trial: Protissucol001," *Cirugia Espanola,* vol. 90, no. 10, pp. 647-655, Dec 2012, doi: 10.1016/j.ciresp.2012.05.007.

[61] J. A. Saldaña-Cortés *et al.*, "Role of fibrin glue in the prevention of cervical leakage and strictures after esophageal reconstruction of caustic injury," (in eng), *World J Surg,* vol. 33, no. 5, pp. 986-93, May 2009, doi: 10.1007/s00268-009-9949-x.

[62] E. Sdralis *et al.*, "Reinforcement of intrathoracic oesophago-gastric anastomosis with fibrin sealant (Tisseel®) in oesophagectomy for cancer: A prospective comparative study," (in eng), *Am J Surg,* vol. 219, no. 1, pp. 123-128, Jan 2020, doi: 10.1016/j.amjsurg.2019.06.013.

[63] G. Silecchia *et al.*, "Clinical evaluation of fibrin glue in the prevention of anastomotic leak and internal hernia after laparoscopic gastric bypass: Preliminary results of a prospective, randomized multicenter trial," *Obesity Surgery,* Article vol. 16, no. 2, pp. 125-131, 2006, doi: 10.1381/096089206775565249.

[64] J. Torres-Melero, J. J. Motos-Micó, M. Lorenzo-Liñán, Á. Morales-González, and R. Rosado-Cobián, "[Use of absorbable fibrin sealant patch to strengthen the gastrointestinal anastomosis performed on patients with peritoneal carcinomatosis treated with intention to cure by debulking surgery and intraoperative hyperthermic intraperitoneal chemotherapy]," (in spa), *Cir Cir,* vol. 84, no. 2, pp. 102-8, Mar-Apr 2016, doi: 10.1016/j.circir.2015.09.005. Aplicación de sellante tisular como refuerzo de las anastomosis digestivas realizadas en pacientes con carcinomatosis peritoneal tratados con intención curativa mediante procedimiento quirúrgico de citorreducción y quimioterapia intraperitoneal intraoperatoria hipertérmica.

[65] V. D. Upadhyaya *et al.*, "Role of Fibrin Glue as a Sealant to Esophageal Anastomosis in Cases of Congenital Esophageal Atresia with Tracheoesophageal Fistula," *World Journal of Surgery,* vol. 31, no. 12, pp. 2412-2415, 2007/12/01 2007, doi: 10.1007/s00268-007-9244-7.

[66] O. Brehant, C. Sabbagh, P. Lehert, A. Dhahri, L. Rebibo, and J. M. Regimbeau, "The gentamicin-collagen sponge for surgical site infection prophylaxis in colorectal surgery: a prospective case-matched study of 606 cases," (in eng), *Int J Colorectal Dis,* vol. 28, no. 1, pp. 119-25, Jan 2013, doi: 10.1007/s00384-012-1557-9.

[67] Y. Huang *et al.*, "Evaluation of Fibrin Sealant in Prevention of Cervical Anastomotic Leakage After McKeown Esophagectomy: A Single-Center, Retrospective Study," *Annals of Surgical Oncology,* Article vol. 28, no. 11, pp. 6390-6397, 2021, doi: 10.1245/s10434-021-09877-0.

[68] J. W. Huh, H. R. Kim, and Y. J. Kim, "Anastomotic leakage after laparoscopic resection of rectal cancer: the impact of fibrin glue," (in eng), *Am J Surg,* vol. 199, no. 4, pp. 435-41, Apr 2010, doi: 10.1016/j.amjsurg.2009.01.018.

[69] H. J. Kim, J. W. Huh, H. R. Kim, and Y. J. Kim, "Oncologic impact of anastomotic leakage in rectal cancer surgery according to the use of fibrin glue: case-control study using propensity score matching method," (in eng), *Am J Surg,* vol. 207, no. 6, pp. 840-6, Jun 2014, doi: 10.1016/j.amjsurg.2013.07.047.

[70] L. Marano and N. Di Martino, "Efficacy of Human Fibrinogen-Thrombin Patch (TachoSil) Clinical Application in Upper Gastrointestinal Cancer Surgery," (in eng), *J*

Invest Surg, vol. 29, no. 6, pp. 352-358, Dec 2016, doi: 10.1080/08941939.2016.1181229.

[71] B. Sieda and O. Gharib, "Comparative study of single-layer anastomosis in high-risk colonic anastomosis versus single layer reinforced using fibrin glue," *The Egyptian Journal of Surgery,* vol. 34, p. 215, 01/01 2015, doi: 10.4103/1110-1121.167380.

[72] P. B. Dobrin, "Mechanical properties of arteries," (in eng), *Physiol Rev,* vol. 58, no. 2, pp. 397-460, Apr 1978, doi: 10.1152/physrev.1978.58.2.397.

[73] Y.-C. Fung, *Biomechanics - Mechanical Properties of Living Tissues*. Springer New York, NY, 1993, pp. XVIII, 568.

[74] Y. C. Fung, *Biomechanics. Its scope, history, and some problems of continuum mechanics in physiology.*, 1 ed. Applied Mechanics Reviews, 1968, pp. 1-20.

[75] H. GREGERSEN, *Biomechanics of the gastrointestinal tract*, 1 ed. Springer London 2003, pp. XV, 268.

[76] X. Hu and M. W. Grinstaff, "Advances in Hydrogel Adhesives for Gastrointestinal Wound Closure and Repair," *Gels,* vol. 9, no. 4, p. 282, 2023. [Online]. Available: https://www.mdpi.com/2310-2861/9/4/282.

[77] A. H. C. Anthis *et al.*, "Chemically Stable, Strongly Adhesive Sealant Patch for Intestinal Anastomotic Leakage Prevention," *Advanced Functional Materials,* vol. 31, no. 16, p. 2007099, 2021, doi: https://doi.org/10.1002/adfm.202007099.

[78] B. Szabo *et al.*, "Biomechanical comparison of microvascular anastomoses prepared by various suturing techniques," (in eng), *Injury,* vol. 51, no. 12, pp. 2866-2873, Dec 2020, doi: 10.1016/j.injury.2020.02.104.

[79] H. Yuk *et al.*, "Dry double-sided tape for adhesion of wet tissues and devices," (in eng), *Nature,* vol. 575, no. 7781, pp. 169-174, Nov 2019, doi: 10.1038/s41586-019-1710-5.

[80] A. Lam, B. Fleischer, and J. Alverdy, "The Biology of Anastomotic Healing-the Unknown Overwhelms the Known," (in eng), *J Gastrointest Surg,* vol. 24, no. 9, pp. 2160-2166, Sep 2020, doi: 10.1007/s11605-020-04680-w.

[81] R. B. Morgan and B. D. Shogan, "The science of anastomotic healing," *Seminars in Colon and Rectal Surgery,* vol. 33, no. 2, p. 100879, 2022/06/01/ 2022, doi: https://doi.org/10.1016/j.scrs.2022.100879.

[82] X. Xue and D. M. Falcon, "The Role of Immune Cells and Cytokines in Intestinal Wound Healing," (in eng), *International journal of molecular sciences,* vol. 20, no. 23, p. 6097, 2019, doi: 10.3390/ijms20236097.

[83] H. Oxlund, H. Christensen, M. Seyer-Hansen, and T. T. Andreassen, "Collagen deposition and mechanical strength of colon anastomoses and skin incisional wounds of rats," (in eng), *J Surg Res,* vol. 66, no. 1, pp. 25-30, Nov 1996, doi: 10.1006/jsre.1996.0367.

[84] D. M. Hayden, C. Forsyth, and A. Keshavarzian, "The role of matrix metalloproteinases in intestinal epithelial wound healing during normal and inflammatory states," (in eng), *J Surg Res,* vol. 168, no. 2, pp. 315-24, Jun 15 2011, doi: 10.1016/j.jss.2010.03.002.

[85] R. Morgan and B. Shogan, "The Science of Anastomotic Healing," *Seminars in Colon and Rectal Surgery,* vol. 33, p. 100879, 03/01 2022, doi: 10.1016/j.scrs.2022.100879.

[86] J. Man and J. Hrabe, "Anastomotic Technique-How to Optimize Success and Minimize Leak Rates," (in eng), *Clin Colon Rectal Surg,* vol. 34, no. 6, pp. 371-378, Nov 2021, doi: 10.1055/s-0041-1735267.

[87] E. Zarnescu, N. Zarnescu, and R. Costea, "Updates of Risk Factors for Anastomotic Leakage after Colorectal Surgery," *Diagnostics,* vol. 11, p. 2382, 12/17 2021, doi: 10.3390/diagnostics11122382.

[88] K. Cira, S. N. Janett, H. Friess, and P.-A. Neumann, "Neue Anastomosentechniken in der Chirurgie bei Morbus Crohn," *Gastro-News,* vol. 10, no. 1, pp. 39-43, 2023/02/01 2023, doi: 10.1007/s15036-023-3189-z.

[89] T. Kono *et al.*, "A new antimesenteric functional end-to-end handsewn anastomosis: surgical prevention of anastomotic recurrence in Crohn's disease," (in eng), *Dis Colon Rectum,* vol. 54, no. 5, pp. 586-92, May 2011, doi: 10.1007/DCR.0b013e318208b90f.

[90] H. GREGERSEN and G. KASSAB, "Biomechanics of the gastrointestinal tract," *Neurogastroenterology & Motility,* vol. 8, no. 4, pp. 277-297, 1996, doi: https://doi.org/10.1111/j.1365-2982.1996.tb00267.x.

[91] M. R. Roach and A. C. Burton, "The reason for the shape of the distensibility curves of arteries," (in eng), *Can J Biochem Physiol,* vol. 35, no. 8, pp. 681-90, Aug 1957.

[92] V. Chlumsky, "Experimentelle Untersuchungen uber die verschiedenen Methoden der Darmvereinigung," *Beitr Klein Chir,* vol. 25, pp. 539-543, 1899.

[93] H. Jiborn, J. Ahonen, and B. Zederfeldt, "Healing of experimental colonic anastomoses. I. Bursting strength of the colon after left colon resection and anastomosis," (in eng), *Am J Surg,* vol. 136, no. 5, pp. 587-94, Nov 1978, doi: 10.1016/0002-9610(78)90315-x.

[94] J. B. Herrmann, S. C. Woodward, and E. J. Pulaski, "HEALING OF COLONIC ANASTOMOSES IN THE RAT," (in eng), *Surg Gynecol Obstet,* vol. 119, pp. 269-75, Aug 1964.

[95] T. T. Irvin and T. K. Hunt, "Reappraisal of the healing process of anastomosis of the colon," *Surgery, gynecology & obstetrics,* vol. 138, no. 5, pp. 741-746, 1974.

[96] H. Christensen, S. Langfelt, and S. Laurberg, "Bursting Strength of Experimental Colonic Anastomoses: A Methodological Study," *European Surgical Research,* vol. 25, no. 1, pp. 38-45, 2008, doi: 10.1159/000129255.

[97] J. N. Maina, *Fundamental Structural Aspects and Features in the Bioengineering of the Gas Exchangers: Comparative Perspectives*, 1 ed. (Advances in AnatomyEmbryology and Cell Biology). Germany: Springer-Verlag Berlin Heidelberg New York, 2002, pp. XII, 117.

[98] C. Micheler, ""Entwicklung eines automatisierten, druckgeregelten Perfusionsbioreaktors zur Kultivierung von 3D-Zellkulturen". Masterarbeit," Department of Orthopaedics and Sport Orthopaedics, Klinikum rechts der Isar, Technische Universität München Munich, 2017.

[99] C. Micheler, P. Foehr, and R. Burgkart, "Integration eines Low-Cost Touchscreen Display als Bedienoberfläche für das myRIO-System," 01/01 2017.

[100] C. Micheler *et al.*, "Bioreactor design for the mechanical stimulation by compression of 3D cell cultures," *Current Directions in Biomedical Engineering,* vol. 7, pp. 899-902, 10/09 2021, doi: 10.1515/cdbme-2021-2229.

[101] T. Berndt, ""Optmierung des Fluidkreislaufs für eine druckgeregelte Perfusionsstimulation im Bioreaktor". Semesterarbeit," Department of Orthopaedics and Sport Orthopaedics, Klinikum rechts der Isar, Technical University of Munich, Munich, 2020.

[102] A. Hangleiter, ""Weiterentwicklung eines Perfusionsbioreaktors und Realisierung eines druckprofilgeregelten Durchströmungsmodus (Tissue Engineering)". Masterarbeit," Department of Orthopaedics and Sport Orthopaedics, Klinikum rechts der Isar, Technical University of Munich, Munich, 2022.

[103] R. Bitter, T. Mohiuddin, and M. Nawrocki, "LabVIEW: Advanced programming techniques," *Crc Press,* 2006.

[104] T. J. Higgins JPT, Chandler J, Cumpston M, Li T, Page MJ, Welch VA (editors). "Handbook for Systematic Reviews of Interventions version 6.2 (updated February 2021) " www.training.cochrane.org/handbook [Accessed March 20, 2022] (accessed.

[105] J. Sterne, M. Hernán, A. McAleenan, B. Reeves, and J. Higgins, "Chapter 25: Assessing risk of bias in a non-randomized study. In: Higgins JPT, Thomas J, Chandler J, Cumpston M, Li T, Page MJ, Welch VA (editors). Cochrane Handbook for Systematic Reviews of Interventions version 6.3 (updated February 2022). Cochrane, 2022." [Online]. Available: Available from www.training.cochrane.org/handbook.

[106] J. Higgins, J. Savović, M. Page, R. Elbers, and J. Sterne, "Chapter 8: Assessing risk of bias in a randomized trial. In: Higgins JPT, Thomas J, Chandler J, Cumpston M, Li T, Page MJ, Welch VA (editors). Cochrane Handbook for Systematic Reviews of Interventions version 6.3 (updated February 2022). Cochrane, 2022." [Online]. Available: Available from www.training.cochrane.org/handbook.

[107] J. A. C. Sterne *et al.*, "RoB 2: a revised tool for assessing risk of bias in randomised trials," *Bmj,* vol. 366, Aug 28 2019, doi: 10.1136/bmj.l4898.

[108] J. A. Sterne *et al.*, "ROBINS-I: a tool for assessing risk of bias in non-randomised studies of interventions," *BMJ,* vol. 355, p. i4919, 2016, doi: 10.1136/bmj.i4919.

[109] O. C. D. Wells GA SB, Peterson J et al. . "The Newcastle-Ottawa Scale (NOS) for assessing the quality of non randomised studies in meta-analyses." www.ohri.ca/programs/clinical_epidemiology/oxford.asp [Accessed January 26, 2022] (accessed.

[110] C. R. Hooijmans, M. M. Rovers, R. B. de Vries, M. Leenaars, M. Ritskes-Hoitinga, and M. W. Langendam, "SYRCLE's risk of bias tool for animal studies," (in eng), *BMC Med Res Methodol,* vol. 14, p. 43, Mar 26 2014, doi: 10.1186/1471-2288-14-43.

[111] C. Kilkenny, W. J. Browne, I. C. Cuthill, M. Emerson, and D. G. Altman, "Improving bioscience research reporting: the ARRIVE guidelines for reporting animal research," (in eng), *PLoS Biol,* vol. 8, no. 6, p. e1000412, Jun 29 2010, doi: 10.1371/journal.pbio.1000412.

[112] T. T. Kararli, "Comparison of the gastrointestinal anatomy, physiology, and biochemistry of humans and commonly used laboratory animals," *Biopharmaceutics & Drug Disposition,* vol. 16, no. 5, pp. 351-380, 1995, doi: https://doi.org/10.1002/bdd.2510160502.

[113] D. Ripken and H. F. J. Hendriks, "Porcine Ex Vivo Intestinal Segment Model," in *The Impact of Food Bioactives on Health: in vitro and ex vivo models*, K. Verhoeckx *et al.* Eds. Cham (CH): Springer Copyright 2015, The Author(s). 2015, pp. 255-62.

[114] W. M. S. Russell and R. L. Burch, *The principles of humane experimental technique*. Methuen, 1959.

[115] G. E. Whalen, J. A. Harris, J. E. Geenen, and K. H. Soergel, "Sodium and water absorption from the human small intestine. The accuracy of the perfusion method," (in eng), *Gastroenterology,* vol. 51, no. 6, pp. 975-84, Dec 1966.

[116] K. Soergel, "Flow measurements of test meals and fasting contents in the human small intestine," *Gastrointestinal motility,* pp. 81-92, 1971.

[117] J. S. Fordtran and B. Saltin, "Gastric emptying and intestinal absorption during prolonged severe exercise," (in eng), *J Appl Physiol,* vol. 23, no. 3, pp. 331-5, Sep 1967, doi: 10.1152/jappl.1967.23.3.331.

[118] H. Cooper, R. Levitan, J. S. Fordtran, and F. J. Ingelfinger, "A method for studying absorption of water and solute from the human small intestine," (in eng), *Gastroenterology,* vol. 50, no. 1, pp. 1-7, Jan 1966.

[119] J. S. Fordtran and T. W. Locklear, "Ionic constituents and osmolality of gastric and small-intestinal fluids after eating," *The American Journal of Digestive Diseases,* Article vol. 11, no. 7, pp. 503-521, 1966, doi: 10.1007/BF02233563.

[120] J. Fordtran and F. Ingelfinger, "Absorption of water, electrolytes, and sugars from the human gut," *Handbook of physiology, section,* vol. 6, pp. 1457-1490, 1968.

[121] S. G. Schultz and A. K. Solomon, "Determination of the effective hydrodynamic radii of small molecules by viscometry," *The Journal of general physiology,* Article vol. 44, pp. 1189-1199, 1961, doi: 10.1085/jgp.44.6.1189.

[122] W. S. Cobb, J. M. Burns, K. W. Kercher, B. D. Matthews, H. James Norton, and B. Todd Heniford, "Normal intraabdominal pressure in healthy adults," (in eng), *J Surg Res,* vol. 129, no. 2, pp. 231-5, Dec 2005, doi: 10.1016/j.jss.2005.06.015.

[123] A. Shafik, O. El Sibai, and A. Shafik, "Study of the duodenal contractile activity during antral contractions," (in eng), *World J Gastroenterol,* vol. 13, no. 18, pp. 2600-3, May 14 2007, doi: 10.3748/wjg.v13.i18.2600.

[124] S. Fink, "The intraluminal pressures in the intact human intestine," (in eng), *Gastroenterology,* vol. 36, no. 5, pp. 661-71, May 1959.

[125] N. S. Painter and S. C. Truelove, "THE INTRALUMINAL PRESSURE PATTERNS IN DIVERTICULOSIS OF THE COLON. I. RESTING PATTERNS OF PRESSURE. II. THE EFFECT OF MORPHINE," (in eng), *Gut,* vol. 5, no. 3, pp. 201-13, Jun 1964, doi: 10.1136/gut.5.3.201.

[126] U. o. I. D. o. Surgery, R. E. Condon, L. M. Nyhus, U. o. I. D. o. Surgery, and U. o. I. a. t. M. C. D. o. Surgery, *Manual of Surgical Therapeutics*. Little, Brown, 1972.

[127] J. L. Daristotle *et al.*, "Improving the adhesion, flexibility, and hemostatic efficacy of a sprayable polymer blend surgical sealant by incorporating silica particles," *Acta Biomaterialia,* vol. 90, pp. 205-216, May 2019, doi: 10.1016/j.actbio.2019.04.015.

[128] T. Kocher and F. Harder, *ANASTOMOSEN-TECHNIKEN IM MAGEN-DARM-TRAKT: mit modernem, monofilem Nahtmaterial*, 2 ed. Switzerland: Covidien Switzerland Ltd. , 2011, pp. V, 235.

[129] N. Mantel and W. Haenszel, "Statistical aspects of the analysis of data from retrospective studies of disease," (in eng), *J Natl Cancer Inst,* vol. 22, no. 4, pp. 719-48, Apr 1959.

[130] M. Kaptein and E. v. d. Heuvel, *Stastistics for Data Scientists: An Introduction to Probability, Statistics and Data Analysis*, 1 ed. (Undergraduate Topics in Computer Science). Switzerland: Springer, Cham, 2022, pp. XXIV, 321.

[131] J. Higgins, T. Li , J. Deeks, and (editors), "Chapter 6: Choosing effect measures and computing estimates of effect. In: Higgins JPT, Thomas J, Chandler J, Cumpston M, Li T, Page MJ, Welch VA (editors). Cochrane Handbook for Systematic Reviews of Interventions version 6.3 (updated February 2022). Cochrane, 2022." [Online]. Available: Available from www.training.cochrane.org/handbook.

[132] S. McGrath, X. Zhao, R. Steele, B. D. Thombs, and A. Benedetti, "Estimating the sample mean and standard deviation from commonly reported quantiles in meta-analysis," (in eng), *Stat Methods Med Res,* p. 962280219889080, Jan 30 2020, doi: 10.1177/0962280219889080.

[133] J. P. Higgins and S. G. Thompson, "Quantifying heterogeneity in a meta-analysis," (in eng), *Stat Med,* vol. 21, no. 11, pp. 1539-58, Jun 15 2002, doi: 10.1002/sim.1186.

[134] J. Deeks, J. Higgins, D. Altman, and (editors), "Chapter 10: Analysing data and undertaking meta-analyses. In: Higgins JPT, Thomas J, Chandler J, Cumpston M, Li T, Page MJ, Welch VA (editors). Cochrane Handbook for Systematic Reviews of Interventions version 6.3 (updated February 2022). Cochrane, 2022." [Online]. Available: Available from www.training.cochrane.org/handbook.

[135] H. R. Rothstein, A. J. Sutton, and M. Borenstein, *Publication Bias in Meta-Analysis: Prevention, Assessment and Adjustments* 1ed. England: John Wiley & Sons, Ltd, 2005.

[136] K. Dickersin, "How important is publication bias? A synthesis of available data," (in eng), *AIDS Educ Prev,* vol. 9, no. 1 Suppl, pp. 15-21, Feb 1997.

[137] P. J. Easterbrook, J. A. Berlin, R. Gopalan, and D. R. Matthews, "Publication bias in clinical research," (in eng), *Lancet,* vol. 337, no. 8746, pp. 867-72, Apr 13 1991, doi: 10.1016/0140-6736(91)90201-y.

[138] K. Dickersin, Y. I. Min, and C. L. Meinert, "Factors influencing publication of research results. Follow-up of applications submitted to two institutional review boards," (in eng), *Jama,* vol. 267, no. 3, pp. 374-8, Jan 15 1992.

[139] J. M. Stern and R. J. Simes, "Publication bias: evidence of delayed publication in a cohort study of clinical research projects," (in eng), *Bmj,* vol. 315, no. 7109, pp. 640-5, Sep 13 1997, doi: 10.1136/bmj.315.7109.640.

[140] E. Hemminki, "Study of information submitted by drug companies to licensing authorities," (in eng), *Br Med J,* vol. 280, no. 6217, pp. 833-836, 1980, doi: 10.1136/bmj.280.6217.833.
[141] A. H. Bardy, "Bias in reporting clinical trials," *British Journal of Clinical Pharmacology,* vol. 46, no. 2, pp. 147-150, 1998, doi: https://doi.org/10.1046/j.1365-2125.1998.00759.x.
[142] I. Kirsch, *The Emperor's New Drugs: Exploding the Antidepressant Myth*. Great Britain: The Bodley Head 2009.
[143] M. Page, J. Higgins, and J. Sterne, "Chapter 13: Assessing risk of bias due to missing results in a synthesis. In: Higgins JPT, Thomas J, Chandler J, Cumpston M, Li T, Page MJ, Welch VA (editors). Cochrane Handbook for Systematic Reviews of Interventions version 6.1 (updated September 2020). Cochrane, 2020." [Online]. Available: Available from www.training.cochrane.org/handbook.
[144] M. Egger, G. Davey Smith, M. Schneider, and C. Minder, "Bias in meta-analysis detected by a simple, graphical test," (in eng), *Bmj,* vol. 315, no. 7109, pp. 629-34, Sep 13 1997, doi: 10.1136/bmj.315.7109.629.
[145] R. DerSimonian and N. Laird, "Meta-analysis in clinical trials," (in eng), *Control Clin Trials,* vol. 7, no. 3, pp. 177-88, Sep 1986, doi: 10.1016/0197-2456(86)90046-2.
[146] H. B. Mann and D. R. Whitney, "On a test of whether one of two random variables is stochastically larger than the other," *The annals of mathematical statistics,* pp. 50-60, 1947.
[147] F. Wilcoxon, "Individual comparisons by ranking methods. Biom. Bull., 1, 80–83," ed, 1945.
[148] R. A. Fisher, "Statistical methods for research workers," in *Breakthroughs in statistics: Methodology and distribution*: Springer, 1970, pp. 66-70.
[149] F. Grieder, H. Gelpke, D. Cadosch, and M. Decurtins, "Fibrin glue reduces the rate of anastomotic leakage in colorectal surgery," in *British Journal of Surgery*, 2010, vol. 97, pp. 4-4. [Online]. Available: <Go to ISI>://WOS:000290664300013. [Online]. Available: <Go to ISI>://WOS:000290664300013
[150] M. J. Page *et al.*, "The PRISMA 2020 statement: an updated guideline for reporting systematic reviews," *International journal of surgery,* vol. 88, p. 105906, 2021.
[151] D. Dindo, N. Demartines, and P.-A. Clavien, "Classification of surgical complications: a new proposal with evaluation in a cohort of 6336 patients and results of a survey," (in eng), *Ann Surg,* vol. 240, no. 2, pp. 205-213, 2004, doi: 10.1097/01.sla.0000133083.54934.ae.
[152] F. Grieder, H. Gelpke, D. Cadosch, and M. Decurtins, "Fibrin glue reduces the rate of anastomotic leakage in colorectal surgery," *British Journal of Surgery,* vol. 97, pp. 4-4, 2010. [Online]. Available: <Go to ISI>://WOS:000290664300013.
[153] D. Dindo, N. Demartines, and P. A. Clavien, "Classification of surgical complications: a new proposal with evaluation in a cohort of 6336 patients and results of a survey," (in eng), *Ann Surg,* vol. 240, no. 2, pp. 205-13, Aug 2004, doi: 10.1097/01.sla.0000133083.54934.ae.
[154] "SMART (Servier Medical Art), licensed under a Creative Common Attribution 3.0 Generic License. http://smart.servier.com/ [Accessed February 09, 2022]." (accessed.
[155] H. C. Pommergaard, M. P. Achiam, and J. Rosenberg, "External coating of colonic anastomoses: a systematic review," (in eng), *Int J Colorectal Dis,* vol. 27, no. 10, pp. 1247-58, Oct 2012, doi: 10.1007/s00384-012-1547-y.
[156] T. Nordentoft, H. C. Pommergaard, J. Rosenberg, and M. P. Achiam, "Fibrin glue does not improve healing of gastrointestinal anastomoses: A systematic review," *European Surgical Research,* Review vol. 54, no. 1-2, pp. 1-13, 2015, doi: 10.1159/000366418.
[157] X. Chen, X. Yuan, Z. Chen, and L. Zhu, "Endoscopic injection of human fibrin sealant in treatment of intrathoracic anastomotic leakage after esophageal cancer surgery,"

Journal of Cardiothoracic Surgery, vol. 15, no. 1, p. 96, 2020/05/14 2020, doi: 10.1186/s13019-020-01127-w.

[158] P. Del Rio, P. Dell'Abate, P. Soliani, S. Ziegler, M. Arcuri, and M. Sianesi, "Endoscopic treatment of esophageal and colo-rectal fistulas with fibrin glue," (in eng), *Acta Biomed,* vol. 76, no. 2, pp. 95-8, Sep 2005.

[159] E. Lippert *et al.*, "Fibrin glue in the endoscopic treatment of fistulae and anastomotic leakages of the gastrointestinal tract," (in eng), *Int J Colorectal Dis,* vol. 26, no. 3, pp. 303-11, Mar 2011, doi: 10.1007/s00384-010-1104-5.

[160] V. D. Plat *et al.*, "The role of tissue adhesives in esophageal surgery, a systematic review of literature," *International Journal of Surgery,* vol. 40, pp. 163-168, Aug 2017, doi: 10.1016/j.ijsu.2017.02.093.

[161] A. Cheragwandi, D. H. Nieuwenhuis, M. Gagner, and E. C. Consten, "An update of available innovative staple line reinforcement materials in colorectal surgery," (in eng), *Surg Technol Int,* vol. 17, pp. 131-7, 2008.

[162] Y. S. Chen, E. W. Loh, S. C. Shen, Y. H. Su, and K. W. Tam, "Efficacy of Fibrin Sealant in Reducing Complication Risk After Bariatric Surgery: a Systematic Review and Meta-analysis," (in eng), *Obes Surg,* vol. 31, no. 3, pp. 1158-1167, Mar 2021, doi: 10.1007/s11695-020-05098-8.

[163] S. Panda, M. P. Connolly, M. G. Ramirez, and J. B. de Heredia, "Costs analysis of fibrin sealant for prevention of anastomotic leakage in lower colorectal surgery," *Risk Management and Healthcare Policy,* Article vol. 13, pp. 5-11, 2020, doi: 10.2147/RMHP.S221008.

[164] S. K. Thompson, E. Y. Chang, and B. A. Jobe, "Clinical review: Healing in gastrointestinal anastomoses, Part I," *Microsurgery,* https://doi.org/10.1002/micr.20197 vol. 26, no. 3, pp. 131-136, 2006/01/01 2006, doi: 10.1002/micr.20197.

[165] F. J. Thornton and A. Barbul, "Healing in the gastrointestinal tract," (in eng), *Surg Clin North Am,* vol. 77, no. 3, pp. 549-73, Jun 1997, doi: 10.1016/s0039-6109(05)70568-5.

[166] D. I. Anderson *et al.*, "Enterococcus faecalis Is Associated with Anastomotic Leak in Patients Undergoing Colorectal Surgery," (in eng), *Surg Infect (Larchmt),* vol. 22, no. 10, pp. 1047-1051, Dec 2021, doi: 10.1089/sur.2021.147.

[167] "Takeda Pharma A/S. TISSEEL (Fibrin Sealant) [package insert]. U.S. Food and Drug Administration. Revised 2013 " https://www.fda.gov/media/71674/download [Accessed January 26, 2022].

[168] "Takeda Pharma A/S. TachoSil (TACHOSIL® Fibrin Sealant Patch) [package insert]. U.S. Food and Drug Administration. Revised July 2015." https://www.fda.gov/media/78698/download [Accessed January 26, 2022]

[169] H. Christensen, J. Chemnitz, B. C. Christensen, and H. Oxlund, "Collagen structural organization of healing colonic anastomoses and the effect of growth hormone treatment," (in eng), *Dis Colon Rectum,* vol. 38, no. 11, pp. 1200-5, Nov 1995, doi: 10.1007/bf02048337.

[170] L. Haverkamp, J. P. Ruurda, and R. van Hillegersberg, "Technical Feasibility of TachoSil Application on Esophageal Anastomoses," (in eng), *Gastroenterology research and practice,* vol. 2015, pp. 534080-534080, 2015, doi: 10.1155/2015/534080.

[171] J. C. Becker, W. Domschke, and T. Pohle, "Biological in vitro effects of fibrin glue: fibroblast proliferation, expression and binding of growth factors," (in eng), *Scand J Gastroenterol,* vol. 39, no. 10, pp. 927-32, Oct 2004, doi: 10.1080/00365520410003371.

[172] P. Kotze, I. Folchini de Barcelos, R. Ropelato, and C. Coy, "Human fibrinogen and thrombin patch for extraluminal protection of intestinal anastomosis," *Journal of Coloproctology (Rio de Janeiro),* vol. 33, pp. 174-178, 09/01 2013, doi: 10.1016/j.jcol.2013.08.004.

[173] T. Michalik, R. Matkowski, P. Biecek, J. Forgacz, and B. Szynglarewicz, "Ultralow anterior resection with implantation of gentamicin-collagen sponge and no defunctioning stoma: anastomotic leakage and local cancer relapse," (in eng), *Radiol Oncol,* vol. 53, no. 1, pp. 77-84, Mar 3 2019, doi: 10.2478/raon-2019-0008.

[174] M. C. Parker, U. Pohlen, I. H. Borel Rinkes, and T. Delvin, "The application of TachoSil® for sealing colorectal anastomosis: a feasibility study," (in eng), *Colorectal Dis,* vol. 15, no. 2, pp. 252-7, Feb 2013, doi: 10.1111/j.1463-1318.2012.03144.x.

[175] J. Torres-Melero, J. J. Motos-Mico, M. Lorenzo-Linan, A. Morales-Gonzalez, and R. Rosado-Cobian, "Use of absorbable fibrin sealant patch to strengthen the gastrointestinal anastomosis performed on patients with peritoneal carcinomatosis treated with intention to cure by debulking surgery and intraoperative hyperthermic intraperitoneal chemotherapy," (in Spanish), *Cir. Cir.,* Article vol. 84, no. 2, pp. 102-108, Mar-Apr 2016, doi: 10.1016/j.circir.2015.09.005.

[176] P. Kelly, "Solid mechanics part ii: Engineering solid mechanics small strain," *The University of Auckland,* 2013.

[177] S. K. Panda and M. L. Buist, "A viscoelastic framework for inflation testing of gastrointestinal tissue," *Journal of the Mechanical Behavior of Biomedical Materials,* vol. 103, p. 103569, 2020/03/01/ 2020, doi: https://doi.org/10.1016/j.jmbbm.2019.103569.

[178] D. Roylance, "Engineering viscoelasticity," *Department of Materials Science and Engineering–Massachusetts Institute of Technology, Cambridge MA,* vol. 2139, pp. 1-37, 2001.

[179] J. Bergström and J. Bergström, "Linear viscoelasticity," *Mechanics of solid polymers,* pp. 309-351, 2015.

[180] V. L. Popov, M. Heß, and E. Willert, *Handbook of contact mechanics: exact solutions of axisymmetric contact problems*. Springer Nature, 2019.

[181] G. Papanicolaou and S. Zaoutsos, "Viscoelastic constitutive modeling of creep and stress relaxation in polymers and polymer matrix composites," in *Creep and fatigue in polymer matrix composites*: Elsevier, 2019, pp. 3-59.

[182] E. P. Weledji, "Perspectives on paralytic ileus," *Acute Medicine & Surgery,* vol. 7, no. 1, p. e573, 2020, doi: https://doi.org/10.1002/ams2.573.

[183] J. H. M. Soffers, J. P. J. M. Hikspoors, H. K. Mekonen, S. E. Koehler, and W. H. Lamers, "The growth pattern of the human intestine and its mesentery," *BMC Developmental Biology,* vol. 15, no. 1, p. 31, 2015/08/22 2015, doi: 10.1186/s12861-015-0081-x.

[184] J. Kang, H. Kim, H. Park, B. Lee, and K. Y. Lee, "Risk factors and economic burden of postoperative anastomotic leakage related events in patients who underwent surgeries for colorectal cancer," *PLOS ONE,* vol. 17, no. 5, p. e0267950, 2022, doi: 10.1371/journal.pone.0267950.

[185] E. Goshen-Gottstein *et al.*, "Incidence and Risk Factors for Anastomotic Leakage in Colorectal Surgery: A Historical Cohort Study," (in eng), *Isr Med Assoc J,* vol. 21, no. 11, pp. 732-737, Nov 2019.

[186] S. R. Hunt and M. L. Silviera, "Anastomotic Construction," in *The ASCRS Textbook of Colon and Rectal Surgery*, S. R. Steele, T. L. Hull, T. E. Read, T. J. Saclarides, A. J. Senagore, and C. B. Whitlow Eds. Cham: Springer International Publishing, 2016, pp. 141-160.

[187] R. E. Cohen, C. J. Hooley, and N. G. McCrum, "Viscoelastic creep of collagenous tissue," *Journal of Biomechanics,* vol. 9, no. 4, pp. 175-184, 1976/01/01/ 1976, doi: https://doi.org/10.1016/0021-9290(76)90002-6.

[188] F. Guan, G. Zhang, X. Jia, and X. Deng, "Study on the Effect of Sample Temperature on the Uniaxial Compressive Mechanical Properties of the Brain Tissue," (in eng), *Appl Bionics Biomech,* vol. 2021, p. 9986395, 2021, doi: 10.1155/2021/9986395.

[189] J. J. KarisAllen and S. P. Veres, "Effect of testing temperature on the nanostructural response of tendon to tensile mechanical overload," *Journal of Biomechanics,* vol. 104, p. 109720, 2020/05/07/ 2020, doi: https://doi.org/10.1016/j.jbiomech.2020.109720.

[190] R. Eisenthal, M. E. Peterson, R. M. Daniel, and M. J. Danson, "The thermal behaviour of enzyme activity: implications for biotechnology," (in eng), *Trends Biotechnol,* vol. 24, no. 7, pp. 289-92, Jul 2006, doi: 10.1016/j.tibtech.2006.05.004.

[191] H. Fraenkel-Conrat and H. S. Olcott, "The Reaction of Formaldehyde with Proteins. V. Cross-linking between Amino and Primary Amide or Guanidyl Groups," *Journal of the American Chemical Society,* vol. 70, no. 8, pp. 2673-2684, 1948/08/01 1948, doi: 10.1021/ja01188a018.

[192] K. J. Burkhart *et al.*, "Influence of formalin fixation on the biomechanical properties of human diaphyseal bone," (in eng), *Biomed Tech (Berl),* vol. 55, no. 6, pp. 361-5, Dec 2010, doi: 10.1515/bmt.2010.043.

[193] Y. C. Fung, "Biorheology of soft tissues," (in eng), *Biorheology,* vol. 10, no. 2, pp. 139-55, Jun 1973, doi: 10.3233/bir-1973-10208.

[194] Z. Jiang, H. N. Do, J. Choi, W. Lee, and S. Baek, "A Deep Learning Approach to Predict Abdominal Aortic Aneurysm Expansion Using Longitudinal Data," (in English), *Frontiers in Physics,* Original Research vol. 7, 2020-January-15 2020, doi: 10.3389/fphy.2019.00235.

[195] B. Rengarajan, S. S. Patnaik, and E. A. Finol, "A Predictive Analysis of Wall Stress in Abdominal Aortic Aneurysms Using a Neural Network Model," (in eng), *J Biomech Eng,* vol. 143, no. 12, Dec 1 2021, doi: 10.1115/1.4051905.

[196] M. Lindquist Liljeqvist, M. Bogdanovic, A. Siika, T. C. Gasser, R. Hultgren, and J. Roy, "Geometric and biomechanical modeling aided by machine learning improves the prediction of growth and rupture of small abdominal aortic aneurysms," *Scientific Reports,* vol. 11, no. 1, p. 18040, 2021/09/10 2021, doi: 10.1038/s41598-021-96512-3.